Republic of Iraq
Ministry of Higher Education and Scientific Research
University of Babylon
College of Engineering
Department of Civil Engineering

Behavior of Reinforced Concrete Inverted T-Beams Retrofitted using Different Repairing Techniques

A Thesis
Submitted to the Council of the College of Engineering, University of Babylon in partial fulfillment of the Requirements for the Degree of Master of Science in Engineering /Civil Engineering/ Structures

By
Duaa Maged Shaker Hamzah
(B.Sc. in Civil Engineering 2015)

Supervised by
Asst.Prof.Dr. Muhammad Jawad Kadhim

2023 A.D **1444 A.H**

بِسْمِ اللَّهِ الرَّحْمَٰنِ الرَّحِيمِ

وَأَنْزَلَ اللَّهُ عَلَيْكَ الْكِتَابَ وَالْحِكْمَةَ وَعَلَّمَكَ مَا لَمْ

تَكُنْ تَعْلَمُ وَكَانَ فَضْلُ اللَّهِ عَلَيْكَ عَظِيمًا ﴿١١٣﴾

صدق الله العلي العظيم

سورة النساء الآية (113)

Dedication

To the Seal of the Prophets and the Master of Beings, the Noble Prophet Muhammad (may God bless him and his family and grant them peace).

To the remnant of the Awaited God (May God hasten his honorable reappearance).

To the master of martyrs, Imam Hussein (peace be upon him).

To my beloved country Iraq.

To my dear family.

To my supervisor Asst. Prof. Dr. Muhammad Jawad Kadhim.

I dedicate this fruit of my humble labour

With all due respect

Duaa Maged Shaker Hamza

2023

ACKNOWLEDGMENTS

In the name of Allah, the most gracious, the most merciful

prayers and peace be upon our master Muhammad and his family and companions. All praise and thanks to God who enabled me to complete this research.

First, I would like to express my appreciation and deep gratitude to my supervisor, Asst. Prof. Dr. Muhammad Jawad Kadhim, for his wonderful suggestions, encouragement and guidance throughout the research period. I really owe him.

I would like to express my sincere thanks and gratitude to my family for their care, patience and great support during the research period.

Thank you to the Dean of the College of Engineering, the President, and faculty members of the Civil Engineering Department at the University of Babylon, and thank you to everyone who supported me and helped me in this scientific career.

Thanks were also given to the staff of the Structures Laboratory at the College of Engineering / University of Babylon for their assistance in using the various facilities.

Duaa Maged Shaker

2023

Abstract

The main purpose of this research is to investigate the behavior and performance of inverted T beams of reinforced concrete by using a variety of retrofits (strengthening and repair) by external bonding technique (EBR) with carbon fiber strips (CFRP) or steel plates to upgrade existing structures and increase their flexural capacity. The current research study consisted of two parts. The first part included the practical part for preparing and checking thirteen reinforced concrete for beams inverted T beams divided into three groups in addition to the reference beam or control beam. The first group consisted of five inverted T beams strengthened with the external bonding of the CFRP strips to show the effect of the effective length and width of the CFRP strips on the beam's behavior and load capacity. The second group consisted of five inverted T beams strengthened with the outer bonding of the steel plates to show the effect of the effective length and width of the steel plates on the conduct of the beams and the amount of bearing. The third group, consisted of two inverted T beams to investigate the bearing and behavior of the inverted T beams, cracked and repaired by external bonding technique (EBR) for carbon fiber strips (CFRP) or steel plates. All inverted T beams had the same dimensions and the same rebar for tension, compression, and shearing. All inverted T beams were examined under simply supported conditions. The load in the first and second groups was examined to the stage of failure, while the beams in the third group were subjected to the load to the stage of cracking and after repaired, the load was brought to the stage of failure. The practical results showed that the use of the strengthening technique by external bonding with carbon fiber strips or steel plates improved the behavior and bearing capacity of the inverted T-reinforced concrete beams. The increase in the load capacity of the inverted T beams reinforced with carbon fiber strips ranged between 10.2% and

45.4% of the load capacity of the reference beam (unstrengthened beam), and the increase in the load capacity of the inverted T beams strengthened with steel plates ranged between 0.7% and % 31.1 of the load capacity of the reference beam (unstrengthened beam). It was noted that the model strengthened with CFRP strips measuring length and width (80% and 60%), respectively, gave the highest increase in the ultimate load when compared with other types of beams strengthened with CFRP strips. The results also showed a high flexural strength when using the CFRP strengthening technique, compared to the other type of strengthening technique by steel plates. The practical results also included a study of the effect of steel plates and CFRP in the repair of reinforced concrete inverted T beams. These results reflected the good susceptibility of steel plates and CFRP in the repair of damaged beams, as the load capacity of the beams increased by rates ranging between (29.6% and 39.3%), compared to the control beam. The results showed that the preferred method for the repair of reinforced concrete beams for inverted T beams was by using CFRP strips compared to steel plates. The second part included the study using nonlinear analysis by the finite element method to suggest the nonlinear behavior of the inverted (T) reinforced concrete beams. Numerical models were represented using ABAQUS Standard/Explicit 2019. The finite element method gave results with good convergence with the practical results, where the difference in the ultimate load of all retrofit beams ranged from -8.62% to 7.51%, and also a good agreement was obtained between the load-deflection curves in the analytical part and the experimental part.

Also, the ABAQUS Standard/Explicit 2019 program was used to develop the study further and give more results to understand the real behavior of the analysis of inverted T-shaped reinforced concrete beams retrofitted by external steel plate or carbon fiber reinforced polymer (CFRP).

List of Contents

List of Tables

List of Figures

List of Plates

Notation

The major symbols used in this study are listed below, all units are metric: dimensions are in millimeters, stresses are in MPa, moduli are in MPa, forces are in kN, and moments are in kN.m.

Symbol	Description
A_s	Area of steel
A_v	Area of two legs of stirrups
a	Shear span
b	Width of the section
bw	Web width
d	Effective depth
d′	Depth of compression longitudinal steel centroid
dbar	Diameter of steel bar
dc	Concrete compression damage parameter
dt	Concrete tension damage parameter
Ec	Concrete modulus of elasticity
Es	Steel modulus of elasticity
fc	Stress of concrete
f'_c	Nominal concrete compressive strength (cylinder test)
f_t	Concrete tensile strength
f_y	Yield stress of steel reinforcement
h	Total depth of the beam
hf	Flange height
M_u	Ultimate Bending Moment
P	Applied load
P_u	Ultimate load
V_c	Shear force carrying by concrete
V_n	Nominal shear capacity of section
Vs	Shear force carrying by stirrup.
V_u	Ultimate Shear Load
$\beta 1$	Concrete stress-block factor controlling the block height
δs	Deflection of member at service load
ε_c	Compressive strain in concrete
ε_{cu}	Ultimate compressive strain of concrete
ρ	Reinforcing bar ratio
ρ_{max}	Maximum steel reinforcement ratio
σc	Axial stress in concrete
S	Spacing of stirrups

List of Abbreviations

Abbreviations	Descriptions
ABAQUS	Analysis System Program
ACI	American concrete institute
ASTM	American society for testing materials
BS	British standard
C3D8R	8-Node Linear Brick Element, with Reduced Integration
CDP	Concrete Damaged Plasticity
CFRP	Carbon Fiber Reinforced Polymer
CFRP	Carbon fiber reinforced polymer
EA	Energy Absorption
EB	Externally Bonded
EBR	Externally Bonded Reinforcement
EXP	Experimental
etc	et cetera
FE	Finite Element
FEM	Finite Element Method
FRP	Fiber reinforced polymer
GPa	Giga Pascal (kN/mm2)
IQS	Iraqi specification
LVDT	linear variable differentia-transformer
MPa	Mega Pascal (MN/m2) (equal to N/mm2)
N.A	Neutral Axis
NSM	Finite Element Method
RC	Reinforced concrete
S4R	Four-node shell element
SFRC	Steel fiber reinforced concrete
T3D2	2-Node, 3D Truss Element
3D	Three-Dimensional

CHAPTER ONE

INTRODUCTION

1.1 General

Reinforced concrete is defined as the material that is composed of a steel bar, which is immersed in the matrix of hardened concrete; concrete bears the compressive forces, while steel bar withstands the tensile forces [1]. Strict considerations led to the use of reinforced concrete inverted beams. The inverted beam is of different types, such as I beam, T beam, etc. as shown in Figure (1-1). The inverted T beam is the RC beam which the slab is connected with it from the bottom, and the depth of the beam is upward, on the contrary, for the dropped beam (T beam), where the slab is connected with the beam from the top and its fall is to the bottom [2-4]. As for the reinforcing steel of the inverted beam, it is the same as the reinforcing steel of the ordinary beam (T beam), except in the inverted beam, it needs intensive reinforcing steel to resist the tensile stress, where the inverted beam is in contact with the slab steel and this characteristic is not present in the ordinary beam (T beam) because the steel will be in the pressure area in relation to arming the flange as mentioned in the ACI- Code 2019 in the section R9.6.1.2 [5]. While, There is no difference between the ordinary beam (T beam) and the inverted beam in terms of the moment of inertia, as both beams give the same efficiency in resisting moments. The design of the inverted T beam is similar to the ordinary beam (T beam) when the flange in the T beam is in tension, whereby the T beam resists the negative moment, so the formula for the rectangular beam design will be used according to the ACI-Code 2019[5].

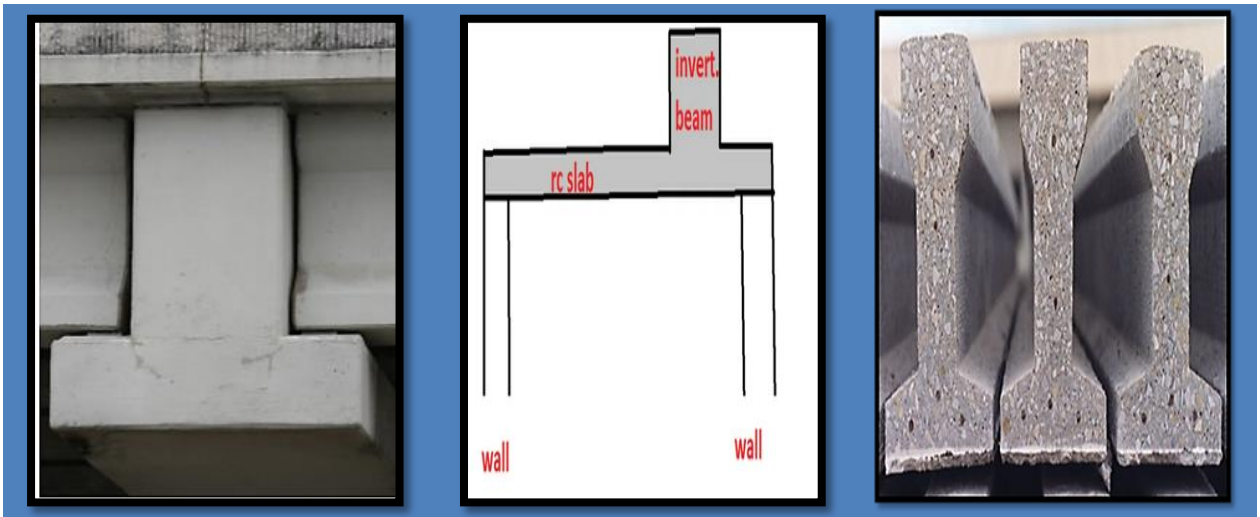

(a):(1-a) and (2-a) represent Inverted T beam (b):Inverted I beam

Figure (1-1): Various shapes of inverted beams [2-4]

In this research project, the study of the inverted beam was chosen due to its multiple benefits, which are as follows: Inverted beams are used to reduce the loads on the slabs, it allows the use of a larger slab range (large space), the inverted beam is used when there is an architectural problem such as the projection of the beam, which hinders service extensions such as air conditioning (it is used in mechanical air ducts), as well as when there are problems in stairs and entrances, lastly, the inverted T beams are provided exclusively for architectural aesthetic purposes inside the building to improve the architectural aesthetic appearance by providing an elegant lower surface.

As for the applications of inverted T beams, they are many and varied, as inverted T beams are used in buildings, bridges, foundations, and floors, in various places of the world. Where are the applications of inverted T beams:

- The inverted T beam is cast either on site, precast, and prestress, the inverted T beam use as bent caps widely in construction especially bridges to improve the clearance beneath beams, reduce the elevation of the bridges and for improving the aesthetic, the bent caps are beams

which support bridge girders over ledges close the bottom of the beam as shown in the Plate (1-1) **[2]**.

Plate(1-1):Typical inverted bent-caps [2]

- Pre-stress inverted T beams have a constant cross-section, where prestress inverted T beams have many uses in floor construction where the floor is made of pre-stress inverted T beams with clay hollow block in fills or with concrete then covered with concrete in the site to form the floor slab and the ribs, where the floor be in different types such as (a)single beam floor, (b) double beam floor and (c) full beam floor as shown in the Figure (1-2) **[4]**.

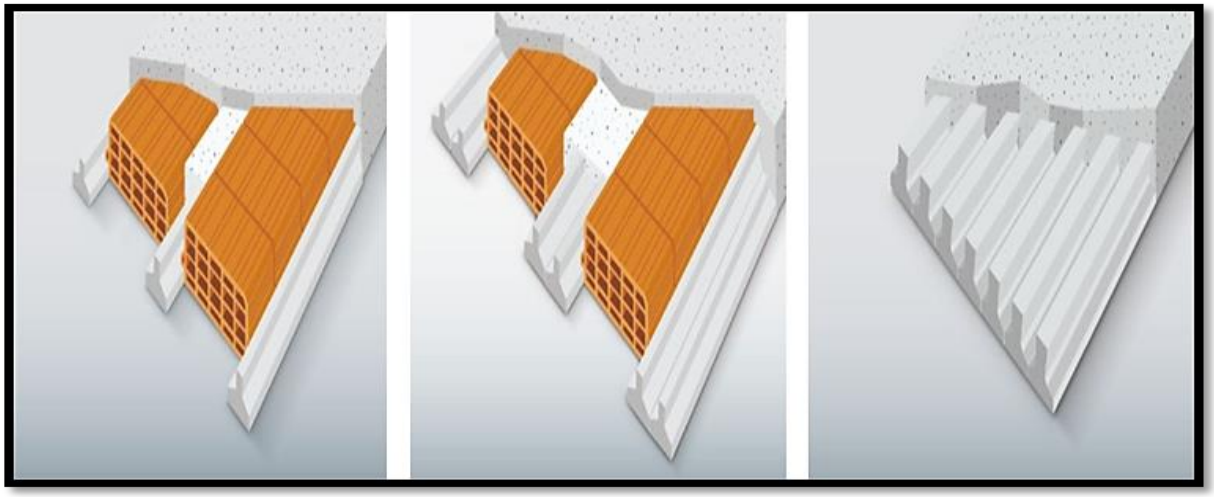

(a) Single beam floor (b) Double beam floor (c) Full beam floor

Figure (1-2):Floor made of pre stress inverted T beam [4]

- The precast concrete inverted T beam was developed by the university of Nebraska to produce short to medium-span bridges, where from benefits the precast inverted T beam are didn't require site formwork, is faster to build than the cast in site reinforced slab bridge, and its weight proper for country bridges where don't need to have heavy lifting equipment as shown in the Plate (1-2) **[5]**.

Plate (1-2): Precast concrete inverted T beam [5]

- Lastly, Inverted T beams are used in foundations to meet weaknesses points in the different soils and for purpose of seismic design **[2]**.

1.2 Retrofitting Techniques for RC Structures

The most popular way to reinforce a concrete construction is to utilize steel reinforcing bars that are placed in the construction before the concrete is cast. Since a structure may have to hold larger loads at a later history or achieve new design standards. In utmost cases, construction will have to be repaired due to an incident such as earthquakes, or fires. A further cause can be found that causes have been made through the design, construction stage, and deterioration due to corrosion happening in the steel caused by exposure to an attacker environment resulting in the requirement for strengthening the structure before employment. If any of these conditions will grow; there are

two likely solutions such as replacement or retrofitting. Full structure the replacement may cause disadvantages like high costs for material and labor, an inconvenience due to interruption of the function structure so it is often better to repair or improve the structure by retrofitting **[6,7]**, where the retrofit is mainly used in some countries for the purpose of seismic modernization of bridges. In other countries, retrofit is used as the term that includes all the strengthening and repair activities**[8]**. The basic concept of retrofitting is the up gradation of the strength of the structures and the increase in stiffness of the structures **[9]**.

The load-carrying capacity of most RC beams requires strengthening to resist early failure and prolong service life. Where the RC beams typically undergo flexural and shear failure. There are several methods used to strengthen RC beams; a common method is the use of externally bonded sheets or plates with high-strength materials, such as fiber-reinforced polymer, polyester, steel plates, wire mesh, and textile fabrics **[10-14]**. It is necessary nowadays to find repair techniques suitable in terms of fast processing time and low cost. Carbon fiber reinforced polymer (CFRP) or steel plates are the famous repairing and strengthening systems or retrofitting systems, therefore, they are used in this study **[15]**, as shown in the Plates (1-3) and (1-4) respectively **[9]**.

Plate(1-3): Retrofitting by CFRP [9]

Plate(1-4): Retrofitting by steel plate [9]

1.3 (FRP) Material

Fiber reinforced polymer (FRP) composite of materials are consist of high strength fiber found in polymer resin matrix. The benefit polymer found in the composite of matrix is used to link the fiber together, also its used to transfer forces between fibers and used to maintain fibers from environment damage and external mechanical as shown in Figure (1-3) **[16]**.

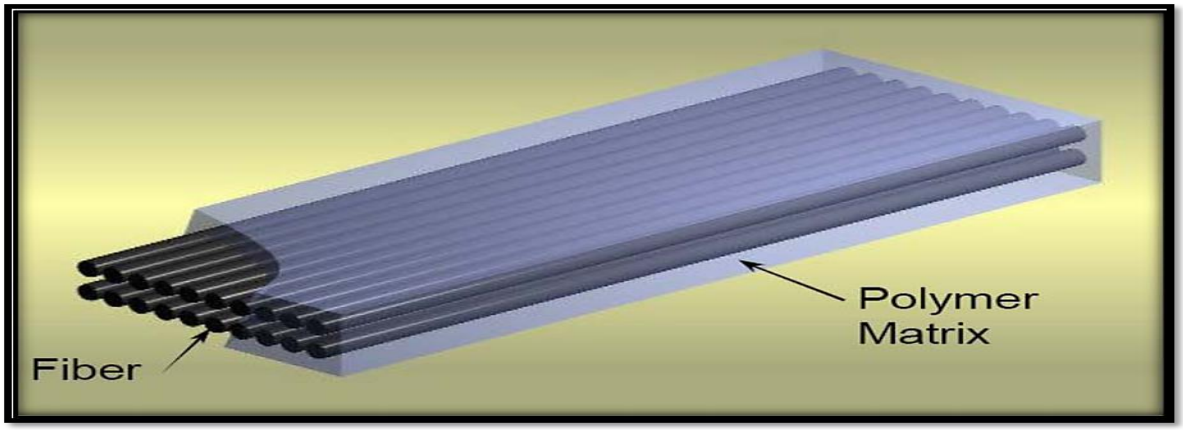

Figure(1-3):Composition of FRP material [16]

Fibers used in the (FRP) are carbon, glass and aramid**[17]**.Table (1-1) gives comparison of properties of FRP sheet generated with different fibers**[18]**.

Table (1-1):Comparison of the properties of the different FRP sheet[18]

Characteristics	Carbon	Aramid	E-glass
Tensile strength	Very good	Very good	Very good
Compressive strength	Very good	Inadequate	Good
Stiffness	Very good	Good	Adequate
Long term behaviour	Very good	Good	Adequate
Fatigue behaviour	Excellent	Good	Adequate
Bulk density	Good	Excellent	Adequate
Alkaline resistance	Very good	Good	Inadequate
Cost	Adequate	Adequate	Very good

1.3.1 Carbon Fiber Reinforces Polymer (CFRP) in (RC)

CFRP combined material consist of the polymer matrix strengthened with the carbon fiber mat, cloth or strands **[19]**. Externally bonded CFRP sheets technology is one of the most important technologies used in

strengthening and repairing or retrofitting reinforced concrete (RC) that was started in 1980s and for now has attracted researchers around world. This is due to advantages and characteristics of CFRP. From applications this method of retrofitting with externally CFRP sheets applied to strengthen and repair many of structures such as beams, columns, slabs, walls, etc. as shown in the Plate (1-5) **[20-22,18]**.

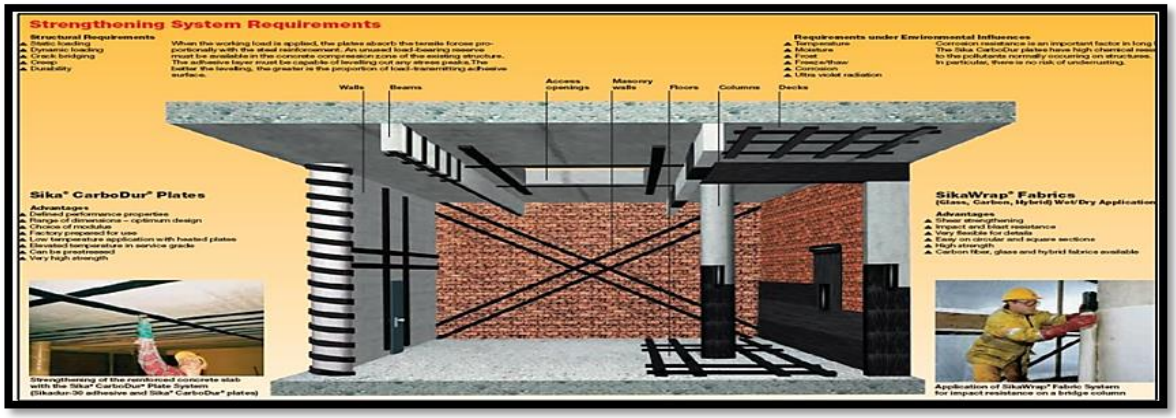

(a) CFRP strengthening[22]

(b) Increase axial load in building[20] (c) Strengthening real bridge[21]

(d) Repair historic old building[20] (f) Strengthening girder bridge[21]

Plate (1-5):Applications of CFRP strengthening and repair system

The CFRP has many advantage compared with steel where it has two times higher in stiffness, five times higher in tensile strength as shown in the Figure (1-4), more durable and corrosion resistance, excellent fatigue properties and environmental and chemical resistance. This is the cause for using like this fiber in strengthen to increase of loading capacity, repair of faults and to prevent of the defects caused by explosions or earthquakes **[23]**.

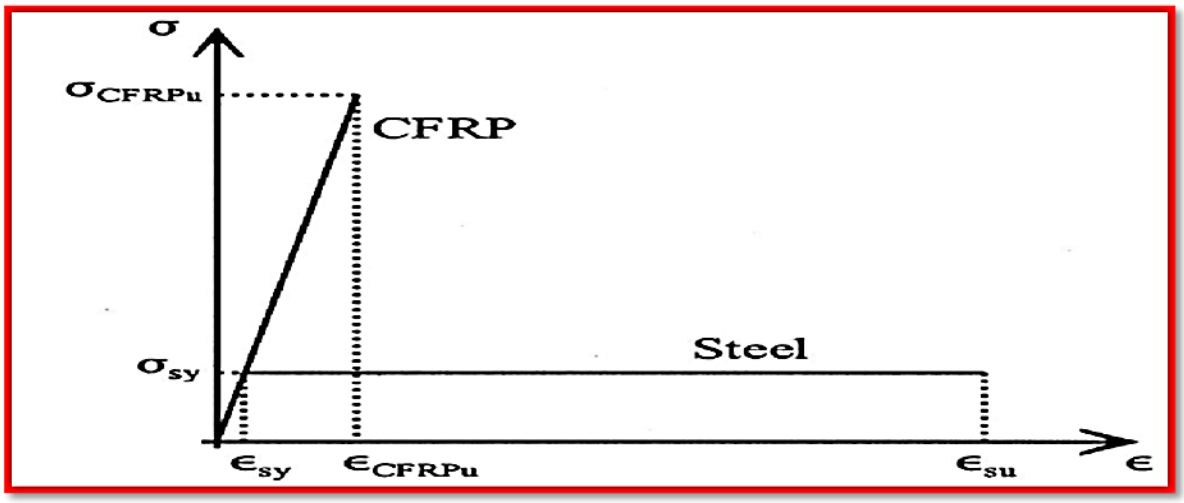

Figure(1-4):Stress-Strain Relationship CFRP Comparison with Steel[23]

1.3.1.1: Advantage of CFRP

The CFRP have several advantages including **[24,18]**:

(1) Very high strength (E > 165000MPa, tensile strength > 2400MPa).

(2) Excellent fatigue strength and high strength to weight ratio.

(3) Availability in any length and ability to be transported in rolls.

(4) Durability of the strengthening system (Resistance to corrosion, alkalis and other aggressive materials).

(5) Light weight and ease of handling.

1.3.1.2: Disadvantage of CFRP

The main disadvantages of CFRP are summarized in the following **[24,18]**:

(1) Erratic plastic behavior and less ductility.

(2) Could burnt easily.

(3) High cost.

(4) Strength depends on adhesive matrix(cohesion material) Epoxy to work.

1.4 Steel Plate

The steel sheets are manufactured from the thin strip or coil material. The steel sheets that are used can be with thickness between (0.8mm-1.2mm). The steel plates are formed in any required shapes to obtain the strength and stiffness contractures with low weight and high efficiency **[25]**.

Externally steel plate technology is common strengthening and repairing or retrofitting that is used in the RC beams, also the technique is used in the strengthening reinforced concrete structures such as bridges, slabs, and buildings in different parts of the world as shown in the plate (1-6), which the external steel plate aims to increase the load carrying capacity and decrease the service load deflections of the structures, also externally steel plate have ductile flexural behavior **[26,27]**.

Mechanical fastening to fix steel plate to sides of the reinforced concrete beam for retrofitting purposes was by adhesion epoxy for steel plate which epoxy bonded mild the steel plate using on the tension face of the beam has been proven to be an effective, economical, efficient, and convenient technique in order to guarantee the flexural and shear performance of RC beams under service and ultimate loads, and many researchers used adhesive with epoxy to connect the steel plate with concrete, although bolted steel plate could have been used and is considered a solution to prevent the deboning failure, but there is the problem with the use of connecting with bolts which needed to planning to set and drilling the bolts, also the failure didn't observe that will happened in the concrete or in the shear connectors due to strong connection who gets between the concrete and steel plate, also the anchorage by bolts leads to initial cracking in the beam near bolts holes

or bolt anchorages leading to the brittle rupture failure of the composed steel plates which this failure is undesirable**[29]**.

(a) bridge under retrofitting **(b) bridge after retrofitting**

Plate(1-6): Retrofitting with steel plate [28]

1.4.1:Advantage of Steel Plate[30,31]

(1) High fatigue strength and high ductility.

(2) Its work with steel plate easily and simple.

(3) Has isotropic material properties (uniform).

(4) Doesn't occur change the overall dimensions of the structures.

(5) Steel plate are cheaper and economical and it is easily available.

(6) It can be ensured without work any damage to the structure.

(7) It has fire resistance.

1.4.2:Disadvantage of Steel Plate [32]

(1) Don't have resistance against corrosion.

(2) Difficulty handling, transporting and installing heavy plates.

(3) Limited delivery lengths of the plates are very clear.

1.5 Comparison between FRP and Steel plate

The steel plate is used although owing FRP composites are activity strengthening or repairing materials such as perfect bonding quality with concrete and high strength, Table (1-2) **[27,34]** shows in the following comparison points the purpose of using steel plate although of found FRP, where both methods are useful when used, they have their own advantages, disadvantage, and failure patterns, both according to the way they are used.

Table (1-2):Comparison between FRP and steel plate[26,33]

FRP	Steel Plate
1-FRP composites are more costly.	1-Steel plates compared with FRP are cheap or lower prices.
2-Fire resistance is low.	2-Fire resistance is good.
3-Brittle stress-strain behavior.	3-Ductile stress-strain behavior.
4-It may available or may not be available in the place to work.	4-Avialable everywhere and reasonable prices.
5-Working with FRP required skilled workers and has work experience, because working with FRP required accuracy.	5-Working with steel plate doesn't required skilled workers or skilled labor, as work with steel plate is fast and can be completed without stop.

1.6 Research Significance

Generally, the use of RC beams with retrofitting become very famous in building structures to introduce different services. However, important status must be given to analysis of such beams by relying on the effect a retrofitting by CFRP or steel plates. Several investigation had studied the effects of retrofitting with CFRP or steel plates with different shape, size, and location on the flexural behavior of RC beams. However, very little researches are found in literature about the effect of retrofitting with CFRP or steel plate on

the behavior of RC inverted T beams and the effect of the length and width of the optimum strengthening, in addition, to repair the RC inverted T beam with the length and width of the optimum strengthening. The important of this research due to the very little of publications and researches on it. This research program is decided to fill in this gap by enhancing and evaluating the information about the behavior of RC inverted T beams with retrofitting by CFRP or steel plate for present buildings.

1.7 Objectives of the Research

1. The main objective of this research project is to study, experimentally and numerically the behaviors and load-carrying capacity of simply supported RC inverted T beams externally retrofitted (strengthened and repaired) with carbon fiber reinforced polymer (CFRP) strips or steel plates in flexural.

2. Comparison between behaviors of strengthened with CFRP strips or steel plates and repaired with CFRP strips or steel plates of the inverted T beams.

3. Finding the sufficient length and width for strengthening .

4. Study effect of the presence CFRP strips or steel plates on the width of the flexural cracks.

4. A 3D finite element method using ABAQUS standard-Explicit 2019 computer program used for nonlinear analysis simply supported RC inverted T beams with and without found strengthening and repairing with CFRP strips or steel plates.

5. Then, comparison between the numerical and the experimental results for knowing the validity and accuracy of the using this technique.

6. Extending the FE (finite element) analysis in order to carry out a parametric study to search of several variables on the behavior of simply supported reinforced concrete inverted T beams such as;

a)- Increase the strengthening length of CFRP strips and also, increase the strengthening length of steel plates.

b)- Increase the strengthening width of the CFRP sheet.

c)- Increase the thickness of the steel plates to (a) 2mm and (b) 3mm.

d)- Increase the number of layers of (CFRP) sheets.

1.8 Research Layout

The present research involves of six chapters as follows:

- **Chapter One**: presents general introduction about behavior of reinforced concrete inverted T beam. Retrofitting of the reinforced concrete structures, FRP materials, steel plate, advantage and disadvantage and comparison of the CFRP or steel plate.
- **Chapter Two**: presents a review on the previous research carried out on the experimental and theoretical investigations in the flexural behavior using CFRP strips and steel plate for retrofitting such as strengthening or repairing reinforced concrete members.
- **Chapter Three**: deals with the experimental work and test including on the materials properties, concrete mix design of the test program, also cast program, strengthening and repair of the reinforced concrete inverted T beam and their test methods.
- **Chapter Four**: presents the test experimental results and discussion of the reinforcement concrete inverted T beam without or with strengthening or repair including : loads, deflection (load deflection curve), flexural crack width and mode of failure is notice.
- **Chapter Five**: use the finite element program ABAQUS to analyze of the beams strengthening or repair by CFRP strips or steel plates, then comparing the experimental results with theoretical results.
- **Chapter Six**: presents of the conclusions, summary of research work and recommendations for the future works.

CHAPTER TWO

REVIEW OF LITERATURE

2.1 General

Retrofitting by externally bonded CFRP or steel plate systems has been used in most countries of the world to strengthen and repair concrete structural members such as slabs, beams, columns, trusses, pipes, walls, etc…

The purpose of this chapter is to give a brief review of the experimental and numerical researches that studied the behavior of the reinforcement concrete beams. Also, studied the retrofitting of the reinforced concrete structures to strengthening and repair by externally steel plate or carbon fiber reinforced polymer composites that will summary according to the major studies in this field.

2.2 Experimental studies on (RC) beams

2.2.1: Reinforced concrete Inverted T beam

2.2.1.1 Experimental studies on RC inverted T beam

There is a little researches carry out about subject of the reinforced concrete inverted T beam

Furlong et al. in (1971) [34] tested six inverted T beams that use as bent cap beams to support precast members (stringer) under loads in order to study shear strength, behavior anchorage bars, and the flexural behavior in the flange. The inverted T beam consists of two components the web and ledge or brackets. The test loads were applied on the top of the flange of the inverted T bent cap to show the accounts about the design of reinforcement in the such beam. Figure (2-1) shows the loads applied to the ledge and

transported to the web. Figure (2-2) show the bracket reinforcement, for flexural the horizontal bar and with additional horizontal bar parallel to the flexural steel at the third point approximately of the bracket depth as shown in Figure (2-2 a) and the diagonal bar would be present as bracket shear reinforced on the face T beam web as shown in Figure (2-2 b) and hangers that represent stirrups in the web of the T beam to transport the bracket load to the upper T beam web as shown in Figure (2-2 c).

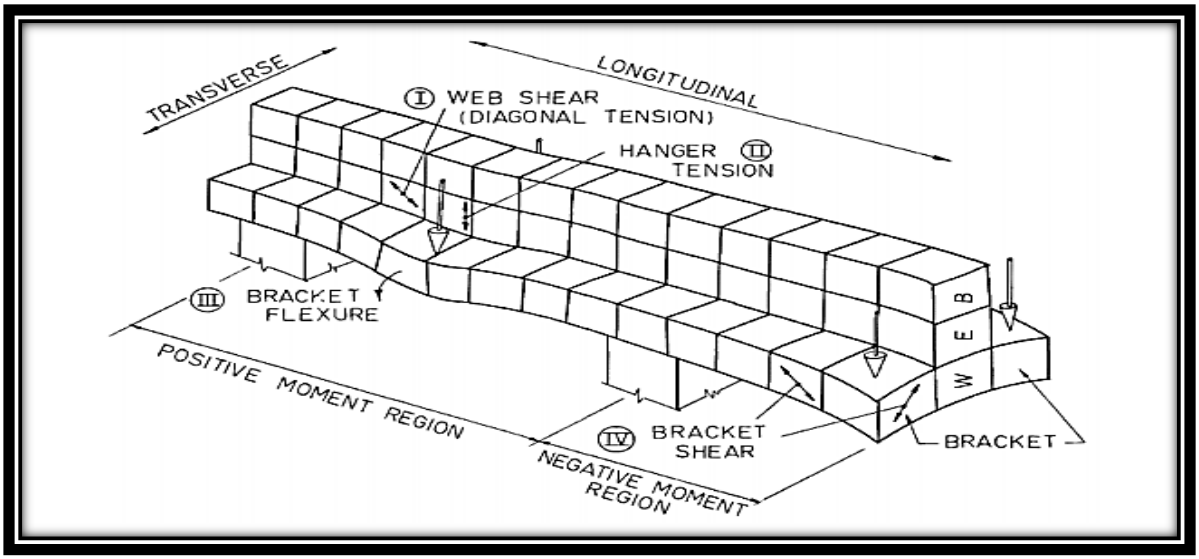

Figure (2-1): Structural load effects on Inverted T bent cap [34]

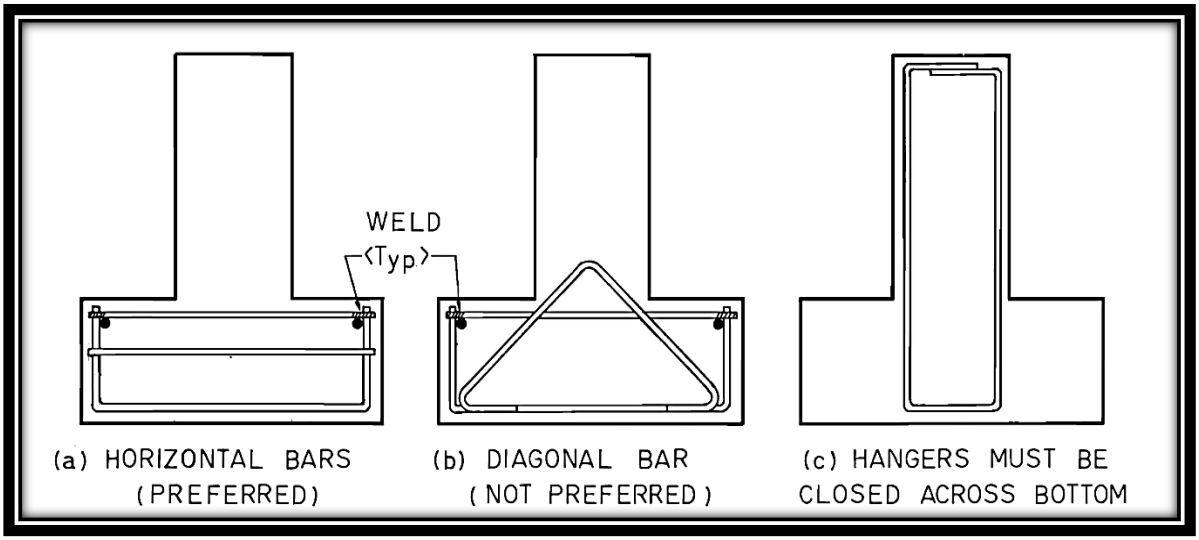

Figure (2-2): Bracket reinforcement [34]

All model beams specimens possessed the ultimate shear strength that was determined of the plain concrete according to the ACI -71 building code that represents between the compression face and the centroid tensile

steel of the beam on all concrete. Based on the experimental results, the authors showed that (1) the flange reinforcement which is perpendicular on the web is very necessary to transport the flange load to the hangers, (2) the stirrups that represent hangers are also very important to transport the vertical loads to the web. (3) the forces transmitted to the flange make a big torsional load on the web.

Furlong and Mirza (1974) [35] reported the same study about inverted T beam bent caps but carried out a study to known strength and serviceability on the seven prestress and nonprestress concrete specimens model inverted T beam bent caps under loads flexural, shear and torsion, four of them were prestressed. The tests appearance that the prestress concrete specimen had little cracks under the service load and the transverse reinforcement had the lower stresses, and the ledge (bracket) must be enough deep to prevent the punching shear and also show that the ledge must have the transverse reinforcement strength sufficiently to keep the shear friction resistance in the face at the web, finally recommended that the web stirrups that represent the hangers should be sufficient to keep on loads transport from ledge to web.

It has been found out the behavior of the inverted T RC beam under combined shear and torsion loads through researchers **Deifalla and Ghobarah (2014) [36]** who suggested it by testing the three inverted T beams. This research was done in order to design specimens to failure under influence combined shear and torsion and under different ratios, see in Figure (2-3) the dimensions and graphic system for tested beam, the middle region (test region) represent combined shear and torsion. The behavior of inverted T beam was influenced by ratio of the torque to shear. They found that decreasing the applied torque to shear ratio produced the following:

i. Significant reduction in the cracking and ultimate torque, spacing between the diagonal cracks, stirrup strain in the flange and web.

ii. Significant increase in the cracking load and failure load, cracking and ultimate shear, and rigidity in the post cracking torsional.

iii. Beam failure that result from reduction in efficiency the stirrup which the diagonal failure in concrete rather than yield in the stirrup.

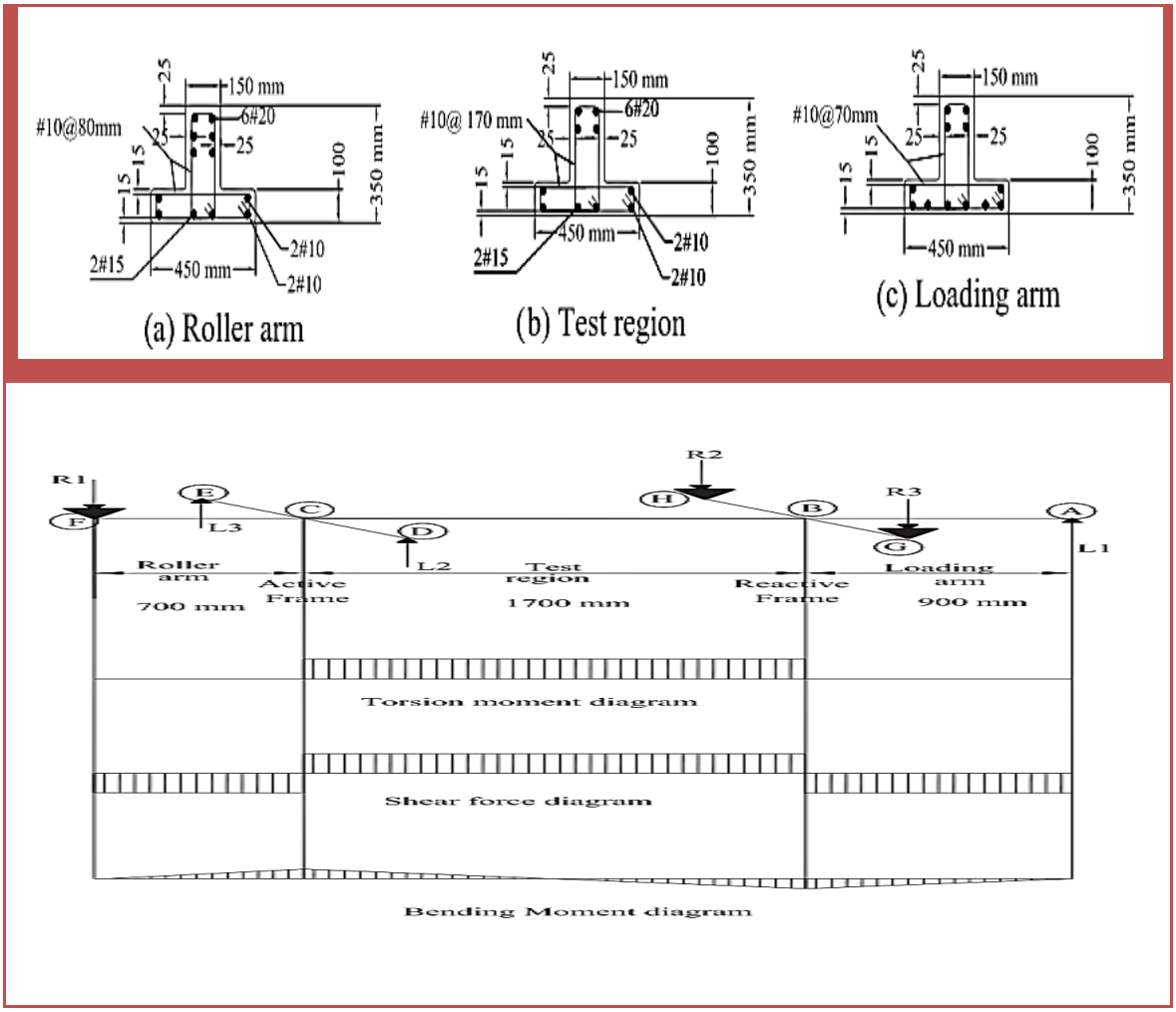

Figure(2-3): Dimension and graphic system for tested beam [36]

2.2.1.2 Failure of the mechanisms inverted T beam in form bent cap

In (1974) Furlong and Mirza [35] classified the failure mechanisms of inverted T bent caps to six failure modes depending on experimental tests, which were: flexural, flexural-shear, hanger, torsion, punching, and ledge (bracket), as shown in Figure (2-4). Flexural failure is represented by

crushing of concrete or fracture of the tensile reinforcement as shown in Figure (2-4a). Flexural-shear failure occurs by forming diagonal cracks that appear in the web after the appearance of the flexural cracks, the flexural-shear failure consists typically when don't adequate flexural strength when span to depth ratio is small to resist the moment that occurs in the shear span as shown in Figure (2-4b). Torsion failure is the appearance when occur crushing along the spiral crack or anchorage failure along reinforcement as shown in Figure (2-4c). Hanger failure is the percent yielding the hanger reinforcement which appearance a vertical separation on the web-ledge in the interface as shown in Figure(2-4d). Punching failure is made up when the applied load overpasses the tensile strength in concrete as noted in the truncated pyramid in Figure (2-4e). The sixth failure is bracket failure which occurs when the flexural failure at the ledge (bracket) or friction failure at the face web, in which the ledge is cut off; see Figure (2-4f).

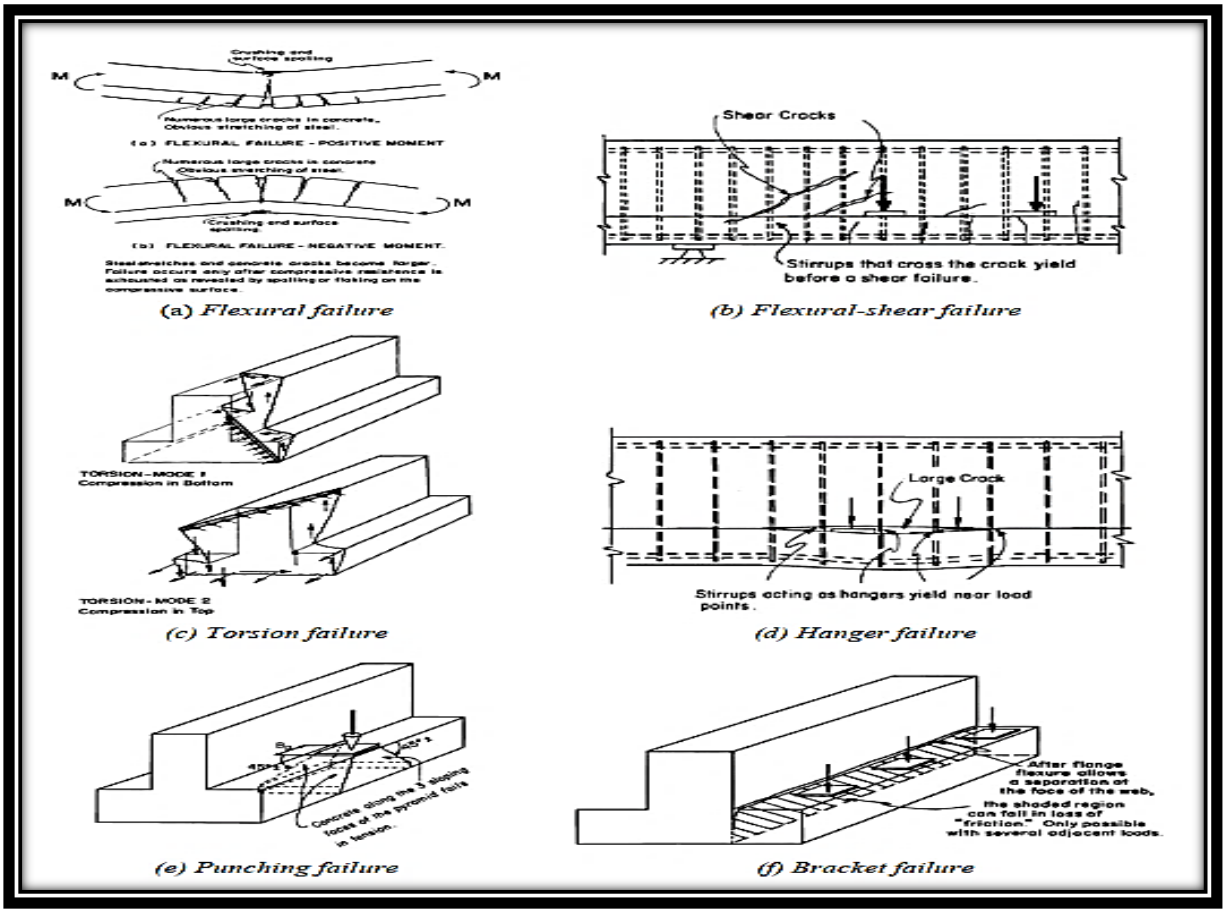

Figure (2-4): Failure mechanism of the inverted t bent caps [35]

2.2.2 : Reinforced concrete T beams

The T–shaped cross-section beam consists of the horizontal part known as the flange for the purpose of resistance compression stresses and the vertical part known as the web below the flange for the purpose of resisting the shear stresses and for the purpose of separating the coupling bending forces **[37]**. In order to form a strong T-shaped beam, this beam must be completely poured with the slab. The T beam compared to the I-shape beam a form that it has a disadvantage because it doesn't have a lower flange that deals with tensile forces so one method to create a T beam more active structurally is to utilize an inverted T beam with a bridge deck connection the tops beams or a floor slab **[38]**. But, the T-beam is better than the rectangular beam in the case of a large span because the deflection of the T-beam is reduced to a good extent.

The history of the T beam goes back to a human the first time who created abridge with a deck and a pier where case T beam has a vertical section (web) connection with a horizontal section (flange) at the top, or connection with a flange in the bottom in case inverted T beam **[39]**. Then, use the T beam in the buildings, precast concrete floors, highway overpasses, and parking garages **[40]**.

2.2.2.1 Experimental studies on reinforced concrete T beam

Bryson and Carpenter (1970) [41] presented an experimental investigation on the prestress T-shape cross-section beam constructed by split beam way, the split T beam was tested under the flexure until it fails. In this investigation, the specimens consisted of beams of the split beams composite structure and of the conventional monolithic structure. The monolithic two beams consisted of post-tensioned while the split beams consisted of both pre-tension and post-tension. All specimens were T-shaped in the cross-section. The dimensions of the specimens were included 3-in the

depth of the flange, 15-in were its width ,18-in were the overall depth and and 19 ft were the long as shown in Figure (2-5).

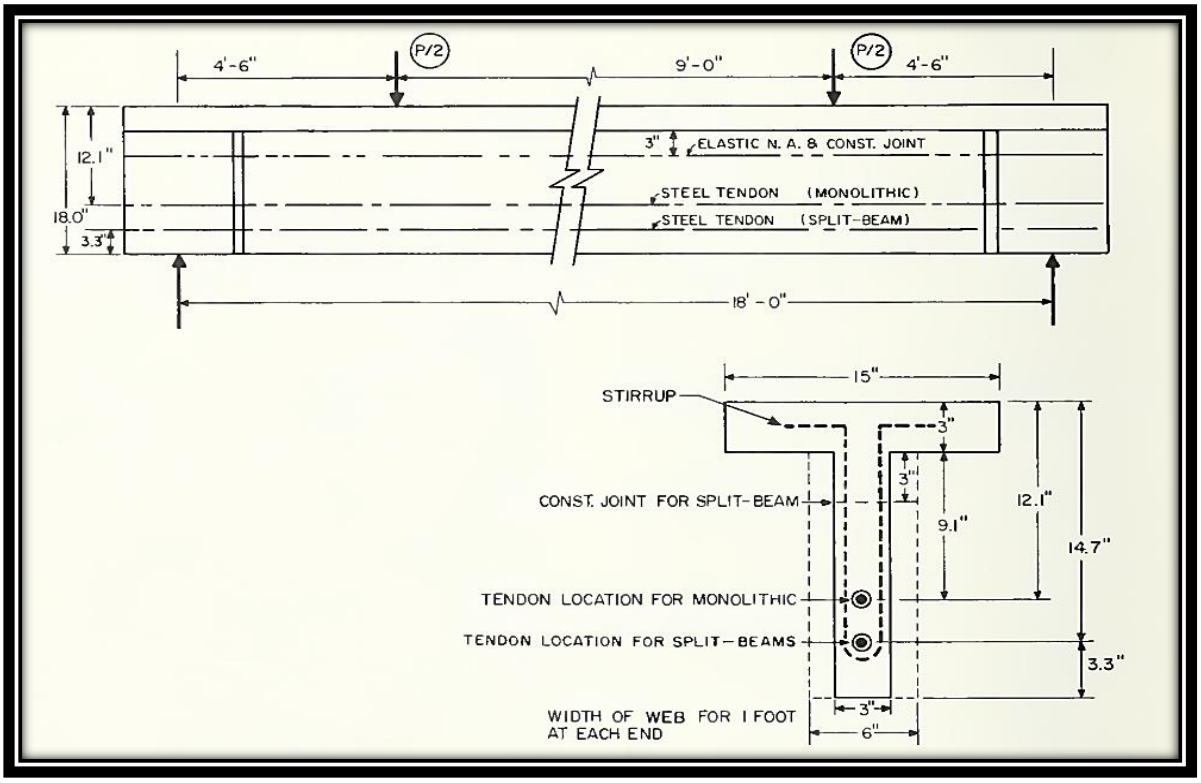

Figure (2-5): Beam dimensions and loading details [41]

The variables in this research were the percentage of prestressed steel, the behavior of prestressing, and the web reinforcement and strength concrete for the composite split beams in the compressive element. They concluded this study as the following:

a) Behavior of split beams were similar to the beams monolithically constructed depend on ultimate loads and flexure response.
b) The strength concrete in the compressive element can be reduced within the required limits for prestressed part without immolate ultimate load capacity.
c) The percentage of reinforcing steel that must be available for split beam was less than the percentage of conventional beam.

In (1980) Hanson [42] conducted a series of tests on T-shaped beams in order to study the problem of shear connections between the cast-in-site concrete slabs and precast concrete beams. The results of these tests gave an indication that the smooth joint had a horizontal shear strength of about (2.1 Mpa), while the rough joint had a strength horizontal shear of about (3.5 Mpa). For the purpose of each reinforced precast through which the joint passes, the increase in the shear strength of the joint was equal to the (1.23 Mpa) .

Ghailan, D. B. (2014) [43] conducted an experimental study on six models of T-section concrete beams, through the use of different types of concrete that are placed in the flange and /or web**.** Two of the models represent the control models and they were made fully of normal concrete and without any additives while the other models were made fully or partially of high-strength concrete or reinforced concrete with steel fibers in the flange and/or the web as shown in the Table (2-1). The test was conducted for the concrete beams with simple support, by applying a single point loading in the middle, as shown in Figure (2-6) which shows the details of the examined beams and the examination program. The author concluded from the experimental results of the two tests, depending on the concrete used, that all models under the load limit of (40- 48 kN) were behaving in an elastic manner. In comparison with the control beams, the increase in the maximum deflection was (152%)for the beam with steel fiber reinforced concrete (SFRC) in both the flange and web and for the beam with normal concrete in the flange and SFRC in the web was (60%) and the decreased that show in beam with high concrete strength in the flange and normal concrete in the web was equal (50.22%). Also, the author concluded that increased by (161%) in the first cracking load for the beam with high-strength concrete in the flange and

SFRC in the web while the other models didn't get any significant changes.

Table (2-1): Properties of the test beams[43]

Beam Designation	Type of Concrete	
	Web	Flange
B2&B6 *	NSC **	NSC
B1	SFRC***	HSC****
B3	SFRC	SFRC
B4	SFRC	NSC
B5	NSC	HSC

*Reference beams

**Normal strength concrete (compressive strength=35Mpa)

***Steel fiber reinforced concrete

****High strength concrete (compressive strength=50Mpa)

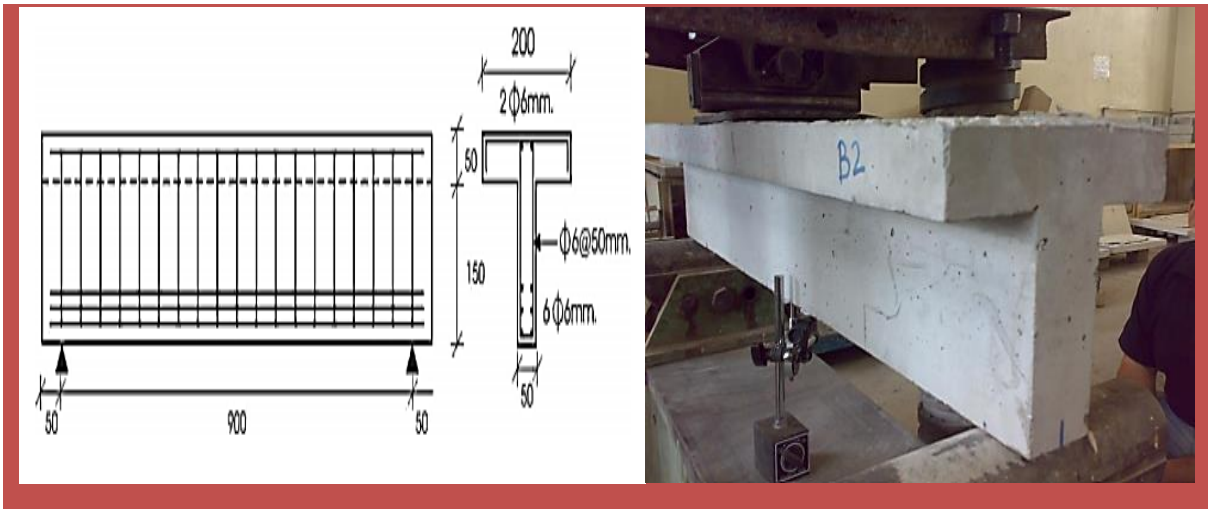

Figure (2-6):Details of the tested beams and the testing program [43]

2.3 Methods of Flexural Strengthening

Table (2-2) shows a general summary of the methods used for flexural strengthening. The main purpose of the flexural strengthening concept is to increase and improve the stiffness and strength of RC flexural structures by bonding reinforcement to RC tensile surface members. Techniques such as steel plate bonding, section enlargement new concrete

overlay, and external post-tensioning by steel tendon, shown in paragraphs (a), (b), and (c) in Table (2-2) have traditionally been widely used. Recently, FRP has been used to flexural strengthen due to its multiple benefits when compared with the strengthening of flexural strengthening traditional and also to increase and develop tensile resistance because it is characterized by high tensile strength as shown in the paragraph (d) and (e) in the Table (2-2) **[44]**.

Table (2-2): Methods of the Flexural Strengthening [44]

Methods	Illustration	Description
(a) Section enlargement	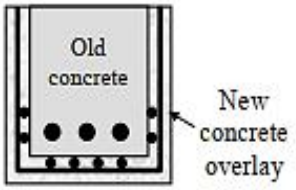	• "Bonded" reinforced concrete is added to an existing structural member in the form of an overlay or a jacket.
(b) Steel plate bonding	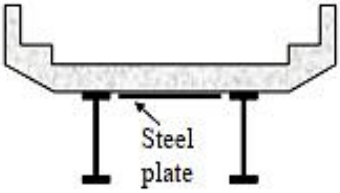	• Steel plates are glued to the concrete surface by epoxy adhesive to create a composite system and improve flexural strength.
(c) External post-tensioning method		• Active external forces are applied to the structural member using post-tensioned (stressed) cables to improve flexural strength.
(d) Externally bonded (EB) system		• FRP composites are bonded to the concrete surface to improve the flexural strength. FRP material could be in the form of sheets or plates.
(e) Near-surface-mounted (NSM) system		• FRP bars or plates are inserted into a groove on the concrete surface and bonded to the concrete using epoxy adhesive.

2.4 Retrofitting (RC) by CFRP or Steel plate

2.4.1: Classification of the Retrofitting

Retrofitting is a process based on new technological developments and scientific knowledge, whereby materials and modern construction methods are applied to the strengthening and repair of structures where retrofit in structures is done to increase survivability functionality. The authors **Harshal and Rao (2019) [45]** classified and define the retrofit process as a general term that consists of a variety of treatments, including (a)rehabilitation, (b)preservation, (c)reconstruction, and (d)restoration. Selecting the appropriate treatment strategy involved in the retrofit process must be determined individually for all projects. Depending on project objectives, renovation and preservation of buildings may involve an array of diverse technical considerations, such as fire life safety, remedies, geotechnical hazards, water infiltration and weathering, structural performance under wind loads, and earthquake.

Rehabilitation refers to the process of creating a new application for a property through repair, additions, and alterations. Preservation is defined as the process of applying measures to sustain the present form, probity, and materials of a historic property. Preservation is preferable than rehabilitation because it saves its historical, cultural, or architectural values. Reconstruction refers to replicating a property at a specific period of time. Restoration is the process of carefully restoring the property as it existed for a specific period of time. The two authors also showed that retrofits are cost-effective techniques to strengthen and repair damaged structures rather than completely replacing them.

2.4.2 : Historical Development of (FRP)

The FRP materials were used early for experimental work in Germany in **1978** by **(Wolf and Miessler)** for retrofitting concrete constructions **[46]**. The initial applications of the externally bonded FRP-strengthening technique occur in Switzerland in the year 1987 the leadership **(Meier) [47]**. The first repair occurred in 1991 on-site by externally bond FRP materials. Then, the strengthening by externally bonded reinforcement (EBR) FRP was studied worldwide. After 1995 Japan obtain a sudden increase in the utilization of FRP composites. In 1997, the reinforced by externally bonded FRP materials were used in more than 1500 concrete constructions **[48]**. After that, there were wide applications for FRP composite reinforcement covering new installations as well as the repair and rehabilitation of the present structures.

2.4.2.1 Experimental and Analytical studies of RC with Retrofitting by EBR (CFRP) in Flexural member

Meier et al. in 1992 [49] tested twenty-six beams whose dimensions are (150x250x1975 mm) were reinforced by externally bonded together with CFRP sheets with minimum steel reinforcement in the bottom and top in addition to shear reinforcement. The beams were simply supported with four loadings. They found from experimental results that the beam strengthening with CFRP sheet with dimensions (0.3x200x1975 mm) and bonded to the tensile face give a percentage increase was 100% in the ultimate load capacity compared with unstrengthened beam (control beam) and also, they found that the strengthened beam has the deflection 50% less than the deflection in the unstrengthened beam (control beam).

Arduini et al. (1997) [50], modeled RC beams that have been strengthened by CFRP sheets and plates using a program (ABAQUS) based on a smeared cracking way. Analyzed the beams strengthened with CFRP plates by using a two-dimensional mesh, while the beams bonded with CFRP sheets were modeled in three dimensions. Applied the FRP reinforcement over concrete elements was directly assuming complete bond. The authors suggested that the results of the FE analysis appeared a good linkage with the data of the experimental work. However, the results of the FE analysis were stiffer compared with the experimental test results. This was back to the assumption of the complete bond and used the limited number of nodes. The FE analysis showed that the delamination failure was caused by high stresses at the end of the FRP plate of the beam.

Shahawy and Beitelman (1999) [51] investigated the experimental programs consisting of sixteen specimens of RC T beams, six with fatigue loading and ten with static loading. All specimens were flange, thickness and width 89, and 584 mm respectively, and tapered web, widths were 150mm in the part near the flange and 91 mm in the far part. The examination was done by applying a load to the top of the T beam as shown in Figure (2-7). The specimens were bonded with external CFRP sheets for flexural strengthening. The webs were wrapped fully or partially with 1,2,3, or 4 layers of the CFRP sheets. Static test was obtained with specimens wrapped fully and partially layer of the CFRP sheets and those specimens were loaded regularly to failure while the Fatigue test was obtained with specimens fully wrapped. The fatigue loading was between (25 to 50) percent of the capacity control specimen and at the frequency of 1 HZ. The results of the test were as follows, effective externally CFRP sheets in improving fatigue and static testing of the RC T beams also concluded that the effective full wrapping technique more than the partial wrapping technique for increasing capacity.

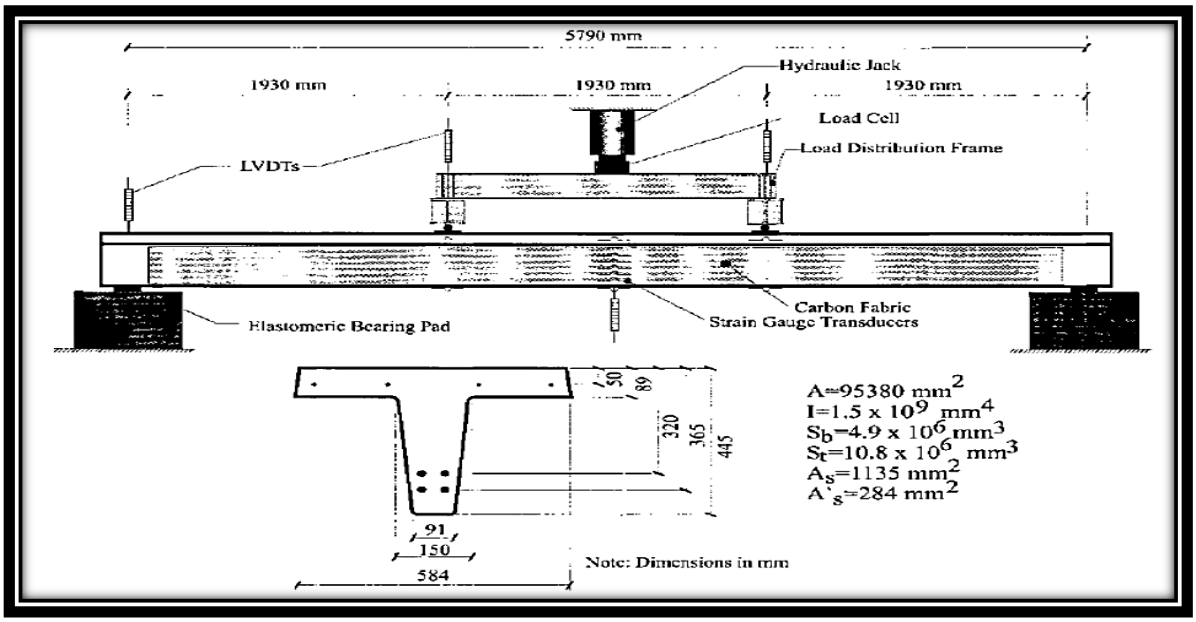

Figure (2-7) :Test setup and details of specimens [51]

Alagusundaramoorthy et al. (2003) [52], the authors conducted an experimental study whose purpose was to evaluate the effectiveness of the external bonding of the CFRP or carbon fiber fabric on the nine specimens strengthened with different layers of CFRP sheets and three specimens strengthened with different layers of anchored CFRP sheets. An analytical way depending on equilibrium forces and compatibility of deformations was found for the flexural behavior of RC beams strengthened by CFRP sheets and carbon fiber fabric. Comparisons between the experimental test results and the analytical results found that the flexural strength was increased by up to 58% on the RC beams strengthened with the anchored CFRP sheets.

Esfahani et al. (2007) [53] was shown through his experimental research the effect of the reinforcing bar ratio ρ of the longitudinal tensile reinforcement on the flexural strength of the strengthened specimens with varied the length, widths, and number of layers of the CFRP sheets in the different beams CFRP sheets. They concluded like previous studies, stiffness and flexural strength of the strengthened specimens increased compared to the control beams. Also, with the small (ρ) values the effect of CFRP sheets

in increasing the flexural strength of the specimens, when compared with maximum value (ρ max). The strengthened beams with great reinforcing bar ratio, near to the maximum value of (ρ max), the failure occurred with sufficient the ductility.

Thiemamn (2009) [54] presented the behavior of beam-to-girder connexion of an inverted-T bent cap beam the bridge using program (ABAQUS) FEM software. Developed an inverted-T bent cap with bridge analysis model, girder, bearing pads, and prestressing strands, and the slab with the reinforcing bars. A damage plasticity model was used, which is suitable to hold the correct behavior of the concrete under low confining pressures, and was conveyed to the concrete material. Monolithically model of the bearing pads to bent cap ledges. The prognosis of the damaged plasticity model worked fully in reservation the effects but was incapable of carefully capturing the tensile manner of the concrete under the flexure.

Yousif (2012) [55] did an experimental study about the behavior of beams strengthened with the (CFRP) sheets, where the loads were divergence in different situations. The CFRP sheets with (100x100x100) mm were bonded with epoxy in a U shape, and where put in the tension face and the web of RC beams to achieve their strengths and ductility. The effect of the CFRP sheets on the stiffness and strength of the RC beams is represented for different lengths of the CFRP sheets with different the distance from the center of the beams, which were increased in the length of the CFRP sheets according to the variety of the distance between two points load. Six beams were strengthened with the CFRP systems in six different lengths. The beams were tested with loaded to the failure. The results from the test were the modes of the failure were depended on the length of the CFRP sheets and loads divergence, when bonded the CFRP sheets to the tension face and web, that leads to an increase in the stiffness and strength and also, they found that

CFRP sheets can be used to increase strength against the load divergence and the stiffness of RC beams without leads to tragic brittle failures related to this the strengthening technique.

Hussein and Razzaq (2017) [56] tested nine prestressed inverted T beams under distribution load. The cross-section is shown in Figure (2-8). The purpose of the study was to study the prestressed inverted T beam with different retrofitting by CFRC sheets for possible application in building construction. The CFRP sheets were applied in compression and tension with three different thicknesses. The theoretical analysis also work, was depending on the coupling moment-curvature relations with the central finite difference formulation. Based on various retrofitting by CFRP sheets, the conclusions have developed an increase in loads capacity of prestressing inverted T beams retrofitting by CFRP sheets and an increase in effective CFRP retrofitting on both the compression and tension, and it most effective in reducing the deflection of the beam. The results also showed that retrofitting by CFRP sheets in prestressing inverted T beam, possible use or applied in the building structures.

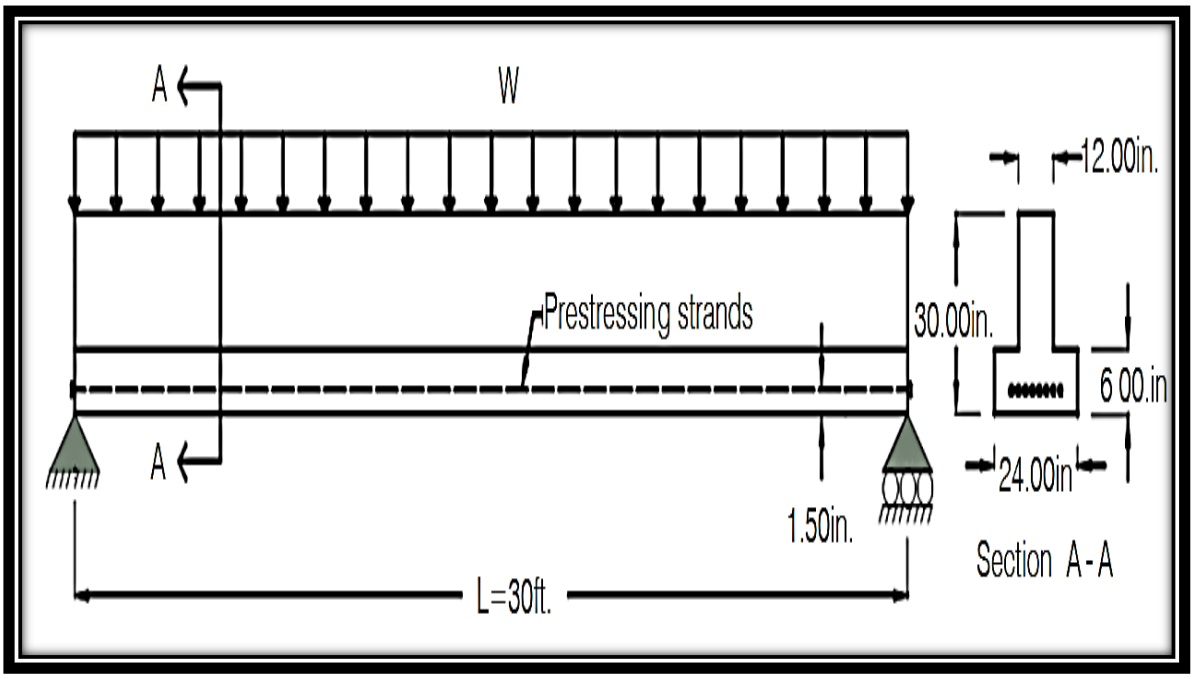

Figure (2-8): Details of beam cross section and the load [56]

Ayssar and Hani (2020) [57] investigated an experimental study about strengthening continuous RC beams. The experimental work was carried out on the 18 T beams, 6 were non-inverted T beams and 12 were inverted T beams. The various in this study were (a) CFRP widths (b) CFRP strengthening configurations with the equal area of the CFRP and (c) using multiple strips, one layer, and use multiple layers.

The investigation was to study these various effects on the ductility and ultimate load capacity of the strengthened RC beams. The main conclusions were :

- The ultimate load capacities for the non-inverted T beams strengthened by CFRP depending on the configuration and area of CFRP enhanced from 4% to 90% compared with control beam.
- When compared the beam with multiple layers of the CFRP and beam with single layer, the multiple layers were prefer due to enhanced the ultimate load capacity, strength, stiffness, and toughness of the strengthened beams.

For the inverted T beams that act negative bending (supports) in the continues beams, the main conclusion were:

- Depending on the configuration and area the CFRP sheets ,the loads were enhanced from 2% to 35% .
- When used multiple CFRP, the failure modes were desired compared with the single.
- When the width the CFRP to width beam ratio increased, that leads to increase the ultimate load and stiffness.

The analytical calculation also investigated and compared with the experimental results, they were very near.

2.4.2.2 Failure modes in RC beams with FRP plate or sheets

A series of experimental research was carried out in various years by the following researchers e.g**. Richie et al.(1991) [58], Saadatmanesh and Ehsani (1991) [59], Triantafillou and Plevris (1992) [60], Chajes et al. (1994) [61], Sharif et al. (1994) [62], Hefferman and Erki (1996) [63], Shahawy et al. (1996) [64], Takeda et al. (1996) [65], Arduini and Nanni (1997) [66], Malek et al. (1998) [67], Grace et al. (1998) [68], GangaRao and Vijay (1998) [69], Ross et al. (1999) [70], Bonacci and Maalej (2000) [71], Maalej and Bian (2001) [72], Nguyen et al. (2001) [73], Rahimi and Hutchinson (2001) [74]** to examine number of failure modes types observed in RC beams bonded with flexural strengthened with FRP sheets as shown in the Figure (2-9) which would be as follows:

1-) Flexural failure: that occur by crushing of the compressive concrete after or before yielding the tensile steel reinforcement.

2-) Rupture FRP failure: that occur after yielding tensile steel reinforcement.

3-) Cover delamination (shear delamination of concrete cover):that occur due to the crack at the end of FRP.

4-) Debonding failure:

4-a)Debonding FRP:that occur when debonding FRP from concrete material.

4-b)Interfacial debonding :that occur by flexural crack.

4-c)Interfacial debonding :that occur by flexural shear crack.

5-) Shear failure: that failure formation of shear crack at the end of plate.

The Malek et al.(1998) [67], Maalej and Bian (2001) [72], also, the author's **Ye (2001) [75] and Lau et al.(2001) [76]** studied analytically and experimentally the failure type (3) and (4-a) and showed that these types of failure occurred in cases the ends the FRP sheets are not completely anchored, and the failure types (4-b) and (4-c) were occurred by bond-slip

behavior between the concrete and FRP sheets. Also the authors **Sebastian (2001) [77] and Teng et al. (2003) [78]** showed that these types of failure occurred by change the reinforcing bar ratio in the neighborhood of the large bending moments, the corrosion of the longitudinal steel bars and also by increase the shear forces.

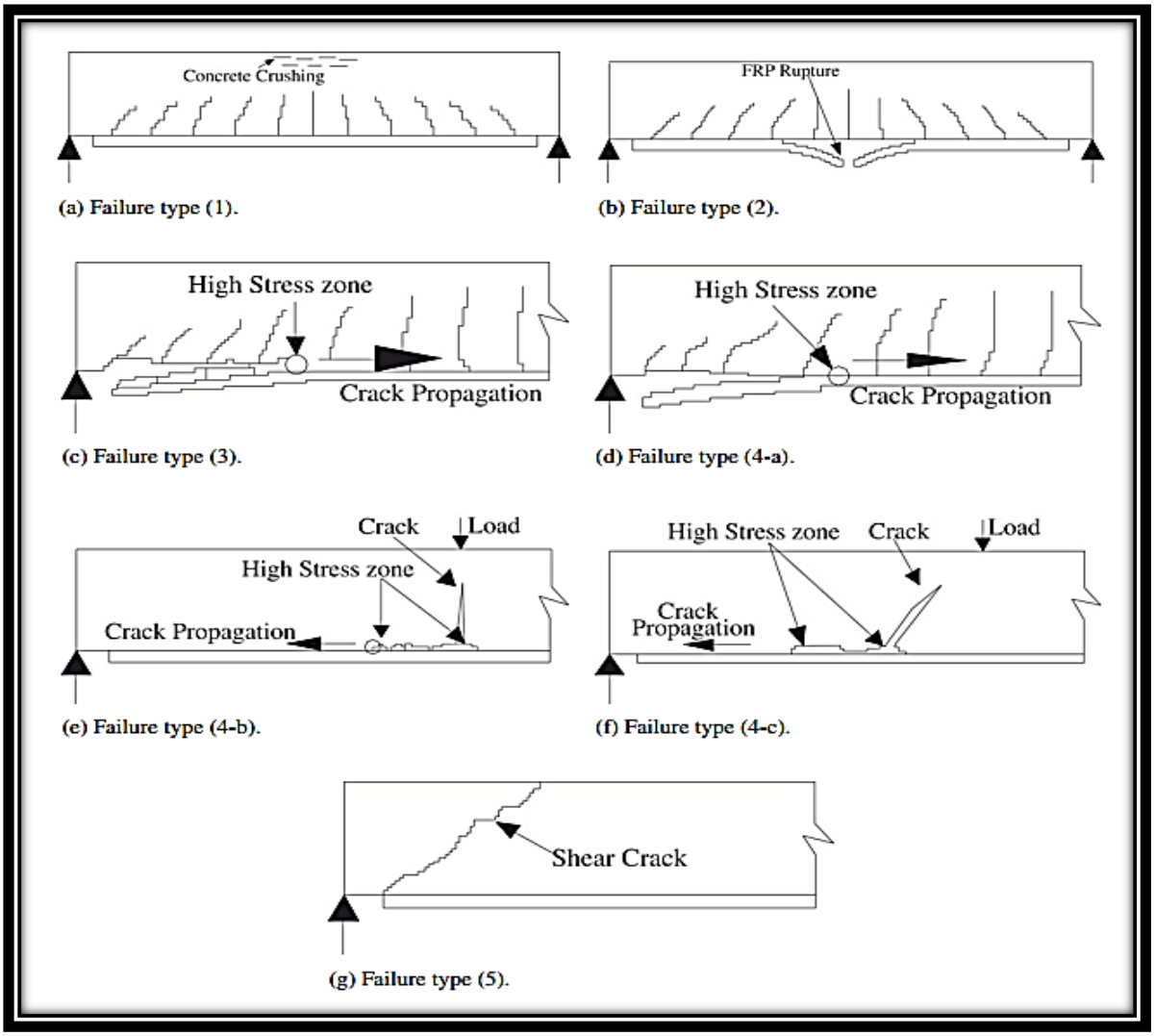

Figure (2-9): Failure modes of RC beams strengthened with FRP sheets

2.4.3 Historical Development of Steel Plate

The steel plate materials were used for the strengthening and repairing of RC structures. This technique is effective for increasing the flexural and shear capacity of RC beams. This technique was investigated early and started in the year the 1960s. The development of use steel plate

strengthened for the purpose of strengthening structures such as bridges and buildings in various countries of the world such as Belgium, France, Japan, Poland, South Africa, Switzerland and the United Kingdom **[79]**.

2.4.3.1 : Experimental and Analytical studies of RC with Retrofitting by EBR (Steel Plate) in Flexural member

Adhikary and Mutsuyoshi (2002) [80] investigated the theory study about strengthening flexural RC beams with epoxy-bonded steel plate, by using the new FEM capable of expecting the strengthened RC beams depending on the development of the various failure modes. The conclusion is that assumption of the perfect bond between the steel plate and RC beams leads to wrong results and cannot use in all cases of the strengthening beams with externally bonded epoxy steel plate, only can be used the perfect bonded when the steel plate was enough long and near from support. When the steel plate was short and reduce at a large distance from support, the failure modes were changed from steel plate yielding to steel plate debonding, while the steel plate was long and extended to a near distance from support or reduce at distance very near from support, the debonding failure was minimized. When the steel plate was thicker, the steel plate was a failure in small loads by debonding failure while the steel plate was a failure in large loads in case the yielding steel plate failed. The anchorage by the bolts did not prevent the full failure modes change from the plate yielding to the plate debonding, it only delay the debonding failure.

Jumaat et al. (2008) [81] investigated the experimental work consisting of four rectangle cross-section beams. One of them represented the control beam and the other beams represented strengthened beams with steel plates. One of the strengthened beams was strengthened without end anchorage, while the other two strengthened beams were strengthened with anchored

using L and U shapes. They found from experimental results that each strengthened beams were given failure loads and cracking loads higher than the control beam and less deflection, strain, and crack width also than from the control beam, and it gave a better crack mode compared with the control beam. The beams with end anchored were given better failure loads compared with strengthened beams without end anchored. The L shape of the end anchored beam compared with the U shaped gave a better execution.

Rakgate and Dundu (2018) [82] presented experimental research of 23 flexural behavior rectangular RC beams, 6 beams in group 1 where one beam represents the control beam, and 17 beams in group 2 where two beams represent control beams, strengthened in the flexural by externally epoxy-bonded steel plates, where the ratio of width to thickness was varied. The group 1, the width of the steel plate varied from 75-175 mm and the increment was 25 mm, while in group 2, the thickness of the steel plate varied. They found that compared with the control beams, the flexural stiffness increased in the case of beams with externally steel plate, also increased the cracking load and decreased the crack width and deflection, also found that the ratio of the width to the thickness as low as 12.5 of steel plate can enhance flexural yielding and wide ductility in the strengthened beams.

2.4.4 Experimental and Analytical studies of RC with Retrofitting (Strengthening with CFRP or Steel Plate)

Jumaat and Alam (2008) [83] tested three RC beams, the first beam was represented the control beam (un strengthened beam), strengthened the second beam with externally steel plate, while the third beam was used the externally CFRP in strengthening. The purpose from this experimental study was compared between the flexural strengthened by externally (CFRP and

steel plate), The details the beams and the strengthening as shown in the Figure (2-10). The results of this the study were :

- ❖ The beam strengthened with CFRP was gave the failure loads a little higher of the beam strengthened with steel plate. The failure was by separation the concrete cover.
- ❖ The beam strengthened with steel plate gave higher cracking load and less strains with concrete and steel reinforcement and less deflection. Also less by crack widths, when compared with the beam strengthened with CFRP. The failure was by debonding the end plate followed by separation the concrete cover.

The analytical study also presented on the three RC beams by using finite element modeling. The analytical results and the experimental results were corresponded.

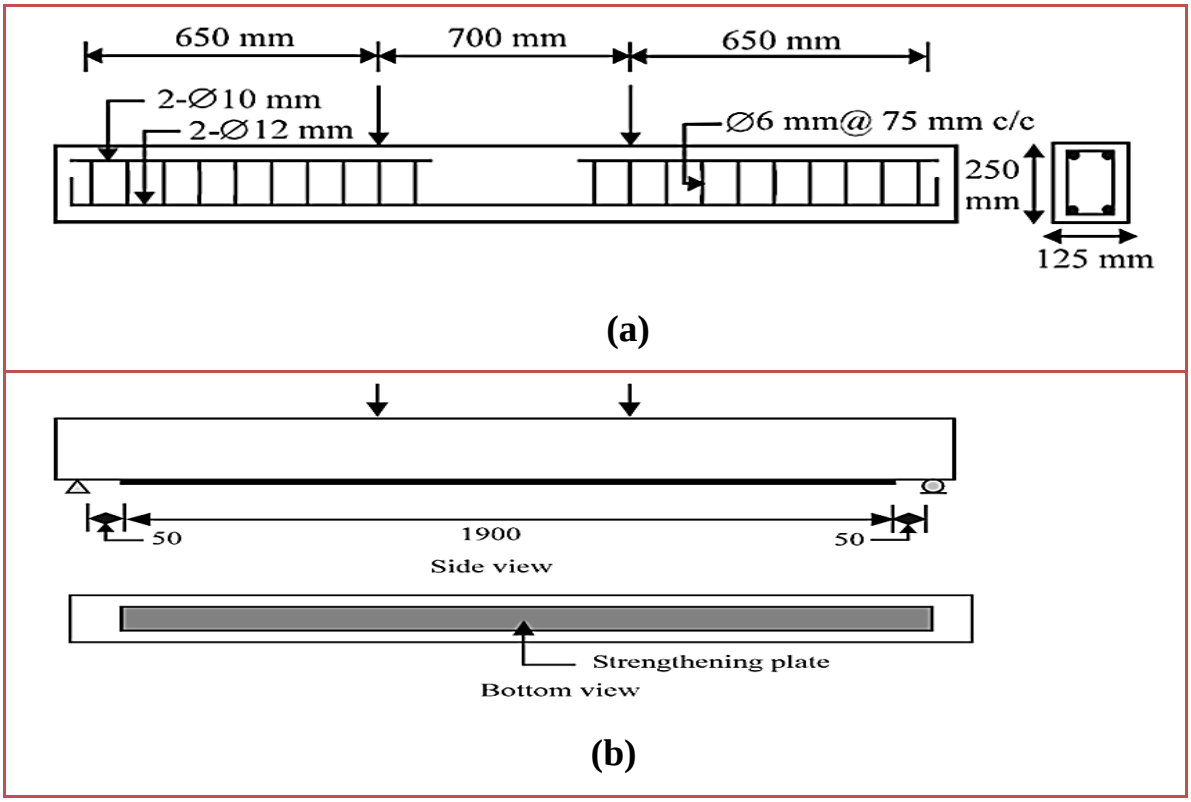

Figure (2-10) [83]:
(a) Details of the RC beam
(b) Details of the strengthened RC beam

Also, the experimental study was conducted in the year **(2018)** by authors **(Ercan et al.) [84]**, on seven beams, one of them represented the control beam and other beams were, three of them were flexural retrofitting by CFRP sheets and the other three were flexural retrofitting by steel plates. This study examined the effectiveness of strengthening by epoxy CFRP sheets and bolted steel plates on the flexural RC beam, and for comparing between the retrofitting by the CFRP and the retrofitting by the steel plate. They concluded from the results of an experimental test that the role of the CFRP sheets in flexural retrofitting RC beams was preferable to the role of steel plates. Also, the beams that were strengthened in flexural were subject to shear failure, which indicates that the specimens had a flexural strength that was increased.

Also, the authors conducted the analytical study by using the ATENA program software (Finite Element Methods (FEM)), and prepared the three-dimensional modeling of unstrengthening and strengthening RC beams. Analytical results were given an indicator that the strengthened RC beams had better moment capacity, The shear failure, however, was evident. Although strengthened specimens were exposed to the shear failure, failure was not brittle.

2.4.5 Experimental and Analytical studies of RC with Retrofitting (Repairing with CFRP or Steel Plate)

Hussian et al. (1995) [85] investigated an experimental program that deals with the repair technique by bonding to the steel plate. The repair process for the RC beams by bonding to a steel plate using different thicknesses without and with end anchorages was carried out after loading the RC beams to 85% of the ultimate load capacity. They concluded that the

repaired beams were given a higher strength than the reference beams. The failure pattern changed from the flexural to the permanent failure when the thickness of the plate increased due to rupture of the plate causing a decrease in ductility. The anchoraging bolts did not prevent permanent failure, but it reduced the yield ultimate strength, and it also improved ductility.

Benjeddou et al. (2007) [86] tested three groups of the eight beams, group one represented two control specimens, group two represented the beam was reinforced directly by using CFRP by bonding with epoxy in the tensile face and the beam was not damaged (not pre-cracked), group three represented the remaining damaged beams and then repaired by using different quantities of CFRP with various damage degree, the width of the CFRP was also various and various the concrete strength types. Table (2-3) was showed the different parameters for all the types of beams. Each of the examined specimens had the same dimensions, the same longitudinal reinforcement, and the same stirrups arrangement. The span length for the tested beams was (1800 mm). The length of CFRP for the purpose of all beams that were repaired was equaled (1700 mm). They concluded from the tested results; the rigidity and load capacity for each tested beams with damage degrees and then repaired were higher compared with the control beams, the failure modes were changed for the repaired beams from the interfacial debonding to the peeling off with increased the width of CFRP from (50 to 100) mm and for any types of the concrete. The CFRP was given a significant amount from load capacity and rigidity of the repaired beams. Similar, the same observations as the result of the experimental study were noted by the authors **(Gao et al. in 2004) [87]**, except that the criterion studied was the thickness of the CFRP layers.

Table (2-3): Details of the various parameters of each beam[86]

Beam reference	Concrete strength f_{c28} (MPa)	Designation	Damage degree (%)	Width of laminate (mm)
CB1	21	Control beam	–	–
CB2	38	Control beam	–	–
RB1	21	Reinforced	0	100
RB2	21	Repaired	80	100
RB3	21	Repaired	90	100
RB4	21	Repaired	100	100
RB5	21	Repaired	90	50
RB6	38	Repaired	90	100

Hawileh et al. (2011) [88] conducted an experimental study on three RC rectangular section beams for the purpose of knowing the behavior of retrofitted beams by CFRP and epoxy injections. The experimental program was as follows, the control primary beam (CB), primary beam +90% CFRP plate (B90P), and cracked beam + epoxy injections + 90% CFRP plate (B90PC). The same concrete mix was used in casting each of the beams. The pre-cracking strengthening was intended in beam (B90PC) by using the load to 35 kN until the flexural cracks, which were 0.03 mm in width and were seen with the telescope, and after obtaining the required crack width, the load was removed immediately. Compared the (CB), (B90P), and the (B90PC), results appear as shown in Figure (2-11) as the following increased the load capacity of beams when were used the epoxy injections more than utilized the bonded CFRP plate, also the Figure showed a reduction of the ductility with increased the strength of RC beams. The control primary beam (CB) failed at a load equal to 48 kN, while the other beams (B90PC) and (B90P) were carried out at the ultimate load failure of 71.6 kN and 61.7 kN respectively. Generally, the retrofitting beams gave effective results in strength compared with the control beam.

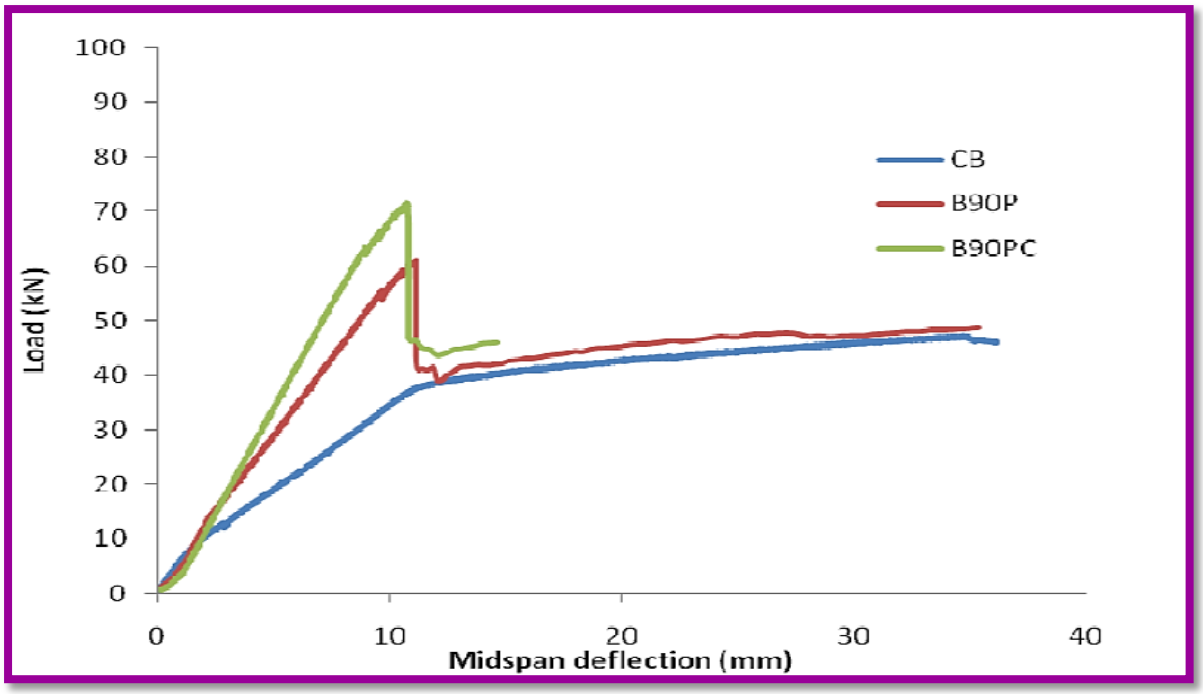

Figure (2-11): Load Response of the tested beams [88]

Ramachandary Murtha (2017) [89] investigated the experimental work consisting of two sets, set-1 represented the damaging stage where the RC beams were loaded to the load (70%) of yield load. Set-2 was the laminates stage where these damaged RC beams were repaired with different amounts of the CFRP laminates bonded externally to the RC beam's tension face and were tested for failure. The experimental results were concluded as follows, the ultimate load capacity for the strengthening beams were given 17% compared with the control beam when was the width and thickness of CFRP and damage degree equal to (100mm), (1.2 mm), (and 70%) respectively. The control beam failed in flexural but, when strengthened with CFRP, the failure mode would flexural shear failure and was more dangerous. When the strengthening was worked to the neutral axis of the beam, the increase in ultimate load capacity was not significant and the cost was higher three times when compared with the strengthening of the beam at the bottom face only by CFRP sheets. Also, the analytical work was carried

out and compared with experimental work for the purpose to utilize the ultimate load capacity. The analytical work was given a lower value compared with the experimental work.

In the same year, Sandle and Morgan [90] investigated experimental test of 12 RC beams with dimensions (175, 300 and 3200) mm wide, deep, and long respectively that consisted of three sets, set one consisting of two referenced beams not repaired with steel plates were tested to failure. Set two were pre-cracked to the serviceability load of the control beams and that were repaired by the steel plate which used epoxy in the bonded and consisted of the five beams, while set three were pre-cracked to 85% of the capacity of control beams and consisted of five beams. The varied parameter was the width of the steel plate that was used in the repair of beams, where the increment in width of the steel plate was equal to 25 mm, and the width varied from (75 to 175)mm. They found that carrying out the external steel plates with epoxy bonded on the repaired RC beams gave an increment in maximum load and stiffness and a decrease in the mid-span deflections. The increment in the strength and rigidity of the repaired RC beams were increased by increasing the ratio width to thickness of the steel plates.

Feng Ya et al.(2020) [91] determined effectiveness of the CFRP sheets for RC beams as the flexural repair through the experimental study on the ten RC beam, one control beam and nine RC beams with CFRP sheets under pre-damaged load equal to 40% or 80% of yield load of the control beam. Details dimensions and shape of the CFRP sheets and various reinforced of the RC beams, for the ten beams, there were six of them reinforced with two 12mm steel bars in the tension area; the remaining four beams were reinforced with two 16mm in the tension area and all the specimens of the RC beams in the pressure area were reinforced with 10mm steel bar as

shown in the Figure (2-12). Two types of failure modes for repaired beams with CFRP sheets under pre-damaged load such as fracture failure and debonding failure of the CFRP sheets. They were found that the flexural capacity of the repaired RC beams was increased with increased the CFRP layers or increased reinforcement ratio, while they were noted that it decreased with increased pre-damaged load. The deflection for the RC beams that repaired with CFRP decreases with the development of the CFRP layer or the ratio of the steel reinforcement or a decrease in the level of the pre-damage load.

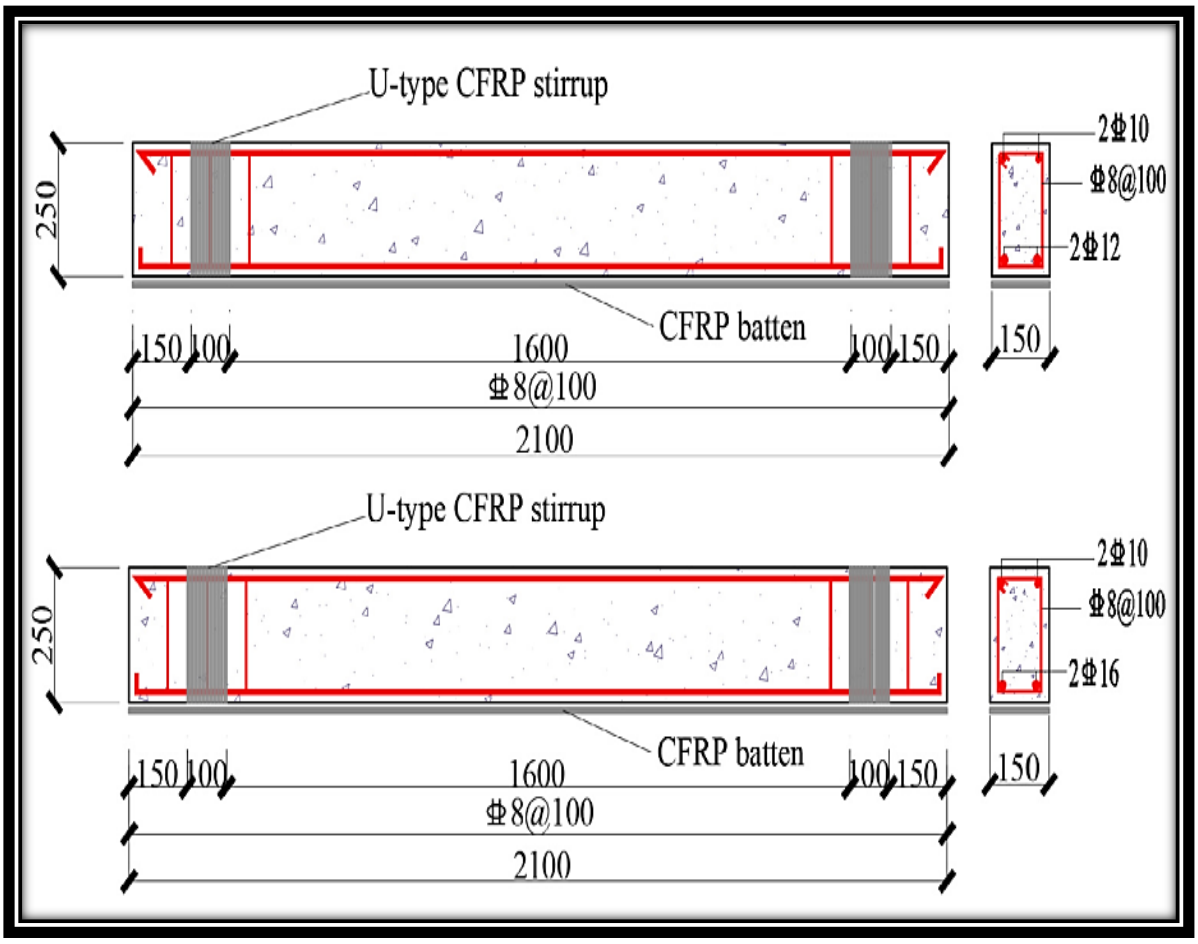

Figure (2-12): Details of the dimension ,reinforcement and steel plate[91]

2.5 Summary

From the previous studies (literature review) stipulated, it is clear that the use of the method of external bonded reinforcement (EBR) for the purpose of retrofitting (strengthening and repairing) the RC beams by means of CFRP sheets or steel plates have been an effective and advanced method so far. Several studies on retrofitting (strengthening and repairing) RC beams by using CFRP sheets or steel plates, but there are very few studies in all universities in the world about retrofitting (strengthening and repairing) an inverted T beams by using CFRP sheets or steel plates.

The following main points can be summery from the available literature review on reinforced concrete inverted T beams retrofitting by CFRP sheets or steel plates:

* The flexural strengthening concept is to increase and improve the stiffness and strength of RC flexural structures by bonding reinforcement to RC tensile surface members.

* With the small (ρ) values the effect of CFRP sheets in increasing the flexural strength of the specimens, when compared with maximum value (ρ max).

* When the width or length of the CFRP sheets or steel plates to width or length beam ratio increased, that leads to increase the ultimate load and stiffness, also increased the cracking load and decreased the crack width.

* The number of failure modes types observed in RC beams bonded with flexural strengthened with FRP sheets such as :
flexural failure, rupture FRP failure, cover delamination (shear delamination of concrete cover), end debonding FRP failure, interfacial debonding FRP failure, and shear failure.

* The rigidity and load capacity for each tested beams with damage degrees and then repaired with CFRP strips or steel plates were higher compared with the control beams.

*When the strengthening was worked to the neutral axis of the beam, the increase in ultimate load capacity was not significant and the cost was higher three times when compared with the strengthening of the beam at the bottom face only by CFRP sheets.

In the current study, in order to know the effective and appropriate length and width of the strengthening, which gives effective results in achieving the strength and stiffness required for the inverted T beams at the lowest cost. In addition to repairing the inverted T beam and comparing the results of strengthening with the repair and comparing the results of strengthening by CFRP sheets with the results of strengthening by using steel plates, as well as comparing the results of repair using CFRP sheets and results of repair using steel plates.

CHAPTER THREE

EXPERIMENTAL WORK

3.1 General

This chapter is an explanation of the proposed experimental work that shows the effect of carbon fiber reinforced polymer (CFRP) strips and steel plates on the structural behavior of strengthened and repaired RC inverted T beam specimens.

The experimental work consists of three parts; the first part includes details of the dimension of the inverted T beams, the arrangement of reinforcing steel, and the strengthening and repair system. The second part shows the properties of materials used in this research. In addition, many required tests are worked to obtain certain mechanical properties such as yield and ultimate strength for reinforcement steel and steel plate, compressive strength, flexural strength, and splitting tensile strength for concrete. Finally, the third part deals with the preparation and pouring of specimens and also, the instruments utilized in this test, and the method of testing the specimens.

3.2 Experimental Program

The experimental program includes 13 beam specimens consisting of three groups of specimens, in addition to control or reference specimen. All the specimens were represented by simply supported RC inverted T beams. Two groups consisting of ten beam specimens represented the strengthening system (Group One consists of 5 beams strengthened with CFRP strips, and the other 5 are represented by group two strengthened with steel plates). Group three consisted of two specimens representing the repair system (one is repaired with CFRP strips, and the other specimen is repaired with steel

plates). Figure (3-1) shows the 3D view for all the inverted T beam specimens.

All inverted T beam specimens had similar dimensions and flexural and shear reinforcement. Also, all the inverted T beam specimens had the cross section (**b**=250, **h**=250, **hf**=50, **bw**=150)mm. The total length was 1700mm and the beams were tested under two-point top loading with a clear span of 1500 mm. The ends of each beams expanded 100 mm behind a support's centerline and the steel bar had a 135˚ hook at all end. Concrete cover of 20 mm to prevent splitting failure. Details of the beam as shown in Figure (3-2).

All the beams are designed according to the specifications of the **(ACI-Code 318-19)** as shown in Appendix A. All specimens of the inverted T beams were designed to have more strength in shear to ensure flexural failure even after the strengthening. Also, all specimens were designed on the least amount of reinforcing steel to conform to the effect of the reinforcement represented by CFRP strips and steel plates.

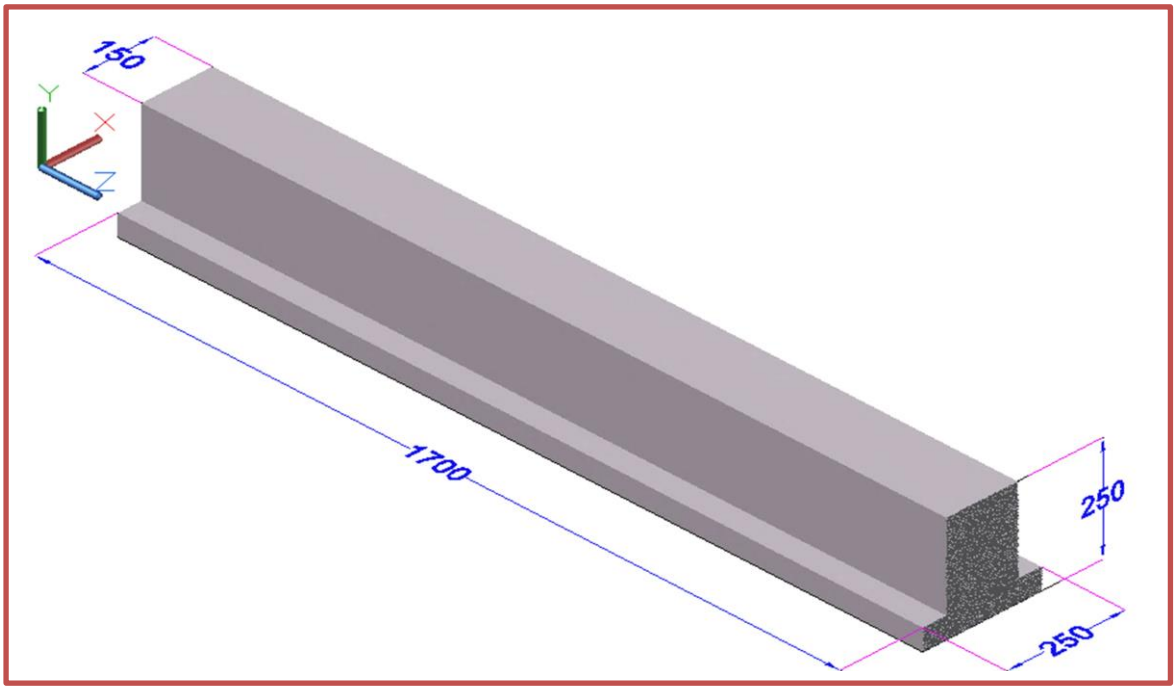

Figure (3-1): The 3D view of the inverted T beam specimen

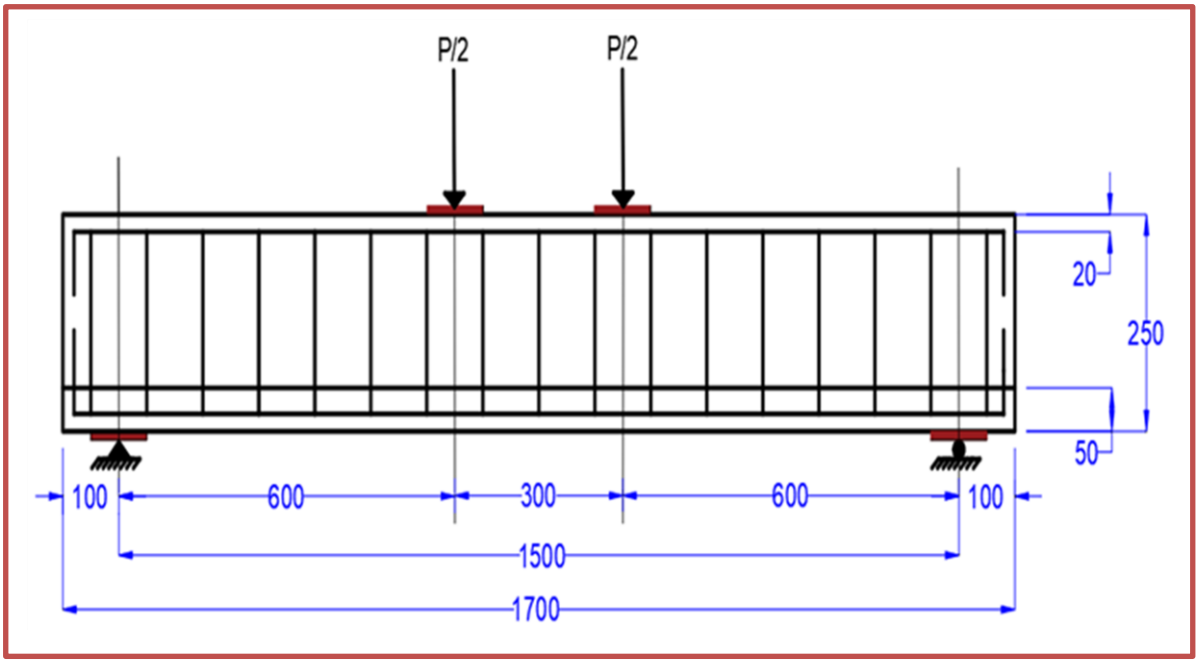

(a)

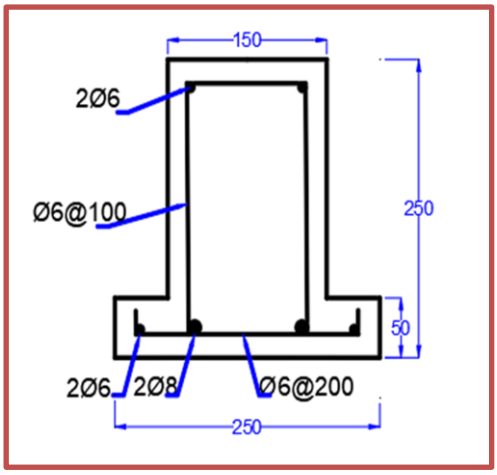

(b)

(a) Loading and supporting details of the beam

(b) Details of cross-sections of beams

Figure (3-2): Details of the beam (All the dimensions in mm)

Details, characteristics, and parameters investigates of the thirteen tested RC inverted T beams are shown in the Table (3-1).

Table (3-1):Details of the tested inverted T beams

NO.	Group No.	Beam Designation	Beam Type	No. CFRP Strips or Steel plates	Length CFRP Strips (mm) or Steel Plates (mm)	Total Width CFRP Strips (mm) or Steel Plates (mm)
1	--------	ITCC	Control	-----	--------	--------
2	Group One	ITF600	Group Strengthened With CFRP Strips	1	600	50
3		ITF900		1	900	50
4		ITF1200		1	1200	50
5		IT2F1200		2	1200	100
6		IT3F1200		3	1200	150
7	Group Two	ITS600	Group Strengthened With Steel Plates	1	600	50
8		ITS900		1	900	50
9		ITS1200		1	1200	50
10		IT2S1200		2	1200	100
11		IT3S1200		3	1200	150
12	Group Three	IT3FR1200	Group Repaired With CFRP strips OR Steel Plates	3	1200	150
13		IT3SR1200		3	1200	150

Note: The characterization of the specimens designation and their significance are found in Table (3-2).

Table (3-2): Significance of Specimens Designation

Specimens designation	Meanings
ITCC	I: Inverted, T: T-section type beam, CC: Concrete Control Reference or control.
ITF600, ITF900, ITF1200 ITS600, ITS900, ITS1200	I: Inverted, T: T-section type beam, F: carbon Fiber with lengths (600, 900 and 1200) mm. S: Steel plate Sheet with lengths (600, 900 and 1200) mm.
IT2F1200, IT3F1200 IT2S1200, IT3S1200	I: Inverted, T: T-section type beam, (2F and 3F): two strips and three strips of carbon fibers with length 1200 mm. (2S and 3S): two strips and three strips of Steel plate sheets with length 1200 mm.
IT3FR1200, IT3SR1200	I: Inverted, T: T-section type beam, (3FR and 3SR), (3FR): three strips of carbon Fiber that used in repairing process with length 1200mm, and (3SR): three strips of Steel plate sheet that used in repairing process with length 1200mm.

In this experimental work tested thirteen inverted T beams, the first beam specimen represents the control concrete beam which is reinforced by flexural and shear reinforcement without any CFRP strips or steel plates as shown in Figure (3-2). The remaining twelve beams were divided into three groups as follows:

Group one: consisted of five inverted T beams ITF600, ITF900, ITF1200, IT2F1200, and IT3F1200 to study the effect of strengthening inverted T beams with CFRP strips on the response for flexural capacity of inverted T beams with variable length and width of the CFRP strips.

Group two: consisted of five inverted T beams ITS600, ITS900, ITS1200, IT2S1200, and IT3S1200 which are tested to study the effect of strengthening inverted T beams with steel plates on the response for flexural capacity of inverted T beams with the constant thickness (0.8 mm) for all the beams and variable length and width of the steel plates.

Group three: consisted of two inverted T beams (IT3FR1200 and IT3SR1200) that were repaired by CFRP strips or steel plates after loading the inverted T beams to 60% of the ultimate load obtained for control inverted T beam ITCC, which were suggested and tested to find out the response of the inverted T beam to the repair technique using CFRP strips or steel plates and to know the difference in the flexural carrying capacity of the inverted T beams for (strengthened and repaired) technique.

Details of the three groups of inverted T beams are shown in Table (3-3).

Table (3-3): Details of three groups of inverted T beams (continue)

Cross Section	Bottom View
Group one and group two (Strengthening Teqnique)	
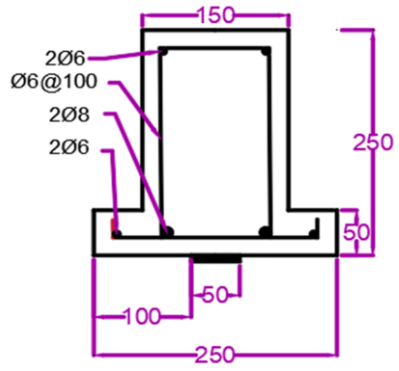	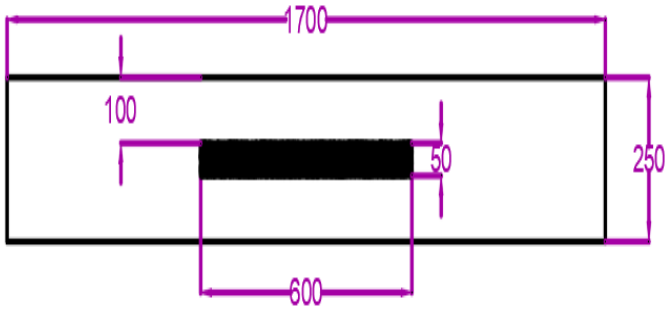
	ITF600 or ITS600

Table (3-3) : Details of three groups of inverted T beams (continue)

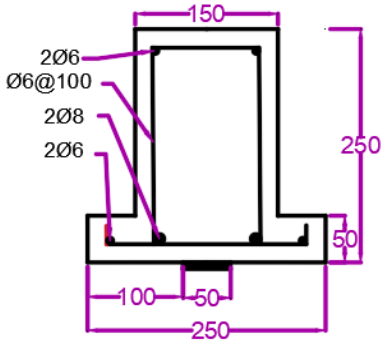	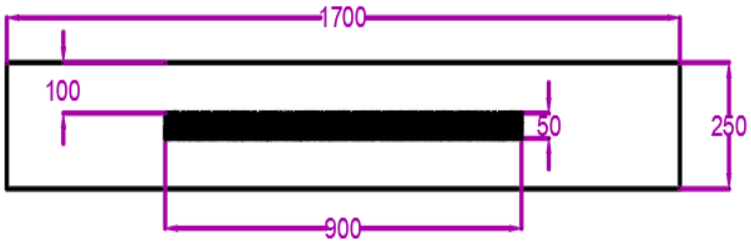 **ITF900 or ITS900**
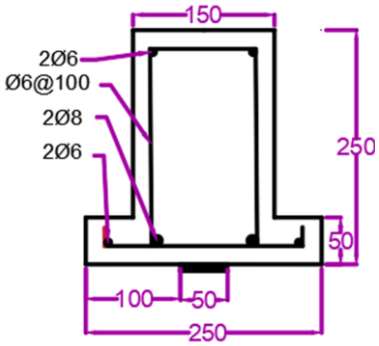	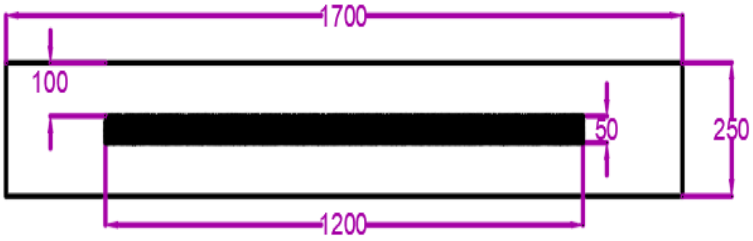 **ITF1200 or ITS1200**
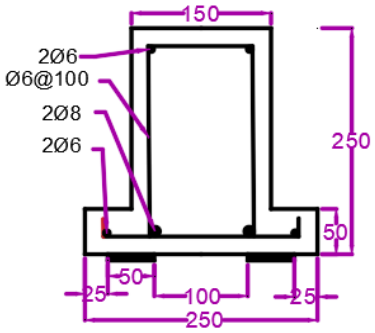	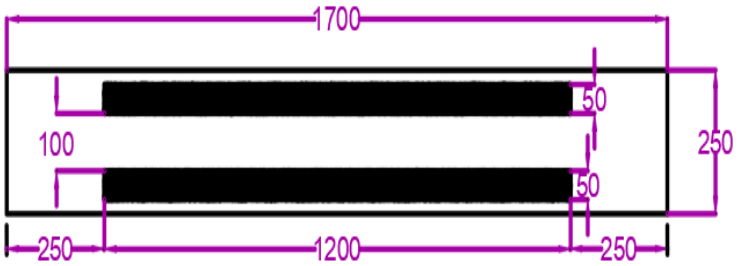 **IT2F1200 or IT2S1200**
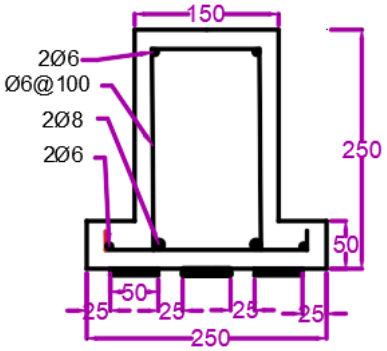	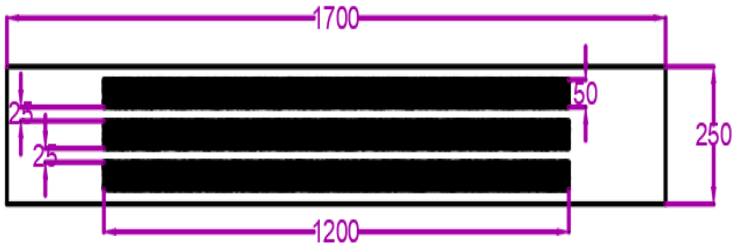 **IT3F1200 or IT3S1200**

Table (3-3): Details of three groups of inverted T beams (continued)

Group Three (Repair Teqnique)	
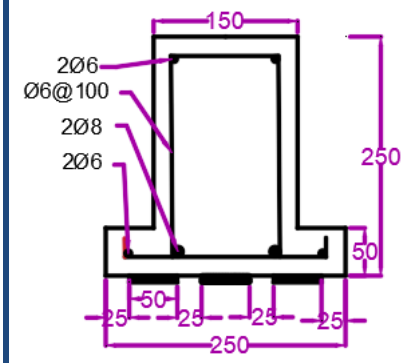	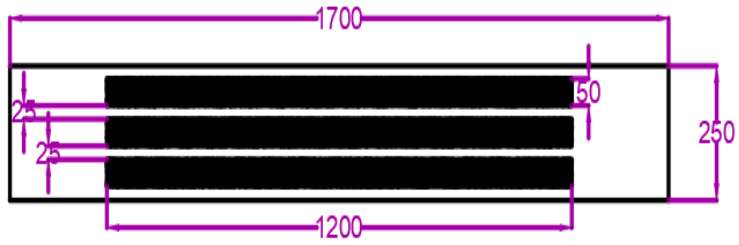 IT3FR1200 or IT3SR1200

3.3 Materials Properties

3.3.1 Cement

Ordinary Portland Cement (OPC) (type I) is used in casting each beams. The properties of cement used are conformed to the Iraqi specification limits (I.Q.S.)NO.5/1984 **[92]**.The chemical and physical properties of the ordinary Portland cement used are given in Table (3-4) and Table (3-5) respectively. For this cement, the physical and chemical properties have been tested in the material laboratory of the civil engineering department at Babylon University.

Table (3-4): Chemical analysis and main compounds of cement (continue)

Chemical Properties	Test Results(%)	Limits of Iraqi specification No.5/1984
Lime (CaO)	62.79	-
Silica (SiO_2)	20.58	-
Alumina (Al_2O_3)	5.6	-
Iron oxide (Fe_2O_3)	3.28	-
Magnesia (MgO)	2.79	≤ 5%

Table (3-4): Chemical analysis and main compounds of cement (continued)

Sulfate (SO_3)	**2.35**	**if C3A < 5% ≤ 2.5% if C3A > 5% ≤ 2.8%**
Loss on ignition (L.O.I.)	**1.94**	**≤ 4%**
Insoluble residue (I.R.)	**1.00**	**≤ 1.5%**
Lime saturation factor (L.S.F.)	**0.9**	**0.66-1.02**
Main Compounds (Bogue's Equation)		
Tricalcium Silicate (C_3S)	**50.12**	**-**
Dicalcium Silicate (C_2S)	**21.26**	**-**
Tricalcium Aluminate (C_3A)	**9.29**	**-**
Tetracalcium Aluminoferrite (C_4AF)	**9.98**	**-**

Table (3-5): Physical Properties of cement

Physical Properties	Test Result	Iraqi specification No. 5/1984
Specific Surface Area (Blaine Method) M^2/Kg	**314**	**≥ 230**
Initial Setting (minute)	**121**	**≥ 45 min**
Final setting (minute)	**194**	**≤ 600 min**
Compressive Strength at:		
3 Days (MPa)	**20.8**	**≥ 15**
7 Days (MPa)	**27.06**	**≥ 23**

3.3.2 Sand (Fine-aggregate)

Natural locally obtainable sand is used. Sand is washed and cleaned several times with water and then left to dry before use. The mechanical and chemical properties of sand as shown in table (3-6). The sieve grading analysis result conformed to the Iraqi specification (I.Q.S) NO.45/1984 zone

(2) **[93]** as shown in Table (3-7). Fine aggregate is tested at the Material Laboratory of the civil engineering department at Babylon University.

Table (3-6) Mechanical and chemical properties for fine aggregate

Properties	Test results	IQ.S No. 45/1984 zone (2)
Specific gravity	2.63	-
Fineness modulus	2.68	-
Sulfate content (SO_3)%	0.344	≤ 0.5
Materials finer than sieve 75 µm %	3	≤ 5

Table (3-7): Grading of Fine Aggregate

No.	Sieve size (mm)	Passing %	Limit of Iraqi Specification No.45/1984, zone (2)
1	10	100	100
2	4.75	94.5	90-100
3	2.36	83.3	75-100
4	1.18	72.8	55-90
5	600 µm	42.7	35-59
6	300 µm	22.1	8-30
7	150 µm	6.5	0-10

3.3.3 Gravel (Coarse Aggregate)

The maximum size (14 mm) of the crushed gravel is used. Also the operation of washing and cleaning gravel with water several times is done before the gravel is used, after that the gravel is spread and leave it in the air to dry before it is used. The chemical and mechanical properties of the coarse aggregate as shown in Table (3-8). The sieve analysis results showed that the coarse grades conformed with the requirements of the Iraqi Specification (IQS) No. 45/1984 **[93]** as shown in Table (3-9).

Table (3-8): Chemical and Mechanical Properties of Coarse Aggregate

Properties	Test results	IQ.S No. 45/1984
Specific gravity	2.68	-
Sulfate content (SO3) %	0.06	≤ 0.1
Absorption %	0.65	-
Clay content %	0.4	≤ 2

Table (3-9): Sieve Analysis Results of Coarse Aggregate

No.	Sieve size (mm)	Passing %	
		Coarse Aggregate	Limit of Iraqi Specification No. 45/1984
1	19	100	100
2	14	96	95-100
3	10	46.6	8-50
4	5	5.1	0-10
5	2.36	0.2	-

3.3.4 Mixing Water

The specimens in this work are casting and curing by using the normal tap water.

3.3.5 Steel Reinforcing Bars

A tensile test was carried out two sizes (Ø8) and (Ø6) mm of Ukrainian steel reinforcing deformed bars that were used in each concrete specimen. The tensile test of the main bars was taking place in the materials laboratory at Babylon University according to the limits of (ASTM A615) **[94]**. The characteristics of steel reinforcing as shown in Table (3-10). The steel bars were checked by the digital machine as shown in the Plate (3-1).

Table (3-10): Testing results of steel Reinforcement

Nominal Diameter (mm)	Measured Diameter (mm)	Yield Stress* (MPa)	Ultimate Strength (MPa)	Elongation Ratio %	Modulus of Elasticity** (GPa)
6	5.7	420	520	7.4	200
8	7.9	523	694	10.34	200

*** Each value is an average of three specimens (each 40 cm length).**

**** Assumed value.**

Plate (3-1): Digital machine used for steel bars testing

3.3.6 Carbon Fiber Reinforced Polymer (CFRP) sheet

Sikawrap® 300C was used as externally reinforcement for strengthening and repairing of the inverted T beams in the flexural as shown in Plate (3-2). The properties of the CFRP used are shown in the product data sheet in the Appendix C.

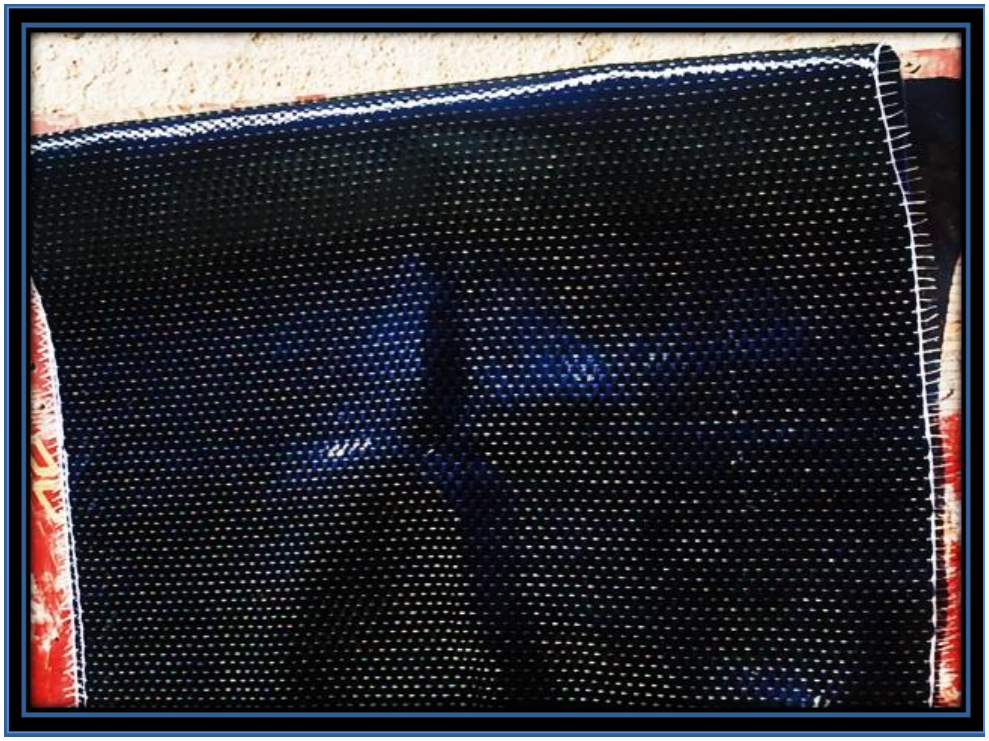

plate (3-2): CFRP sheet

3.3.7 Epoxy adhesive for CFRP sheet

Sikadur®-330 is the most proper adhesive substance for CFRP sheet as shown in the plate (3-3). The type of the adhesive is represented by two components. The compound A is represent the (white color) and the compound B represent the (black color). The mix ratio for the two compounds A:B is 4:1 respectively. The main properties of Sikadur®-330 are founded in the Appendix C.

Plate(3-3): Epoxy adhesive for CFRP strips

3.3.8 Steel plates

Steel plates used in this work have a thickness of (0.8 mm). By testing the two coupons to find out the actual yield and actual ultimate strength as shown in the Plate (3-4). All steel sheets used must have a minimum particular yield stress that is equal to or greater than (230) MPa (33 ksi) **[95]**. The "dog-bone" specimens model that works for tensile testing were of specific dimensions according to the specification ASTM (E8/E8M-13a) **[96]** as shown in Figure (3-3). The two coupon specimens were prepared by cutting using the computerized laser chopping machine as shown in the Plate (3-5). Failure in the coupon specimens occurs in the middle part as a result of high stresses in this part due to the clear and sufficient difference in width between the middle and final parts of the examined pieces. Tensile tests were conducted in the materials engineering laboratory at the University of Babylon. The test results of the two steel coupons are given in Table (3-11).

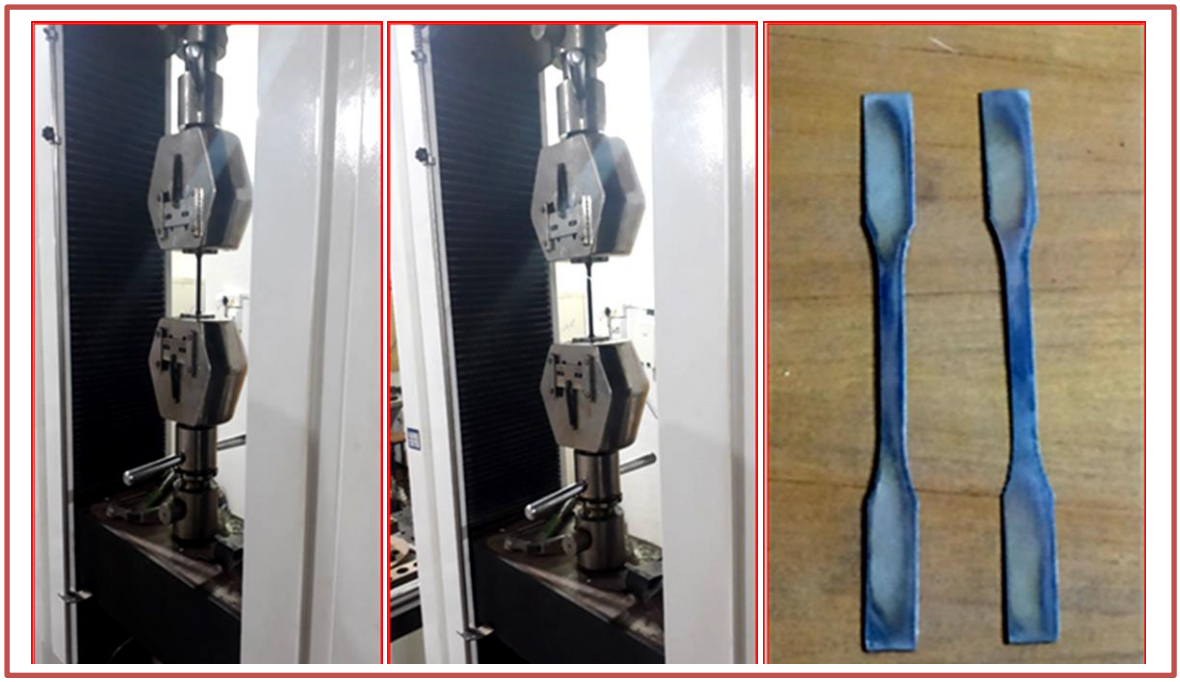

Plate (3-4): The machine used for tensile testing and the tested coupons

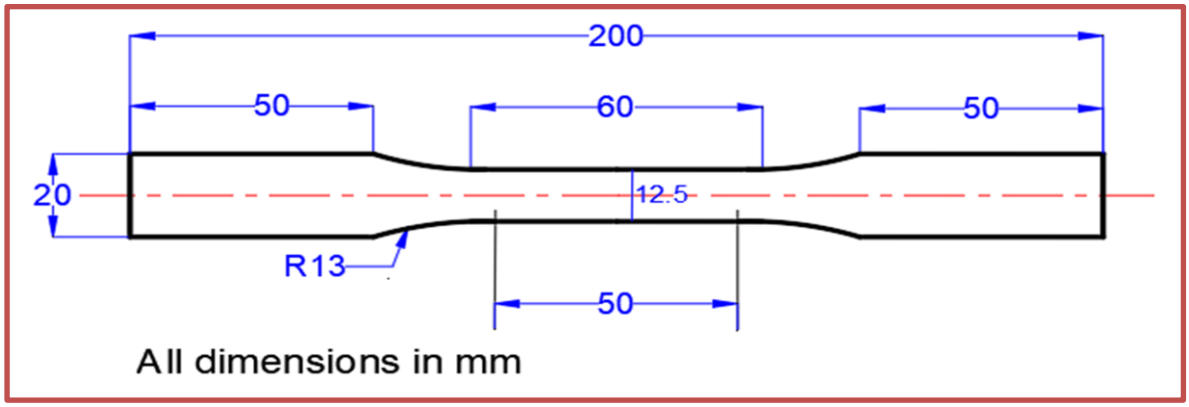

Figure (3-3): Dimensions of Standard Specimens According to ASTM (E8/E8M-13a)

Plate(3-5): computerized laser machine for chopping the coupons

Table (3-11): Tested Results of two steel coupons

Specimens No.	Yield Stress (MPa)	Ultimate Strength (MPa)
1	266.9	359.54
2	264.7	364.6
Average	265.8	362.07

3.3.9 Epoxy adhesive for Steel Sheet

Sikadur®-31 CF Slow is the most proper adhesive substance for steel sheets as shown in the Plate (3-6). The type of adhesive is represented by two components. Compound A represents the (white color) and compound B represents the (black color). The mix ratio for the two compounds A: B is 2:1 respectively. The main properties of the Sikadur®-31 CF Slow are founded in Appendix C.

Plate (3-6): Epoxy adhesive for Steel sheets

3.4 Preparation of Test Specimens

3.4.1 Concrete Mix Proportions

Several experimental mixtures were carried out in order to obtain the required compressive strength of 30 MPa after 28 days for normal-weight

concrete according to the recommendations (ACI 211.1-97) **[97]**. The quantities by weight for casting each beam's specimens were as follows (1 cement:1.73 sand:2.22 gravel). From the trail mix found that the mixture used in this study produces good workability and a uniform mixture of concrete without segregation. Table (3-12) shows the mixing ratios by weight for the purpose of the selected normal-weight concrete mix.

Table (3-12): Proportions of Concrete Mix

Materials	The selected concrete mix
Water/cement ratio	**0.49**
Water (kg/m^3)	**207**
Cement (kg/m^3)	**423**
Fine aggregate (kg/m^3)	**732**
Coarse aggregate (kg/m^3)	**934**

3.4.2 Formwork Fabrication and Reinforcement Cages

13 molds of plywood formworks were fabricated. The molds were made as a T-section with the internal dimensions of 250mm total height, 250mm width of the flange, 150mm width of the web and its height is 200mm, 50mm height of the flange, and 1700mm total length of the beam as shown in the Plate (3-7). The deformed steel reinforcement is utilized to make the reinforcement cages for all inverted T beams. Two sizes were used for each concrete specimen. Bars of the size (Ø8) and (Ø6) were used, (Ø8) was used as the main reinforcement for the flange, the bar of size (Ø6) was used as the main reinforcement for the flange and for top reinforcement, and as stirrups to resists the shear force. Plate (3-8) shows the shape reinforcement bars used in this experimental work. After completing the preparation of the wooden molds, the reinforcement cage is carefully placed inside the wooden molds while achieving the required cover by using plastic spacers on the

sides and the bottom in order for the mold to be ready to cast as shown in the Plate (3-7).

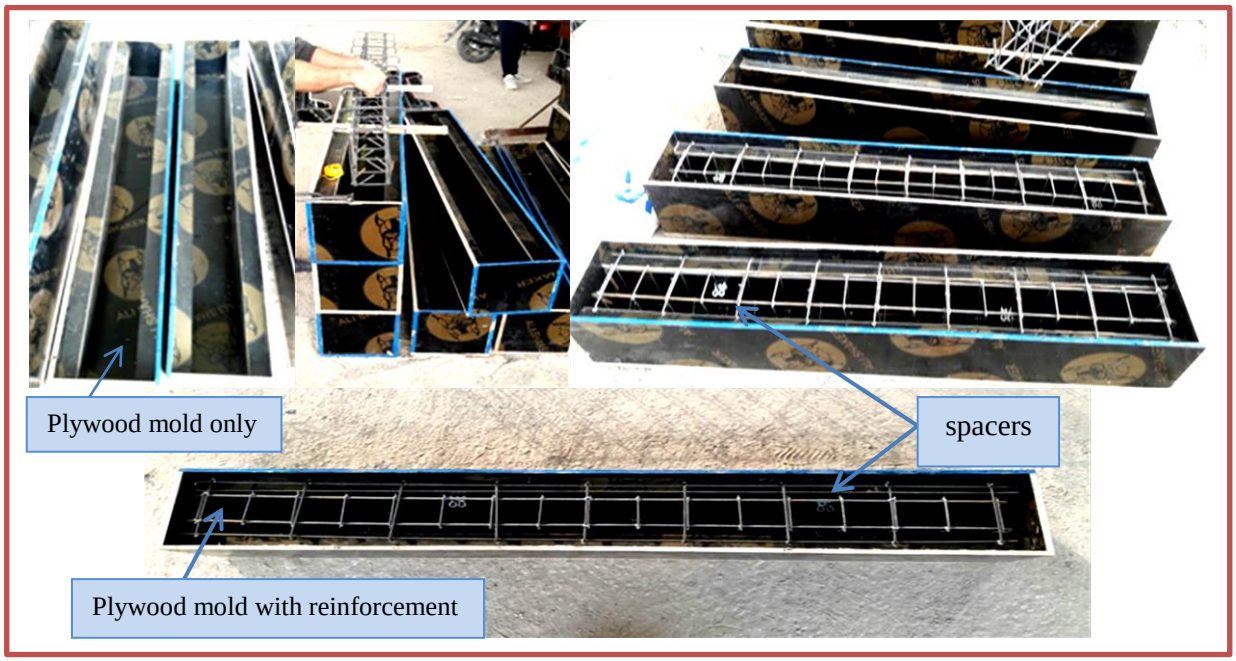

Plate (3-7):Plywood formworks and Reinforcement cages in formworks

Plate(3-8):The shape of reinforcement bars used in this experimental work

3.4.3 Concrete Casting and Curing

Thirteen beam specimens were poured and then cured under the laboratory conditions of the civil engineering department at the University of Babylon. Also, standard specimens such as (cylinders, cubes, and prisms) were casted with dimensions (300x150) ,(150x150x150) and (100x100x400)

respectively. The method of pouring and curing specimens is explained in the following points below:

- At first, the wooden molds of the beam specimens are lubricated before placing the reinforcing iron cage or casting the specimens, as well as the (cylinders, cubes and prism) molds are lubricated before placing the concrete in the molds.
- After that, the reinforcing iron cage is placed inside the wooden molds, while adjusting the side and bottom required cover accurately by using plastic spacers so that the iron cage does not move and remains stable after placing the concrete on it.
- Concrete was poured into the wooden molds on two layers, and each layer was stacked using a mechanical vibrator that had a metal rod with a diameter of 50mm for a period of 5 seconds. As well as for pouring specimens of (cylinders, cubes and prisms), they were filled with concrete on three layers and each layer stacked twenty five blow using a steel bar. For all specimen, a hand trowel is used to level the concrete face.
- After 24 hours of casting, the molds are removed from the specimens. After that, wet burlap bags are placed on top of the beams, and then plastic sheets are placed over them in order to prevent water evaporation from the beams during the treatment days. During the curing period, the burlap bags are monitored and remain wet throughout the curing period until the end of the 28 days. Likewise for cylinders, cubes and prisms, they are placed in water tanks and kept wet, according to the standard specifications. After the 28 days are over, they are taken out of the water and then tested. After the curing period for beam specimens, the concrete surface are painted in white, print the symbols and hang them on them, and then prepare them for testing. Plate (3-9) show the casting, curing and painting stages.

Plate(3-9): casting, curing and painting stages

3.4.4 Surface Preparation

The most important portion of any retrofitting application is a bond between the surface to which the steel plates or CFRP strips are to be attached. The appropriate bond is achieved when the force is effectively

transferred from the structural member to the steel plates or CFRP. Before placing steel plate or CFRP on the bottom of the surface of the beam, the concrete surface of the beam is ground by using an electric manual grinder in order to obtain the appropriate surface for pasting, clean the surface free of all dirt and pollutants such as dust and cement as shown in the Plate (3-10).

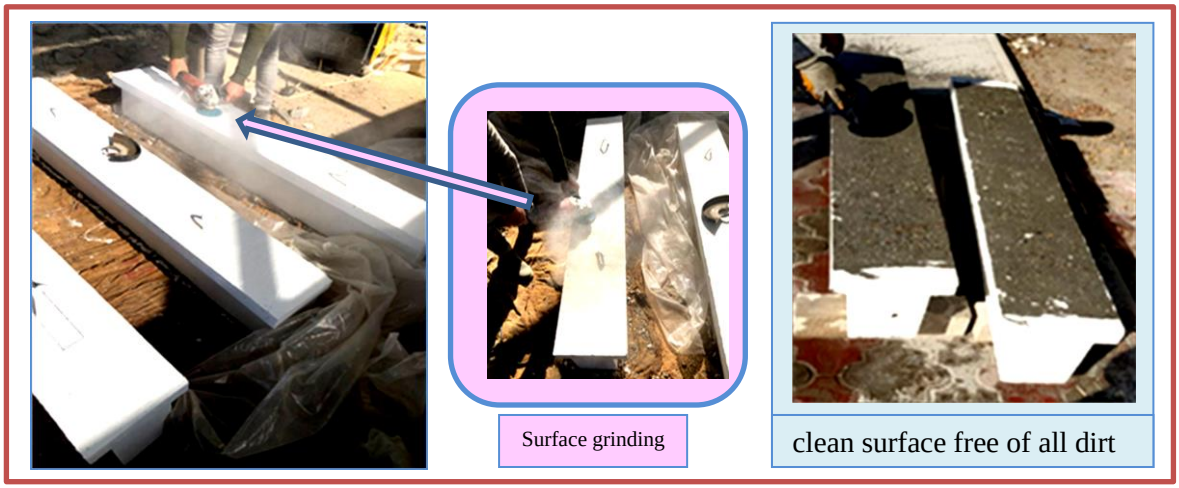

Plate (3-10): Concrete surface preparation

3.4.5 Retrofitting by Application of CFRP Composites or Steel Plates

3.4.5.1 Strengthening by Application of CFRP Composites or Steel Plates:

3.4.5.1.1 Strengthening by Application of CFRP Composites

External strengthening follows the manufacturer's recommended procedure which is described in the following steps :

- At the beginning, the CFRP was cut into the wanted length and widths. Then, before installing the CFRP on the surface of the beam, the surface of the beam is cleaned to remove any dust, dirt, oils or any kind of pollutants stuck on it.
- Mixing the two parts epoxy (Sikadur-330) adhesive (part A:white color and part B:black color) together with proportions (4:1)

respectively, until a homogenous grey color is obtained, then the epoxy is shed on the surface of the beam and on the CFRP sheet with a thickness of 1.5 mm.

- Put the CFRP strips on concrete surface of the beam, which was previously covered with epoxy, and compress it sufficiently with a rubber cylinder to install it in an exact and correct manner so that the excess epoxy is released on the sides of the sheets and the air behind the CFRP sheets is extracted, and then the excess epoxy is removed on the sides of the CFRP sheets. Plate (3-11) shows the steps of installing the CFRP strips on the RC beams.

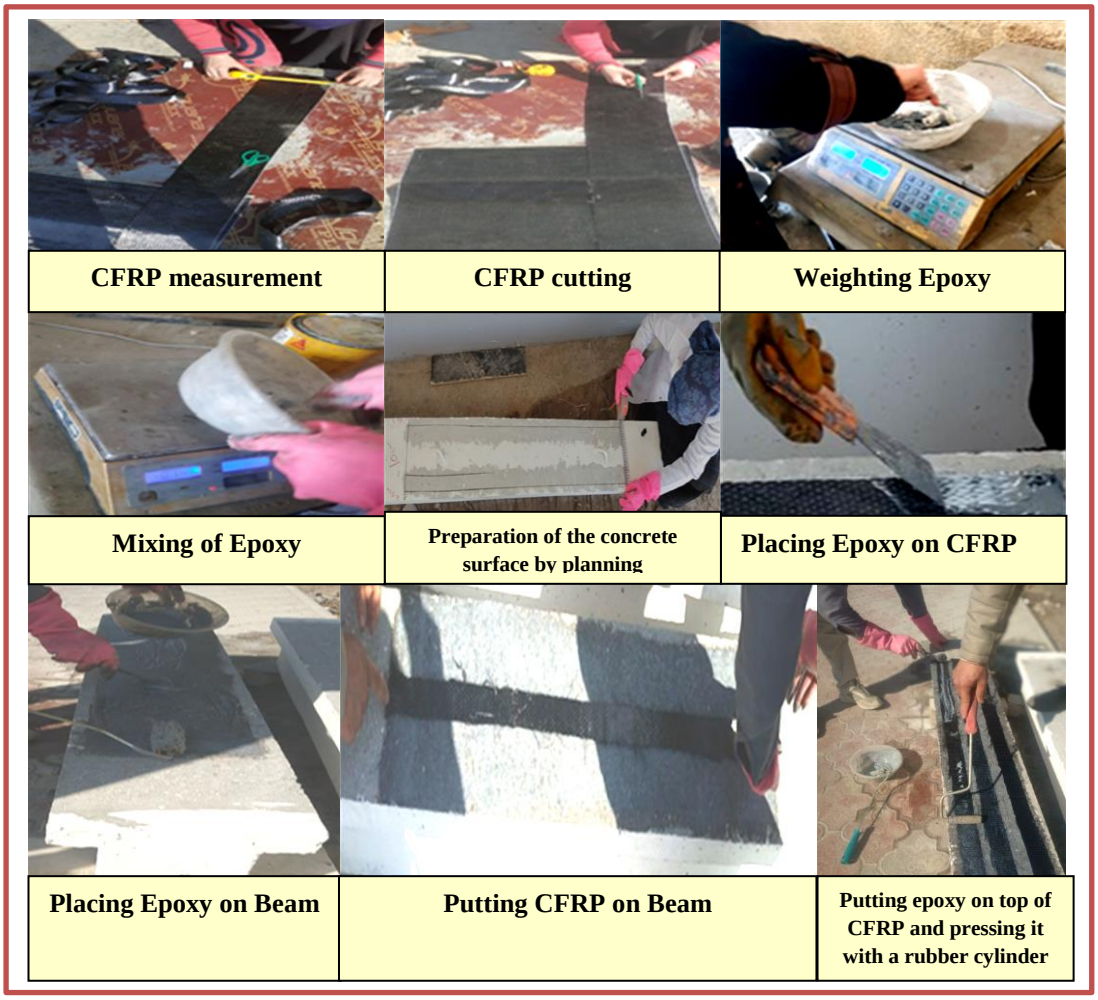

Plate (3-11): Steps of installing the CFRP strips on the RC beams

3.4.5.1.2 Strengthening by Application of Steel Plates

External strengthening by using steel plate is explained in the following steps:

- At the beginning, the steel plates was cut by using a computerized laser chopping machine into the wanted length and widths. Then, before installing the steel plates, the surface of the beam is roughened with X-shaped marks at an angle of approximately 45º, in order to increase the adhesion of the epoxy to the concrete surface and to increase the bonding between surface, epoxy and the steel plate, and then the surface of the beam is cleaned to remove any dust, dirt, oils or any kind of pollutants stuck on it.

- Mixing the two parts epoxy (Sikadur®-31) adhesive (part A:white color and part B:black color) together with proportions (2:1) respectively, until a homogenous grey color is obtained, then the epoxy is shed on the surface of beam with a thickness of about 2 mm.

- Put the steel plates on concrete surface of the beam, which was previously covered with epoxy, and compress it sufficiently by using an iron traps or something heavy to put on the steel plates to install it in an exact and correct manner so that the excess epoxy is released on the sides of the plates and the air behind the steel plates is extracted, and then the excess epoxy is removed on the sides of the steel plates and adjusted. Plate (3-12) shows some of the steps for installing the steel plates on the RC beams.

Cut steel plates by using the computerized laser chopping machine

The surface is roughened in an x shape and at an angle of approximately 45º

Mixing the Epoxy after weighing

Preparation of the concrete surface by planning

Placing Epoxy on Beam

Placing steel plates on the beam and press it

Plate(3-12): Steps of installing the steel plates on the RC beams

3.4.5.2 Repairing by Application of CFRP Composites or Steel Plates

The same steps are followed in the strengthening using CFRP strips or steel plates in terms of measuring the strips of CFRP or steel plates, cutting them to the required size, weighing the epoxy, and mixing the epoxy, but what happened in the repair was that the specimens were escalated to the examination device and a load of (60%) of the ultimate load was shed for the control beam on the specimens so that the appearance of cracks was observed. After that, the specimens are downloaded from the examination device, and begin to repair the specimens using CFRP strips or steel plates by preparing the concrete surface and then shedding epoxy on the CFRP strips or steel plates and on the concrete surface and then placing the CFRP strips or steel plates on the concrete surface and placing epoxy on top of them and pressing them and removing the excess of epoxy. Plate (3-13) shows surface preparation and repair of inverted specimens using CFRP strips or steel plates.

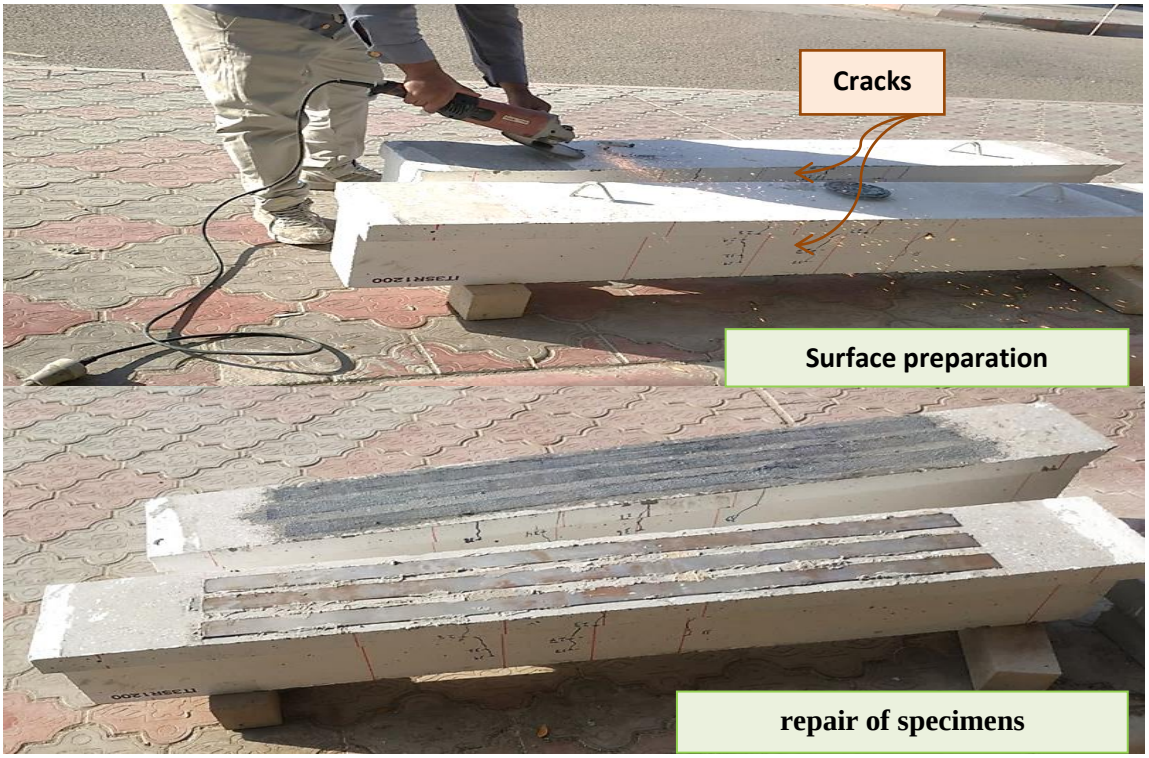

Plate (3-13): Surface preparation and repair of inverted T beam specimens using CFRP strips or steel plates

3.5 Instrumentation

The beam test devices were arranged and designed in order to check and monitor the properties of the structural behavior with each loading stage. The devices, during the test, measured load and deflection in three locations on the beam. also, the width of the crack is recorded during the loading process.

•As for the measurement of deflection in the beam specimens, three sensors called LVDT, which takes the applied pressure and translates it into deflection, were placed as follows: LVDT1 in the middle, LVDT2 under load and LVDT3 placed at a one-third of the beam length in order to obtain the correct shape of the deformation as shown in the Plate (3-14). The crack-meter device is used for all beam specimens to measure the width of the crack and works with an accuracy of 0.01 mm as shown in the Plate (3-14).

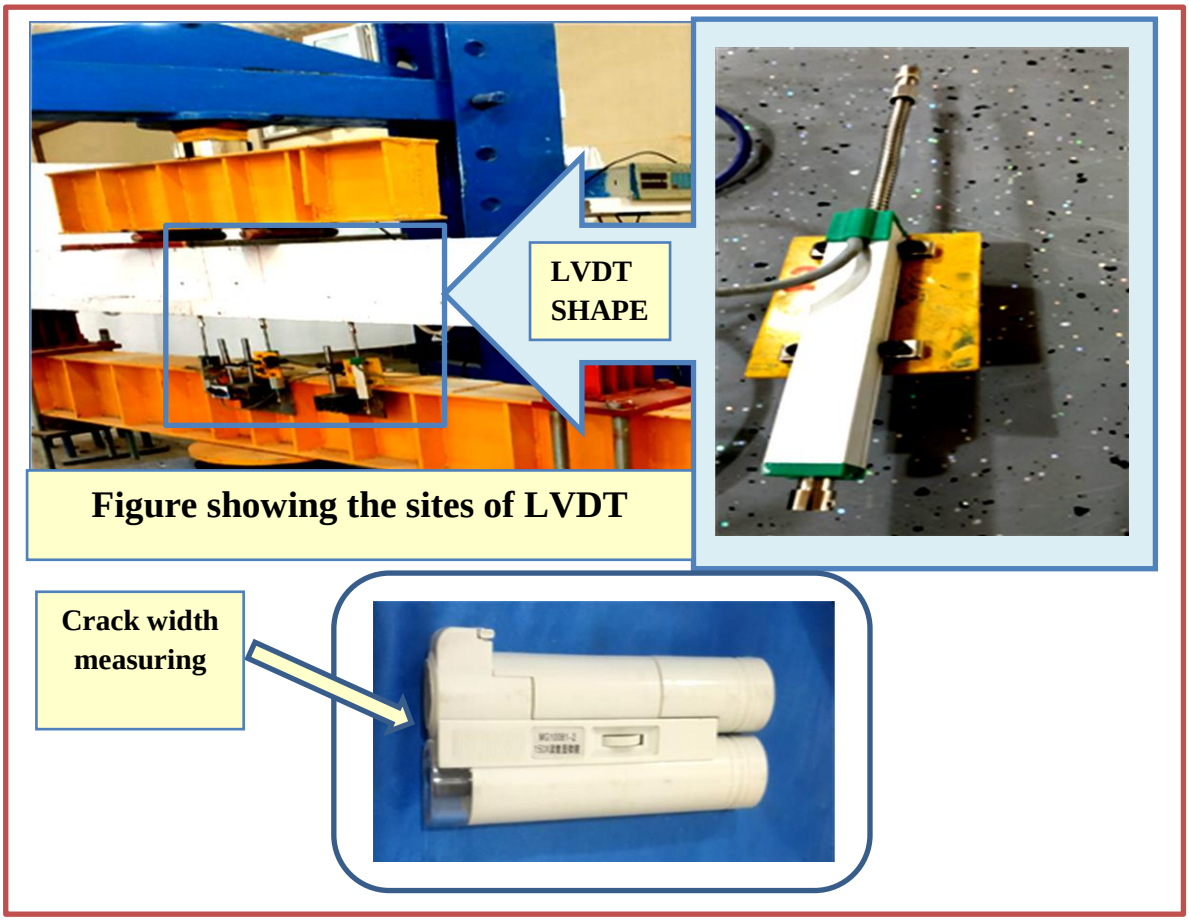

Plate (3-14): Instruments used in this testing

3.6 Test Setup and testing procedure

After curing, the beam specimens were transferred to the construction laboratory of the civil engineering department at the university of Babylon for testing. Thirteen simply supported RC beams were tested above 1500 mm span under the equal two concentrated static loads till failure by utilizing a capacity 600 kN hydraulic testing machine. At the loading points bearing plates with dimensions (500x100x10) mm and supports with dimensions (300x100x10) mm, were used to prevent local crushing of the concrete. The supports used for each beam were at one end a hinge was placed, and at the other end a roller was placed, Figure (3-4) shows the details of the supports used in this test.

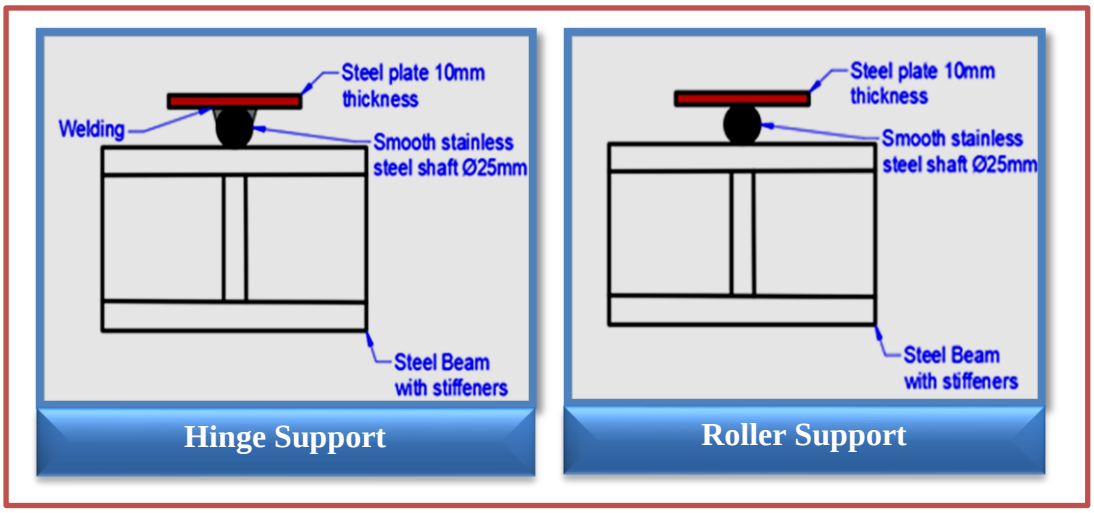

Figure (3-4): Details of the supports

The load applied to the examined beam was transmitted from the load cell and distributed by using the beam steel spread, Plate (3-15) shows details the machine used in this test.

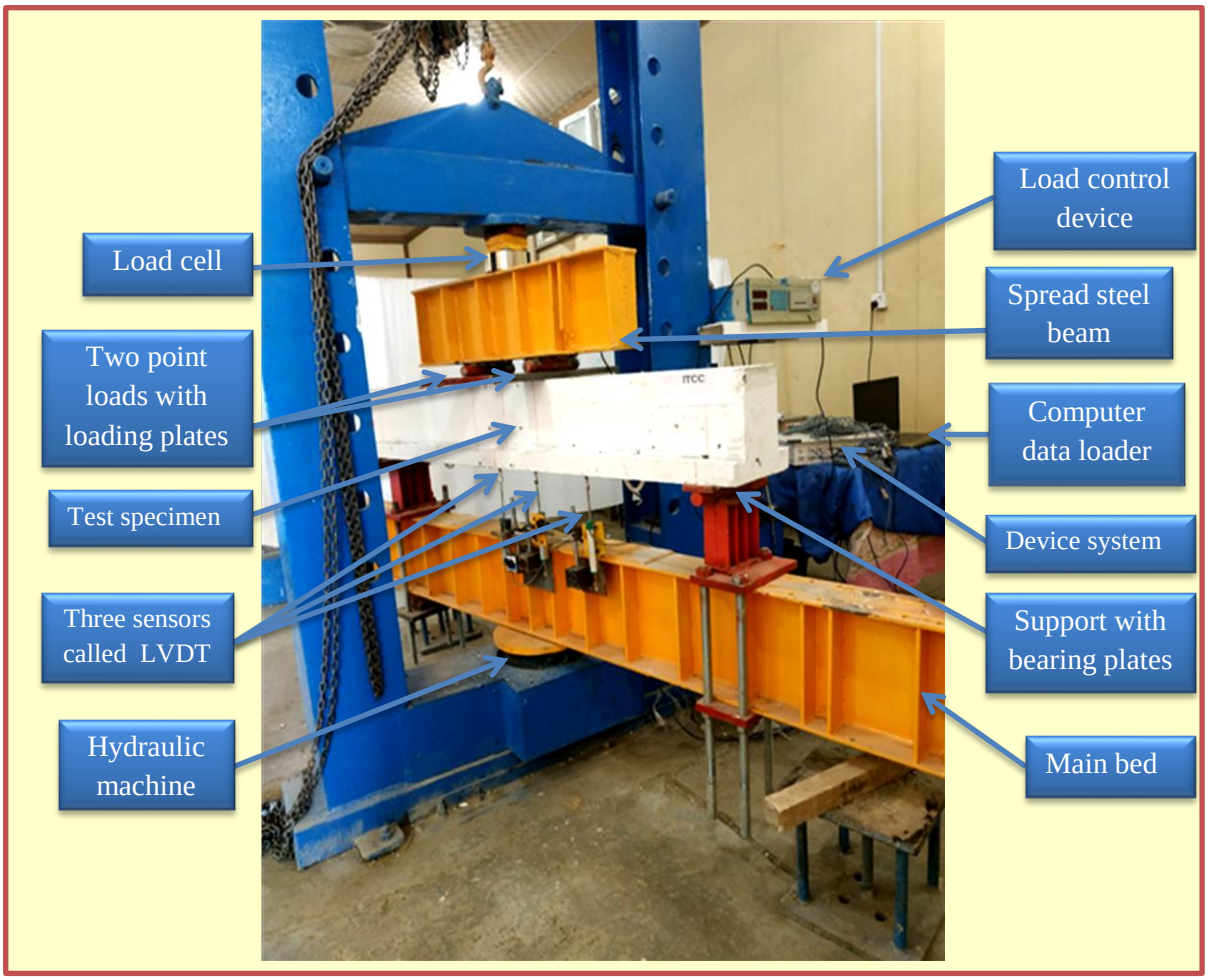

Plate (3-15) : Details of the flexural test machine

The beam specimens were painted white color before the test to watch the development of cracks that were determined by the use of colored pencils. For strengthening specimens, cracks were identified with colored pencils. As for repair specimens, cracks before repair were identified with a blue marker pencil, and after repair and test, cracks were identified with a red marker pencil to distinguish them because cracks before repair are different from cracks after repair. With the increase in the load, the first cracked load, ultimate load, and deflection, in addition to the crack widths are recorded during the test. After the test was completed, the failure mode was studied, and then pictures of the concrete beam were taken.

3.7 Tests of Fresh Concrete

3.7.1 Slump Test

The slump test of concrete was worked in accordance with (ASTM C143/C143M, 2015) **[98]**. The cone and a tamping rod represented equipment for the slump test. The dimensions of the cone were 30 cm in height, 10 cm in diameter at the top, and 20 cm in diameter at the bottom. The cone was filled in with concrete in three equal layers, all layer was stroked 25 times by a steel rod and then, the cone slowly lifted. The slump of concrete is measured by the difference in height between the top of the mold and to concrete level after the concrete is slumped down. Plate (3-16) shows the slump values ranged from (20-110) mm, as it is designed.

Plate (3-16): Slump test for fresh concrete

3.8 Mechanical Properties of the Hardened Concrete

3.8.1 The Test of Compressive Strength

The compressive strength test of the hardened concrete was specified according to (BS. 1881: Part 116:1989) **[99]**, (ASTM C 39-2016) **[100]**. The cubes of dimensions (150×150) mm and cylinders of dimensions (300×150) mm were tested in the construction laboratory of the Department of Civil Engineering at the University of Babylon by using a hydraulic compression machine of maximum capacity equal to (2000kN). Table (3-13) show the test results of the average of six cubes

and cylinders that were tested after 7 days and after 28 days and tested at the date of the testing beams to obtain the compressive strength. Plates (3-17) show the compressive test specimens and machine.

Table (3-13): Hardened concrete Compressive Strength test

Test		At 7-day	At 28-day	At time of testing
Compressive strength(MPa)	**Cube**	**31.84**	**35.65**	**40.55**
	Cylinder	**27.06**	**30.30**	**34.46**

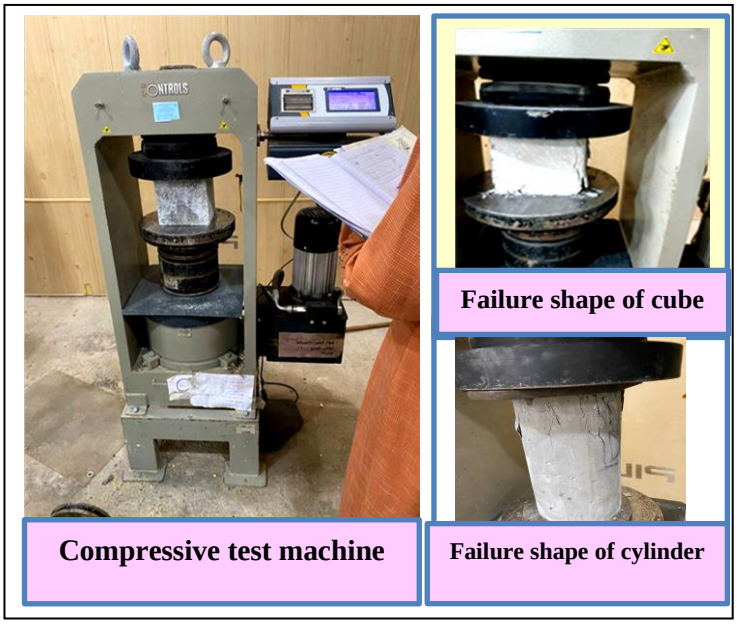

Plate (3-17): Compressive Test Specimen and Machine

3.8.2 Splitting Tensile Strength

According to the (ASTM C496-2011) **[101]**, the split-tensile strength test was carried out on the average of six cylindrical concrete specimens (150x300mm) as shown in the Plate (3-18) and Table (3-14) presents the splitting tensile strength test results.

Table (3-14): Splitting tensile strength test result

Specimens No.	Splitting tensile MPa at 28-days	Splitting tensile MPa at time of testing
1	4.23	4.47
2	4.20	4.81
3	4.12	4.45
4	4.09	4.27
5	4.10	4.64
6	4.21	4.52
Average value	4.16	4.53

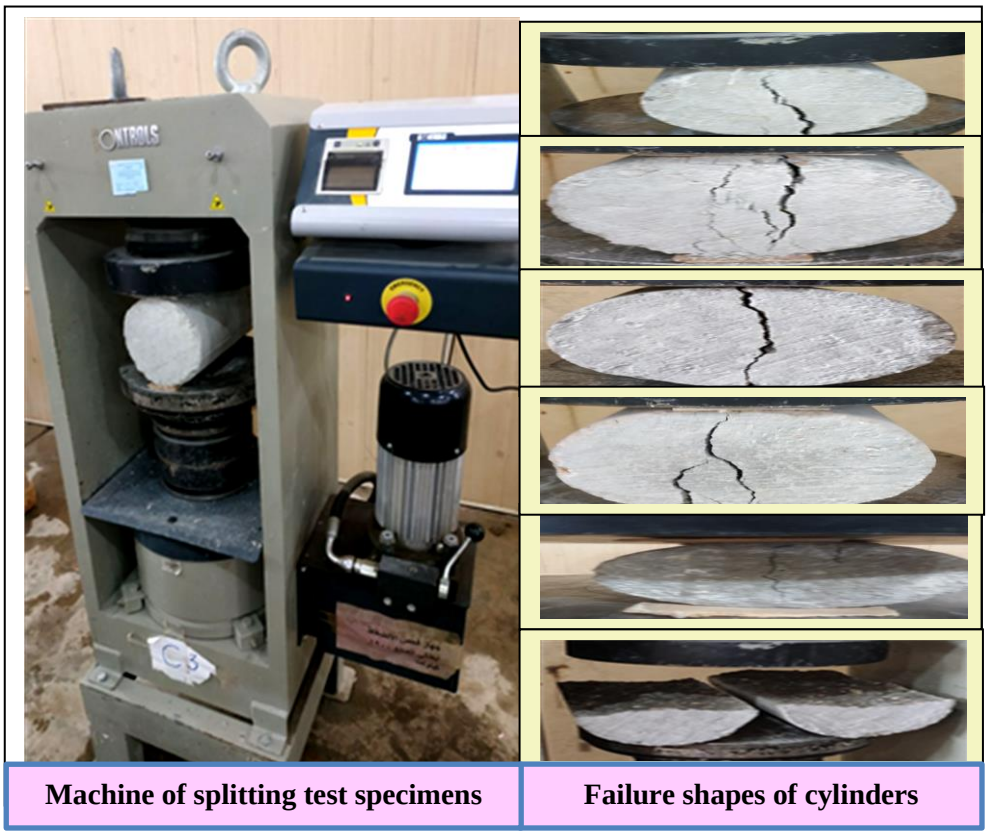

Machine of splitting test specimens | Failure shapes of cylinders

Plate (3-18): The test of splitting tensile strength and Machine

3.8.3 Flexural strength test (Modulus of Rupture)

The concrete prisms of dimensions (100×100×400) mm were tested at 28 days and at the date of testing according to ASTM C78-2010 **[102]** with loading in third points. This test was conducted using the flexural test

machine with a capacity equal to 150 kN, rate of the load was equal to 1 MPa per minute. Table (3-15) show the test specimens results and Plate (3-19) shows the modulus of the rupture test and machine.

Table (3-15): The test results of Modulus of rupture

Specimens No.	Modulus of rupture (MPa) at 28-days	Modulus of rupture (MPa) at time of testing
1	4.22	4.79
2	3.99	4.11
3	4.10	4.43
4	4.14	4.63
5	4.18	4.67
6	4.42	4.95
Average	4.175	4.600

Flexural test machine | Failure shapes of prisms

Plate (3-19): Modulus of rupture test specimens and machine

CHAPTER FOUR

RESULTS AND DISCUSSION

4.1General

The main aim of this experimental work is to study the effect of CFRP strips or steel plates on the structural behavior of strengthened and repaired RC inverted T beams. The experimental work consisted of testing thirteen specimens in three groups of reinforced concrete inverted T beams. In additional control beam specimen, the first group consisted of five beam specimens strengthening with CFRP strips, the second group consisted of also five beam specimens strengthening with steel plates, and lastly, the third group consisted of two beam specimens, one of them repaired with CFRP strips and the other repaired with steel plates. The variables in this experimental work include the length of CFRP strips, width of CFRP strips, length of steel plates, and width of steel plate sheets on the behavior of strengthened RC inverted T beams.

Also, the behavior and load-carrying capacity of repaired cracked RC inverted T beams by CFRP strips or steel plates have been investigated in this experimental work.

In this chapter, the test results from experimental work include, ultimate load capacity, load versus mid-span deflection curves, flexural crack patterns, mode of failure, cracking load, and ductility are also prepared.

Each tested RC inverted T beam specimens had similar dimensions and, flexural and shear reinforcement. The control, strengthened and repaired cracked RC inverted T beams were tested to failure. It may be discovered that the CFRP system or the steel plate system, is a highly effective technique to increase the serviceability and ultimate flexural strength of RC

inverted T beams, compared with control beam, thus the flexural strength of RC inverted T beam can be restored by using CFRP or steel plate.

4.2 Test Results of Experimental work

The thirteen inverted T beams tested in this study were divided into three groups, in addition to the control beam. Table (4-1) shows the results of the cracking load, ultimate load, and mid-span deflections. The failure modes occur for each inverted T beams were typical flexural cracks that cause debonding of CFRP strips or steel plates located in the tensile zone at the ultimate load level. The results obtained from all groups are discussed in the following sections.

Table (4-1): Experimental results of the tested inverted T beams

Group no.	Tested Beams	Pc* (kN)	Pu** (kN)	Mid-span Deflection (Δu) (mm)	***Percentage increase in ultimate load%
-------	ITCC	21	71.652	22.31	----------
Group one	ITF600	22	78.690	24.35	10.2***
	ITF900	24.2	85.754	11.79	19.7
	ITF1200	27.8	89.088	16.43	24.3
	IT2F1200	25	95.899	13.91	33.8
	IT3F1200	26.4	104.155	27.85	45.4
Group two	ITS600	23.3	78.654	22.41	9.8
	ITS900	25.7	72.160	26.41	0.7
	ITS1200	21.6	79.671	28.55	11.2
	IT2S1200	27	85.602	23.99	19.5
	IT3S1200	29	93.937	20.91	31.1
Group three	IT3FR1200	29.4	99.808	14.41	39.3
	IT3SR1200	21.6	92.877	27.84	29.6

*..... Refer to load at initiation of first flexural crack.

…….Refer to load at ultimate level. *……. $= \frac{pu(ITF600) - pu(ITCC)}{pu(ITCC)} * 100.$

4.3 Cracking Behavior

During the testing phase, the crack formation was monitored in order to know the behavior of the strengthened beam specimens and compare it with the behavior of the unstrengthened (control beam). First cracking load, the cracking patterns, and the crack width of all specimens explain in the next subsections.

4.3.1 Cracking Patterns

All specimens are divided into the following sub-parts in order to know the cracking behavior of each beam.

4.3.1.1: Control beam (ITCC)

The control beam specimen represents an unstrengthened specimen. The control specimen is tested for comparison with beams strengthened or repaired with CFRP strips or steel plates. The control specimen behaves in the expected shape under the influence of flexural loading. It is gradually loaded until cracks appear. The first flexural crack appeared at (21 kN) in the area of the constant moment and it is almost vertical. After an increase in the load, flexural cracks increased and widen and continue to develop in the web area as shown in the Plate (4-1). At load (45 kN), cracks are formed in the area of shear span soon on the flexural area. At (68kN), no additional cracks in the constant moment area continued to widen with increasing load to the point of failure. Beam failure was typically a tensile flexural failure due to the increase in flexural stresses in the constant moment area. Plate (4-1) shows the crack pattern at the failure of the control beam (ITCC). No failure occurred in the compression area, and the dominate failure was a tensile failure.

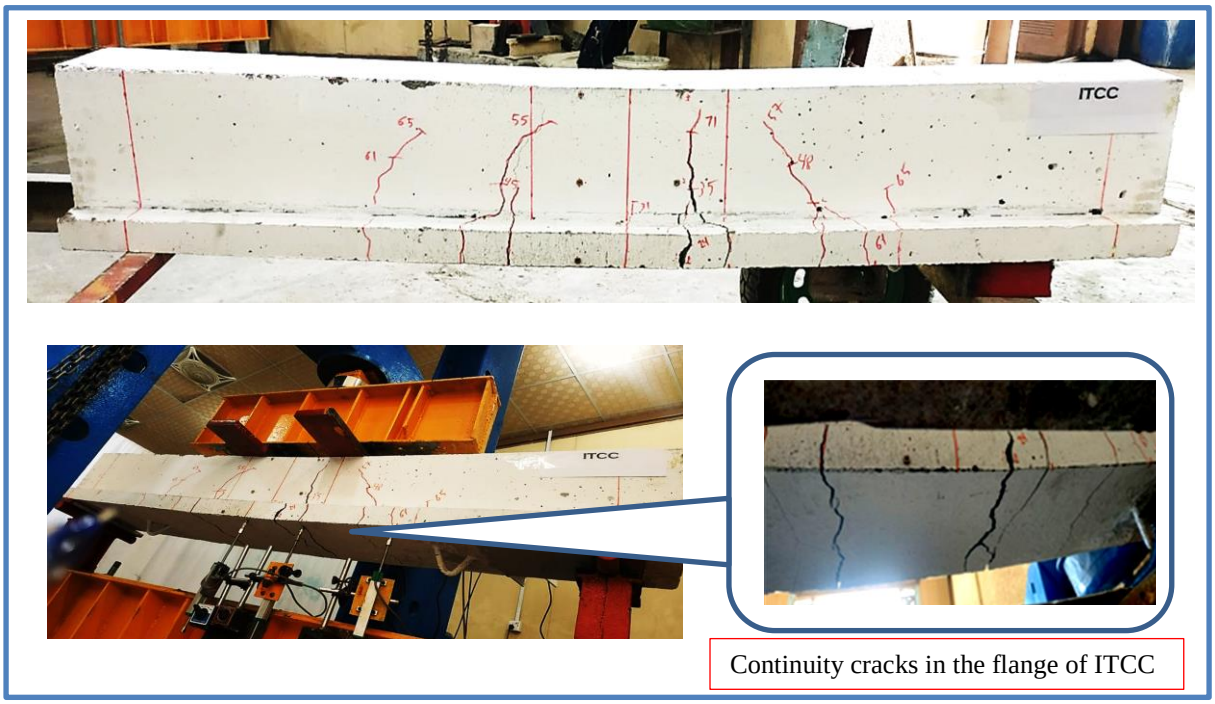

Plate (4-1): Crack pattern after failure for control beam (ITCC)

4.3.1.2: Group One (strengthening with CFRP Sheet)

This group of beam specimens shows the effect of the External Bonding (EB) technique by using a CFRP sheet on the crack pattern after failure as follows:

4.3.1.2.1 Strengthened Beam Specimen (ITF600)

The beam specimen (ITF600) is strengthened with only one strip of CFRP, the length of the strip was (600 mm) and the width was (50mm). The first cracking occurred at a load of (22 kN) forming an initial crack in a constant moment area. With increased load, new cracks were spreading in the beam specimen. Crushing of concrete in the compression area also occurred as shown in the Plate (4-2). Lastly, this beam is a failure by debonding the CFRP strip as shown in the Plate (4-2). The debonding happened at (78.690 kN) which is higher than the control beam (ITCC) by 10.2%. Occurring the debonding in CFRP strip for strengthened RC beam member due to high-stress concentration in this region of the strengthened RC beam member.

Debonding also occurred due to the presence of cracks and their propagation in concrete parallel to bonded sheet and adjacent to the adhesive to the concrete. These cracks begin from the critically stressed parts towards one of the ends of the sheet. The term “debonding failure” is often indicated to describe a significant decrease in beam member capacity due to the propagation or initiation of a major crack in the vicinity of the interface area. Plate (4-2) shows the crack pattern at the failure for the ITF600 beam and debonding failure in this beam.

Plate (4-2): Crack pattern after failure for strengthened beam (ITF600)

4.3.1.2.2 Strengthened Beam Specimen (ITF900)

Beam specimen ITF900 was strengthened with CFRP strip of the length (900 mm) and width (50 mm) and was installed on the tension bottom face of the RC inverted T beam. Plate (4-3) shows the cracks pattern of this RC beam specimen. The first crack appeared at a higher load than the control specimen (unstrengthened beam ITCC). The first crack was seen at an applied load of (24.2 kN). Interfacial debonding failure which was induced by the generation and expansion of flexural cracks, occurred at load (85.754 kN) which is higher than the control beam (ITCC) by 19.7%.

Flexural cracking occurs as a result of high stresses in the flexural area, and then the cracking begins to multiply towards the end of the CFRP strip, causing the CFRP strip to separate.

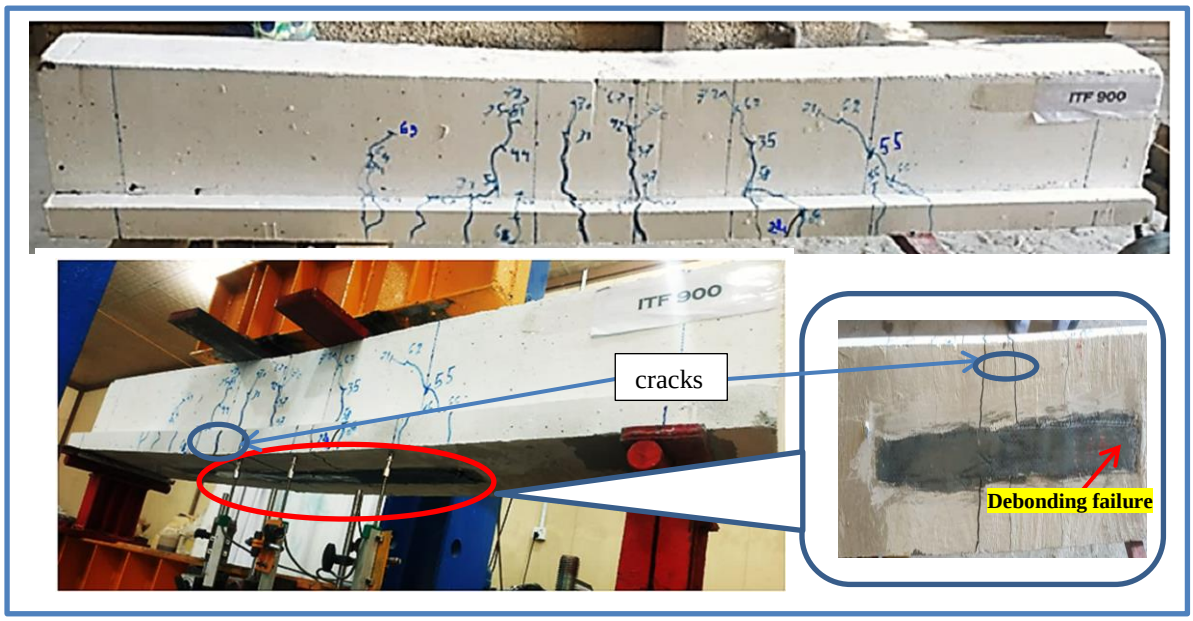

Plate (4-3): Crack pattern after failure for strengthened beam (ITF900)

4.3.1.2.3 Strengthened Beam Specimen (ITF1200)

Beam specimen ITF1200 was strengthened with only one CFRP strip of length (1200 mm) and width (50mm). The first cracking was seen at a load of (27.8kN), which was the initial crack observed in the constant moment area. After that, the load was increased, forming new cracks. Beam failed due to the splitting in the CFRP strip at load (89.088 kN) which is greater than the control beam (ITCC) by 24.3%. The rupture of the CFRP strip occurred due to the strain in the CFRP strip reaching to design rupture strain ($\varepsilon f = \varepsilon fu$). In this beam, when the load reached the amount of 75.2 kN, it began to decrease, and then the load rise to 75 kN and continued to rise until the ultimate load. This behavior of the load, going up and down, explains the steel reinforcement yields when the load went down and then the load increased due to the presence of the CFRP strip and the role of its resistance in this until the failure of the beam due to the rupture of CFRP. In this beam

also occurred the crushing of concrete in the compression area was similar to beam ITF600 but this beam failed by rupture of CFRP. Crack pattern after failure for strengthened beam (ITF1200) as shown in the Plate (4-4). Noted from this failure that the CFRP strip doesn't debond, and this is evidence that the length of the CFRP =1200mm is an appropriate length for strengthening without occurring the phenomenon of debonding if compared to this the length in previous beams of lengths 600mm and 900mm.

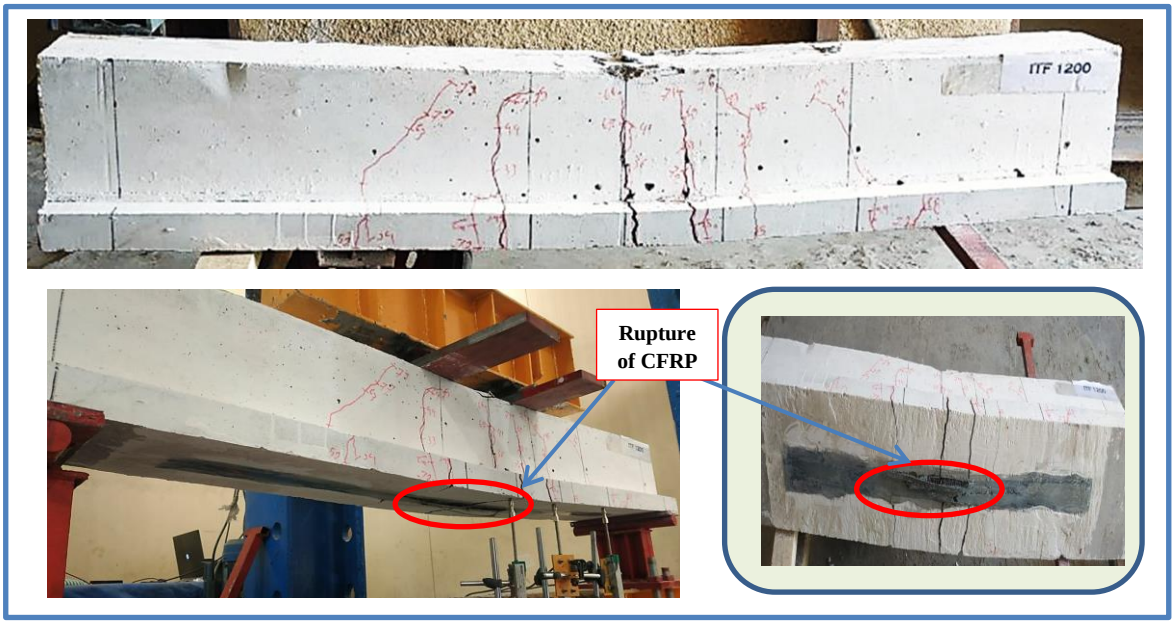

Plate (4-4): Crack pattern after failure for strengthened beam (ITF1200)

4.3.1.2.4 Strengthened Beam Specimen (IT2F1200)

Beam specimen IT2F1200 was strengthened with two strips of the CFRP sheet of length (1200 mm) and the total width of two CFRP strips was (100mm) which the two CFRP strips were installed on the tension bottom face of the RC inverted T beam. The cracks pattern after the failure of this strengthened beam specimen is shown in the Plate (4-5). The first crack was observed at a higher load than of an unstrengthened control beam specimen ITCC. The first crack occurred at an applied load of 25 kN. Mid-span debonding failure of this beam occurred at load (95.899kN) which is higher

than the control beam (ITCC) by 33.8%. It was initiated by the flexural crack. This failure occurred due to crack propagation in the concrete layer that parallels the bonded CFRP sheet and adjacent to the adhesive to the concrete interface. This failure is believed due to high interfacial normal stresses concentrated at the crack along this beam.

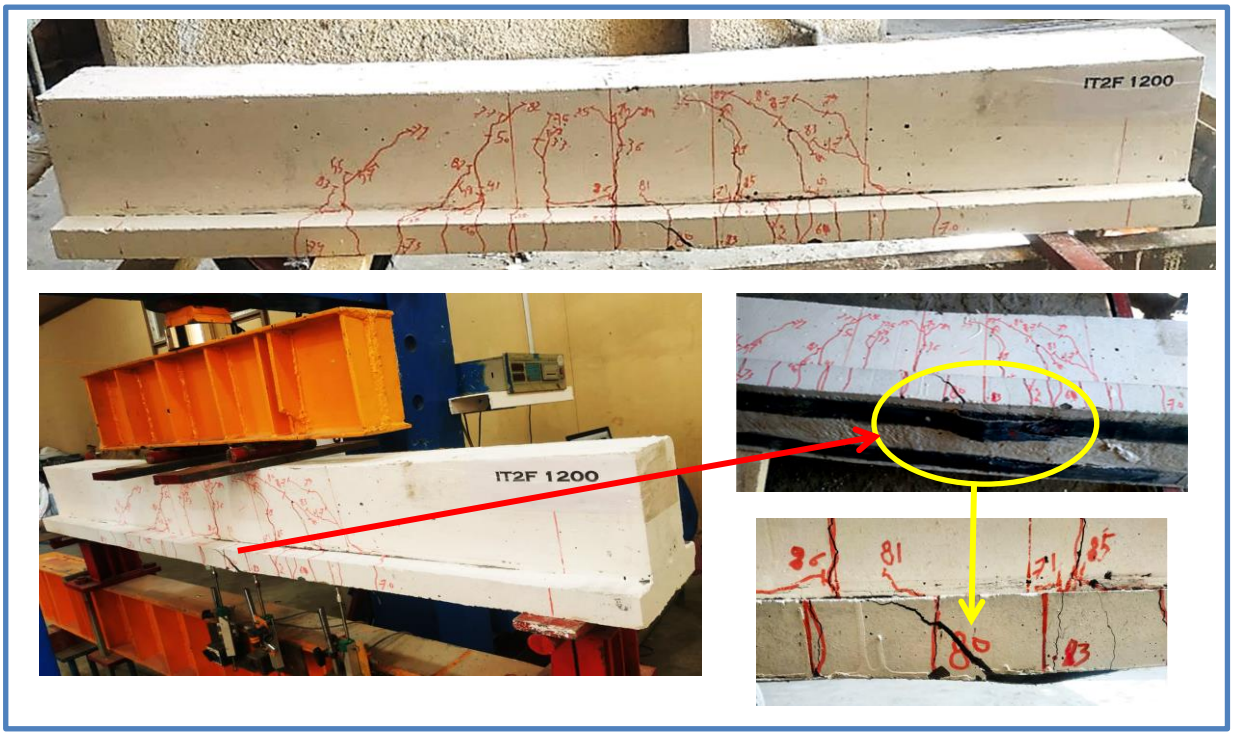

Plate (4-5): Crack pattern after failure for strengthened beam (IT2F1200)

4.3.1.2.5 Strengthened Beam Specimen (IT3F1200)

Finally strengthened beam specimen of group one was (IT3F1200), which is strengthened with three CFRP strips of length (1200 mm) and the total width of three CFRP strips was equal to (150 mm), the first cracking occurred at the load of 26.4 kN. The initial crack observing in the constant moment area. With increased load, new cracks were formed along this beam. lastly, mid-debonding failure occurred at (104.155 kN) which is higher than the control beam (ITCC) by 45.4%. Mid debonding in CFRP strengthened RC beam formed in an area of high-stress concentrations, which are associated with the found of flexural cracks. When occurring "mid-

debonding failure" a significant decrease in the beam capacity due to propagation and widening of a flexural crack in the flange area of this strengthening RC inverted T beam specimen. The crack pattern after failure for the strengthened beam (IT3F1200) is shown in the Plate (4-6).

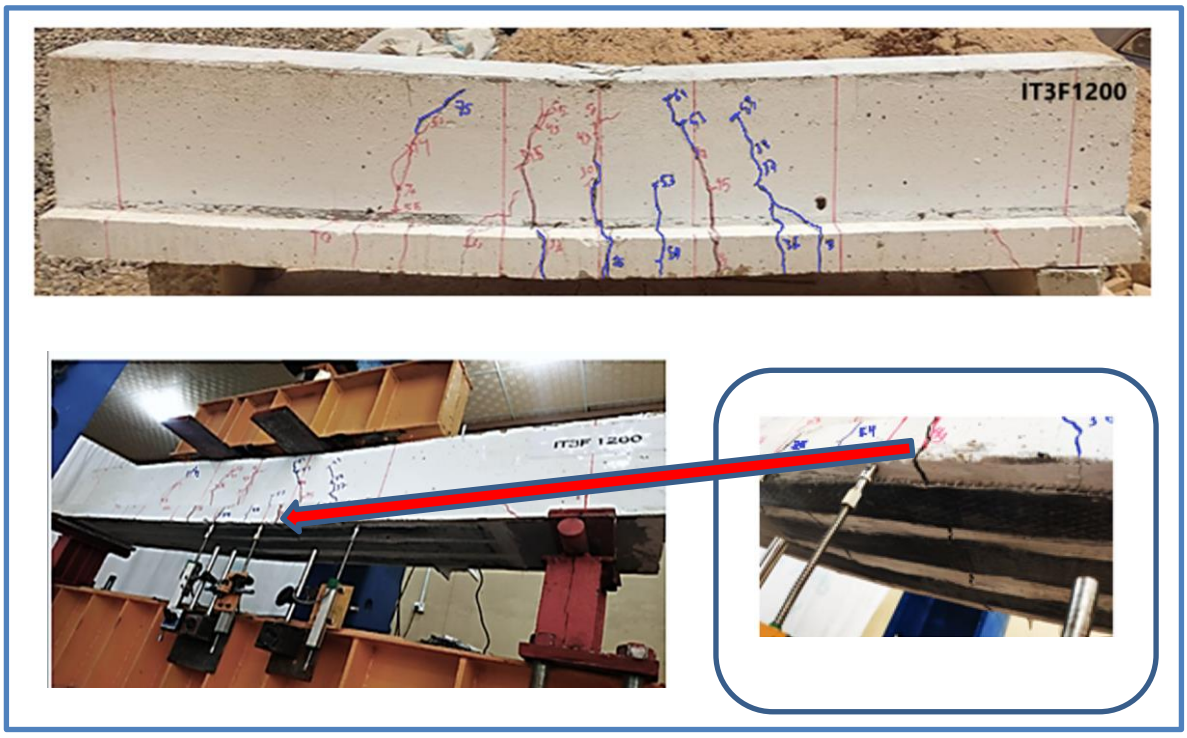

Plate (4-6): Crack pattern after failure for strengthened beam (IT3F1200)

4.3.1.3: Group two (strengthening with steel plates)

This group of beam specimens shows the effect of the External Bonding (EB) technique by using steel plate on the crack pattern after failure as follow:

4.3.1.3.1 Strengthened Beam Specimen (ITS600)

Beam specimen ITS600 was strengthened with one steel plate of length (600 mm) and width (50mm). This beam specimen is similar to the beam specimen (ITF600), but only the difference is the type of externally bonded

technique. The first cracking was formed at a load of (23.3 kN) with forming an initial cracks in the very near area of the constant moment area. when the load was increased, the new cracks induced in the beam specimen. Crushing in the concrete of the compression area followed by failed debonding in the steel plate sheet at the load (78.654 kN) which is higher than the control beam (ITCC) by 9.8%. The debonding occurs in this beam specimen due to the propagation of the flexural cracks in the center moment area and heading toward the end of the plate due to high-stress concentrations in this area. The expression “debonding failure” is used often to characterize enough decrease in beam capacity due to propagation or initiation of the flexure crack in the vicinity of the interface area. Plates (4-7) show the crack pattern after failure for the strengthened beam (ITS600).

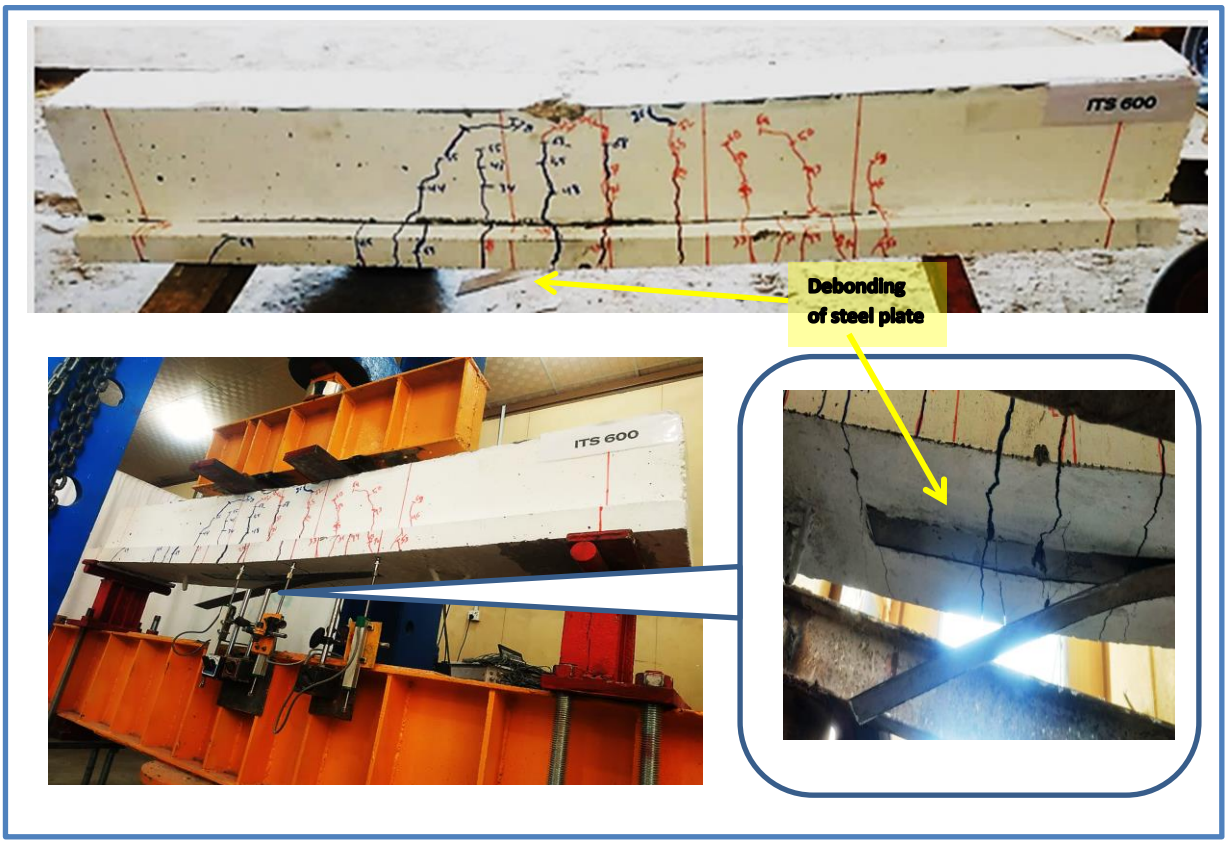

Plate (4-7): Crack pattern after failure for strengthened beam (ITS600)

4.3.1.3.2 Strengthened Beam Specimen (ITS900)

Beam specimen ITS900 was strengthened with a steel plate of length (900mm) and width (50 mm), it was installed on the tension bottom face of the RC inverted T beam. Plate (4-8) shows the cracks pattern of this RC beam specimen. The first crack appeared at a higher load than the control specimen (unstrengthened beam ITCC). The first crack was seen at an applied load of (25.7kN). Crushing in the concrete in the compression area followed by end debonding failure which was induced by the generation and expansion of flexural cracks. It occurred at load (72.160 kN) which is higher than the control beam (ITCC) by 0.7%. Flexural cracking occurs as a result of high stresses in the flexural area, and then the cracking begins to multiply toward the end of the steel plate, causing the steel plate to separate.

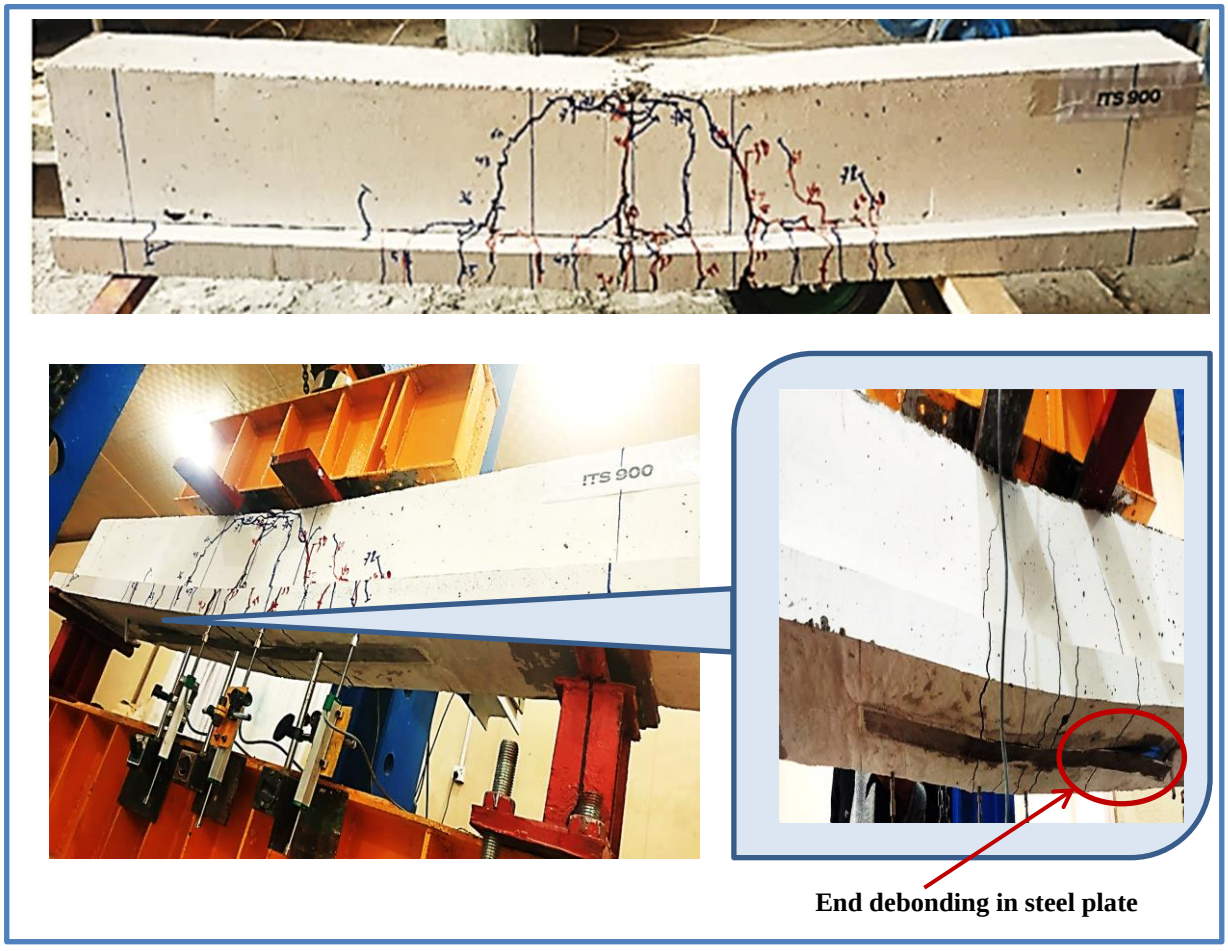

Plate (4-8): Crack pattern after failure for strengthened beam (ITS900)

4.3.1.3.3 Strengthened Beam Specimen (ITS1200)

Beam specimen ITS1200 was strengthened with one sheet of steel plate of length (1200 mm) and width (50 mm), which the steel plate was installed on the tension bottom face of the RC inverted T beam. The cracks pattern after the failure of this strengthened beam specimen is shown in the Plate (4-9). The first crack was observed at a higher load than of an unstrengthened control beam specimen ITCC. The first crack occurred at an applied load of 21.6 kN. Mid-span debonding failure of this beam occurred at load (79.671 kN) which is higher than the control beam (ITCC) by 11.2%. Such a pattern of failure can occur in regions adjacent to flexural cracks in regions of the high flexural moment. This failure leads to the concentration of sufficient stresses adjoining the edge of the crack.

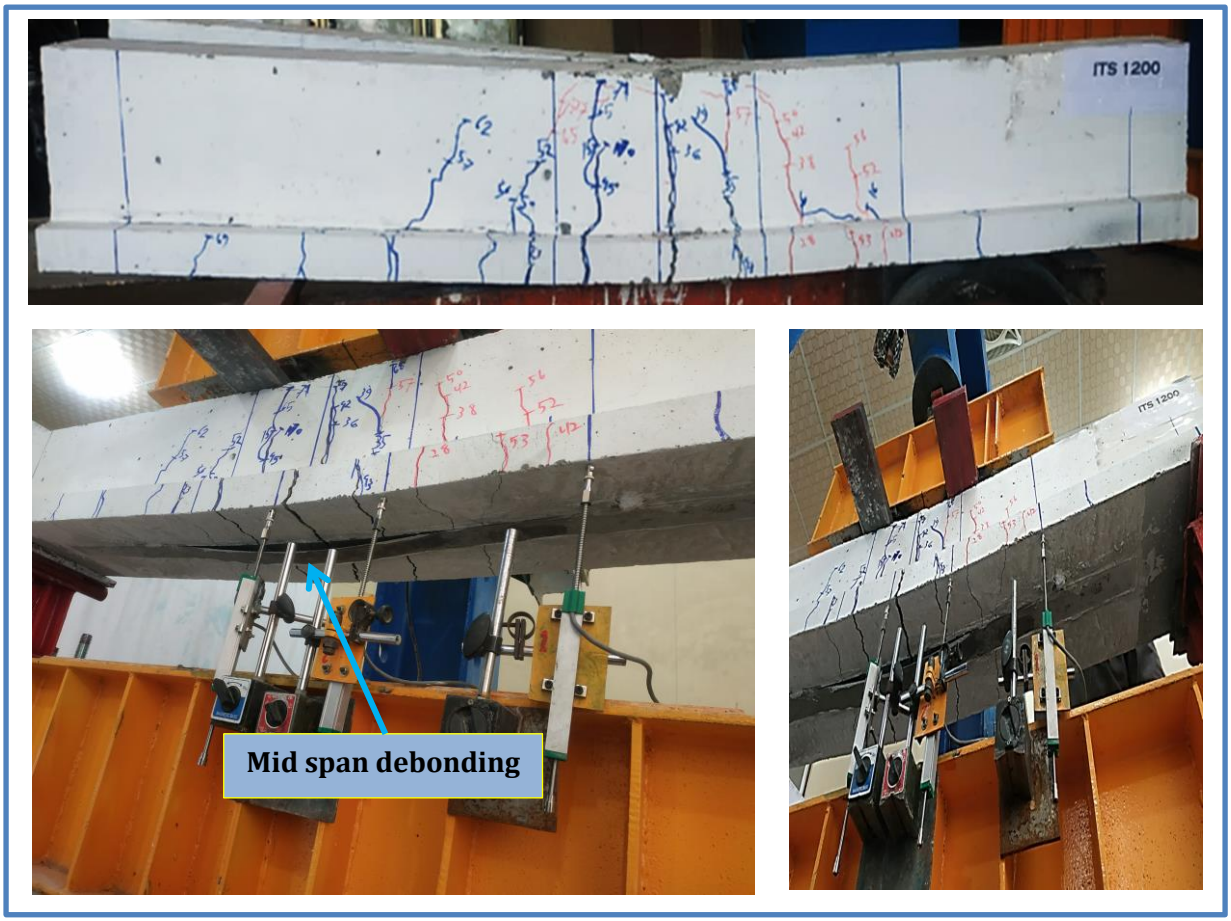

Plate (4-9): Crack pattern after failure for strengthened beam (ITS1200)

4.3.1.3.4 Strengthened Beam Specimen (IT2S1200)

Beam specimen IT2S1200 was strengthened with two sheets of the steel plate of length (1200 mm) and total width were (100 mm), which the steel plates were installed on the tension bottom face of the RC inverted T beam. The cracks pattern after failure of this strengthened beam specimen is shown in the Plate (4-10). First crack observed at a higher load than of an unstrengthened control beam specimen ITCC. The first crack occurred at an applied load of 27kN. The initial crack observing in the constant moment area. One of the steel plates on the back side of the flange of the inverted T beam had an mid span debonding followed the failure by debonding the front steel plate at load (85.602 kN) which is higher than the control beam (ITCC) by 19.5%. The debonding failure occurs due to the concentration of sufficient stresses adjoining to the edge of the flexural cracks which propagation towards the end of the plate.

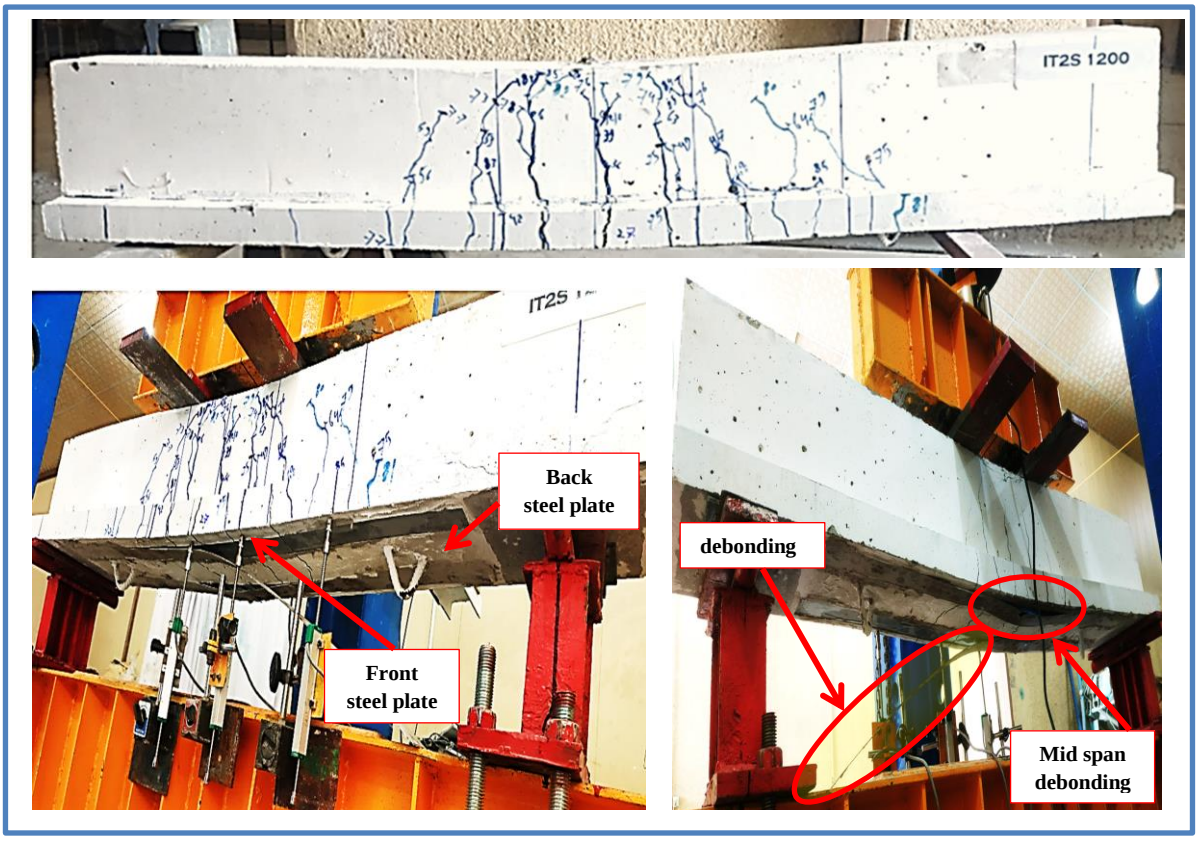

Plate (4-10): Crack pattern after failure for strengthened beam (IT2S1200)

4.3.1.3.5 Strengthened Beam Specimen (IT3S1200)

Beam specimen IT3S1200 was strengthened with three sheets of steel plate of length (1200 mm) and total width (150 mm), which the steel plates were installed on the tension bottom face of the RC inverted T beam. The cracks pattern after the failure of this strengthened beam specimen is shown in the Plate (4-11). The first crack was observed at a higher load than of an unstrengthened control beam specimen ITCC. The first crack occurred at an applied load of 29kN. The initial crack forms in the center of the moment area. The middle steel plate had a partial debonding, then the back steel plate had a partial debonding as well. At a load of 93.937 kN, the beam specimen failure occurred as a result of the end debonding of the front steel plate, which was 31.1% higher than the control beam specimen. Flexural cracks are formed, and then their growth and increase in their width and propagation in this beam specimen was the reason behind the partial or end debonding.

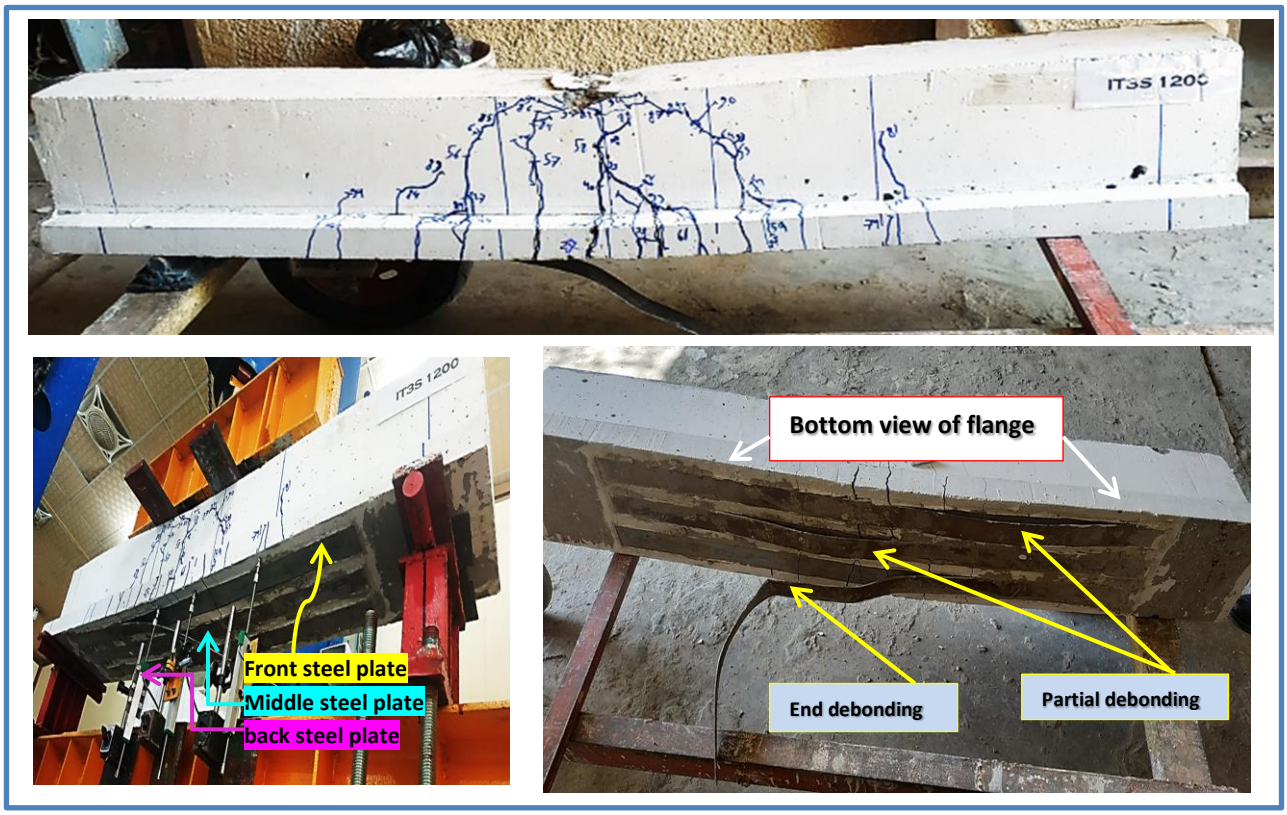

Plate (4-11): Crack pattern after failure for strengthened beam (IT3S1200)

4.3.1.4: Group three (Repaired with CFRP strips or steel plates)

The group of beam specimens described the effect of the repair technique by using CFRP strip or steel plate on the crack pattern after failure , this group of beam specimens shows as follow:

4.3.1.4.1 Repaired Beam Specimen (IT3FR1200)

In this repair specimen, the loading was done in two stages, as follows:

1) The first stage is to apply a load of approximately 60% of the ultimate load on the control specimen (ITCC). The visible cracks on the model were indicated by a blue colored pencile to distinguish it on the stage after repair. Plate (4-12) (a) is showed the crack pattern before repairing for beam (IT3FR1200).

2) In the second stage, the beam is repaired with CFRP strip, then applied the load from zero until failure load (99.808kN) which is higher than the control beam specimen (ITCC) by 39.3%. Plate (4-12) (b) show the crack pattern for this beam after repair (at the failure) for the beam specimen (IT3FR1200). This beam is failed by debonding of three CFRP strip. Debonding occurs from areas of high tensile stress concentration and continues to the end of the strips, this is related to the presence of the cracks, in addition to the properties of the bonding materials and their resistance. The high tensile stress in concrete close to the adhesive layer is the reason for removing CFRP strips from concrete.

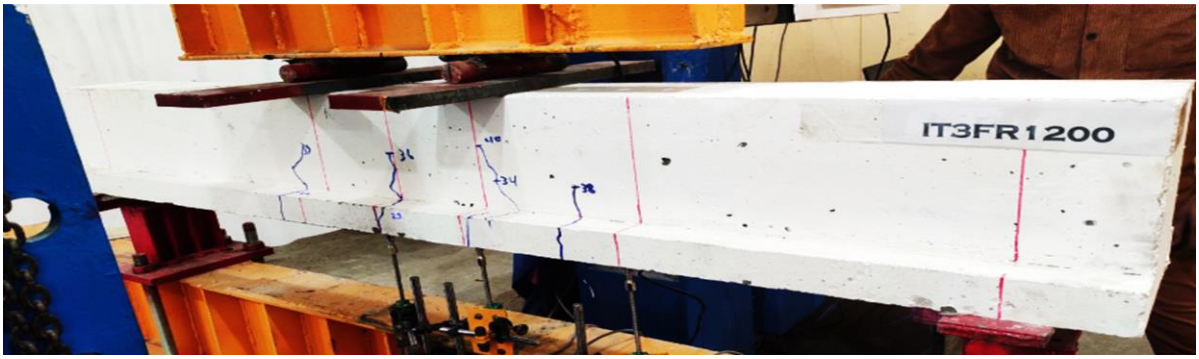

(a) Crack pattern before repairing for beam (IT3FR1200)

(b) Crack pattern after repairing (after failure) for beam (IT3FR1200)

Plate (4-12): (a) Crack pattern (before repairing) for beam (IT3F1200)
(b) Crack pattern (after repairing) after failure for beam (IT3F1200)

4.3.1.4.2 Repaired Beam Specimen (IT3SR1200)

This beam specimen is similar to the beam specimen (IT3FR1200), but only difference is the type of external bonded technique (repaired with steel plate). Also the loading was done in two stages, as follows:

1) The first stage is to apply a load of approximately 60% of the ultimate load on the control specimen (ITCC). The visible cracks on the model were indicated by a blue colored pencile to distinguish it on the stage after repair. Plate (4-13) (a) is showed the crack pattern before repairing for beam (IT3SR1200).
2) In the second stage, the beam is repaired with steel plates, then applied the load from zero until failure load (92.877kN) which is higher than the control beam specimen (ITCC) by 29.6%. Plate (4-13) (b) show the crack pattern for this beam after repair (at the failure) for the beam specimen (IT3SR1200). Crushing concrete in compression area followed by failure by mid debonding of three steel plates. Mid debonding occurs in the areas of high tensile stress concentration. Mid debonding related to the initiation of flexural crack.

(a)Crack pattern before repairing for beam (IT3SR1200)

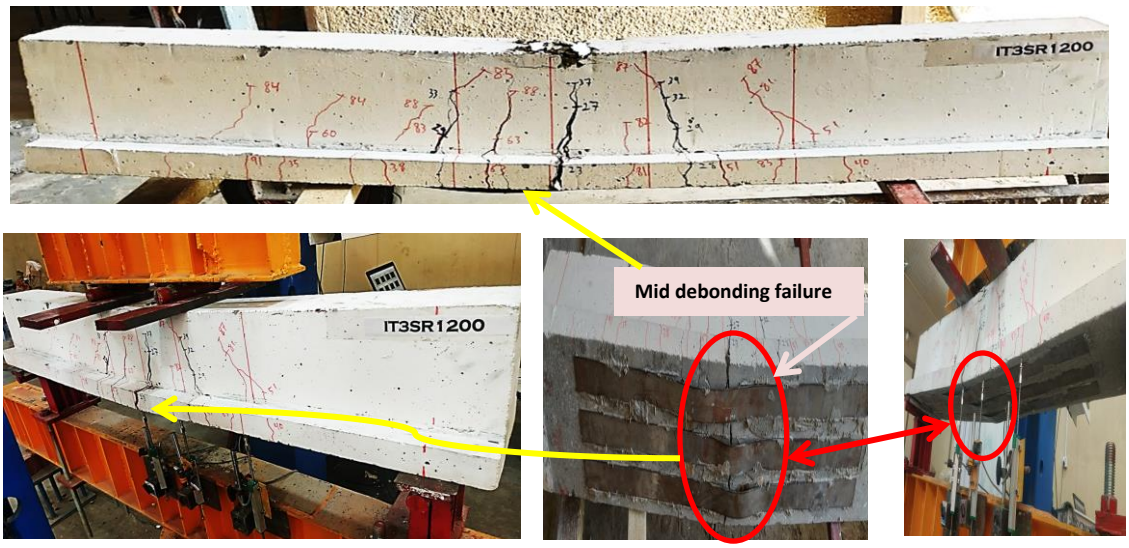

(b) Crack pattern after repairing (after failure) for beam (IT3SR1200)

Plate (4-13): (a) Crack pattern (before repairing) for beam (IT3S1200)
(b) Crack pattern (after repairing) after failure for beam (IT3S1200)

4.3.2 First cracking load and crack width

Steel plates strengthening technology of RC inverted T beam in group two showed the highest first cracking load compared to the control beam and the specimens in the first group (strengthening with CFRP strips technology), except for the model, group one ITF1200, showed higher first cracking loads when compared with ITS1200 in group two as shown in Table (4-2).

Crack measurement in this study was done by using the crack meter machine. With an increase in the load, the formation of the first crack is monitored and compared with the width of the rest of the cracks that appear on the beam specimen during the test period, and recording which of the cracks gives the largest width relative to the width of the first crack. Plate (4-14) shows how to measure the width of cracks by using the crack meter machine. The maximum crack widths occurred in the constant moment area. Control beam specimen without strengthening exhibited given greater crack width at the ultimate load as shown in the Table (4-2). Also, this table show the details of measured crack width at the service load.

Plate (4-14): Measurement the width of the cracks by using the crack meter

Table (4-2): Experimental first cracking load and crack width for flexural beams

Group no.	Tested Beams	First cracking load (kN)	*Service load (kN)	Crack width(mm) at service load	Ultimate load (kN)	Crack width(mm) at ultimate load
-------	ITCC	21	42.9912	0.25	71.652	4.63
Group one	ITF600	22	47.214	0.23	78.69	3.2
	ITF900	24.2	51.4524	0.21	85.754	2.4
	ITF1200	27.8	53.4528	0.19	89.088	2
	IT2F1200	25	57.5394	0.15	95.899	1.58
	IT3F1200	26.4	62.493	0.12	104.155	0.73
Group two	ITS600	23.3	47.1924	0.18	78.654	1.8
	ITS900	25.7	43.296	0.15	72.16	1.68
	ITS1200	21.6	47.8026	0.11	79.671	1.5
	IT2S1200	27	51.3612	0.8	85.602	1
	IT3S1200	29	56.3622	0.66	93.937	0.8
Group three	IT3FR1200	29.4	59.8848	0.19	99.808	0.67
	IT3SR1200	21.6	55.7262	0.16	92.877	1.5

* Assumed service load = 60% * Ultimate load **[103]**.

It is clear from the above table that all beam specimens strengthened with steel plate have a crack width at the service load and at the ultimate load less than the CFRP beam specimens, this may be due to the rise of stiffness of the strengthened steel plate beam specimens. However, the crack width at the ultimate load of the strengthened or repaired beam (IT3F1200 or IT3FR1200) is less than the crack width of all the beam specimens strengthened or repaired with steel plate, this may be due to the fact that in this beam the number of cracks increased and their width decreased. Also, a note from the above table is that the width of the crack will be decreased when the strengthening length or width became greater. This also shows in

drawing Figures (4-1) to (4-13). These figures explain the relationship between the applied load tracking with the crack width for all tested models.

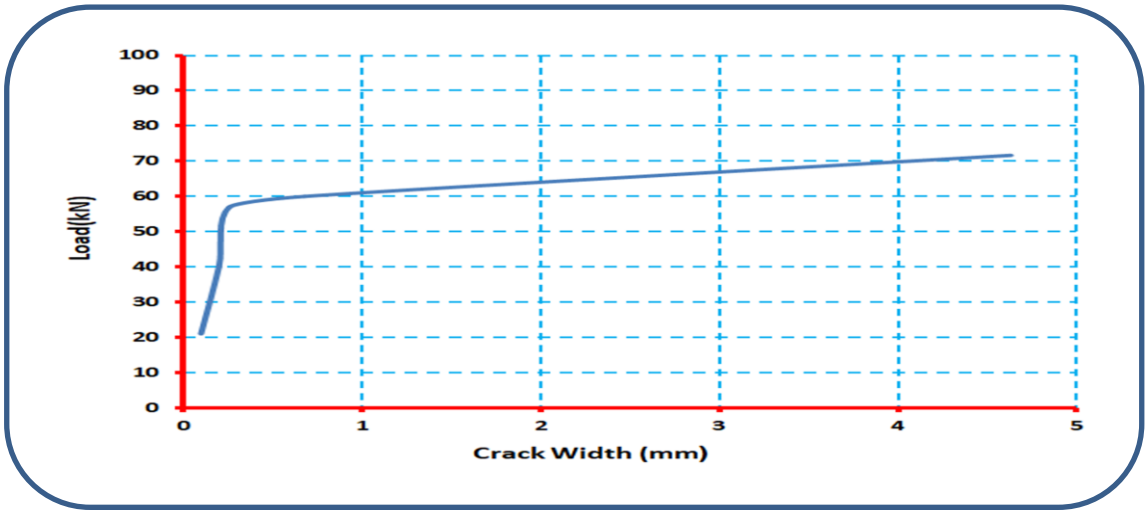

Figure (4-1) Load versus crack width of inverted T control beam ITCC

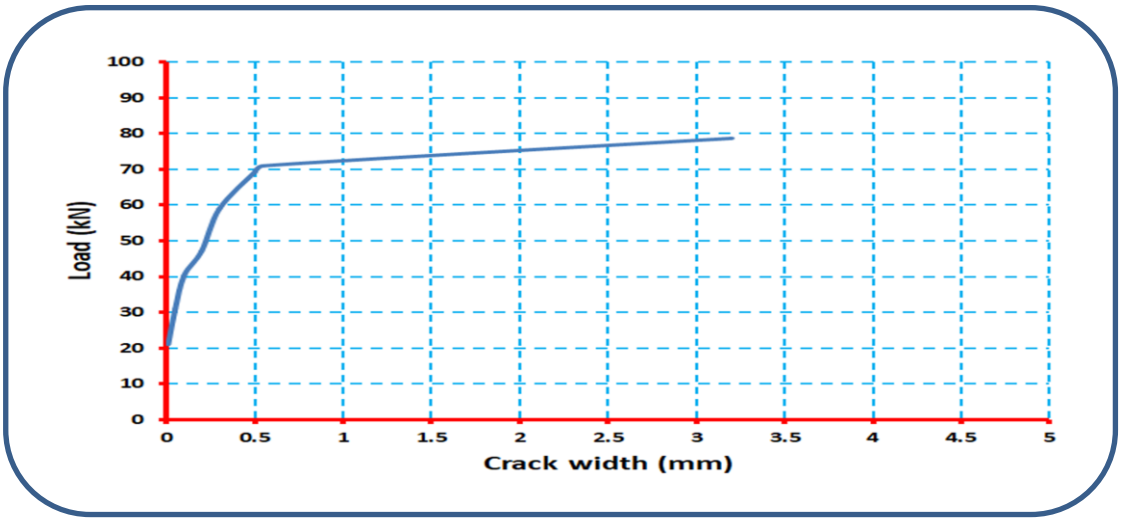

Figure (4-2) Load versus crack width of strengthened inverted T beam ITF600

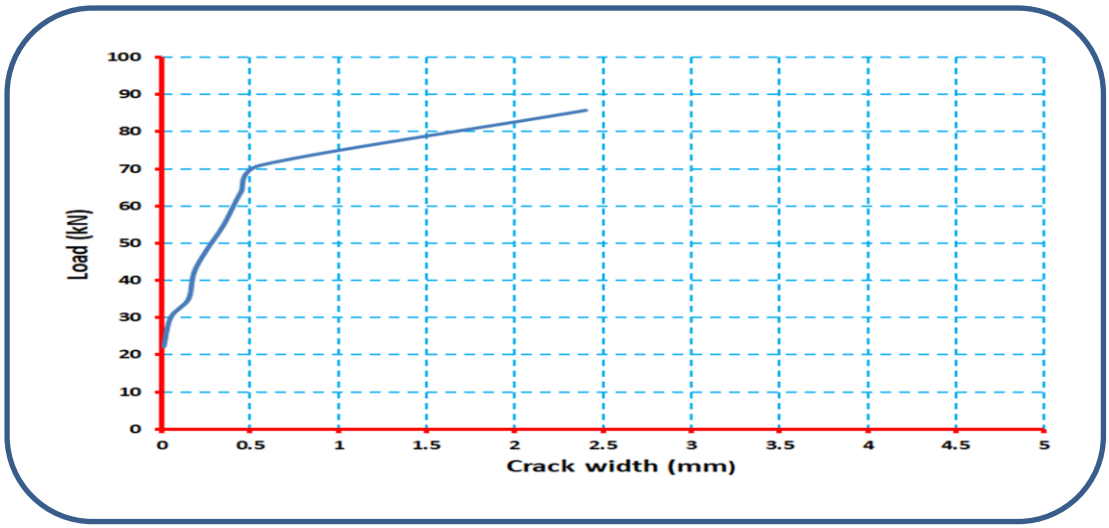

Figure (4-3) Load versus crack width of strengthened inverted T beam ITF900

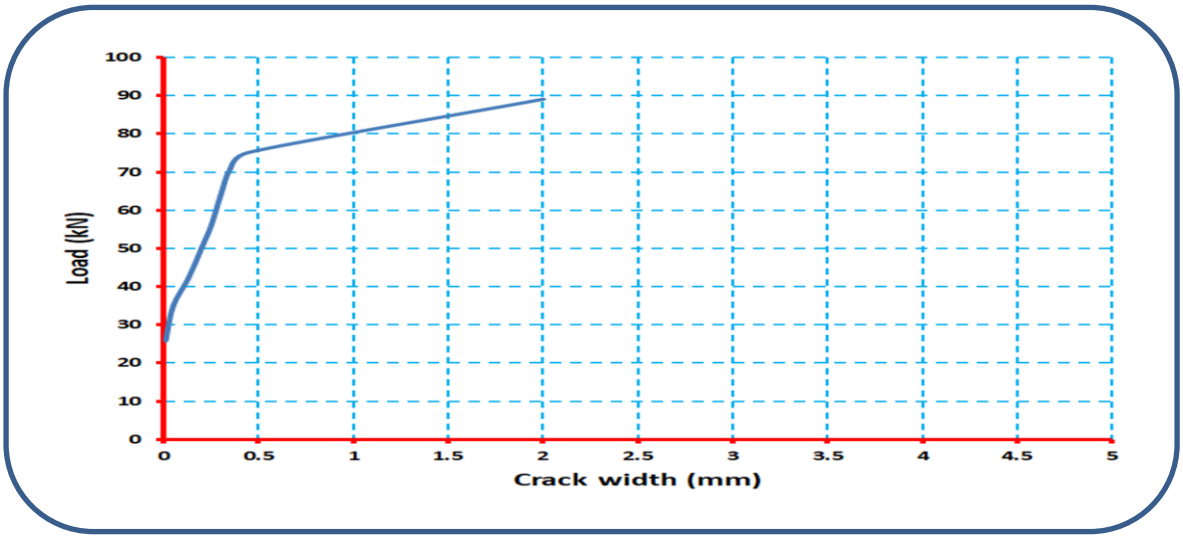

Figure (4-4) Load versus crack width of strengthened inverted T beam ITF1200

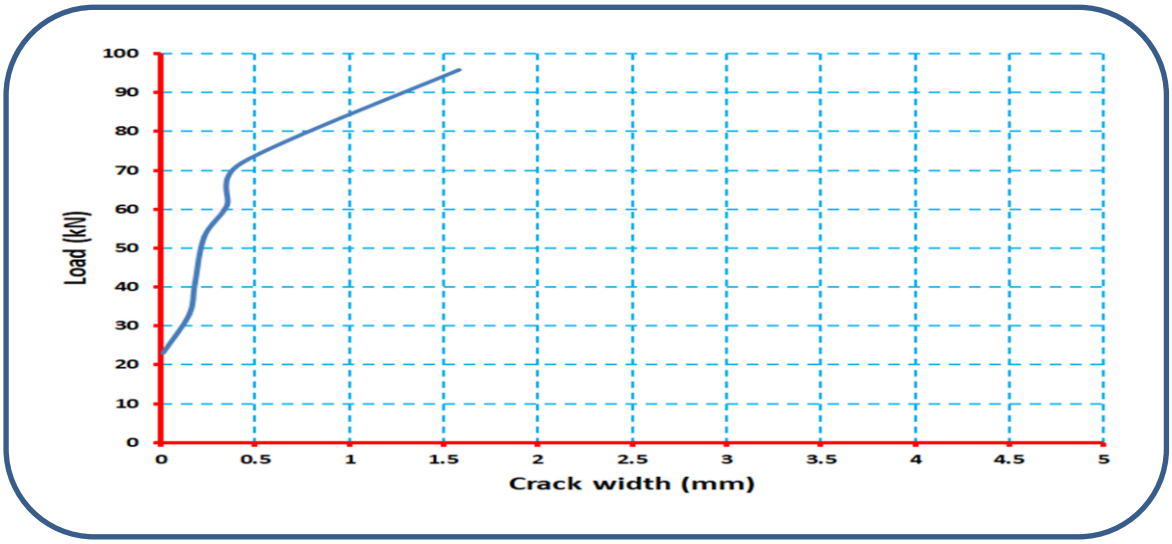

Figure (4-5) Load versus crack width of strengthened inverted T beam IT2F1200

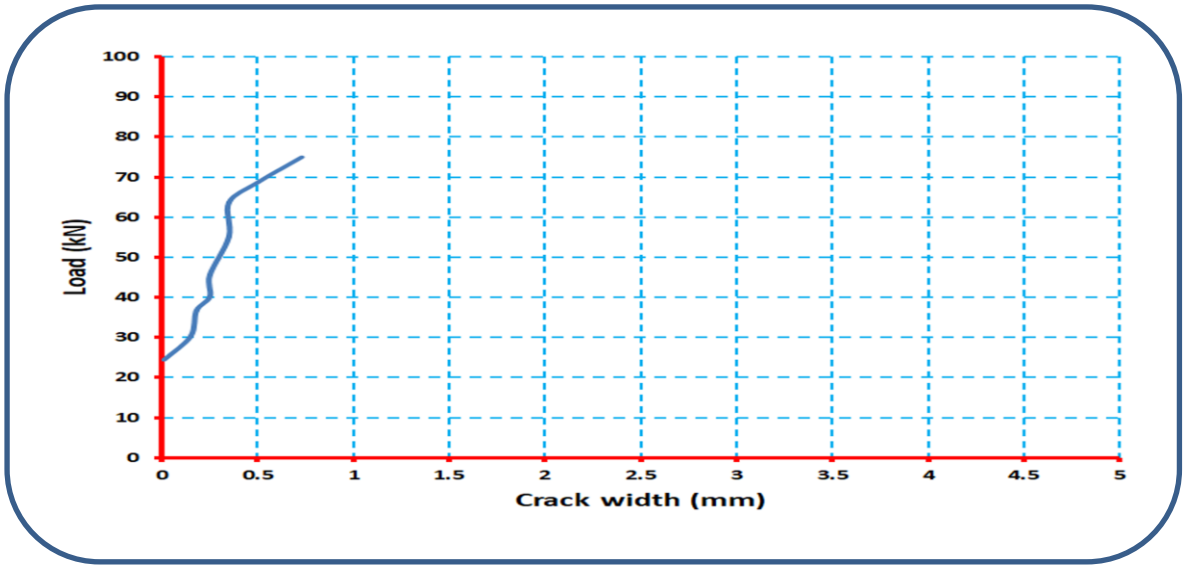

Figure (4-6) Load versus crack width of strengthened inverted T beam IT3F1200

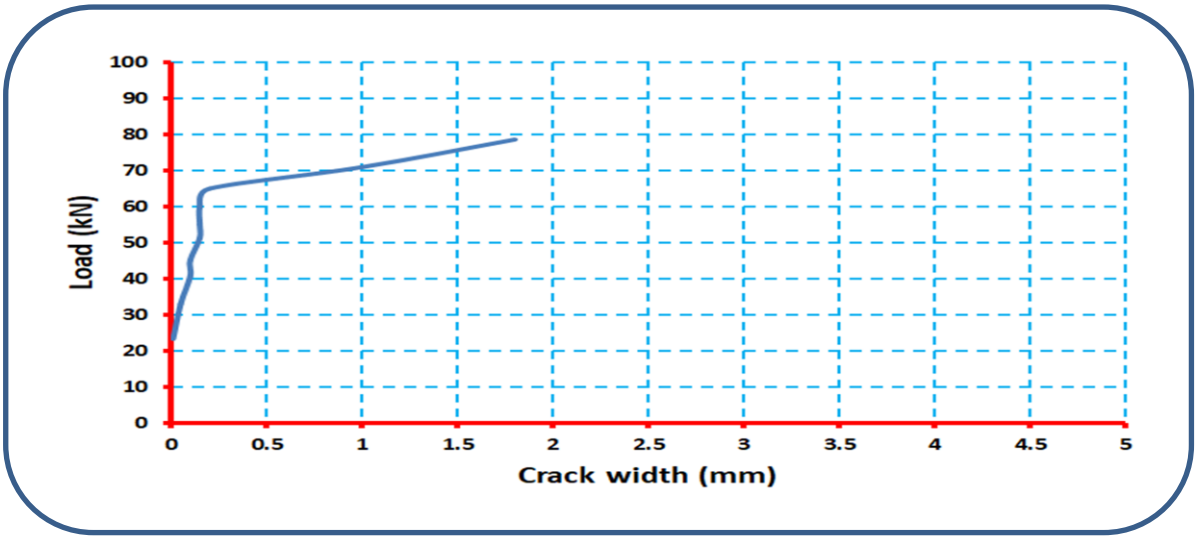

Figure (4-7) Load versus crack width of strengthened inverted T beam ITS600

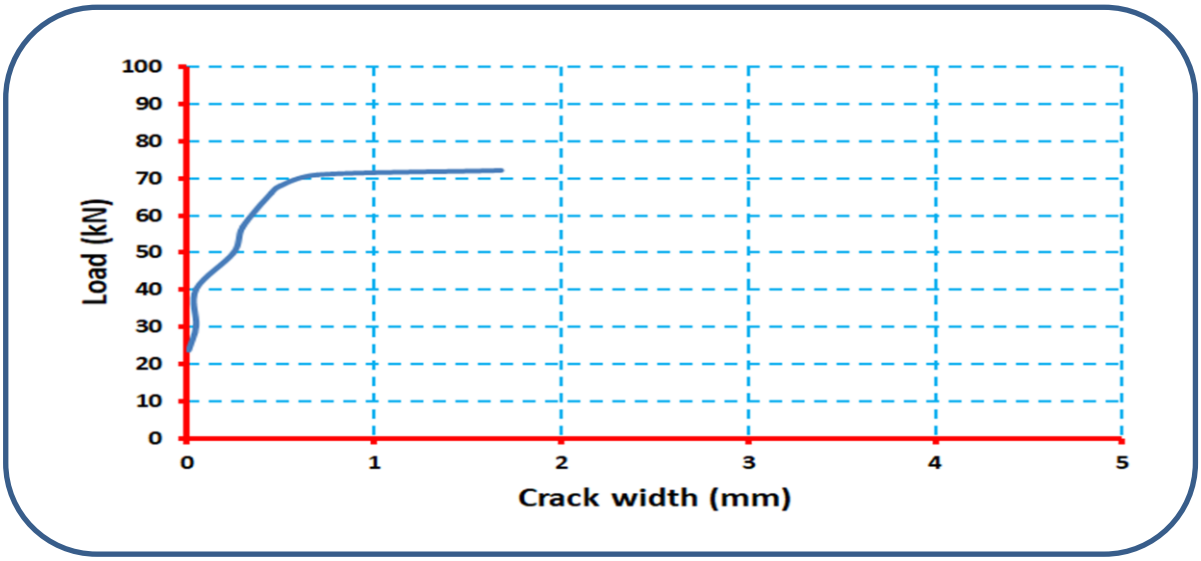

Figure (4-8) Load versus crack width of strengthened inverted T beam ITS900

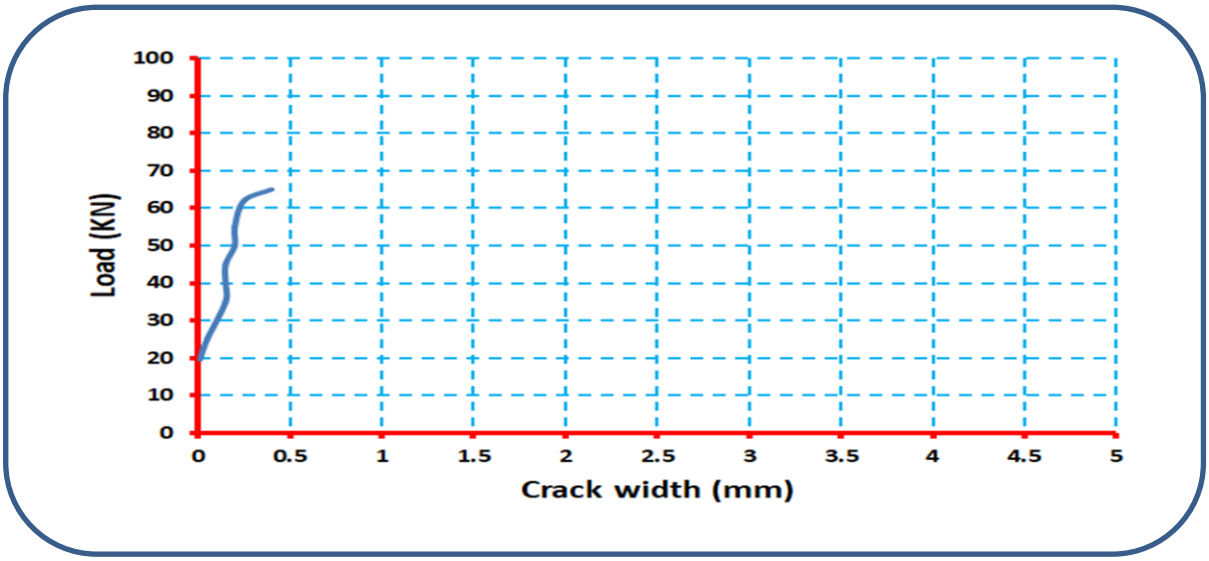

Figure (4-9) Load versus crack width of strengthened inverted T beam ITS1200

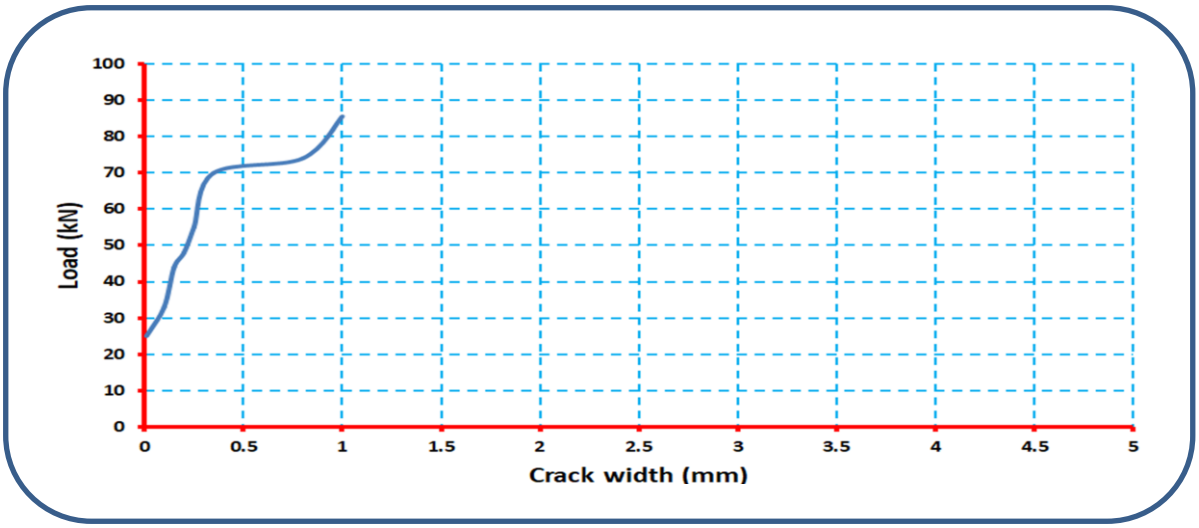

Figure (4-10) Load versus crack width of strengthened inverted T beam IT2S1200

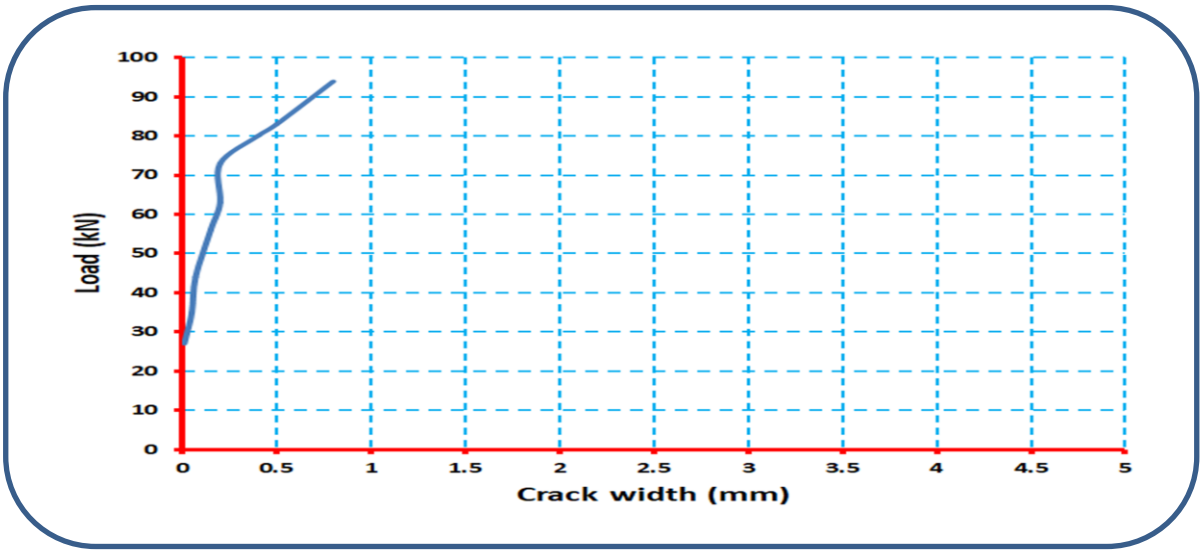

Figure (4-11) Load versus crack width of strengthened inverted T beam IT3S1200

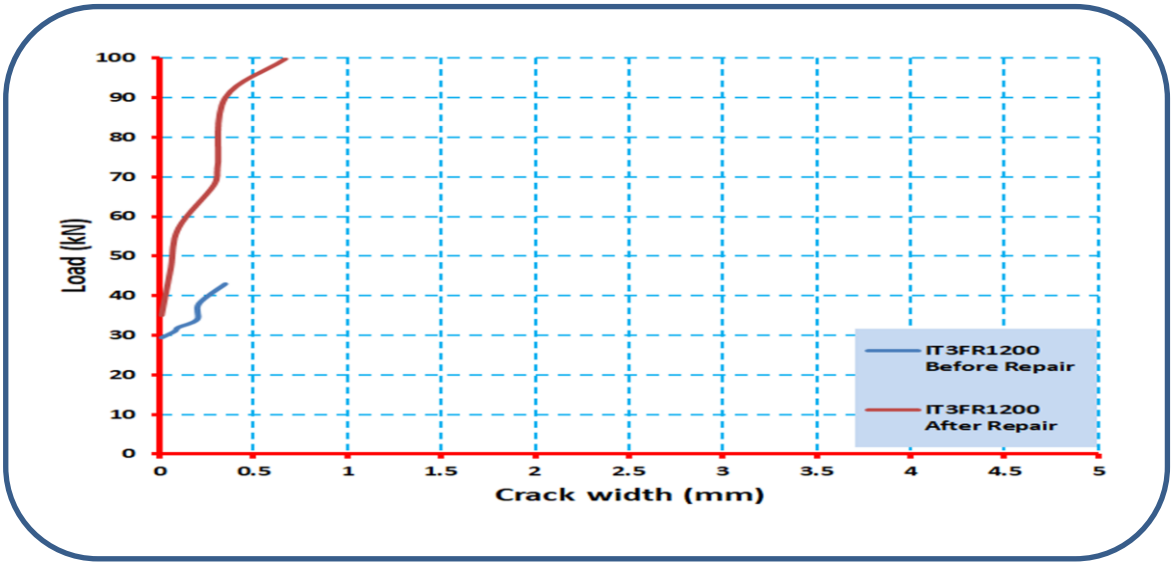

Figure (4-12) Load versus crack width before and after repaired inverted Tbeam IT3FR1200

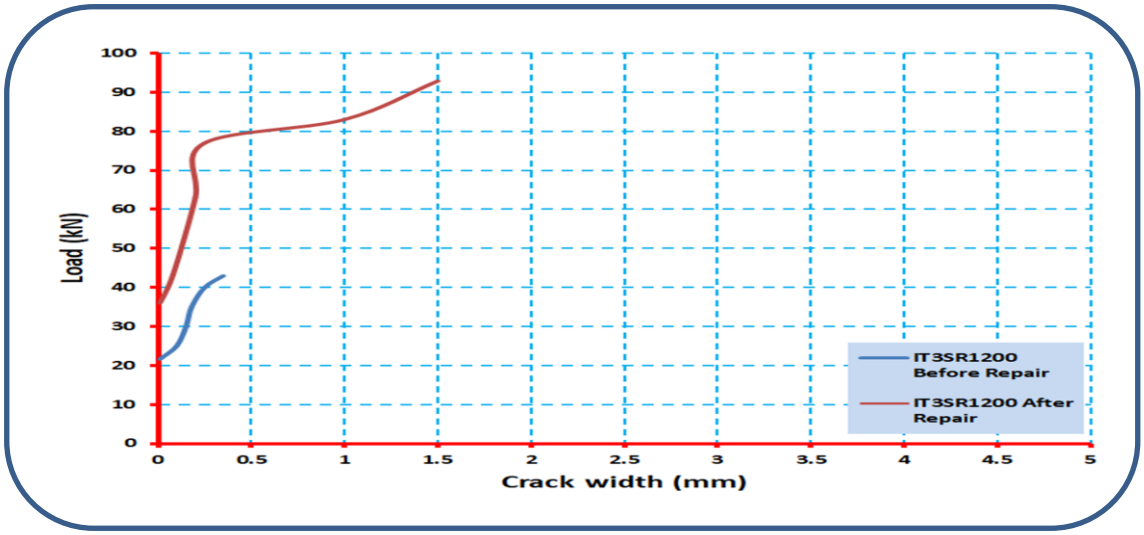

Figure (4-13) Load versus crack width before and after repaired inverted T beam IT3SR1200

4.4 Load Versus Mid-Span Deflection Results

Thirteen reinforced concrete inverted T beams were strengthened or repaired with CFRP strips or steel plates, in addition to the control beam specimen, all these beams were tested under two-point loads to show the effect of strengthening and repairing patterns on their behavior and ultimate load capacity. To measure the deflection, three LVDT sensors were placed, one at the mid-span point, under the load point, and at the third of the supported length. This section shows the experimental work investigation on the behavior of load versus mid-span deflection curves for these inverted T beams. The load-deflection curves of the control beam (ITCC), group one, group two, and group three of inverted T beams show in Figures (4.14) to (4.26). Group one consisted of five strengthening inverted T beams designated as ITF600, ITF900, ITF1200, IT2F1200, and IT3F1200. Group two also consisted of five strengthening inverted T beams ITS600, ITS900, ITS1200, IT2S1200, and IT3S1200. These inverted T beams differ from group one in the type of strengthening. The load-deflection curves of the repaired inverted T beams IT3FR1200 and IT3SR1200 of group three are shown in Figures (4.25) and (4.26). From the load-deflection curves of tested

inverted T beams, it can be discovered that the load versus mid-span deflection response can be divided into three stages of behavior.

The first stage represents the linear behavior of the load-deflection response. This stage covers up to the first crack load area (where the first crack load is defined as the load corresponding to the first deviation from the straight line in the load-deflection curve). Below this limit, the materials were behaving in an elastic fashion and the cracks in the cross-section specimens in the tension areas remain stable. After that, as the load increases, the cracks begin to spread, and their width increases. The concrete and reinforcement in the compression area are still stable.

The second stage of the load-mid span deflection curve represented the behavior of the materials after the initial cracking in the composite section. The stiffness of the beam was decreasing as indicated by the decrease in the inclination relative to the load versus deflection curve. This stage can be distinguished by the inelastic behavior with respect to steel reinforcement.

Finally, in the third stage, the load-mid span deflection curve was distinguished by a decrease in its inclination. The tensile steel reinforcement reaches the stage of strain hardening, as well as the applied load near its final value.

For the control unstrengthened inverted T beams, the decrease in the slope of the curve is more than the decrease in the slope of the curves of strengthening inverted T beams. Also, it can be observed that the strengthened inverted T beams failed suddenly and appeared no ductility.

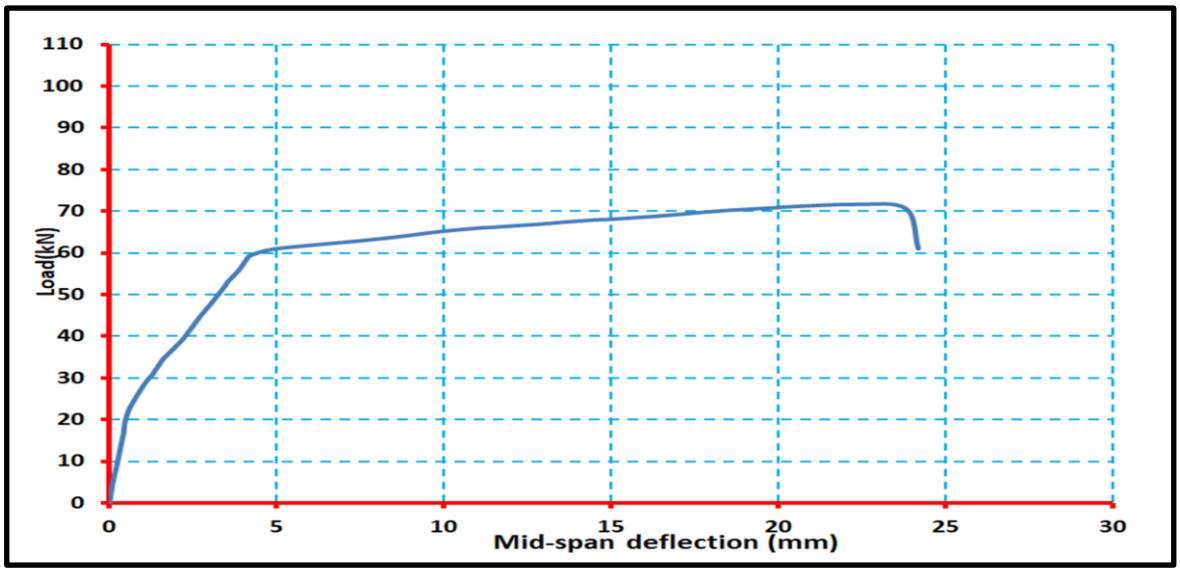

Figure (4-14): Load Vs. Mid-Span Deflection Curve of inverted T beam (ITCC)

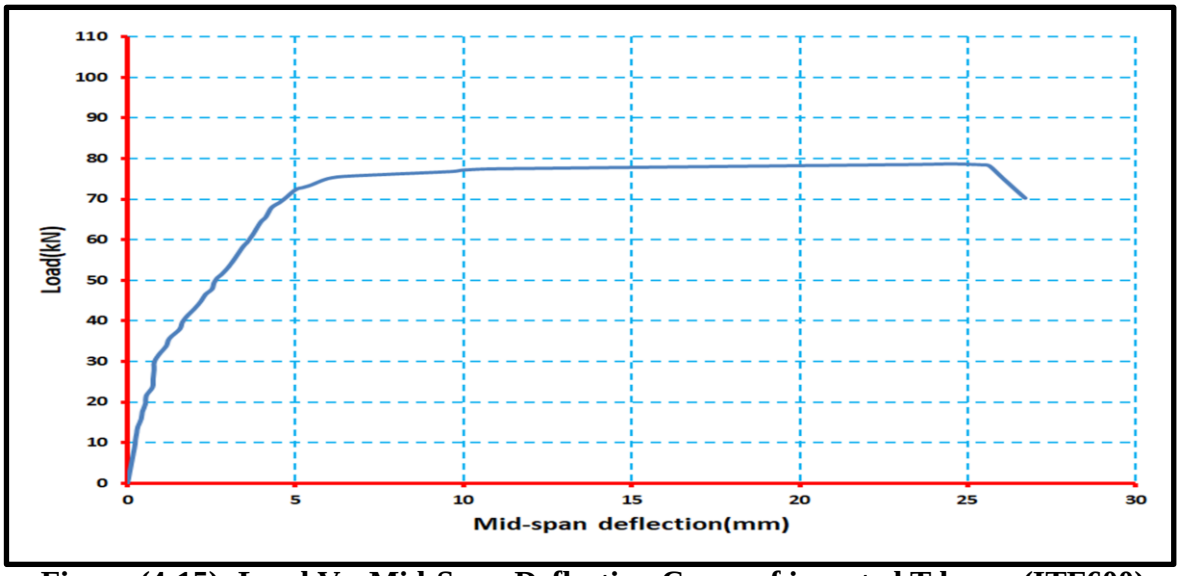

Figure (4-15): Load Vs. Mid-Span Deflection Curve of inverted T beam (ITF600)

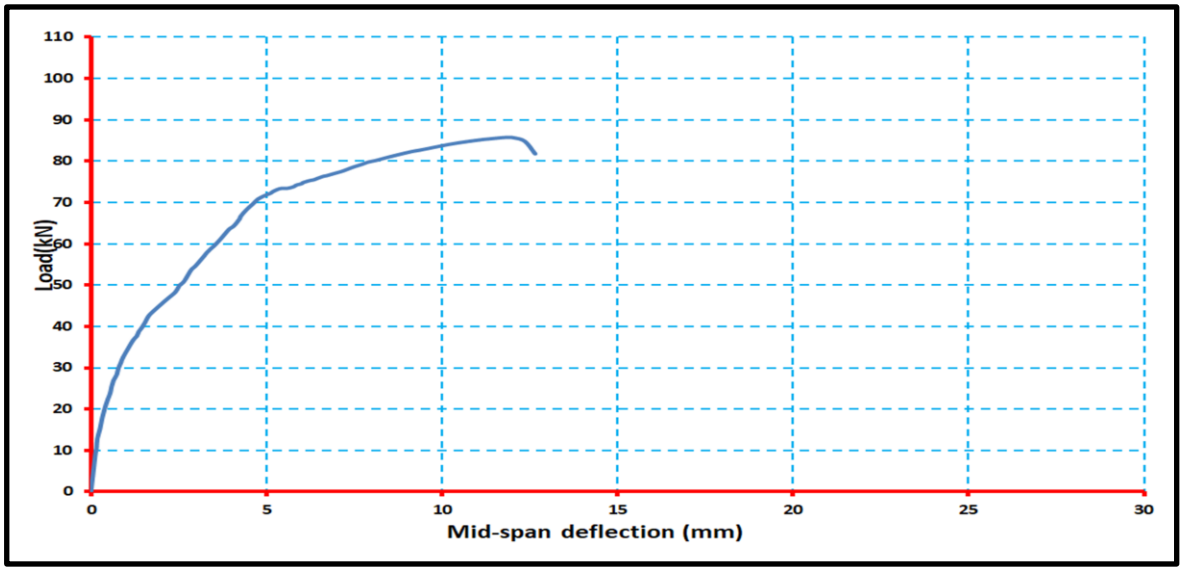

Figure (4-16): Load Vs. Mid-Span Deflection Curve of inverted T beam (ITF900)

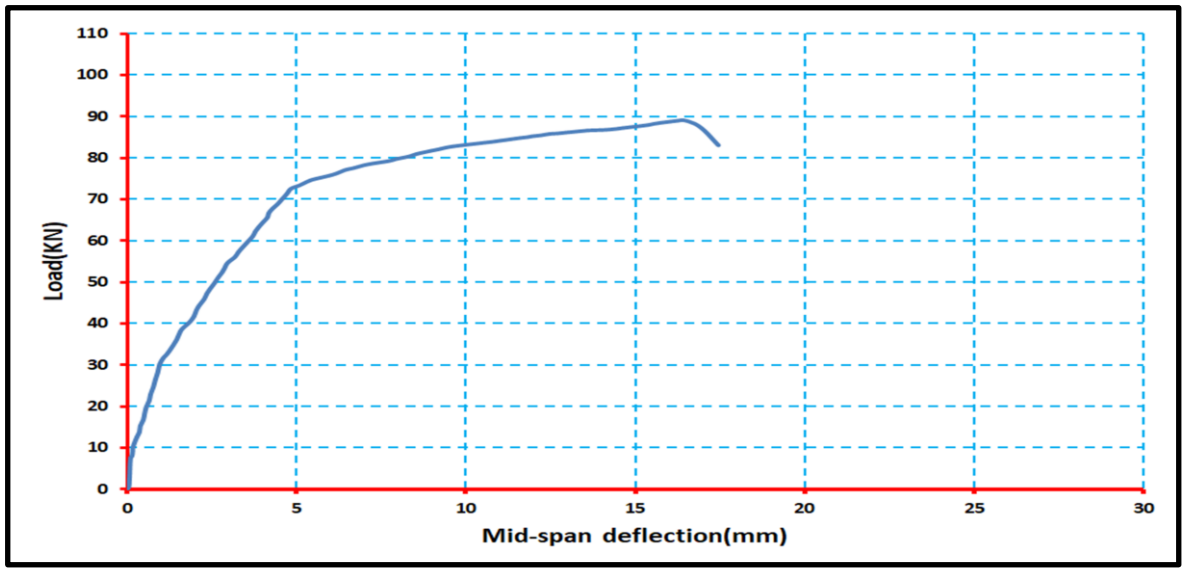

Figure (4-17): Load Vs. Mid-Span Deflection Curve of inverted T beam (ITF1200)

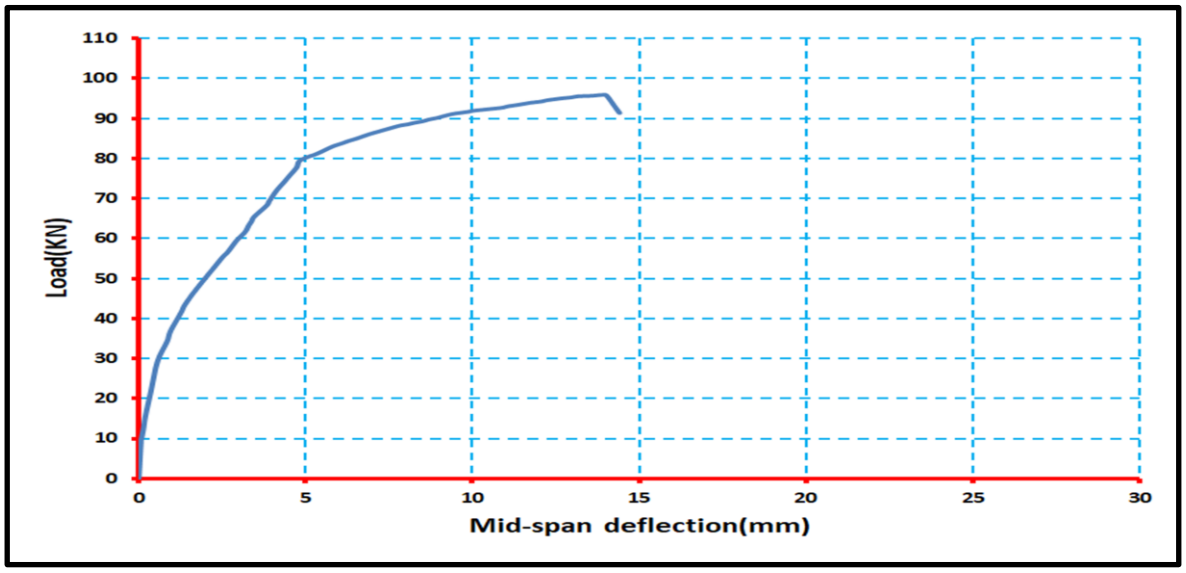

Figure (4-18): Load Vs. Mid-Span Deflection Curve of inverted T beam (IT2F1200)

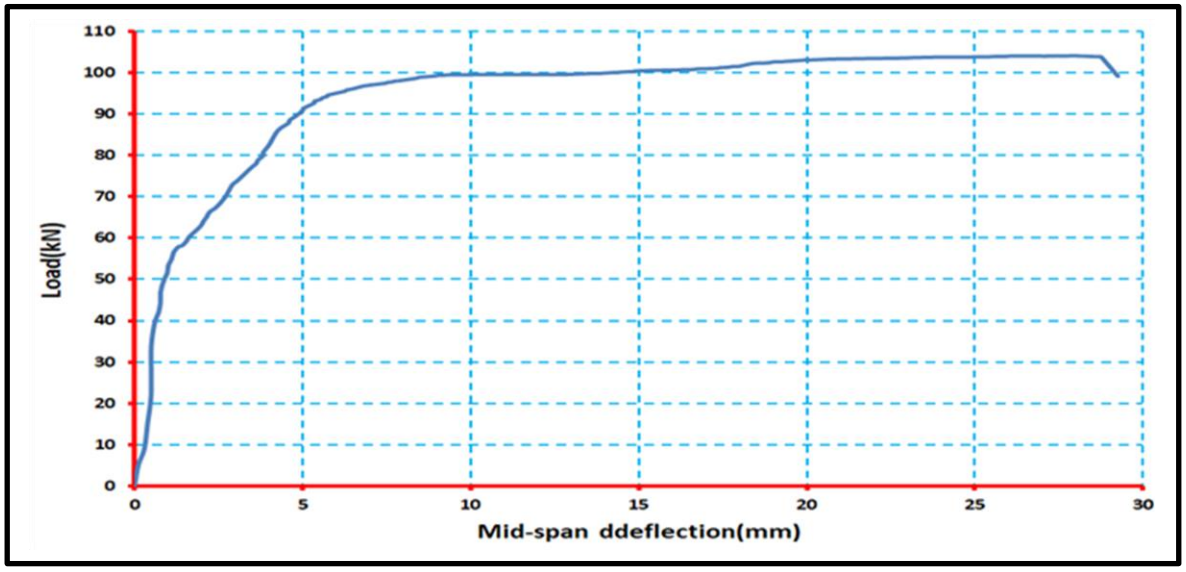

Figure (4-19): Load Vs. Mid-Span Deflection Curve of inverted T beam (IT3F1200)

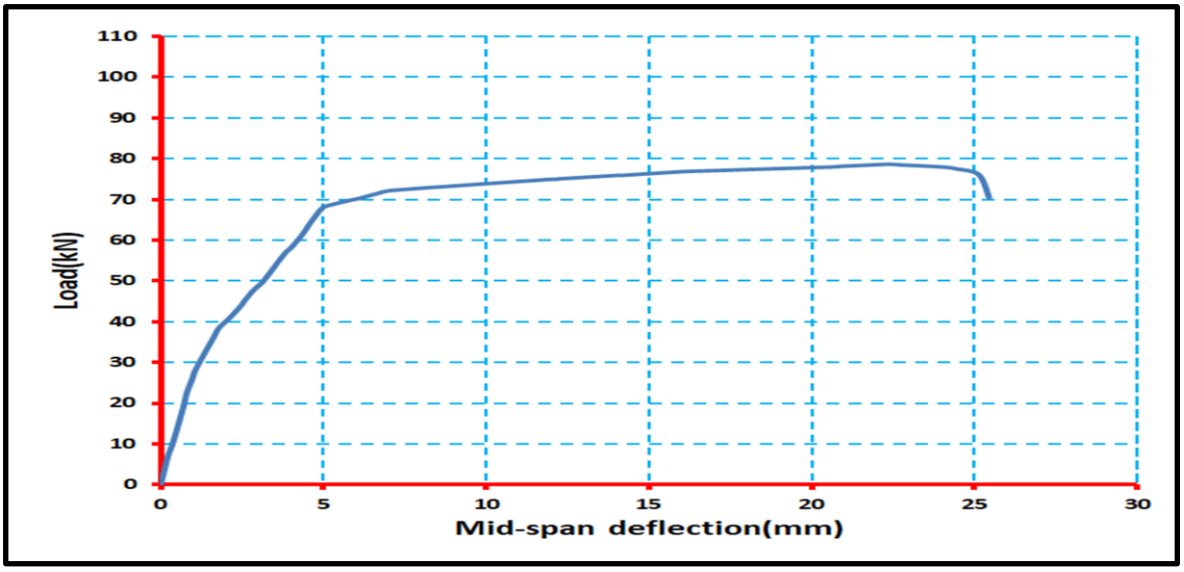

Figure (4-20): Load Vs. Mid-Span Deflection Curve of inverted T beam (ITS600)

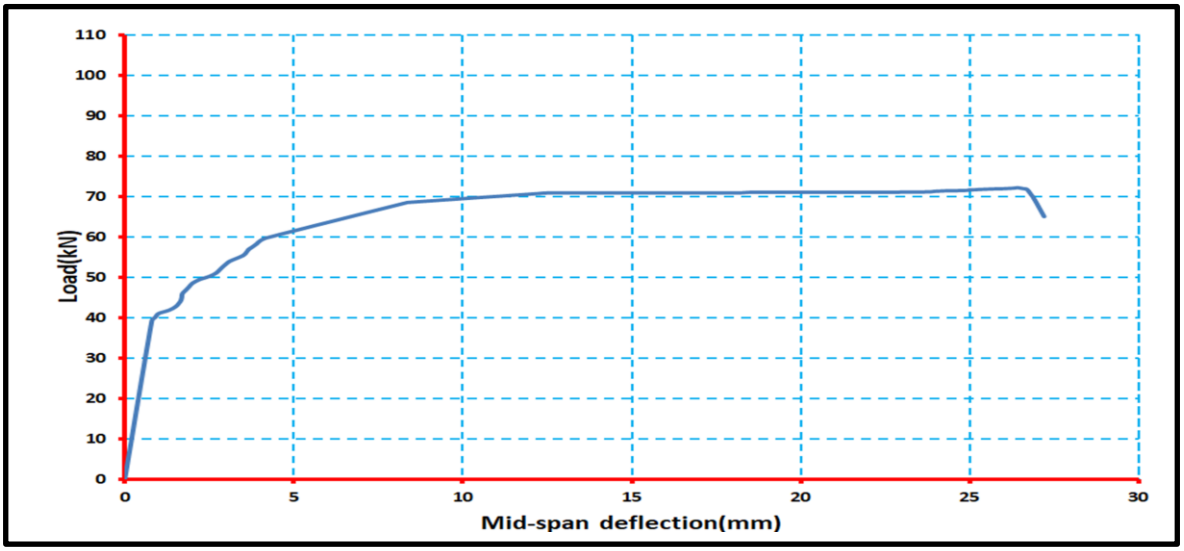

Figure (4-21): Load Vs. Mid-Span Deflection Curve of inverted T beam (ITS900)

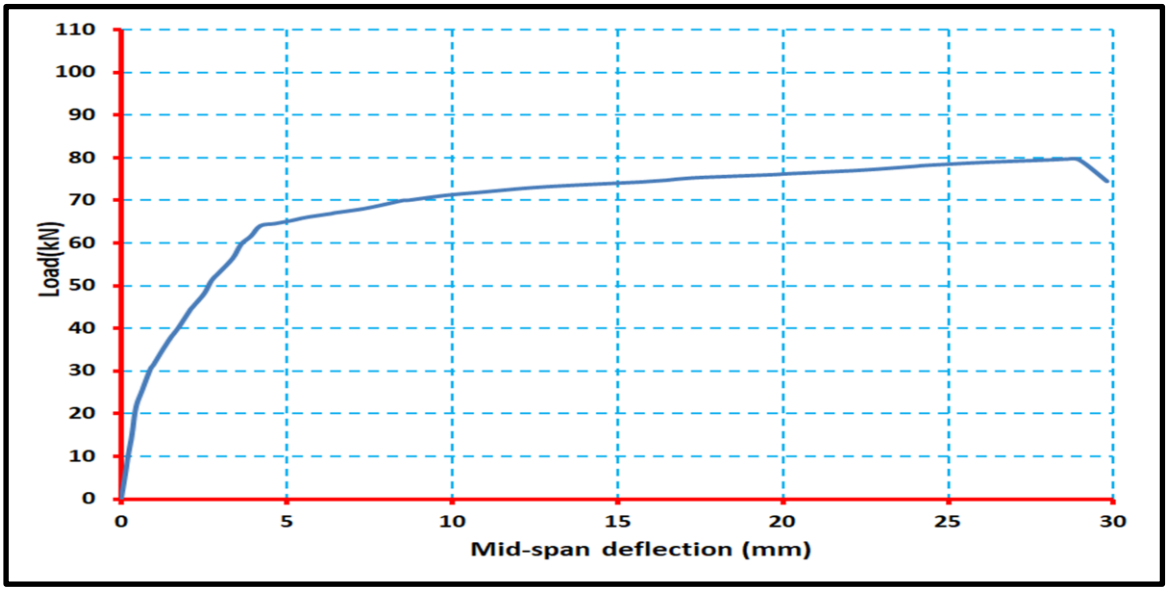

Figure (4-22): Load Vs. Mid-Span Deflection Curve of inverted T beam (ITS1200)

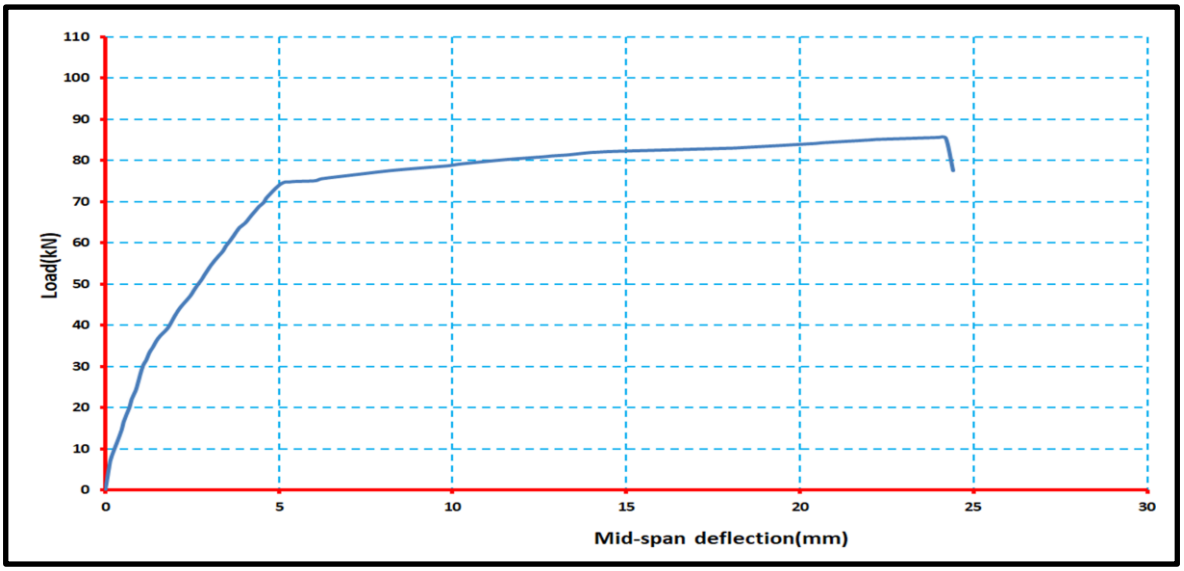

Figure (4-23): Load Vs. Mid-Span Deflection Curve of inverted T beam (IT2S1200)

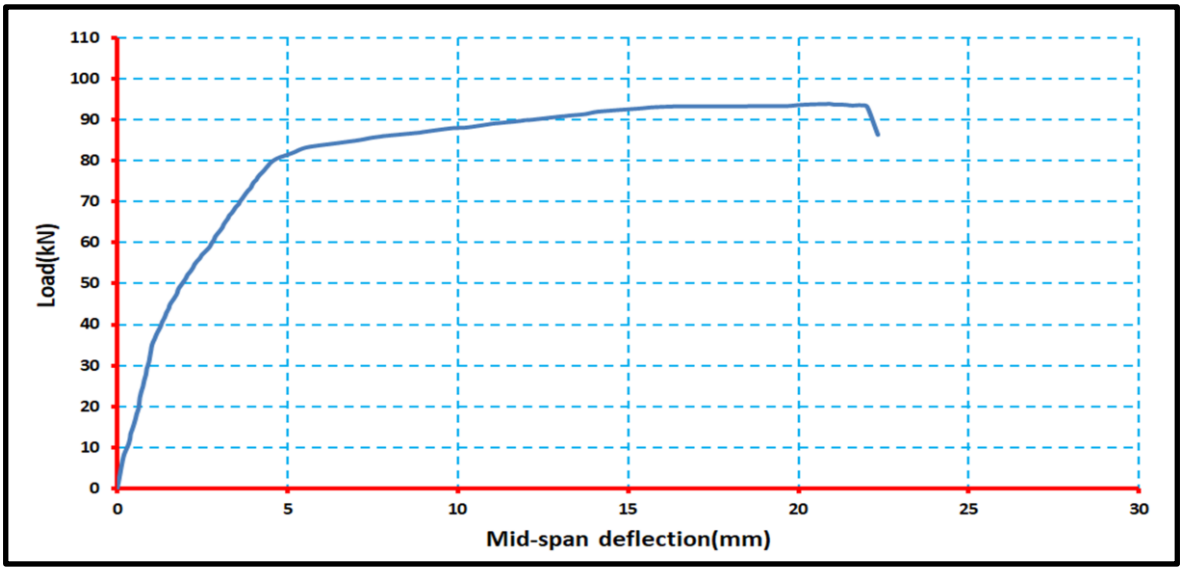

Figure (4-24): Load Vs. Mid-Span Deflection Curve of inverted T beam (IT3S1200)

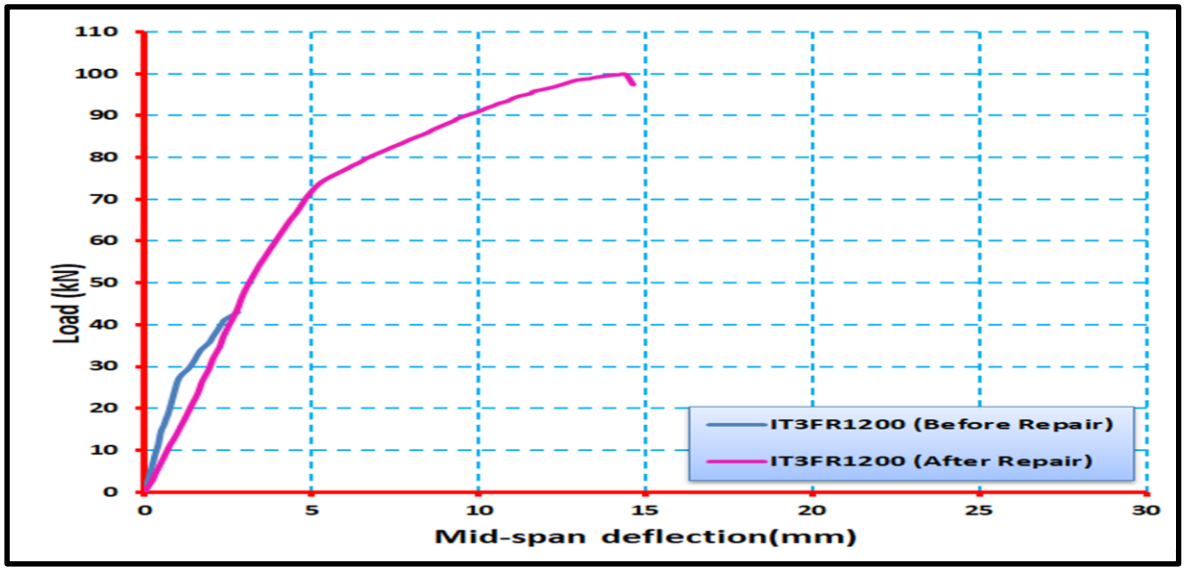

Figure (4-25): Load Vs. Mid-Span Deflection Curve of inverted T beam (IT3FR1200)

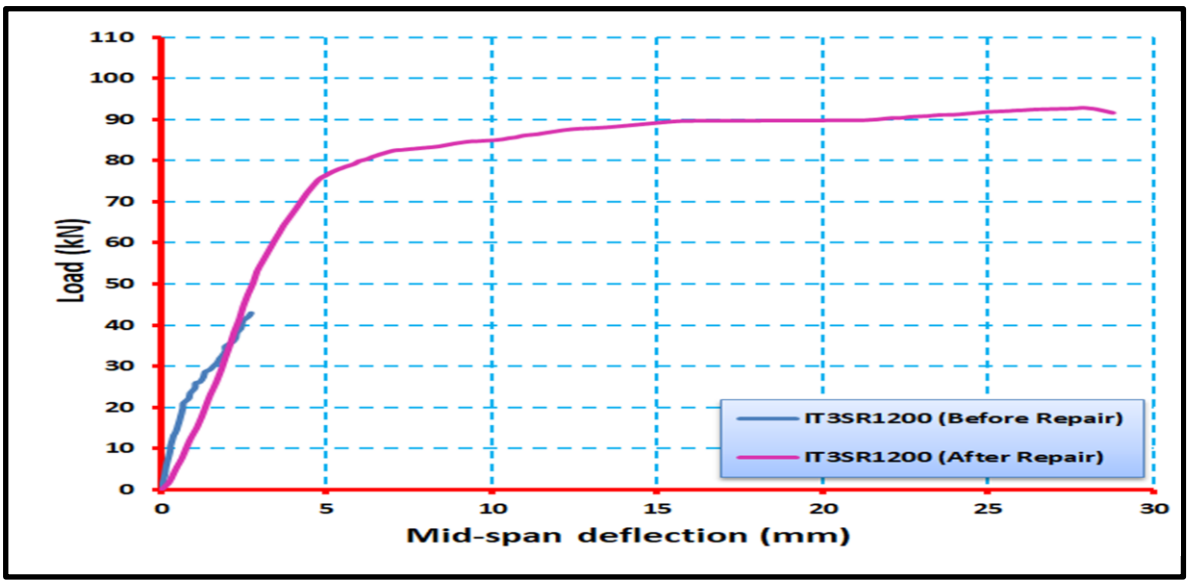

Figure (4-26): Load Vs. Mid-Span Deflection Curve of inverted T beam (IT3SR1200)

Figure (4.27) exhibits the load-deflection curves for group one which consists of the five inverted T beams that were strengthened with CFRP strips ITF600, ITF900, ITF1200, IT2F1200 and, IT3F1200 and control inverted T beam ITCC. Of those curves, it can be noticed that all the strengthened beams give a higher ultimate load capacity compared to the control beam. Also, it can be noticed that the deflection of the strengthened beams ITF600 and IT3F1200 are more than that of the control beam because those strengthened beams have sufficient yield and high plasticity than the control beam.

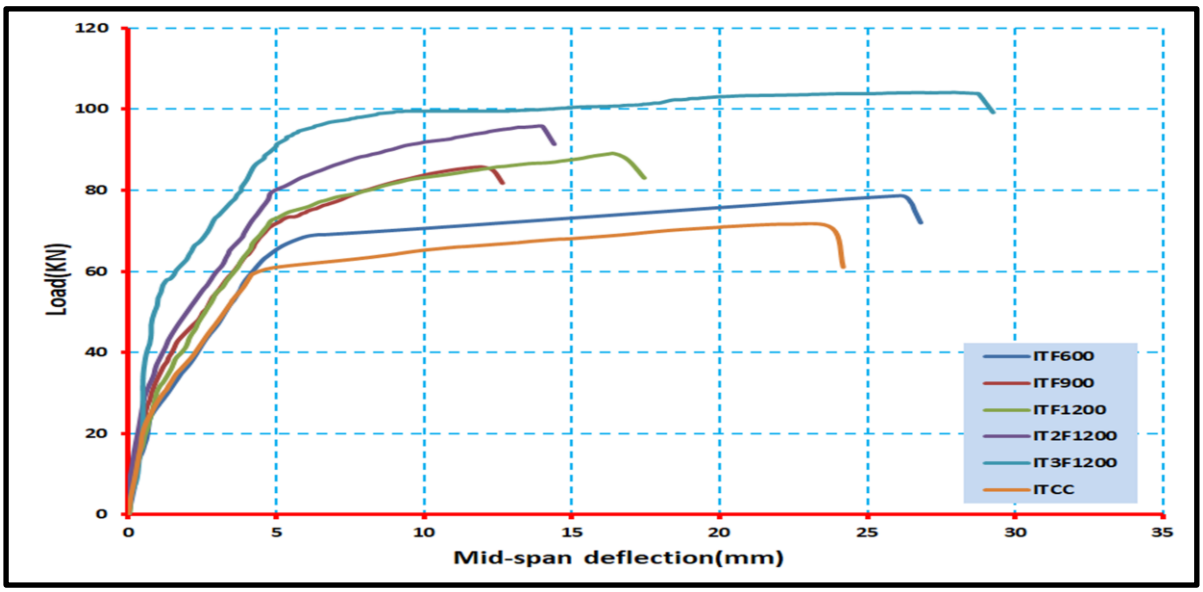

Figure (4-27): Load Vs. Mid-Span Deflection Curve of group one strengthened inverted T beams and control inverted T beam

Figure (4.28) exhibits the load-deflection curves for group two which consist of the five inverted T beams were strengthened with steel plates ITS600, ITS900, ITS1200, IT2S1200, and IT3S1200 and control inverted T beam ITCC. Of those curves, it can be noticed that all the strengthened beams give a higher ultimate load capacity compared to the control beam. Also, it can be noticed that the deflection of all strengthened beams without beam IT3S1200 are more than that of the control beam because those strengthened beams have sufficient yield and high plasticity than the control beam.

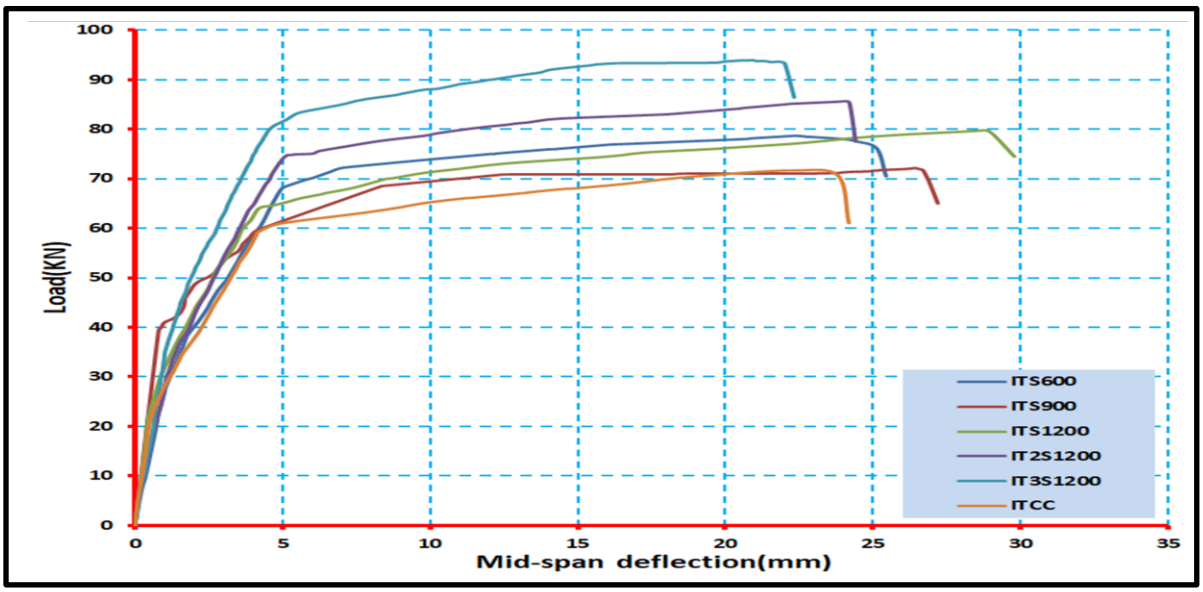

Figure (4-28): Load Vs. Mid-Span Deflection Curve of group two strengthened inverted T beams and control inverted T beam

Figure (4.29) represented the load-deflection curves for group one which consists of the five inverted T beams strengthened with CFRP strips and group two which consisted of the five inverted T beams strengthened with steel plates and control inverted T beam. Of those curves, it can be noticed that all the strengthened beams give a higher ultimate load capacity compared to the control beam. Also, it can be noticed when comparing the strengthened beams with each other, it is noted that the beam IT3F1200 has the highest strength, and the beam ITS1200 has the highest deflection.

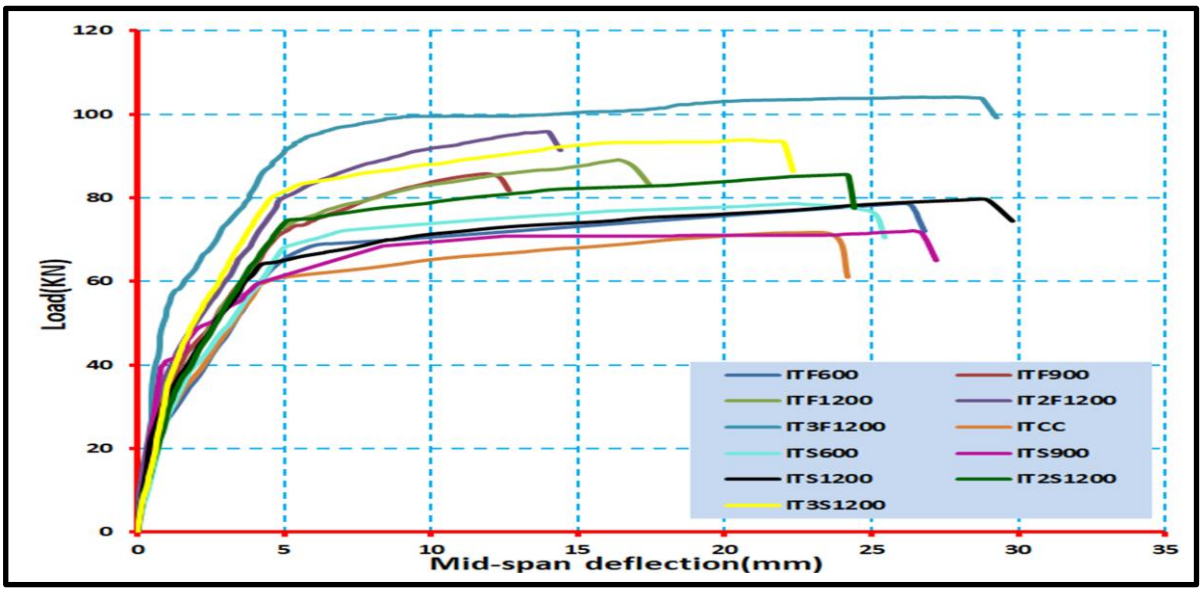

Figure (4-29): Load Vs. Mid-Span Deflection Curve of group one and group two strengthened inverted T beams and control inverted T beam

Figure (4.30) explain the load-deflection curves for group three which consist of the two inverted T beams where one of them was repaired with CFRP sheets IT3FR1200, and the other beam was repaired with steel plates IT3SR1200. When comparing the results with the control beam, it was noticed that both repaired beams gave the highest strength. Beam repaired with CFRP strips gives the highest strength compared to the beam repaired with steel plate and control beam, while the beam repaired with steel plate gives higher deflection because steel plate is more ductility than CFRP sheet.

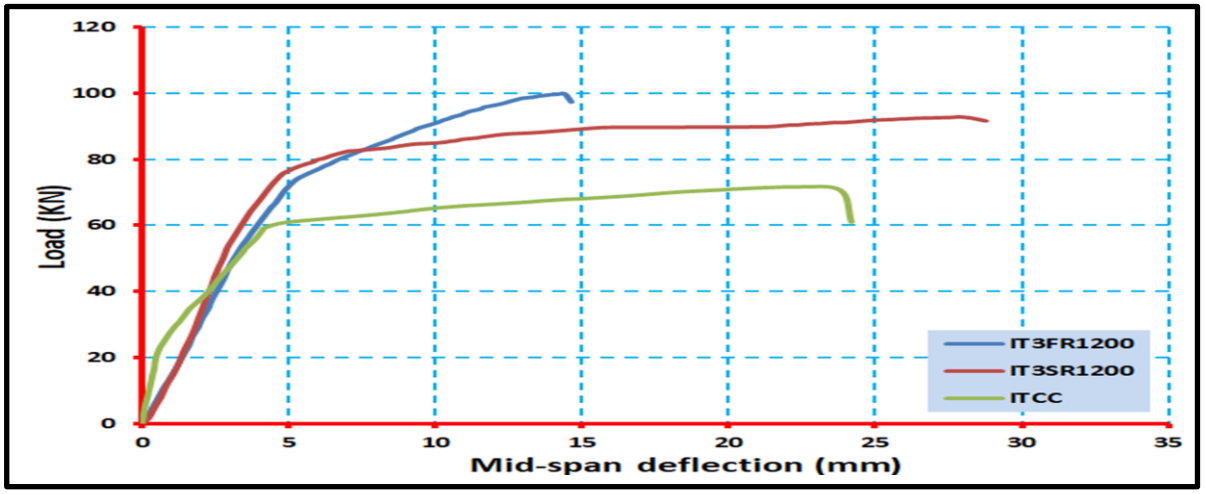

Figure (4-30): Load Vs. Mid-Span Deflection Curve of group three repaired inverted T beams and control inverted T beam

Finally, Figure (4-31) represents the comparison between the control beam and the two retrofitted beams or strengthened beams IT3F1200 and IT3S1200 where these beams loaded until failure, and the other two retrofitted or repaired beams IT3FR1200 and IT3SR1200 where these beams preloaded until appeared the flexural cracks and then retrofitted or repaired with CFRP strips or steel plates, then these beams loaded until failure. The results of the comparison of the curves show that all the strengthened and repaired beams give the highest strength when compared with the control beam. The results also show that all the strengthened beams give more strengthened when compared with the repaired beams.

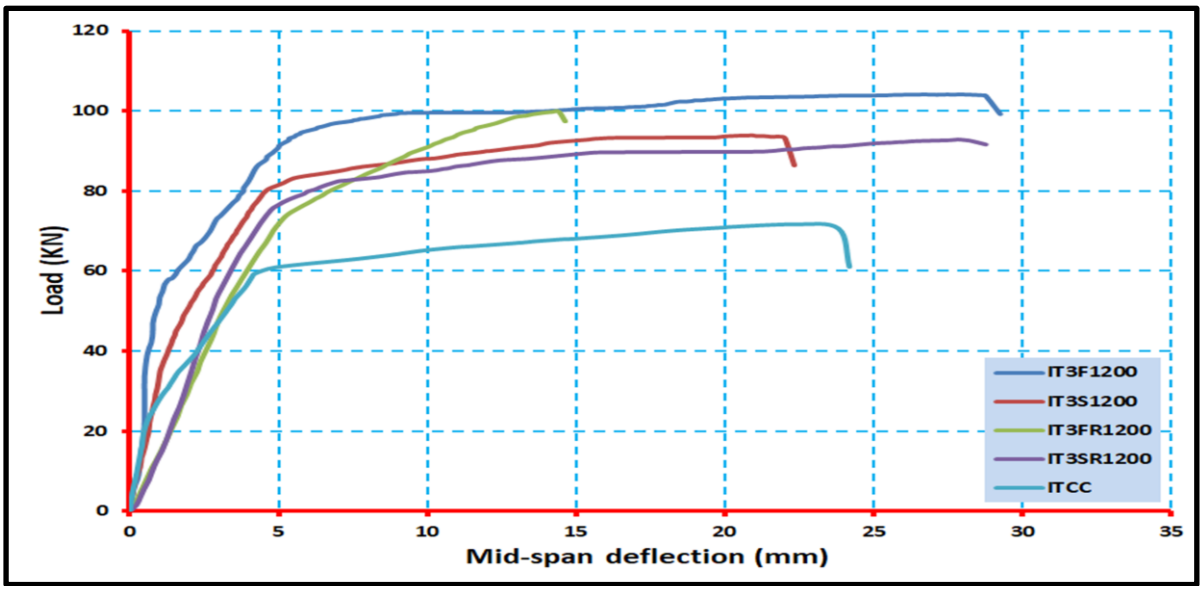

Figure (4-31): Load Vs. Mid-Span Deflection Curve of retrofitted (strengthened and repaired) inverted T beams and control inverted T beam

4.5 Failure Modes and Ultimate Loads

The unstrengthened beam and all the strengthened beams were tested up to failure except the two beams being preloaded then repaired and then tested up to failure. The recorded failure modes and ultimate loads for these beam specimens are founded in Table (4-3).

Table (4-3): The failure modes and the ultimate loads for all tested beam specimens

Group no.	Tested Beams	Pu (kN)	Failure Modes
-------	ITCC	71.652	Flexural failure
Group One	ITF600	78.690	Flexural failure by CFRP debonding
	ITF900	85.754	Flexural failure by CFRP debonding
	ITF1200	89.088	Flexural failure by CFRP rupture
	IT2F1200	95.899	Flexural failure by mid span debonding of CFRP strips
	IT3F1200	104.155	Flexural failure by mid span debonding of CFRP strips
Group Two	ITS600	78.654	Flexural failure by steel plate debonding
	ITS900	72.160	Flexural failure by steel plate debonding
	ITS1200	79.671	Flexural failure by mid span debonding failure of steel plate
	IT2S1200	85.602	Flexural failure by front steel plate debonding
	IT3S1200	93.937	Flexural failure by front steel plate debonding
Group three	IT3FR1200	99.808	Flexural failure by three CFRP strips debonding
	IT3SR1200	92.877	Flexural failure by three steel plates mid debonding

4.6 Ductility

The ductility of reinforced concrete elements is defined as the ability to resist inelastic deformation without any reduction in the bearing capacity until failure. In other words, ductility can be defined as the ratio between the deformations at the ultimate stage to the deformations of the yield. This deformation can represent (curvatures, strains and deflections) **[104]**. In this current study, the ductility index is calculated as the ratio between deflection at the ultimate load (Δu) to yield deflection (Δy).

From the load-deflection curves, the yield deflection (Δy) can be defined as the intersection of the two straight lines for elastoplastic behavior; one line represents the tangent and the other line represent the horizontal line

which passed through the ultimate load as shown in the Figure (4-32). Table (4-4) showed the ductility index results for all tested beam specimens.

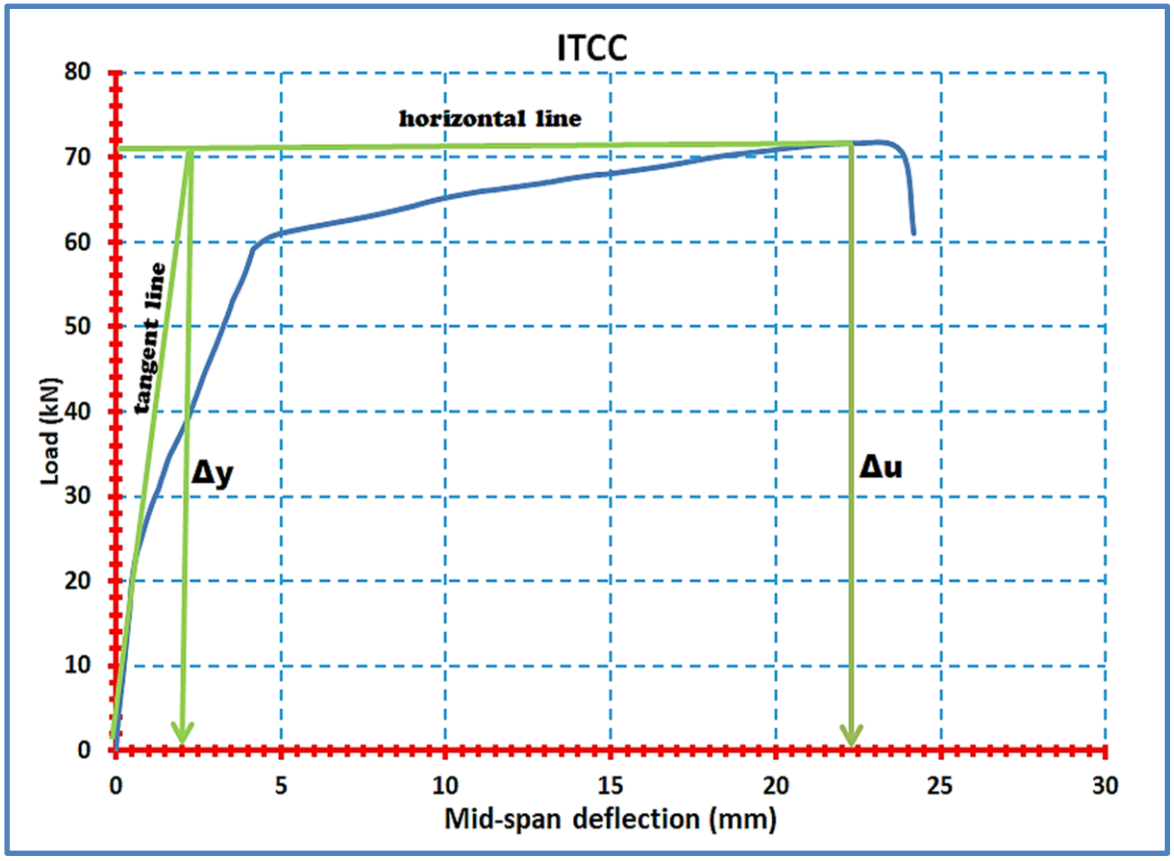

Figure (4-32): Typical diagram for calculating the ductility index of RC beams (ITCC beam specimen)

From Table (4-4) can be noticed that all inverted T beam specimens in the first group and the second group strengthened with CFRP strips or steel plates, respectively, gave lower values of ductility index compared to the control beam specimen, which depends on the values of deflections and may also prove the brittle property possessed by CFRP that makes the current ductility property unadaptable.

Finally, the ductile behavior in all inverted T beam specimens in the third group repaired with CFRP strips or steel plates, respectively, also gave very lower ductile index values compared to the control beam specimen.

Table (4-4): Ductility index for the all tested beam specimens

Group no.	Tested Beams	Deflection (mm)		Ductility index = (Δu/Δy)
		Δy	Δu	
-------	ITCC	2	22.31	11.16
Group one	ITF600	2.5	26.11	10.44
	ITF900	1.5	11.79	7.86
	ITF1200	1.7	16.43	9.66
	IT2F1200	1.4	13.91	9.94
	IT3F1200	3.8	27.85	7.33
Group two	ITS600	2.9	22.41	7.73
	ITS900	2.8	26.41	9.43
	ITS1200	2.6	28.55	10.98
	IT2S1200	2.2	23.99	10.90
	IT3S1200	2	20.91	10.46
Group three	IT3FR1200	5.2	14.41	2.77
	IT3SR1200	5.8	27.84	4.80

4.7 Effect of the length or width of CFRP strips or steel plates on the load capacity of RC inverted T beam specimens

CFRP strips or steel plates are an effective means to increase the ultimate load capacity of the RC beam specimens in the flexure. Twelve RC beam specimens were utilized to investigate the optimum or effective length or width with different lengths or widths of CFRP strips or steel plates and in different percentages relative to the total span length, as the details are shown in Table (4-5). The relationship of ultimate loads capacity with the percentage of lengths or widths of each beam specimens is shown in the Figures (4-33), (4-34), and (4-35). From these figures, it was noted that in strengthening CFRP strips groups in Figure (4-33) that the greater percentage of the chosen length to the total span length, the greater of ultimate load capacity. When the appropriate length of the reinforcement or

strengthening is obtained, the length of the reinforcement is fixed and begins with an increase in the width of the reinforcement or strengthening. Also, when increased the percentage of the chosen width is to the total width, the increased of ultimate load capacity. It was noted that the same behavior occurs in the second group (strengthening with steel plates) as shown in Figure (4-34) except that beam ITS900 gave less ultimate load capacity than beam ITS600 despite the continuous increase in percentage in length and this may be due to the weak link between concrete and steel plates or as a result of the occurrence of debonding failed early as a result of the high concentration of stresses caused by cracks in concrete material. Group three was repaired group, which used the longest length and width, suitable for obtaining the ultimate load capacity, as shown in Figure (4-35).

It can be concluded that the optimal ratio of length or width for CFRP strips or steel plates in all cases and to increase the ultimate load capacity was 80% and 60% respectively of the total length and width of the span, and this has been chosen as the maximum optimum increase in length and width to take into account the cost of materials.

In general, when comparing the CFRP strips group with the steel plates group with respect to the investigation length or width of the strengthening or the repair in order to increase the ultimate load capacity, it was noted that all beam specimens that were strengthened or repaired by CFRP strips gave the highest ultimate load capacity as shown in the Figures (4-36) and (3-37) respectively.

Table (4-5): Beam specimens evaluated in this study

Group no.	Beam specimens	Description
-------	ITCC	----------
Group one	ITF600	The effective length of CFRP strip represent 40%** of the total span length The effective width of CFRP strip represent 20%*** of the total span width
	ITF900	The effective length of CFRP strip represent 60% of the total span length The effective width of CFRP strip represent 20% of the total span width
	ITF1200	The effective length of CFRP strip represent 80% of the total span length The effective width of CFRP strip represent 20% of the total span width
	IT2F1200	The effective length of CFRP strips represent 80% of the total span length The effective width of CFRP strips represent 40% of the total span width
	IT3F1200	The effective length of CFRP strips represent 80% of the total span length The effective width of CFRP strips represent 60% of the total span width
Group two	ITS600	The effective length of steel plate represent 40%** of the total span length The effective width of steel plate represent 20%*** of the total span width
	ITS900	The effective length of steel plate represent 60% of the total span length The effective width of steel plate represent 20% of the total span width
	ITS1200	The effective length of steel plate represent 80% of the total span length The effective width of steel plate represent 20% of the total span width
	IT2S1200	The effective length of steel plates represent 80% of the total span length The effective width of steel plates represent 40% of the total span width
	IT3S1200	The effective length of steel plates represent 80% of the total span length The effective width of steel plates represent 60% of the total span width
Group three	IT3FR1200	The effective length of CFRP strips represent 80% of the total span length The effective width of CFRP strips represent 60% of the total span width
	IT3SR1200	The effective length of steel plates represent 80% of the total span length The effective width of steel plates represent 60% of the total span width

** (600/1500)*100	***(50/250)*100

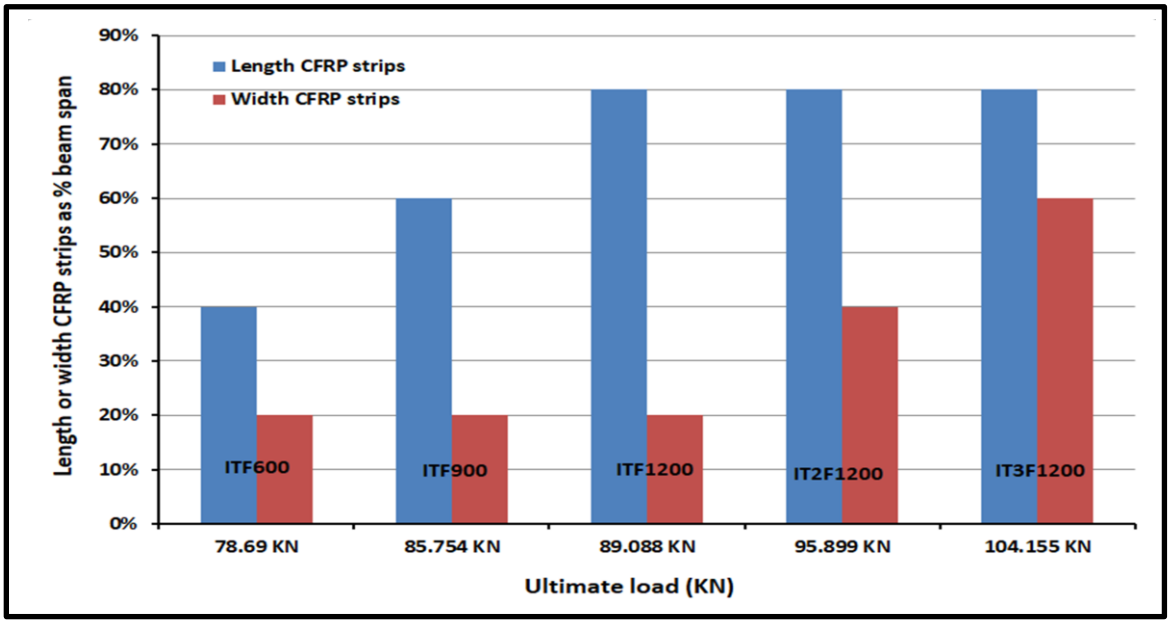

Figure(4-33):Group one, comparisons of the ultimate load capacity vs length or width CFRP strips

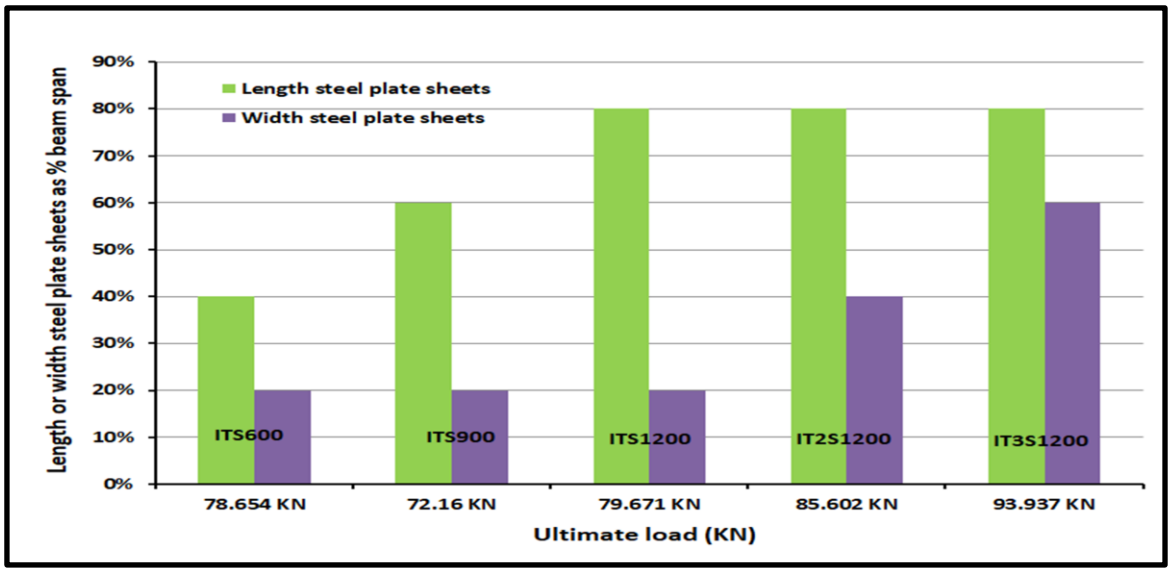

Figure(4-34):Group two, comparisons of the ultimate load capacity vs length or width

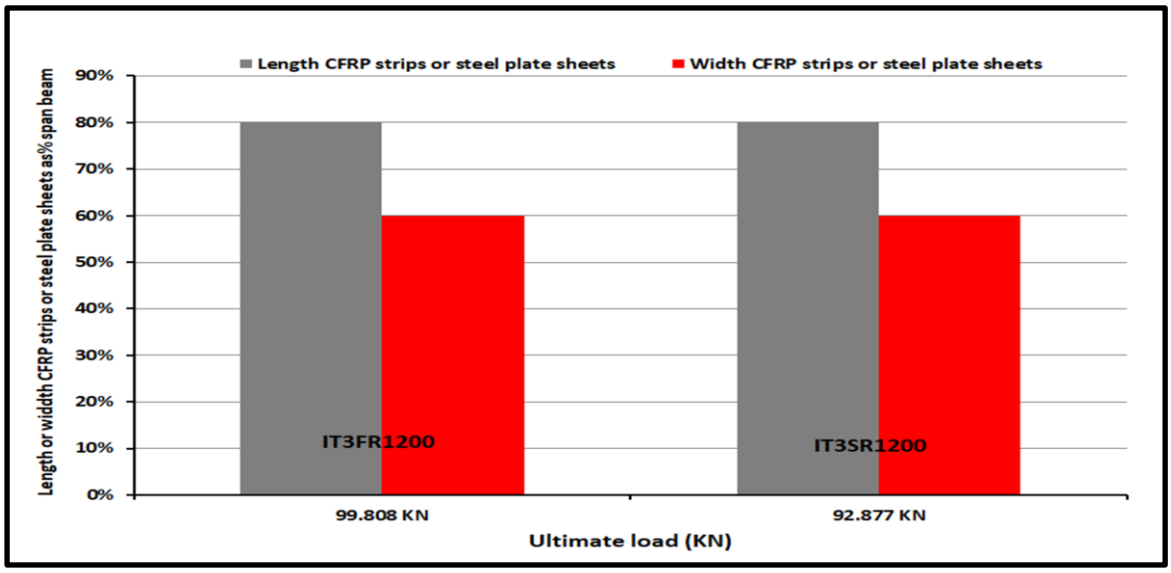

Figure(4-35):Group three, comparisons of the ultimate load capacity vs length or width CFRP strips

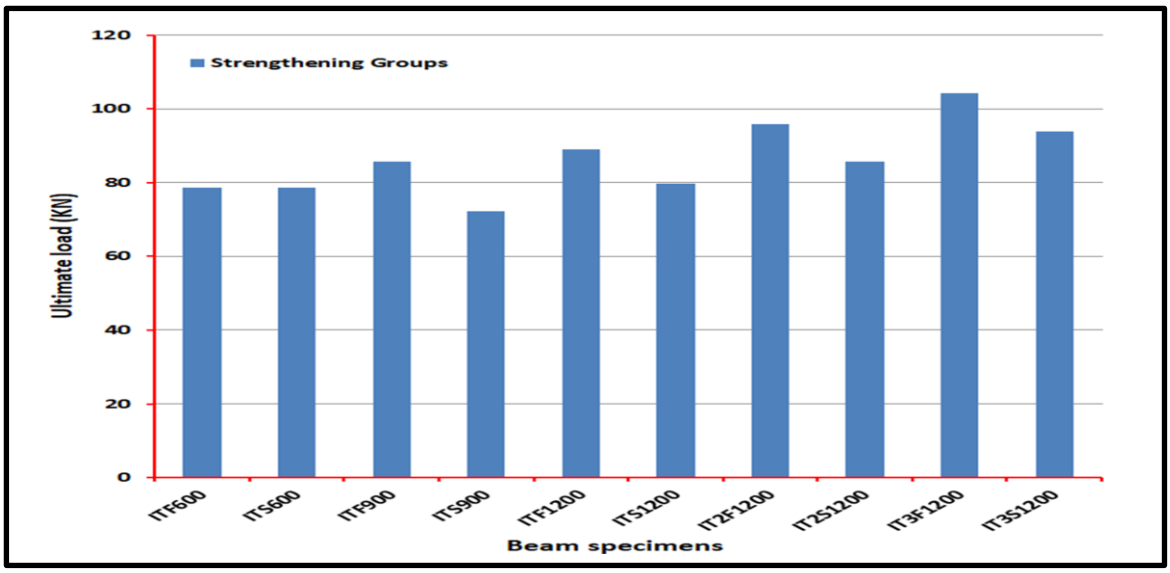

Figure (4-36): Strengthening groups, Ultimate load for experimental beam specimens

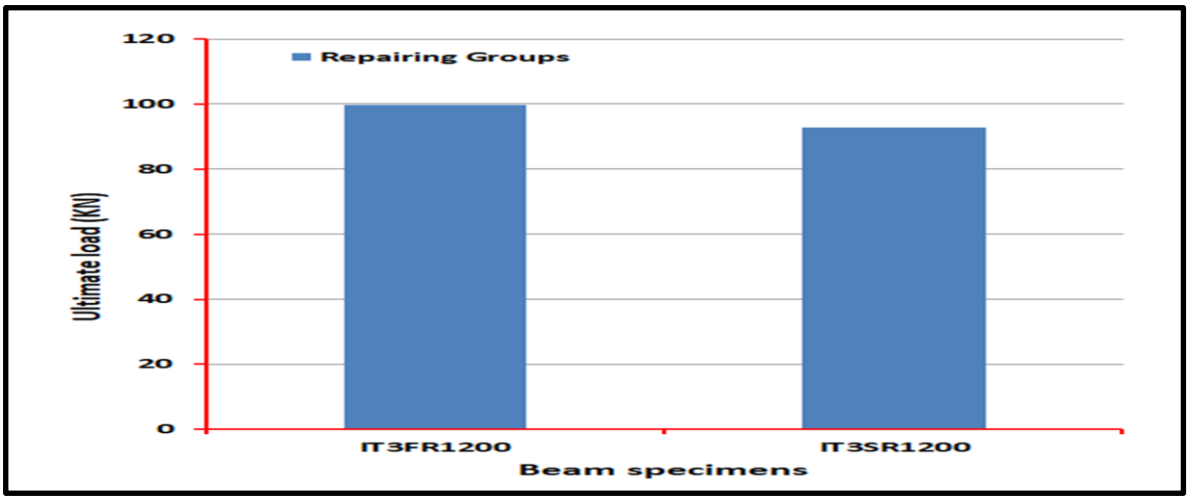

Figure (4-37): Repairing groups, Ultimate load for experimental beam specimens

4.8 Stiffness Criteria

Stiffness is defined as the load needed to produce a unit deformation at any time in a concrete member. In this study, the stiffness criterion was represented by a slope of the secant line drawn in the load-deflection curve at 0.75 times of ultimate load **[105]**. The stiffness calculations for all the tested beam specimens are shown in Table (4-6). It was noted from this table that the stiffness of all strengthening beam specimens in the first or second group increases in comparison with the stiffness of the control beam specimen. In the third group, the repaired beams were exposed to the load, emptied, strengthened, and then subjected to the load, the CFRP strips tried to restore the stiffness of the repaired beam to a value higher than that of the control beam, also the steel plate restored the stiffness of the repaired beam higher than that of the control beam.

It was also noted that the beam that has the longest strengthening length and the widest strengthened was given more stiffness, because the beam that is strengthened with the longest strengthening length is more efficient in the crack area because this sufficient length extends outside the region of the maximum moment. In general, when compared to the strengthening system,

CFRP is more effective in giving greater stiffness but in the repair system, steel plate is more effective in giving greater stiffness.

Table (4-6): Stiffness parameter for the tested beam specimens

Group no.	Beam specimens	pu*0.75 (kN)	Deflection at 0.75 pu (mm)	stiffness K (kN/mm)
-------	ITCC	53.739	3.6	14.928
Group one	ITF600	59.018	3.9	15.133
	ITF900	64.316	3.7	17.378
	ITF1200	66.816	4.33	15.431
	IT2F1200	71.924	4.19	17.166
	IT3F1200	78.116	3.7	21.113
Group two	ITS600	58.991	3.8	15.524
	ITS900	54.120	3.1	17.458
	ITS1200	59.753	3.6	16.598
	IT2S1200	64.202	3.77	17.030
	IT3S1200	70.4523	3.6	19.570
Group three	IT3FR1200	74.856	4.99	15.001
	IT3SR1200	69.658	4	17.414

4.9 Moment-Curvature Relationships

The moment-curvature relationships for the test beam specimens can be obtained by using the data of the experimental load-deflection.

The curvature of the tested beam specimens can be calculated depended on the reference **[106]** as the following:

$$Ø=\frac{1}{R} \quad \text{---------- 1}$$

From figure (4-38) obtained on as following:

OC'=OD'=OE'=R ----------2

Where the denote (R) means the radius of circle .

Using the pythagoream theorm:

$OD'^2=OC'^2 + CD'^2$ ----------3

OC'=OM-CM'

=R-(Δmid – ΔL)

OC'=R-y ----------4

Substituting this value in equation (3) and obtained:

$R^2=(R^2-2Ry+y^2) +\frac{L^2}{100}$ ----------5

$2Ry=(y^2 + \frac{L^2}{100})$ → $R=\frac{y^2+\frac{L^2}{100}}{2y}$ ----------6

Substitute Equation (6) into Equation (1), produces the following:

$Ø=\frac{1}{R}$ → $Ø=\frac{2y}{y^2+\frac{L^2}{100}}$ ----------7

y = Δmid – ΔL ----------8

Substituting equation (8) in equation (7) in order to obtain the curvature of the tested beam specimen

$Ø=\frac{2(Δmid-ΔL)}{(Δmid-ΔL)^2+\frac{L^2}{100}}$ ----------9 which is required

Where :

Ø=Curvature of tested beam specimens.
Δmid=Deflection value from LVDT which placed in mid span.
ΔL=Deflection value from LVDT which placed under the load.
L=The clear span length of tested beam specimens.

Moment can be calculated at mid span of simply supported beam as followed:

$$M=\frac{PL}{5} \quad \text{----------10}$$ which is required

Where :

M=moment at mid span of the simply supported beam.
P= load of tested beam specimens.
L=The clear span length of tested beam specimen.

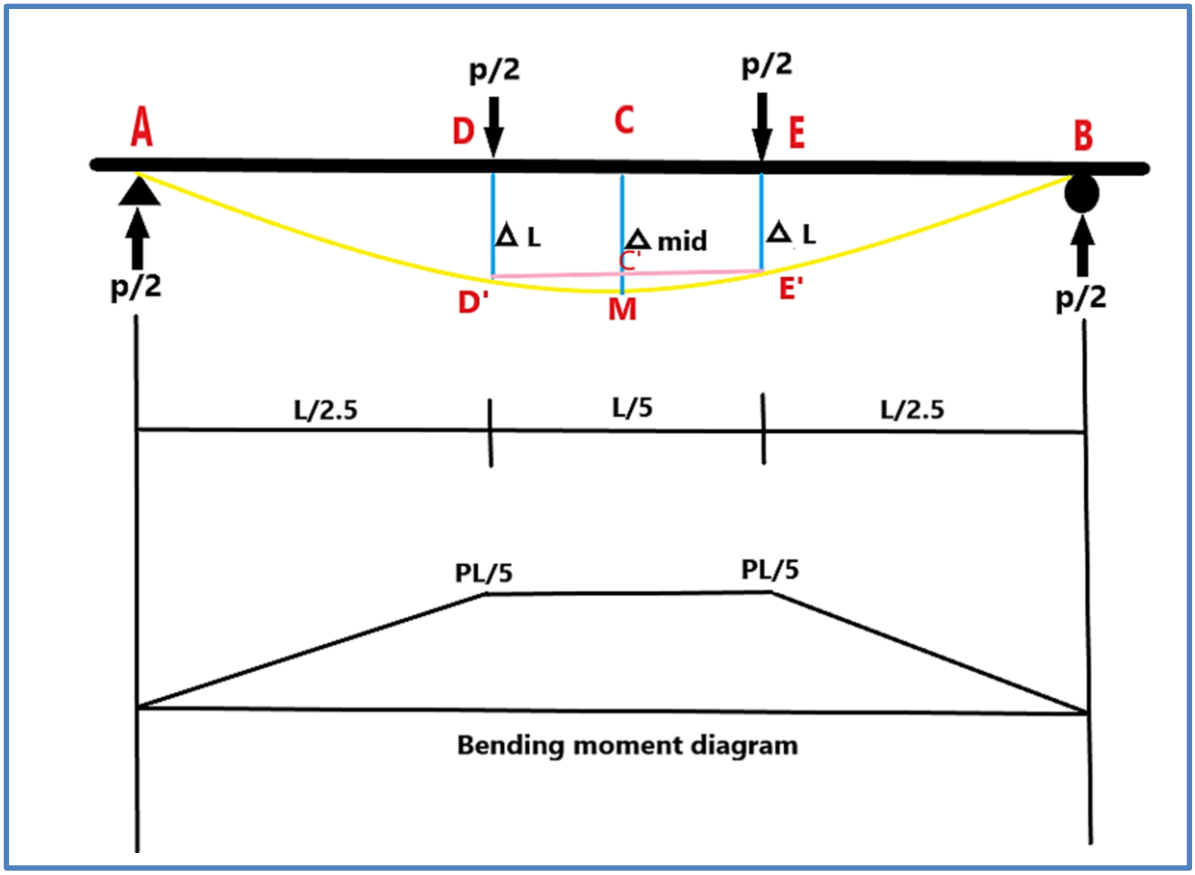

Figure (4-38): Bending moment diagram and Deflection profile for tested beam specimens (continue)

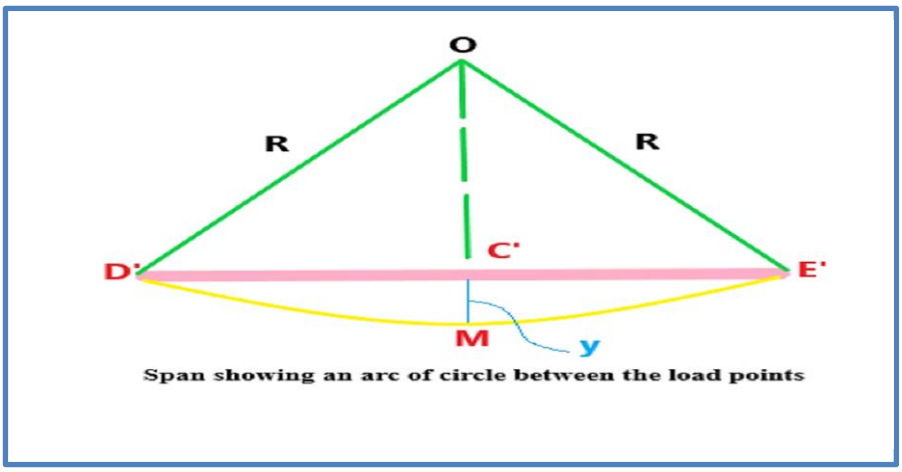

Figure (4-38): Bending moment diagram and Deflection profile for tested beam specimens (continued)

Applying Equation (9) and (10) to the load –deflection curves for the test beam specimens, gives Figures (4-39) to (4-43) which represent the moment –curvature relationship.

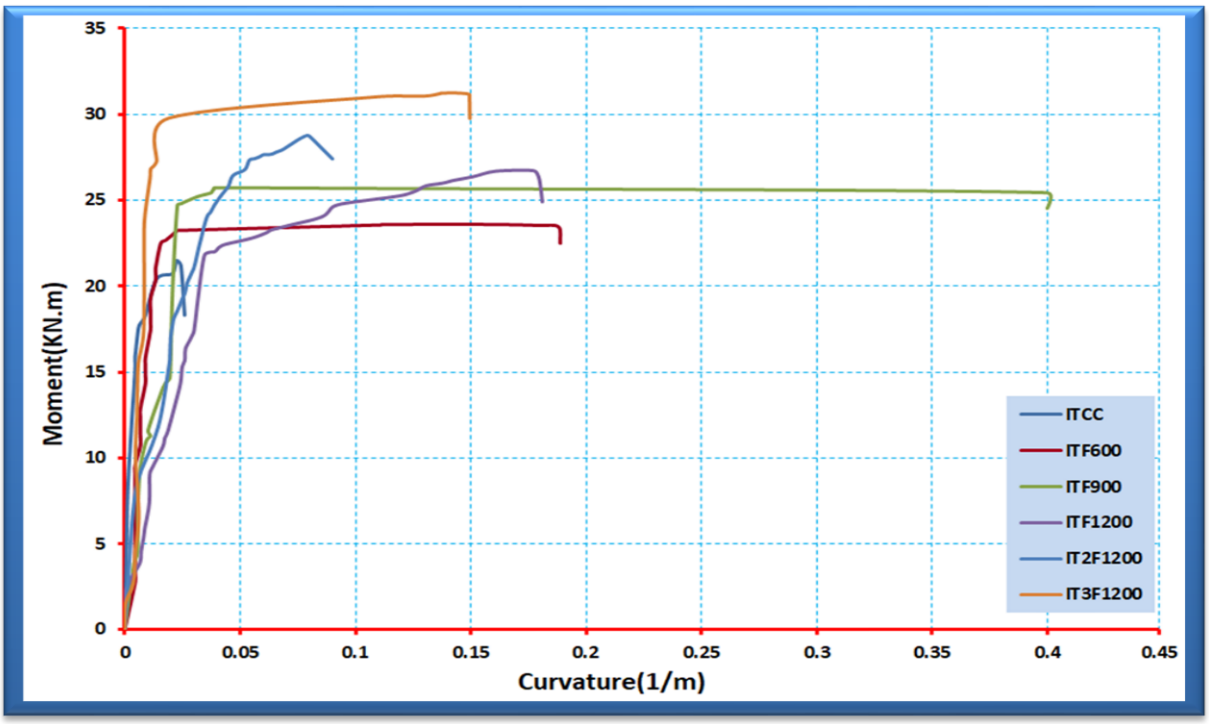

Figure(4-39):Moment-Curvature Relationship of CFRP strip Group with Control beam specimen

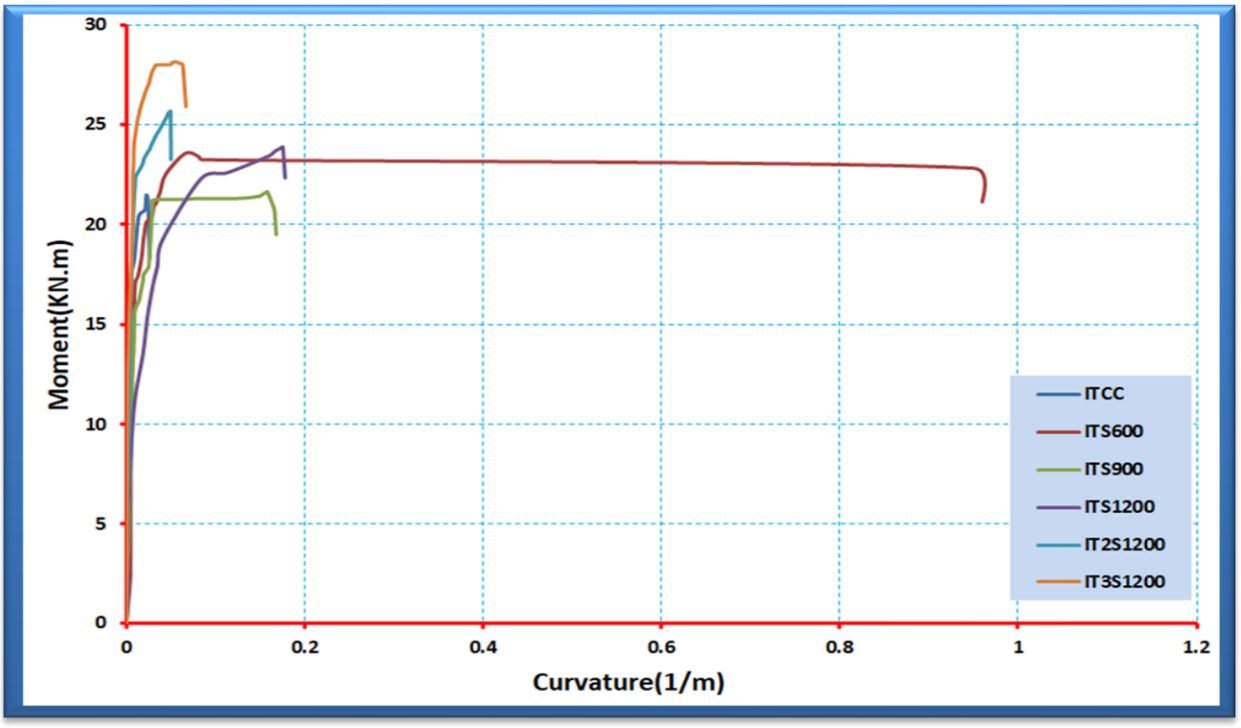

Figure(4-40):Moment-Curvature Relationship of steel plate group with Control beam specimen

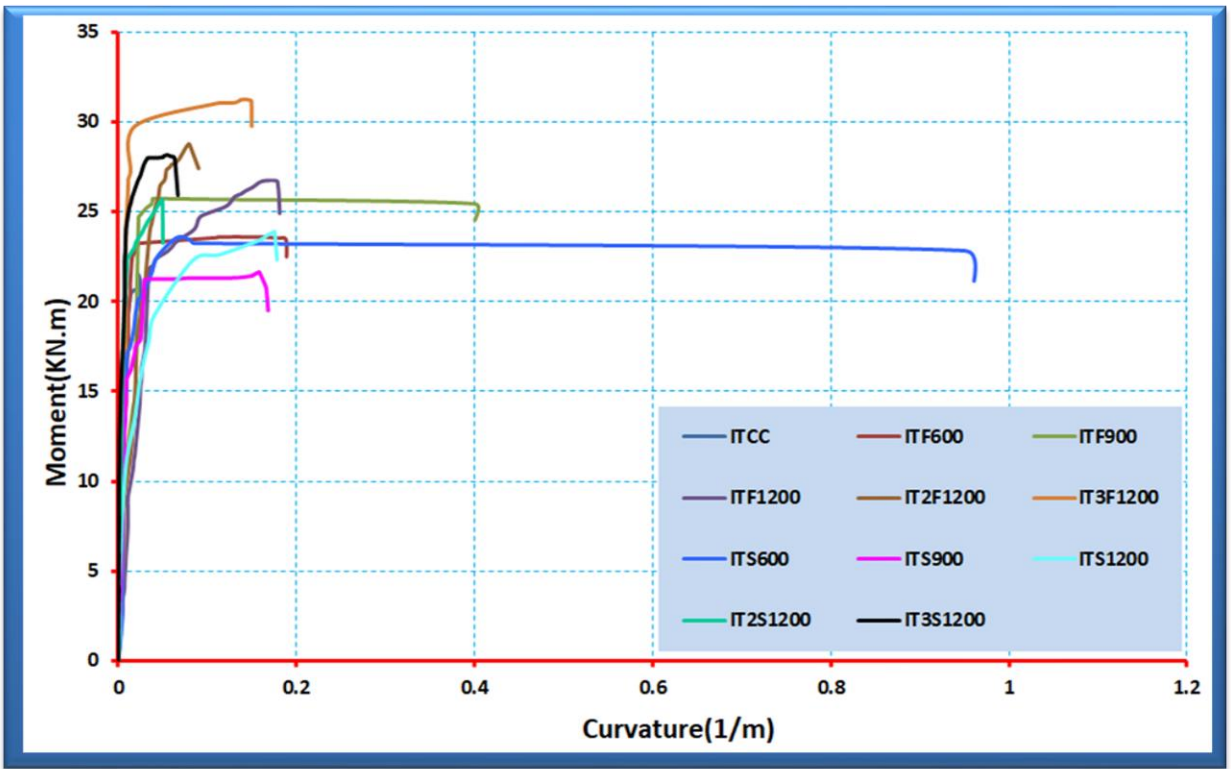

Figure(4-41):Moment-Curvature Relationship of all strengthening groups with Control beam specimen

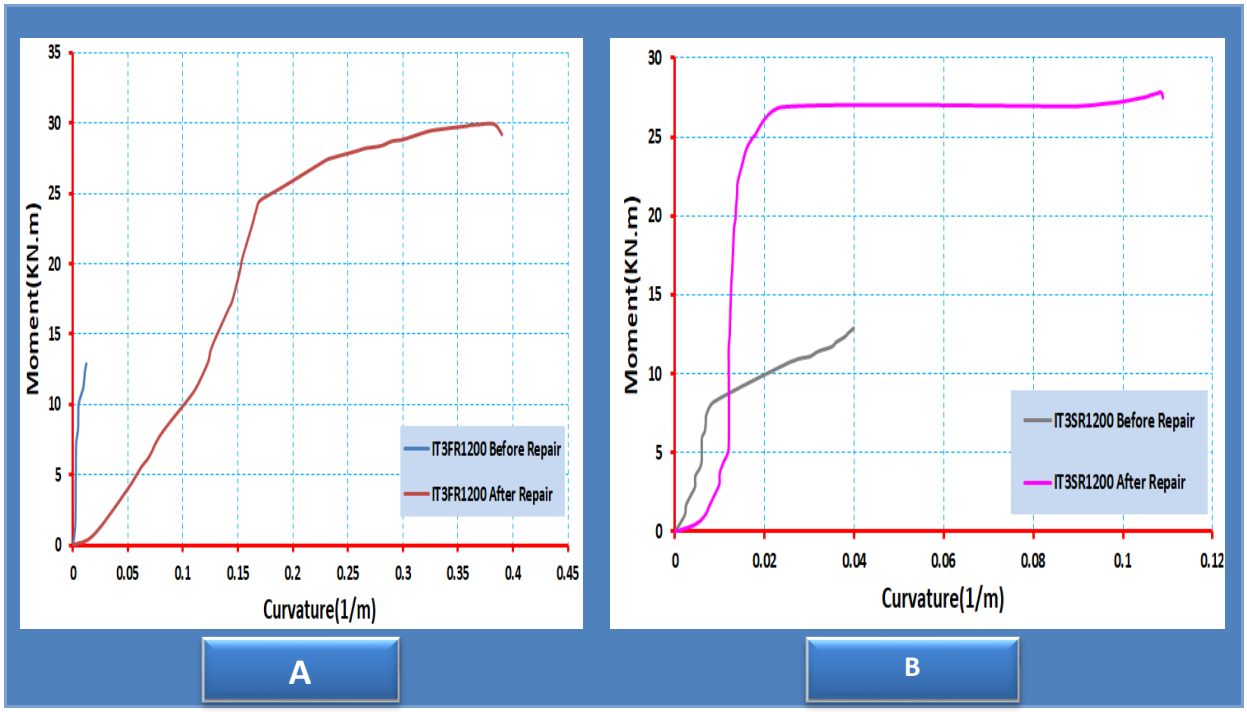

Figure (4-42): Moment-Curvature Relationship of Repaired Group

A: Represent Moment-Curvature Relationship of inverted T beam specimen before and after Repaired with CFRP strips.

B: Represent Moment-Curvature Relationship of inverted T beam specimen before and after Repaired with steel plates.

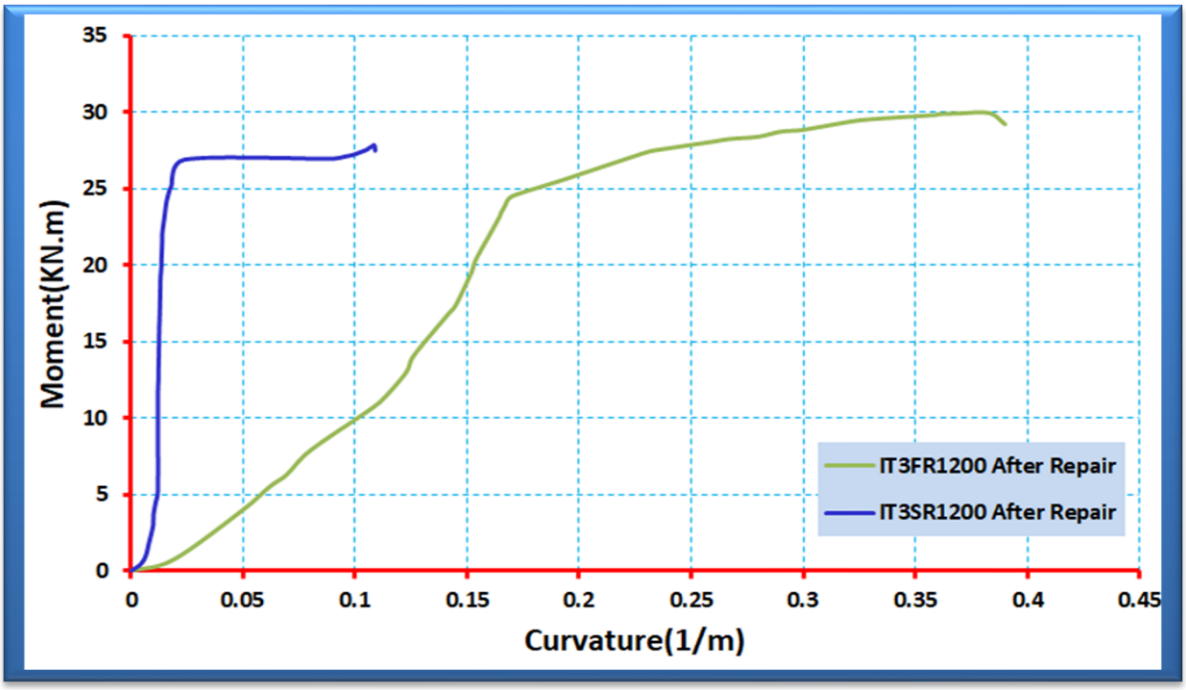

Figure(4-43):Moment-Curvature Relationship for specimens IT3FR1200 and IT3SR1200 (After Repair)

4.10 Energy Absorption (EA)

In this section, the energy absorption (EA) is estimated by calculating the areas under the curve of load versus mid-span deflection **[107]**. Figure (4-44) shows how to calculate the energy absorption in this study. In general, the results of the test in the Table (4-7), through which the energy absorption was calculated, indicating that the ITF600 beam has higher absorption energy compared to the control beam. Also, in the first group, an increase in energy absorption was observed in the IT3F1200 beam, and this beam is of sufficient length and width of carbon fiber, which in turn provides high absorption energy. As for the second group, all beams strengthened with steel plate gave higher absorption energy compared to the control beam. The third group had a beam repaired with a steel plate, which also gave higher absorption energy compared to the control beam and the beam repaired with a CFRP strips.

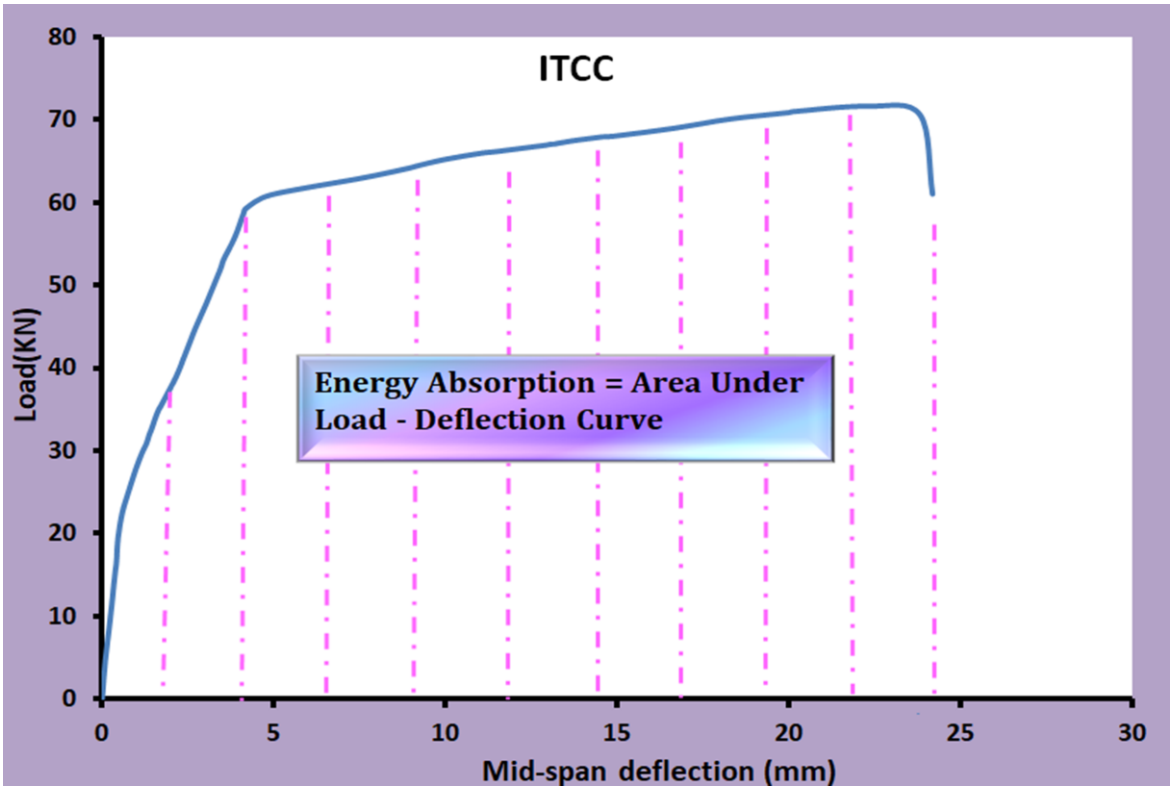

Figure (4-44): Example of diagram for determinations of area under the load-displacement curve for Inverted T beam (ITCC)

Table (4-7): The energy absorption capacity for the tested beam specimens

Group no.	Beam specimens	Energy Absorption Capacity (kN.mm)
-------	ITCC	1498.13
Group One	ITF600	1910.47
	ITF900	856.44
	ITF1200	1268.23
	IT2F1200	1114.26
	IT3F1200	2770.47
Group Two	ITS600	1753.93
	ITS900	1784.89
	ITS1200	2074.19
	IT2S1200	1804.50
	IT3S1200	1827.83
Group Three	IT3FR1200	1048.85
	IT3SR1200	2304.43

CHAPTER FIVE

Finite Element Analysis

5.1General

Finite Element Analysis is an accurate, economical, and effective method for studying the complex behavior of various structural elements in civil engineering. The ABAQUS program is one of the most common programs used in finite element analysis for the purpose of obtaining accurate modeling results. In this study, ABAQUS/CAE 2019 is utilized for simulating numerically the behavior of reinforced concrete (RC) inverted T beams. The experimental test method is more reliable in order to know the behavior of the structural structures, but despite that, this method has several disadvantages, including that the results in each test can be different in addition to that, the experimental test method is expensive and takes a long time to complete. The importance of the finite element method, as well as for comparing and verifying theoretical results with experimental results **[108]**. In this chapter, the results of the experimental tests will be compared with the results of the analytical modeling for thirteen beams consisting of three groups in addition to the control beam with and without strengthening and repair by using CFRP sheets or steel plates, which were summarized in Figure (5-1); details developed for a finite element model include the element types, the constitutive model, the mesh size, and the boundary conditions of each component. Finally, a parametric study will be conducted.

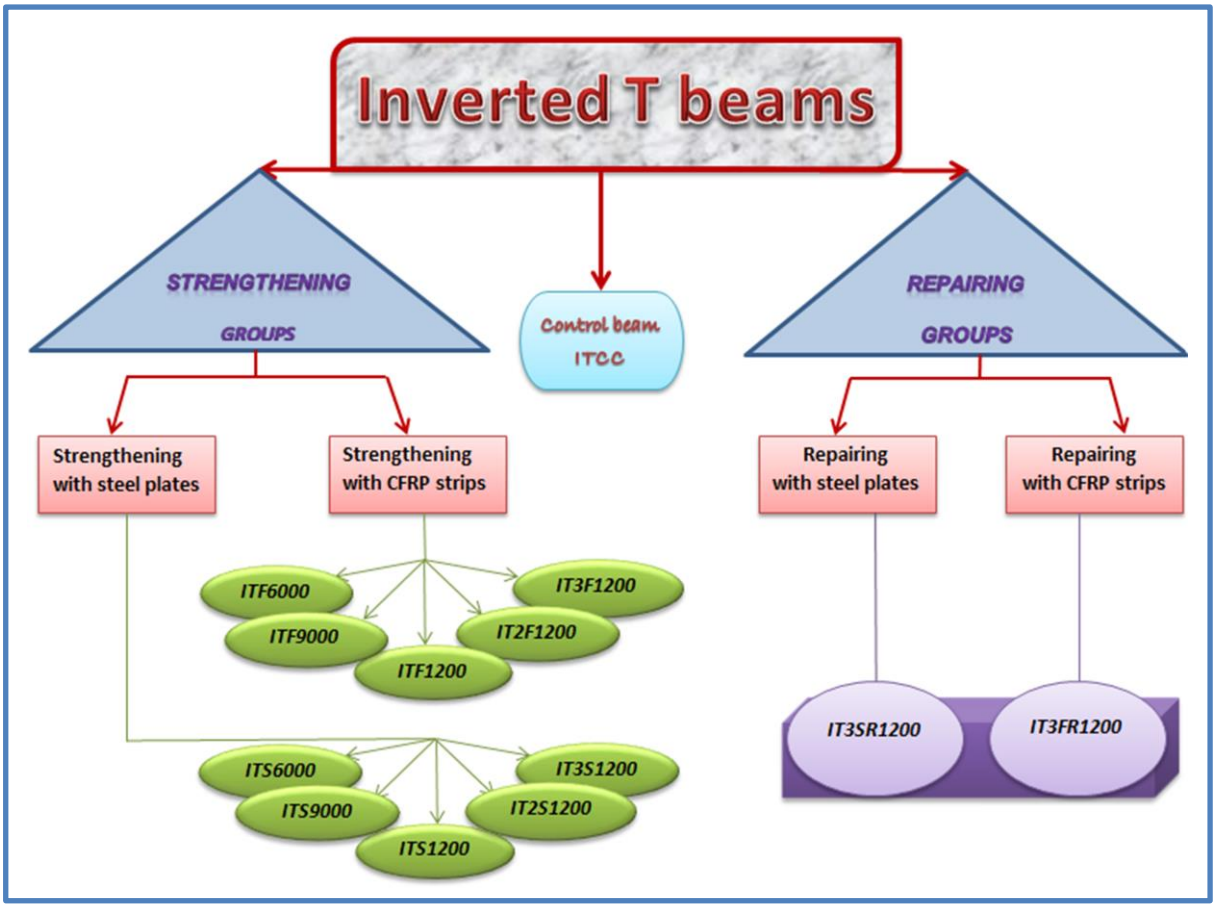

Figure (5-1): The selected inverted T beams for the theoretical study

5.2 Element Type and Material Properties

For modeling the truth behavior of reinforced concrete beams, the modeled concrete according to recommended is with an 8-nodded linear 3D brick solid element with reduced integration (C3D8R) **[109]**, see Figure (5-2a). The element type supplies dependable solutions to most applications. All 3D solid elements consist of eight nodes with three degrees of freedom per node. Also, it can be utilized for both linear and complex non-linear analysis involving contact, plasticity, and large deformations. For steel reinforcements used two nodded linear truss elements (T3D2), see Figure (5-2b). In addition to the concrete beam, the three-dimensional solid element (C3D8R) was selected to model the steel plates in both the supporting situation and the loading situation. The third element type utilized in this study for the purpose of modeling CFRP strips and steel sheets is the (S4R) shell element, see Figure (5-2c) **[110].**

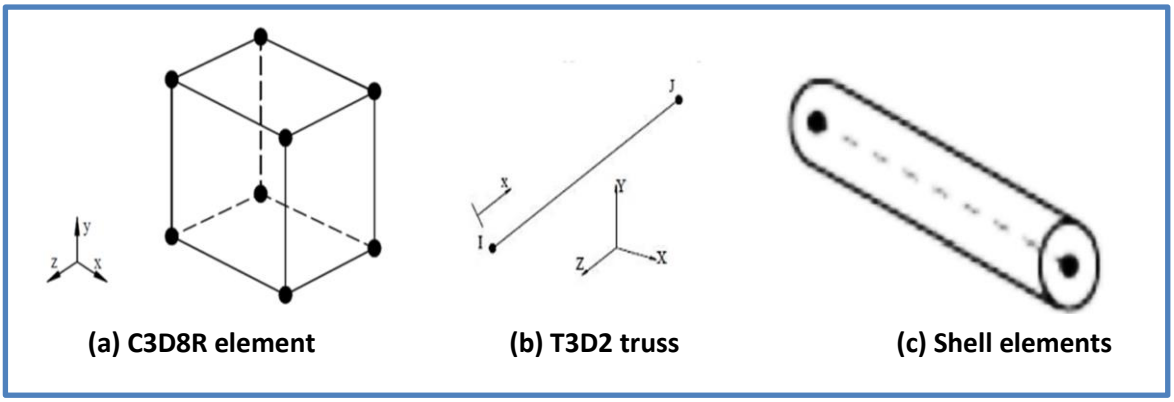

Figure (5-2): Element type used in FE simulation [110],[111]

The used model in ABAQUS for simulating the behavior of concrete is the concrete damaged plasticity model (CDP). Appendix B shows details of the (CDP) model which includes the behavior and properties of the concrete.

5.3 Model Geometry and Boundary Conditions

Three-dimensional (3D) simulations were carried out to obtain an approximate and accurate estimation of the behavior and failure modes of all RC inverted T beam specimens with and without CFRP strips or steel plates. All models were used in the simulation. Figure (5-3) gives a 3D view of the geometry of the FE model developed for the control beam. The Z axis is along the longitudinal direction of the beam, and the X-Y plane represents the cross-section of the beam.

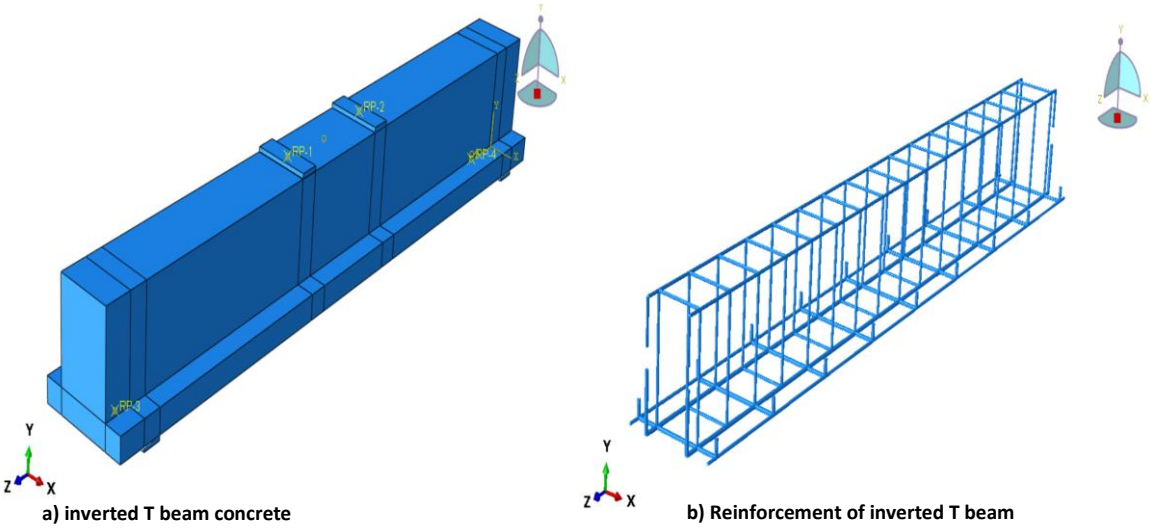

Figure (5-3): 3D view of the RC inverted T beam FE model

The bond simulation between the concrete and the steel reinforcement was by an embedded method. In this constraint, steel reinforcement bars were chosen as the embedded region and the concrete served as the host region, also, the constraint simulation between concrete and steel was a perfect bond see Appendix B. A surface-to-surface option was the usual connection between the beam and steel plates found in both loading and supporting situations which represent a rigid body in the constraint manager. The ability of the ABAQUS shown in Figure (5-4) in modeled variation types of the elements during the constraints function.

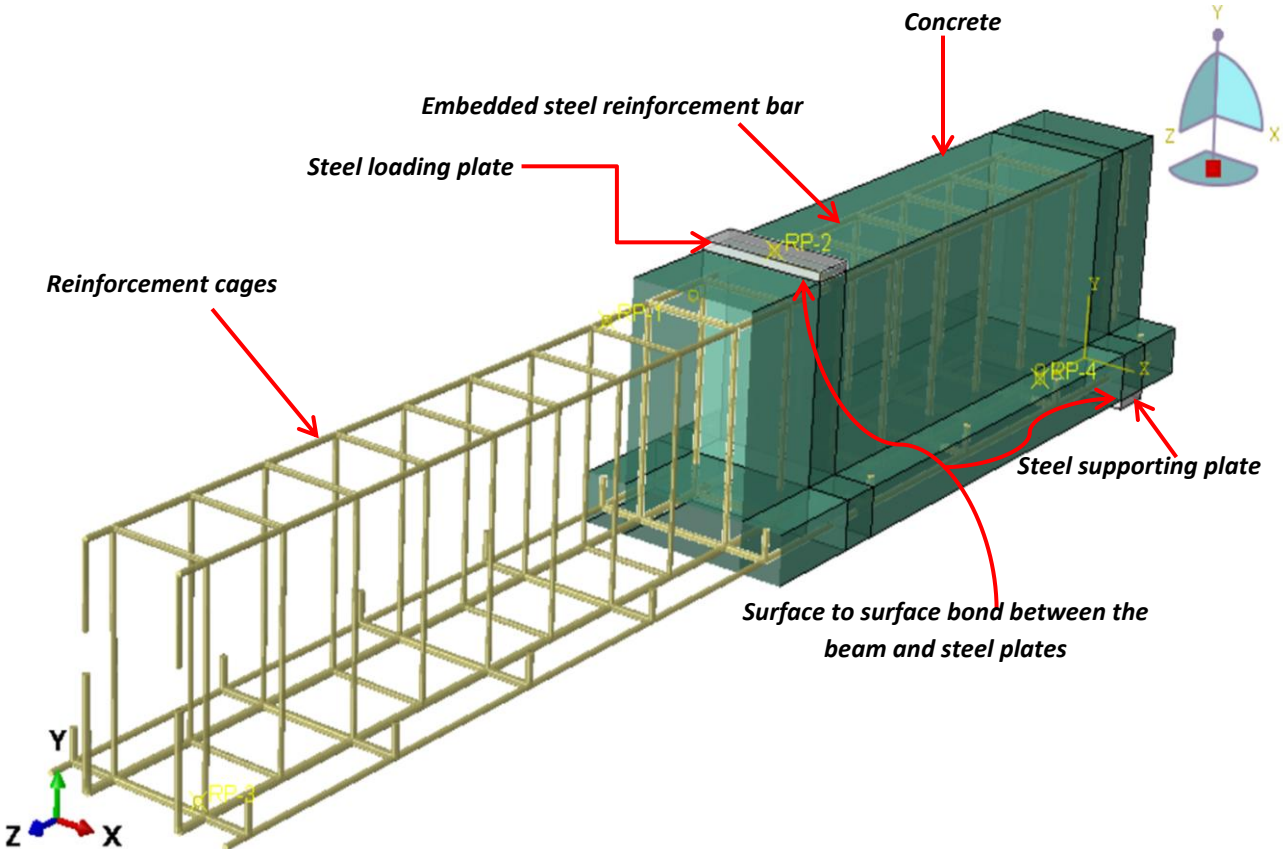

Figure (5-4): FE model of the constraints function in ABAQUS (ITCC beam)

The RC inverted T beams had been analyzed in ABAQUS/Explicit by utilizing static step analysis; a nonlinear dynamic implicit procedure was preferred to analyze all the beams. The load was applied in the static analysis as a displacement on the mid-point (reference point [RP]) of the upper steel

loading plates. This applied displacement was 30 mm for all inverted T beam specimens. The boundary condition of the beam supports of all inverted T beams were represented by making a fix on the (reference point [RP]) and the type of this fix is symmetry/antisymmetry/encastre as (U1=U2=U3=UR1=UR2=UR3=0).

Figure (5-5) shows details boundary conditions for beam specimens utilized in the simulations.

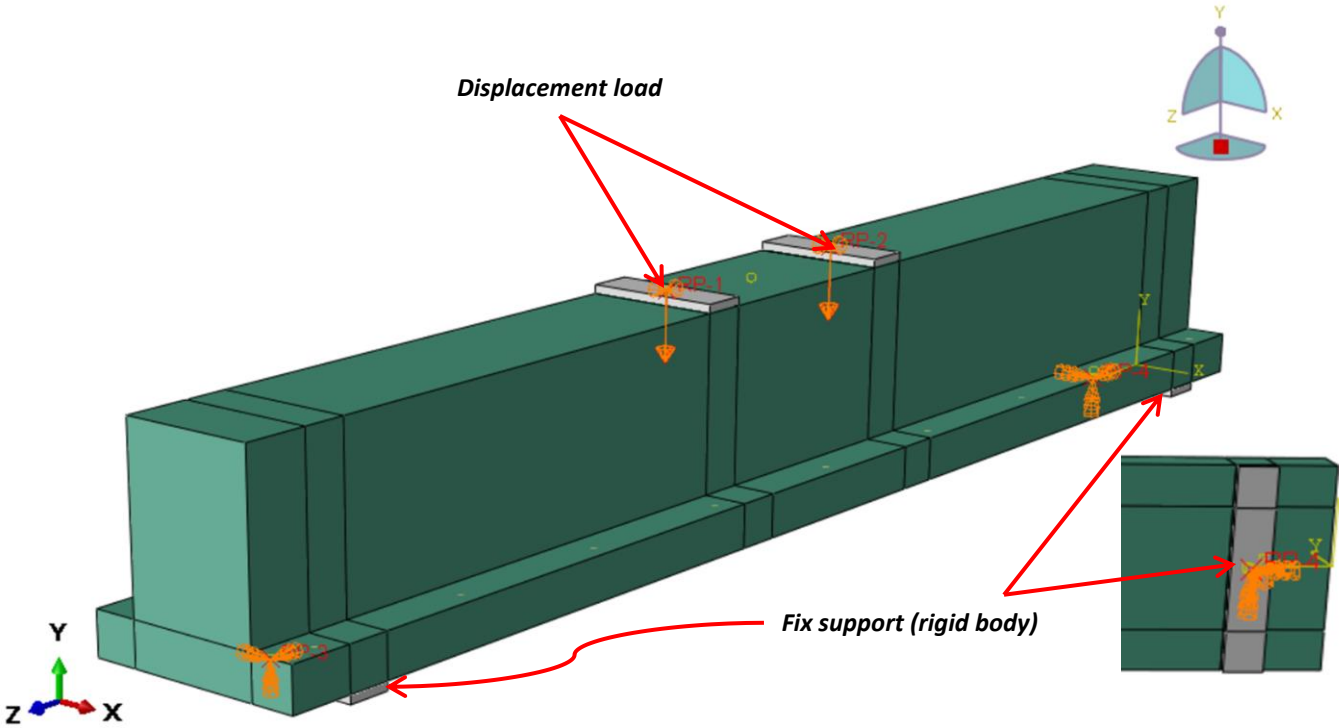

Figure (5-5): Typical boundary conditions and apply load of modeled inverted T beams

5.4 Finite element Mesh and Convergence Analysis

The study of convergence is the main objective in determining the size of the mesh for the purpose of modeling the beam model with fewer elements and higher affinity with experimental test results. Practically, this is achieved when there is a small effect on the results with a decrease in mesh size when compared with the effect of structural analysis complexity and processing time. The beam specimens molded with element size reduced (Increasing the number of elements in each X, Y, and Z direction) (10, 15,20, 25), see Figure (5-6). The model was cut to match the nodes in each

beam element to each other by creating a partition-type cell in a method extend face for steel loading and support plates with beam, as shown in the beam ITCC in Figure (5-6), while when adding strengthen or repair using CFRP strips or steel plates, and for the mesh consistency, the cutting process is done utilizing a datum plane for each side of the CFRP strips or steel plates as shown in the beam IT3F1200 in Figure (5-6). The convergence analysis study, showed that the difference can be ignored when the number of element increased from 15625 elements (mesh size of 20 mm) to 31250 elements(mesh size of 10 mm), therefore; the 20 mm model is suitable mesh in the modeling for all tested specimens as shown in Figure (5-6). All beam specimens were analyzed with the same load, as well as for material properties, all beam specimens strengthened or repaired with CFRP strips were similar in properties to each other, as well as beam specimens that were strengthened or repaired with steel plates were also similar in properties to each other.

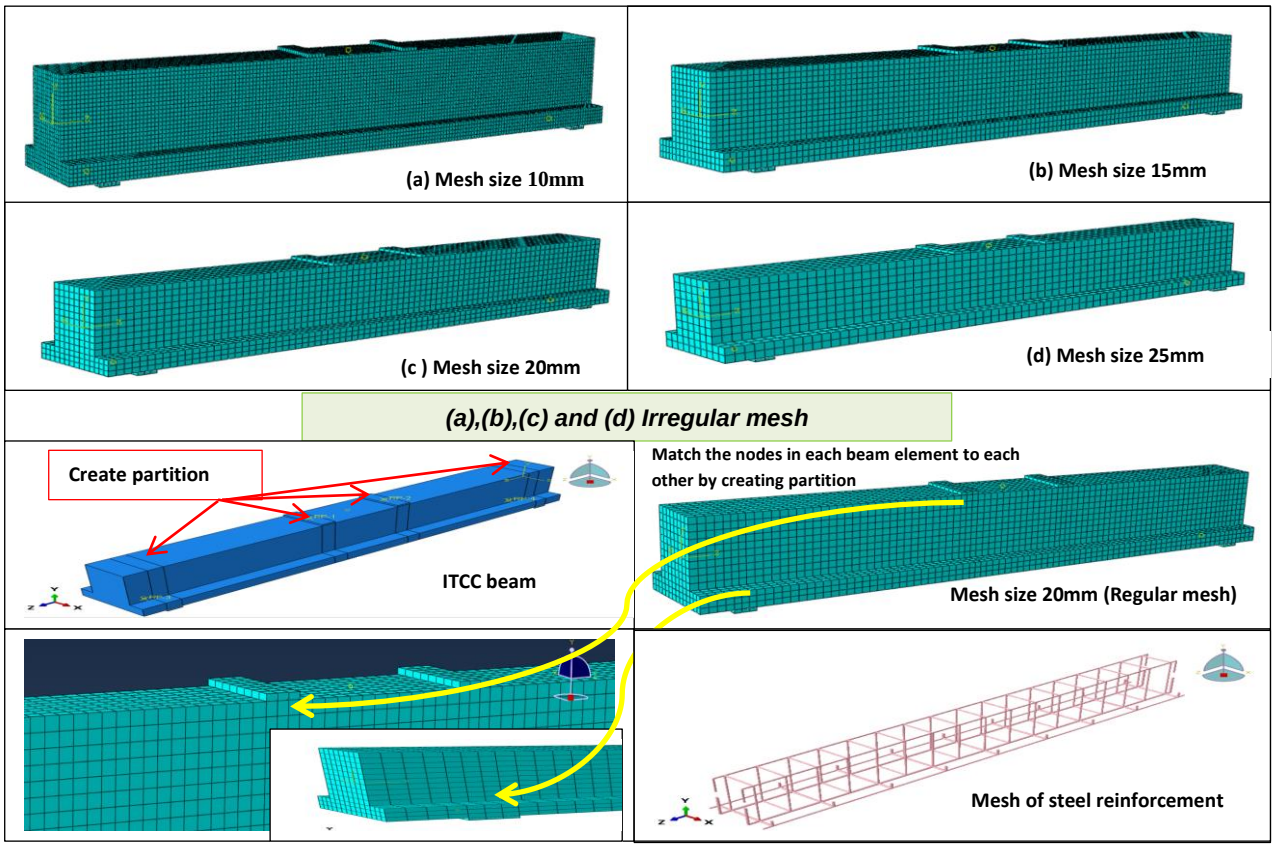

Figure (5-6): Typical mesh applied for the RC inverted T beams (continue)

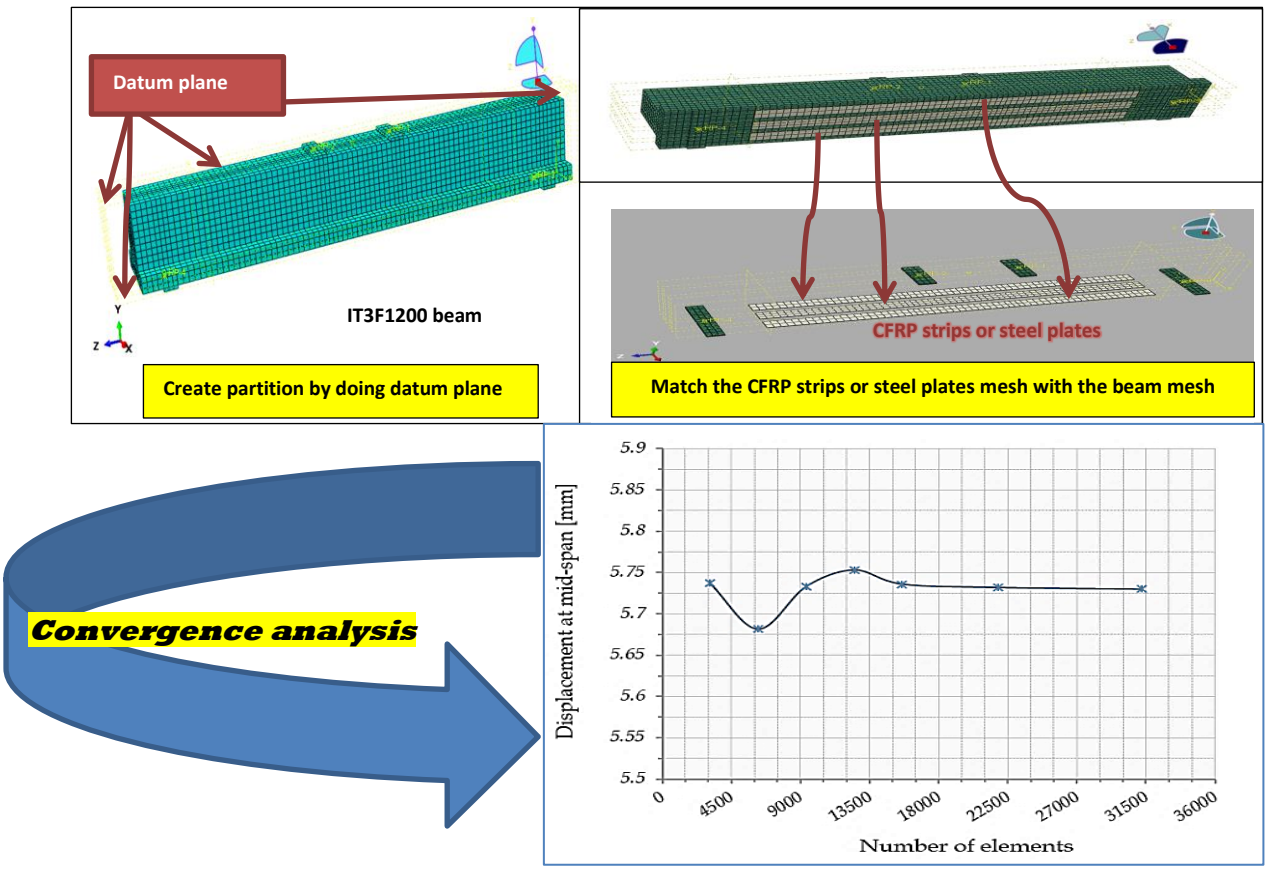

Figure (5-6): Typical mesh applied for the RC inverted T beams (continued)

5.5 CFRP strips or steel plates modeling

5.5.1 CFRP strips Modeling

In the ABAQUS program, the CFRP strips are modeled as follows:

1. The CFRP strips sections are made as a shell layer with a thickness equal to (0.167mm).
2. The CFRP strips material has defined in two stages :

(A) The first stage is represented as an elastic stage, CFRP strips are represented as a laminate which formed of modulus of elasticity in two directions longitudinal and transverse, Poisson's ratio in the longitudinal direction and values shear modulus of elasticity in all directions as shown in Table (5-1) **[112]**.

(B) The second stage is represented as a plastic stage, this stage is defined as the failure stage which is molded by utilizing the hashin model formed of tensile strength, compressive strength, and shear strength in two directions as shown in Table (5-1) **[112]**.

3. Also, the completion of the definition of the behavior of the material, in addition to knowing the elastic and hashin damage, is done by knowing the density of the CFRP strips, which is equal to 1.82E-09. See the Appendix B.

Table (5-1): Elastic and Hashin Damage Properties of CFRP strips Used in ABAQUS [112]

Parameter	magnitude
Elastic properties	
Elastic modulus of CFRP strips: **E1** **E2**	 **230 Gpa** **16.58 Gpa**
Longitudinal Poisson's ratio	**0.3**
Shear modulus: **G12** **G13** **G23**	 **9188.5 MPa** **12259 MPa** **5911 MPa**
Hashin Damage properties	
Longitudinal tensile strength	**3900 MPa**
Longitudinal compressive strength	**3120 MPa**
Transverse tensile strength	**210.6 MPa**
Transverse compressive strength	**643.5 MPa**
Longitudinal shear strength	**210.6 MPa**
Transverse shear strength	**276.9MPa**

4. It is necessary to know the direction of the CFRP strips in order to know the ABAQUS program that $E1$ is the initial Young's modulus in the long direction in the fiber direction and $E2$ is Young's modulus in the short direction in the direction perpendicular to the fibers as shown in the Plate (5.1).

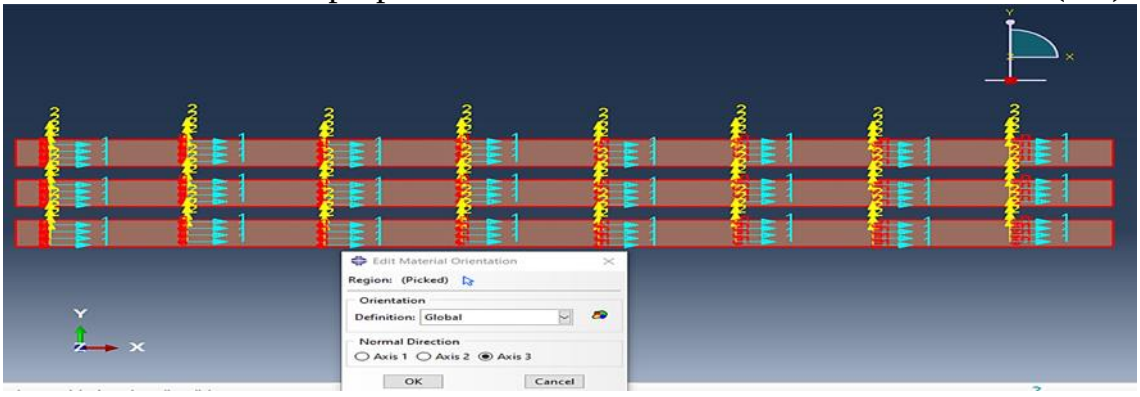

Plate (5-1): Determine the orientation of CFRP strips

5.5.2 Steel Plates Modeling

In the ABAQUS program, the steel plates are modeled as follows:

1. The steel plates sections are made as a shell layer with a thickness of equal to (0.8mm).
2. the steel plates material have defined in two stages:

(A) The first stage is represented as an elastic stage which is formed by young's modulus and Poisson's ratio as shown in Table (5-2).

(B) The second stage is represented as the plastic stage formed of yield stress and plastic strain, yield stress, and plastic strain data obtained from the dog bone test found in chapter three as shown in Table (5-2).

Table (5-2): Elastic and plastic Properties of steel plates used in ABAQUS

Parameter	magnitude
Elastic properties	
Young modulus	200000 MPa
Poisson's ratio	0.3
Plastic properties (for two steel coupons)	
Yield stress : **1- 266.9 MPa** **2- 264.7 MPa**	**Plastic strain :** **0** **0.19**

3. Also, the completion of the definition of the behavior of the material, in addition to knowing the elastic and plastic, is done by knowing the density of the steel plates, which is equal to 7.85E-09.

5.6 Adhesive Interface Modeling

In this study, the surface-to-surface connection is used in the bond between CFRP strips or steel plates and adhesive and between adhesive and concrete in each strengthening and repairing, where the concrete connected

to CFRP strips or steel plates are represented as the master surface, while the slave surface represents CFRP strips or steel plates, as shown in the Plate (5-2).

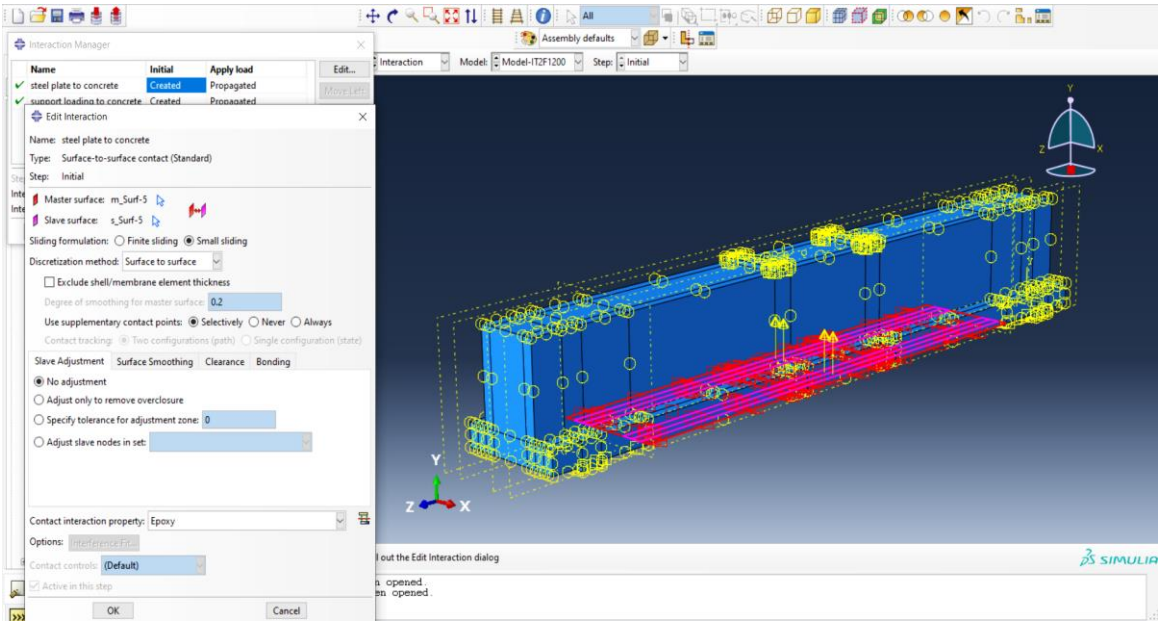

Plate (5-2): Adhesive Interface Modeling (IT2F1200 beam specimen)

The behavior of the bond interface between the CFRP composite strips or steel plates and the concrete beam was modeled in ABAQUS by using the cohesive surface interaction method. The surface is an epoxy that is dependent on cohesive behavior and damage, epoxy is defined as a surface interaction property. The response of the cohesive behavior interaction is based on traction-separation behavior. The traction-separation behavior consists of the initial stiffens in the normal direction in MPa/mm (normal stiffness) (Knn) and the initial stiffens in the tangential direction in MPa/mm (shear stiffness) ($Kss = Ktt$). The second contact property option of the surface of epoxy was represented by damage behavior. The response of the damage behavior interaction is based on maximum nominal stress. The maximum nominal stress consists of the normal strength, σn (MPa), shear-1 strength, τt (MPa), and shear-2 strength, τs (MPa). See appendix B. The data of interaction property for epoxy was taken according to the requirements of

previous research on strengthening concrete beams. Data of mechanical properties of the bond interface material (epoxy resin) as shown in Table (5-3) **[113]**.

Table (5-3): Mechanical properties of the interface material (epoxy resin) [113]

Properties	magnitude
Normal stiffness, Knn (MPa/mm)	**626**
Shear stiffness, Kss (MPa/mm)	**626**
Shear stiffness, Ktt (MPa/mm)	**626**
Normal strength, σn (MPa)	**1.81**
Shear-1 strength, τt (MPa)	**1.5**
Shear-2 strength, τs (MPa)	**1.5**

5.7 Repaired Beam Modeling

The method used in this study for the purpose of modeling the repair of RC beam with externally bonded CFRP strips or steel plates is as follows:

- In the beginning, two models are made, one representing the previous model (pre-loading model) (model-1) and the other representing the model after adding CFRP strips or steel plates (model-2) (IT3FR1200 or IT3SR1200).
- Pre-loading model is the first model that is without any repair. In this model, a pressure force distribution as total force and its value is 60% of the ultimate load of the control beam and is divided by 2 in order to put it on each load plate and as shown in the Plate (5-3). After that, an incremental refined execution was employed to gain a solution for the loading programs and analyzed beams.
- After completing the entries for this model (pre-loading model) as explained in the previous paragraphs of this chapter, a (run) is made for the pre-load model and the results are stored in a special case that

is made so that the results are called when needed in the second model.

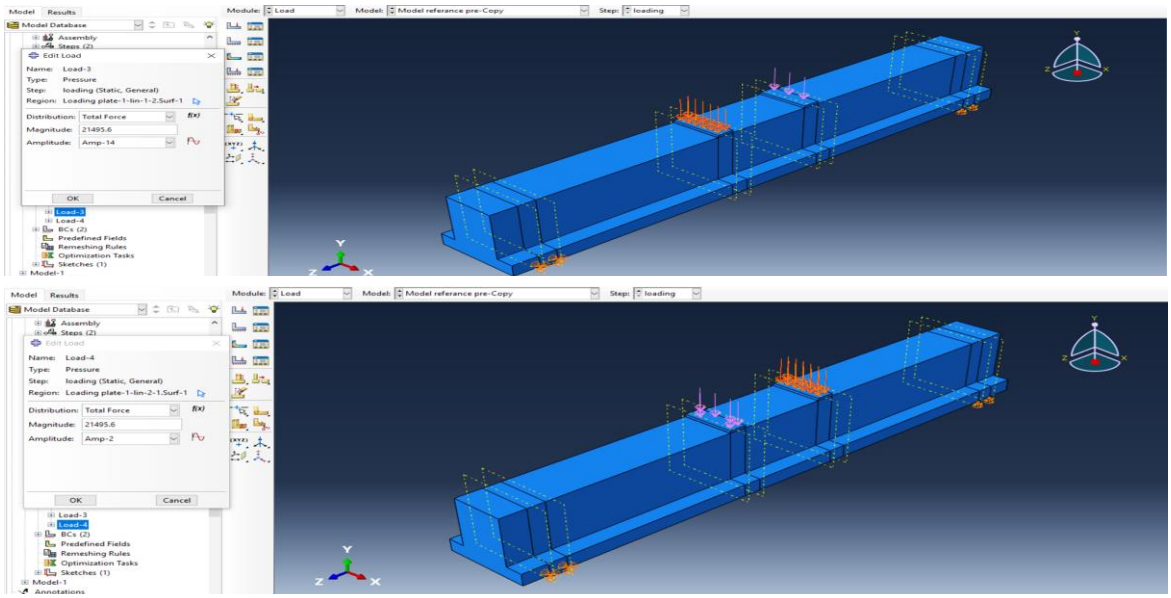

Plate (5-3): Apply load in pre-model (model-1)

❖ After that, the second model (model-2) is used and CFRP strips or steel plates are added (repair phase) , and all the connection details explained in the previous paragraphs of this study remain the same as shown in a Plate (5-4).

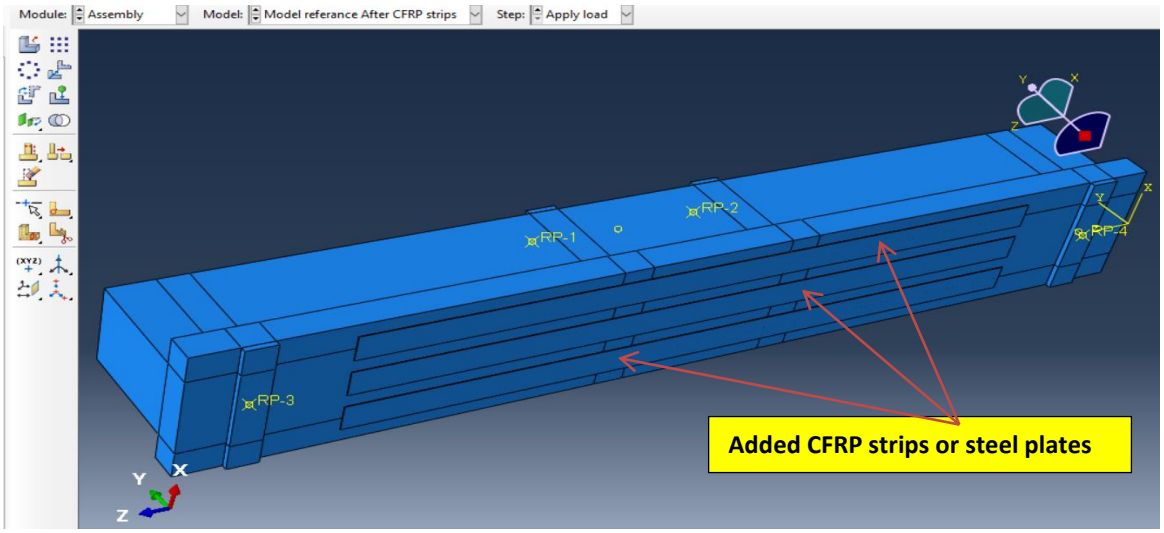

Plate (5-4): assembly CFRP strips or steel plates with beam

❖ Then the outputs of the initial stress are selected from the first model (model-1) and placed as the initial stress for the second model (model-2) by creating a predefined field, step initial, and types for selected

step stress as shown in a Plate (5-5). The increment value is taken from the last increment in which the first model (model-1) was executed and as shown in its Plate (5-5).

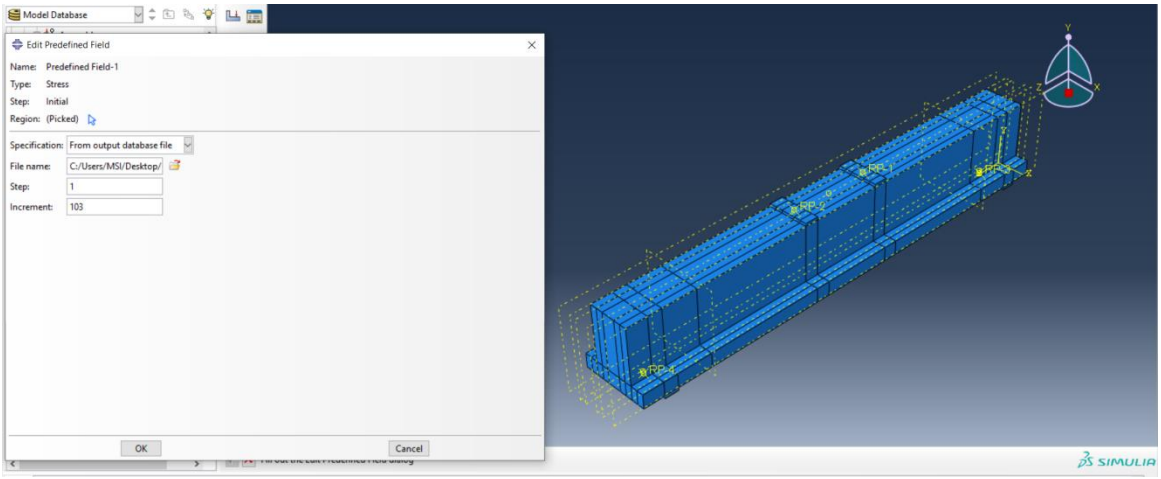

Plate (5-5): Applied initial stress from (model-1) to initial stress for (model-2)

5.8 Results of Finite Element Analysis and Discussion

5.8.1 Load - Deflection Response

The behavior of the study members is reflected in the relationship between load and mid-span deflection during the study compared with the results of the load-mid-span deflection responses obtained from FEM with the experimental results of the control beam, group I, group II and group III of beams as shown in Figures 5-7, 5-8, 5-9 and 5-10 respectively. Load-mid-span deflection expected by FEM was similar to the experimental data in general. However, the results obtained from FEM showed more stiffness compared to the results obtained from experimental specimens. There can be several reasons behind the high stiffness in the FEM and the most important these reasons are, it is the development of micro-cracks due to environmental influences, dry shrinkage, and curing of concrete, in the case of experimental examination results. These small cracks do not appear in the simulation by FEM **[114]**. Also, the perfect bond between steel reinforcement rebar and concrete is not actually ideal, the models in FEM represent the concrete to be a homogeneous material, but it is a heterogeneous material in actually.

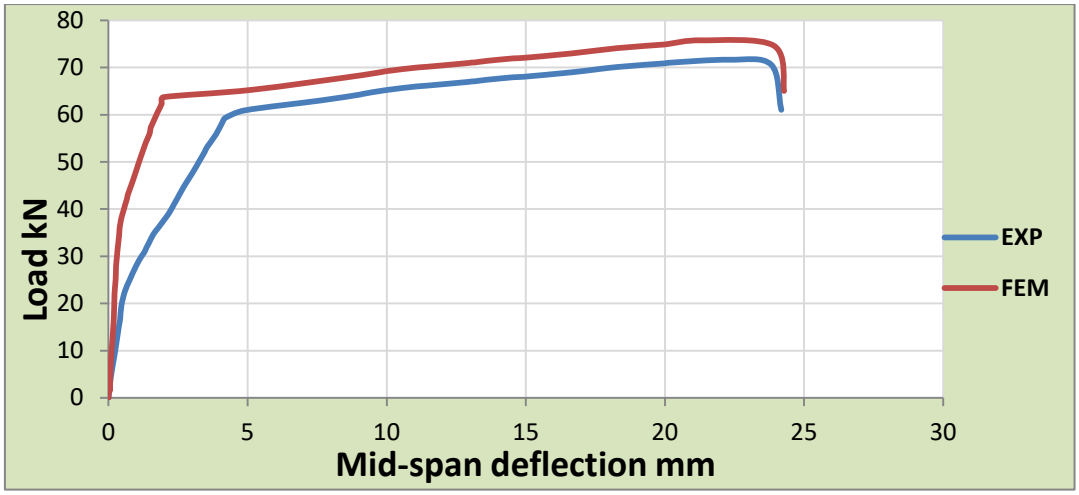

Figure (5-7): Experimental and numerical load-mid-span deflection curves for ITCC beam specimen

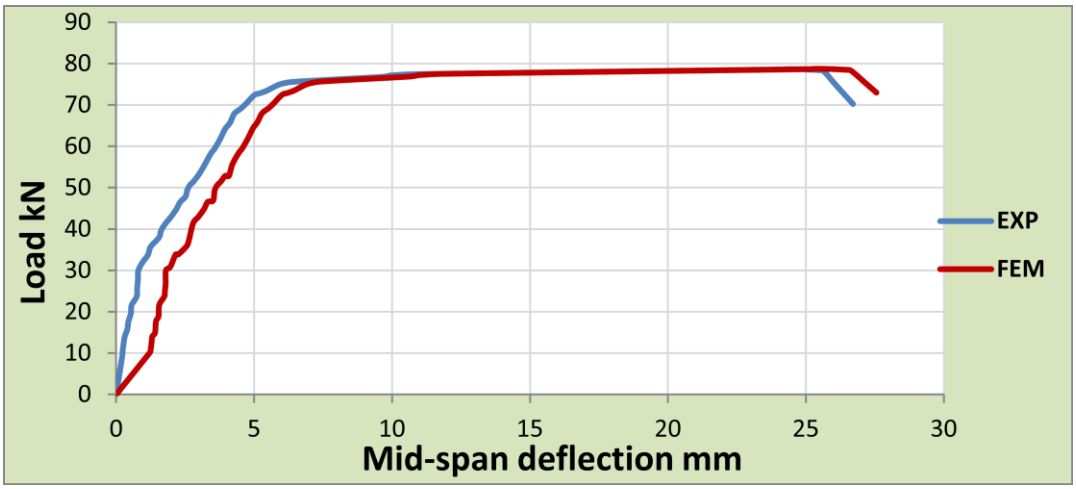

(a) ITF600 specimen

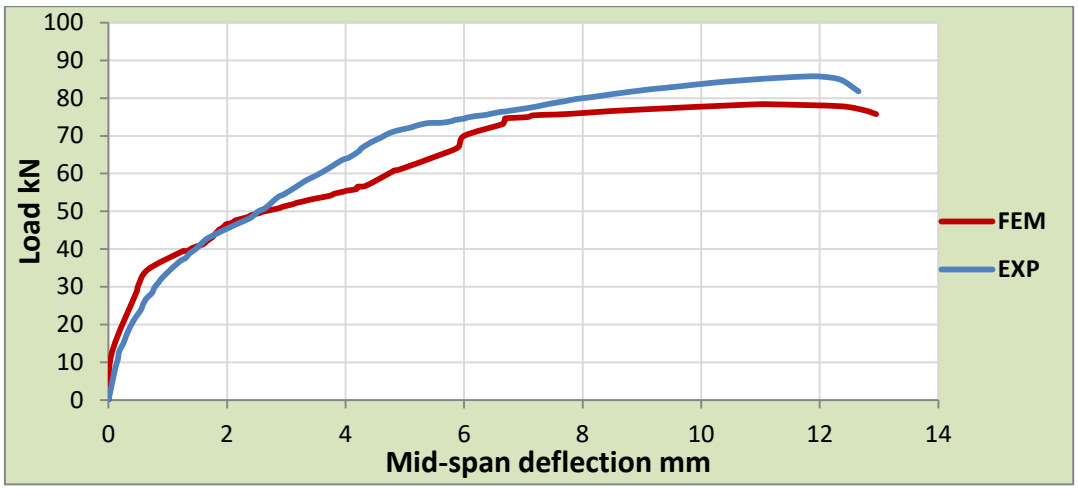

(b) ITF900 specimen

Figure (5-8): Experimental and numerical load-mid-span deflection curves for group I strengthening beams with CFRP strips (continue)

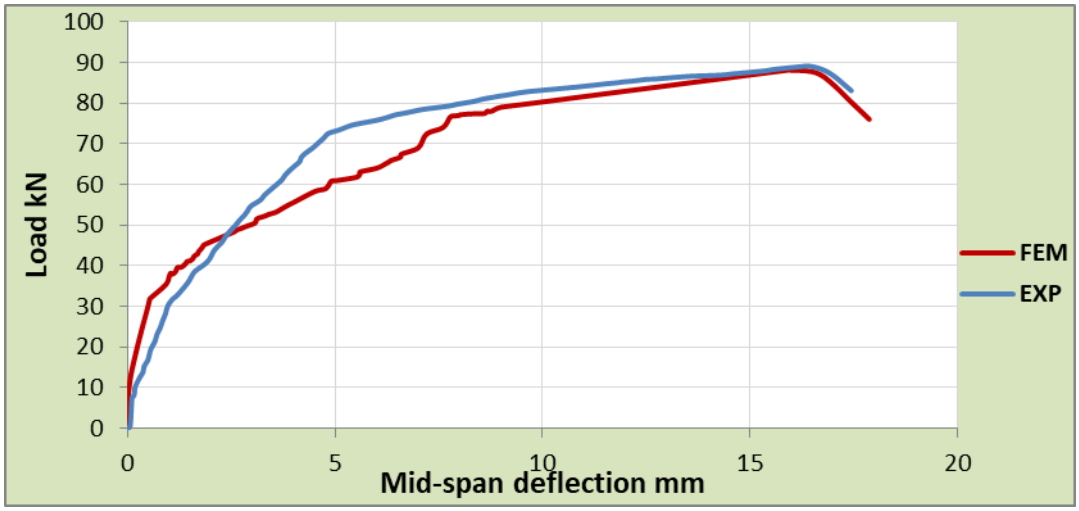

(c) ITF1200 specimen

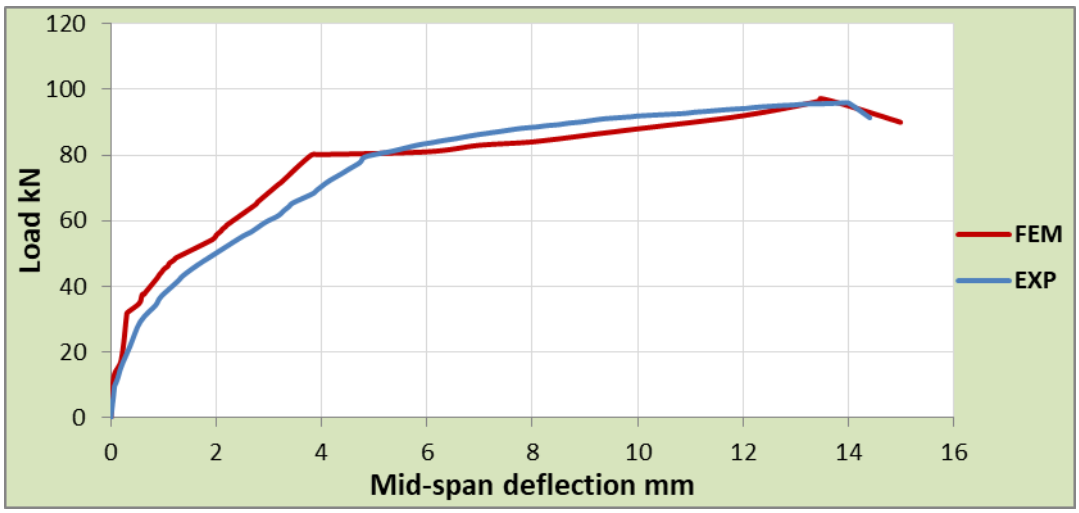

(d) IT2F1200 specimen

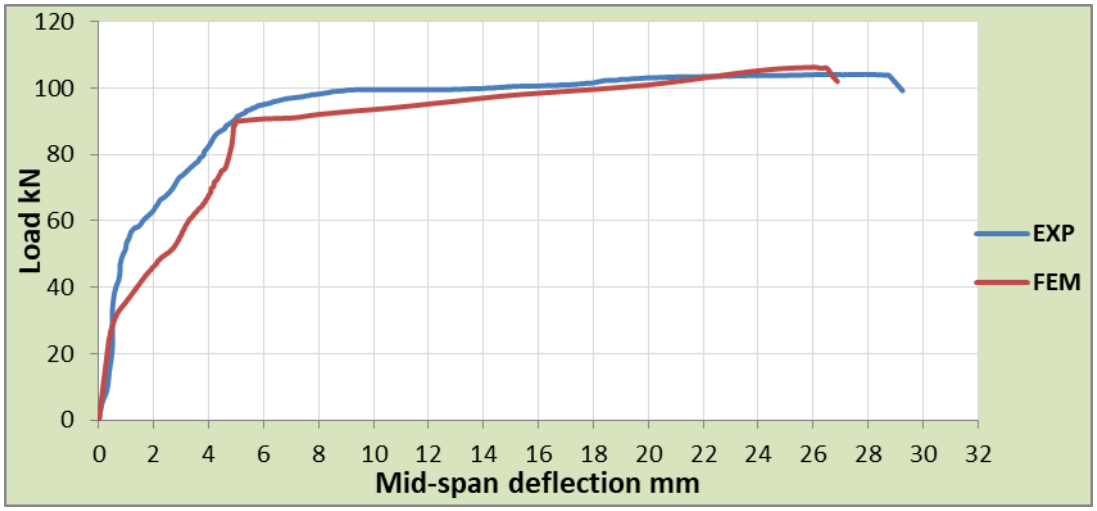

e) IT3F1200 specimen

Figure (5-8): Experimental and numerical load-mid-span deflection curves for group I strengthening beams with CFRP strips (continued)

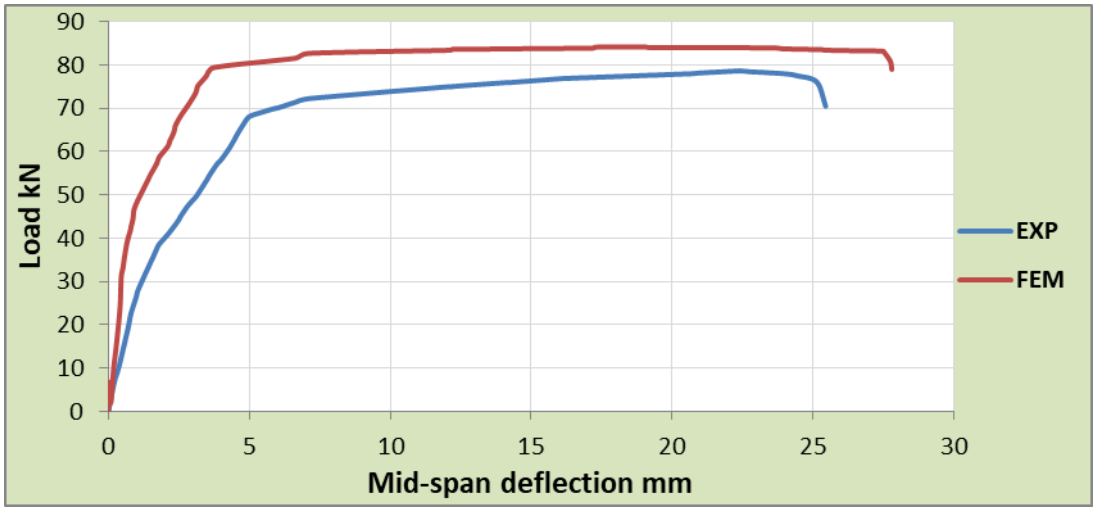

(a) ITS600 specimen

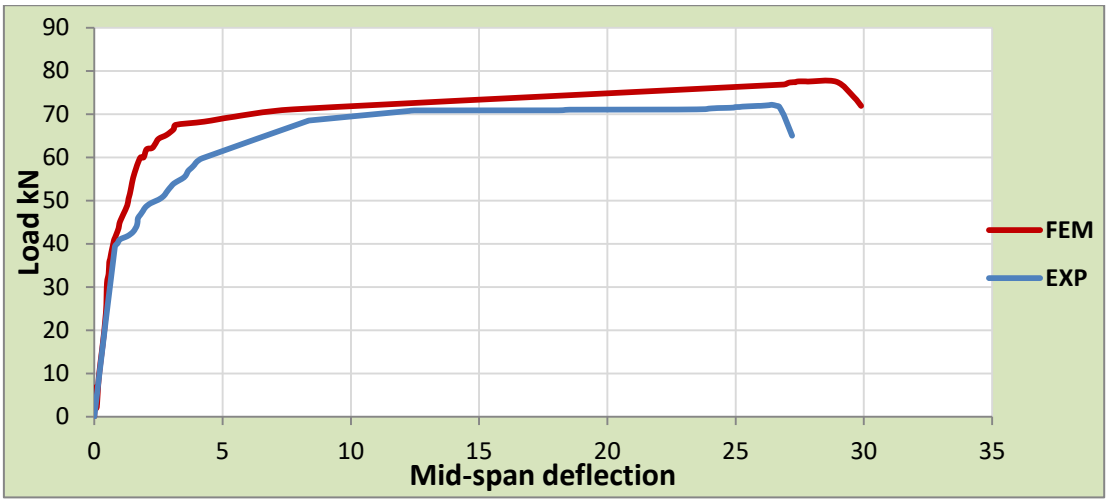

(b) ITS900 specimen

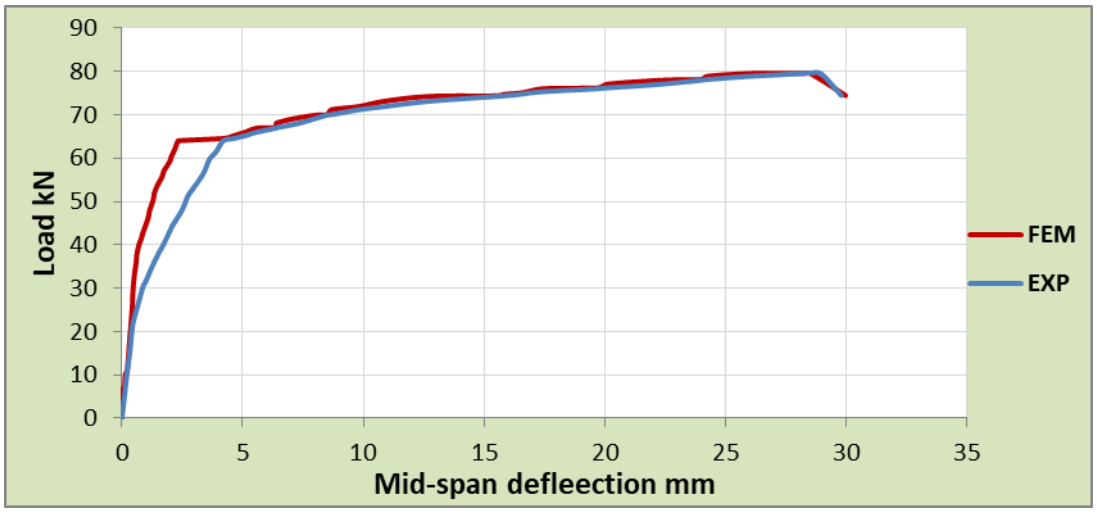

(c) ITS1200 specimen

Figure (5-9): Experimental and numerical load-mid-span deflection curves for group II strengthening beams with steel plates (continue)

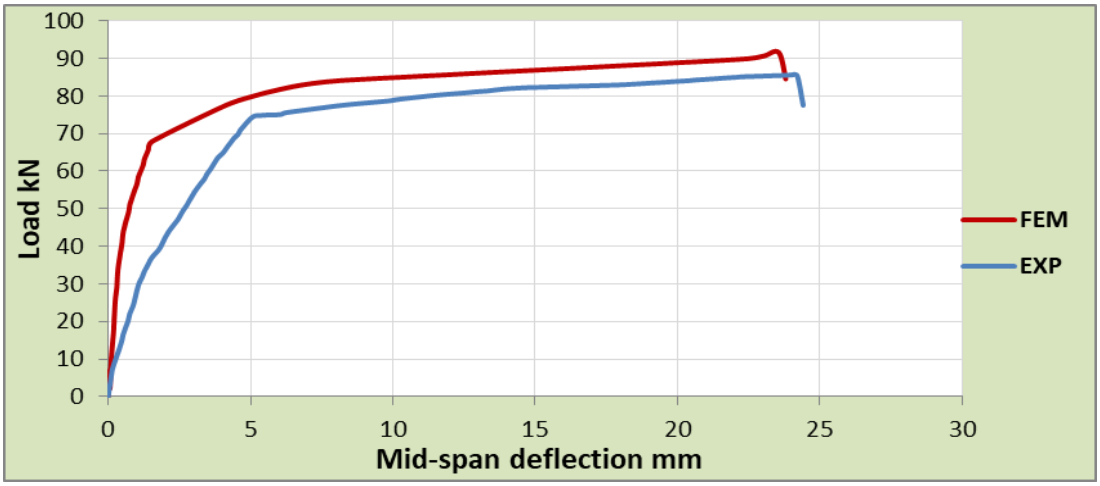

(d) IT2S1200 specimen

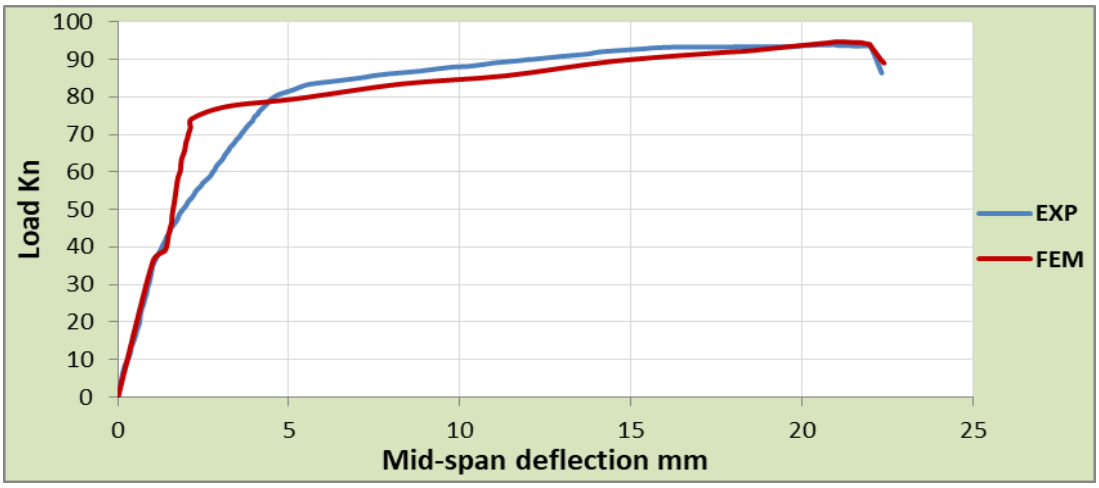

(e) IT3S1200 specimen

Figure (5-9): Experimental and numerical load-mid-span deflection curves for group II strengthening beams with steel plates (continued)

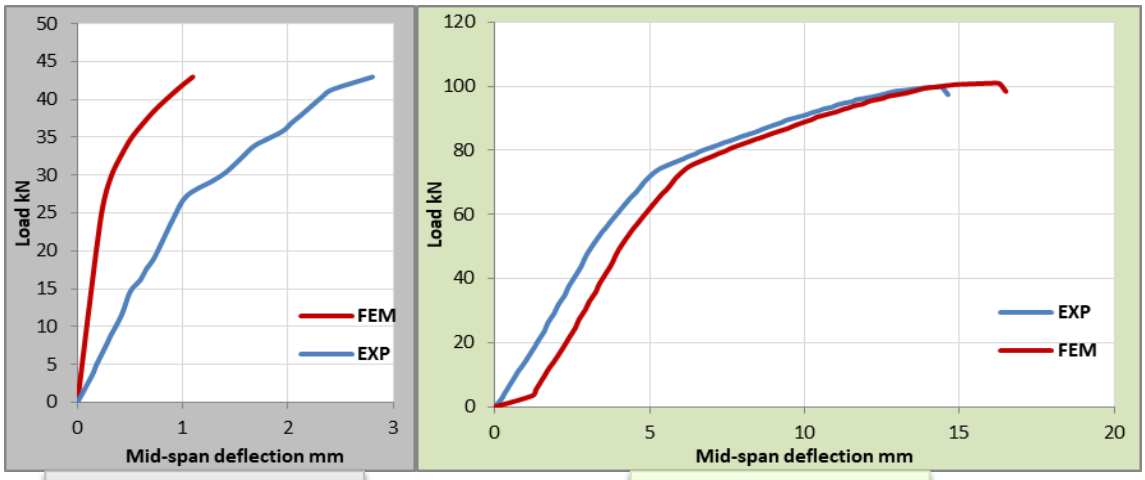

a-1) Before repairing a-2) After repairing

(a) IT3FR1200 specimen

Figure (5-10): Experimental and numerical load-mid-span deflection curves for group III repairing beams with (a) CFRP strips and (b) steel plates (continue)

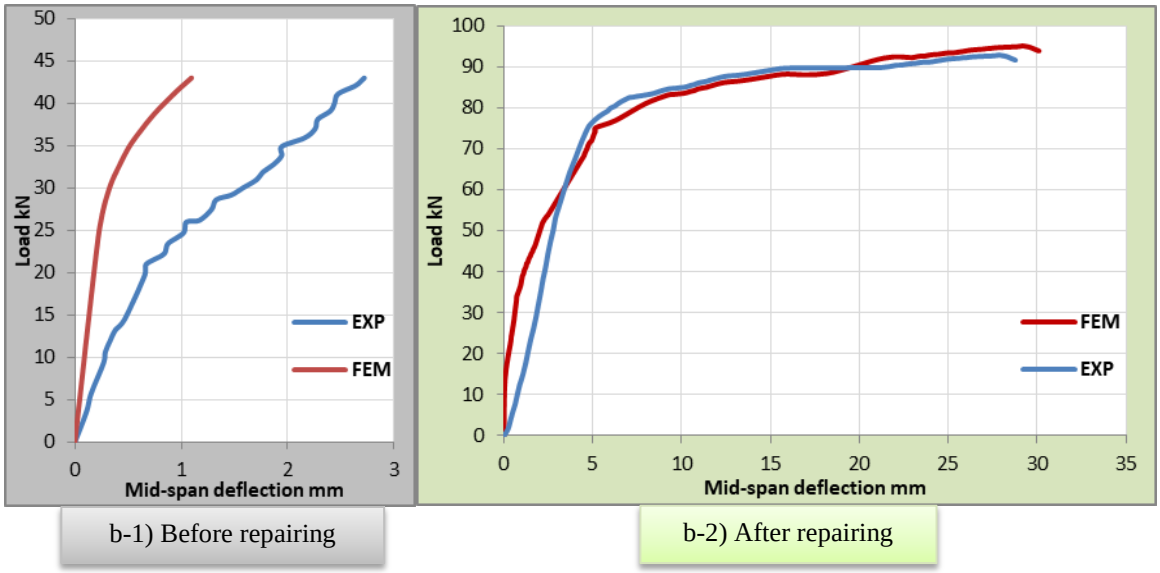

(b) IT3SR1200 specimen

Figure (5-10): Experimental and numerical load-mid-span deflection curves for group III repairing beams with (a) CFRP strips and (b) steel plates (continued)

All of these Figures usually consider a good agreement between the experimental curves and the finite element method curves. Table (5-4) offers summary results in the comparison between experimental and analytical results for reference beam or control beam (ITCC), group I strengthening beams with CFRP strips, group II strengthening beams with steel plates, and group III repairing beams with (a) CFRP strips and (b) steel plates. The maximum difference for all beams strengthened with CFRP strips or steel plates varied in the results between the (-8.62%) reduction to (7.51%) ultimate load increase. While the maximum difference in the maximum deflection at mid-span was between (-15.04%) as a reduction to (4.43%) as an increase. As for the beams repaired with CFRP strips or steel plates, the maximum difference in ultimate load ranges from (1.2%) to (2.40%), and the maximum deflection at mid-span varied in the results between (4.78%) to (12.28%). However, there is an acceptable and good agreement between the results from the FEM analysis and the experimental study results.

Table (5-4): Experimental and Numerical Results for all tested beams

Beam specimens	Ultimate loads (kN)		$\frac{Pu)FEM - pu) EXP}{pu) EXP}$ %	Max. deflection (mm)		$\frac{\Delta u)FEM - \Delta u)EXP}{\Delta u)EXP}$ %
	$Pu)_{EXP}$	$Pu)_{FEM}$		$\Delta u)_{EXP}$	$\Delta u)_{FEM}$	
ITCC	71.652	75.764	5.74	22.31	21.31	-4.48
ITF600	78.690	78.760	0.09	24.35	25.35	4.11
ITF900	85.754	78.362	-8.62	11.79	11.19	-5.09
ITF1200	89.088	88.091	-1.12	16.43	15.90	-3.23
IT2F1200	95.899	97.262	1.42	13.91	13.47	-3.16
IT3F1200	104.155	106.301	2.06	27.85	26.06	-6.43
ITS600	78.654	84.185	7.03	22.41	19.04	-15.04
ITS900	72.160	77.578	7.51	26.41	27.58	4.43
ITS1200	79.671	79.571	-0.13	28.55	28.17	-1.33
IT2S1200	85.602	91.595	7.00	23.99	23.55	-1.83
IT3S1200	93.937	94.696	0.81	20.91	20.99	0.38
IT3FR1200	99.808	101.001	1.20	14.41	16.18	12.28
IT3SR1200	92.877	95.111	2.40	27.84	29.17	4.78

5.8.2 Behavior of Von Mises stress for inverted T beams

The distribution of concrete stresses for all tested flexural strengthened and repaired beams at failure loading is illustrated in Figures (5-11) to (5-16). The stresses were determined in units of (MPa). The stress gradient is shown by a colored bar placed on the gantry of the specimens' shapes.

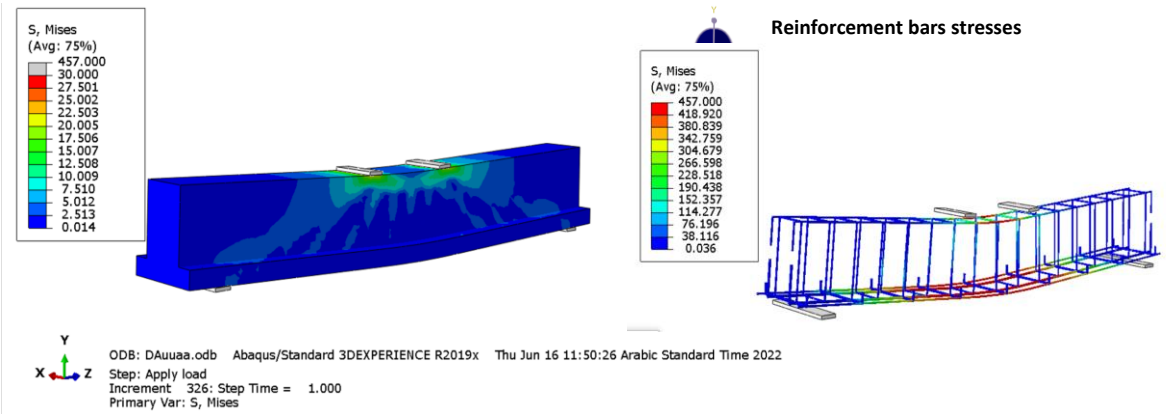

Figure (5-11): Stresses distribution of FEM for flexural beam (ITCC)

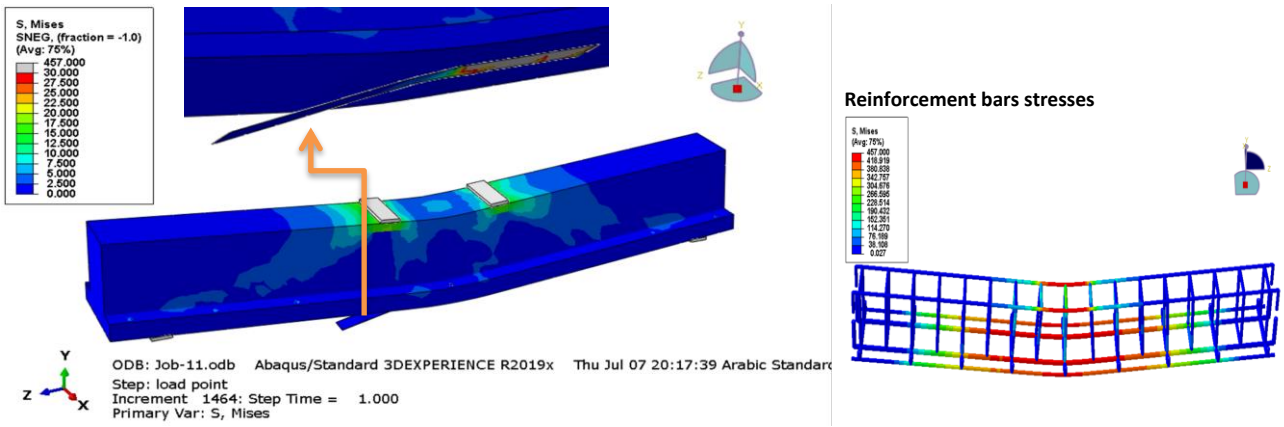

(a) ITF600 beam

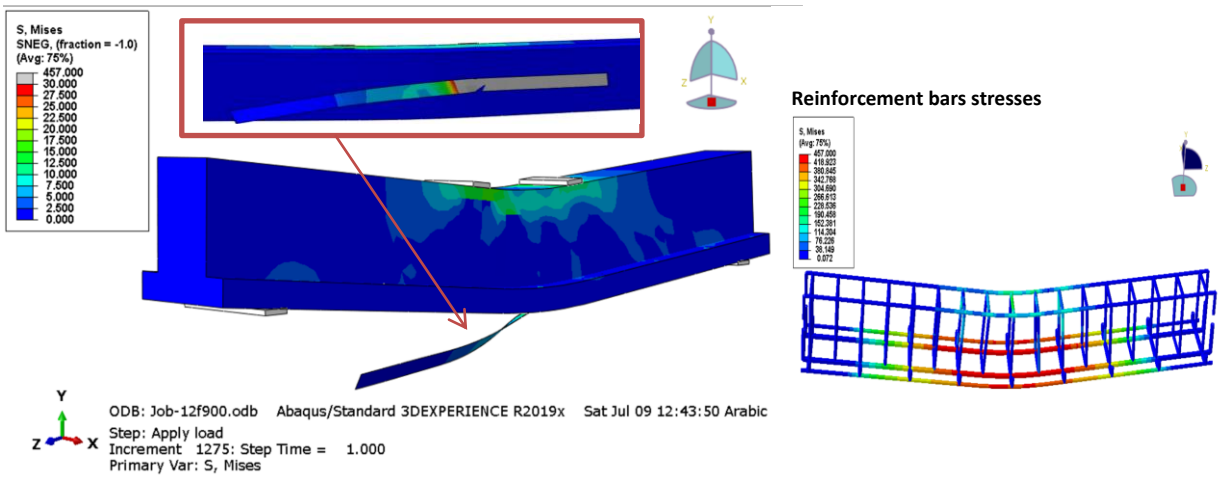

(b) ITF900 beam

Figure (5-12): Stresses distribution of FEM for strengthening beams with CFRP strips (continue)

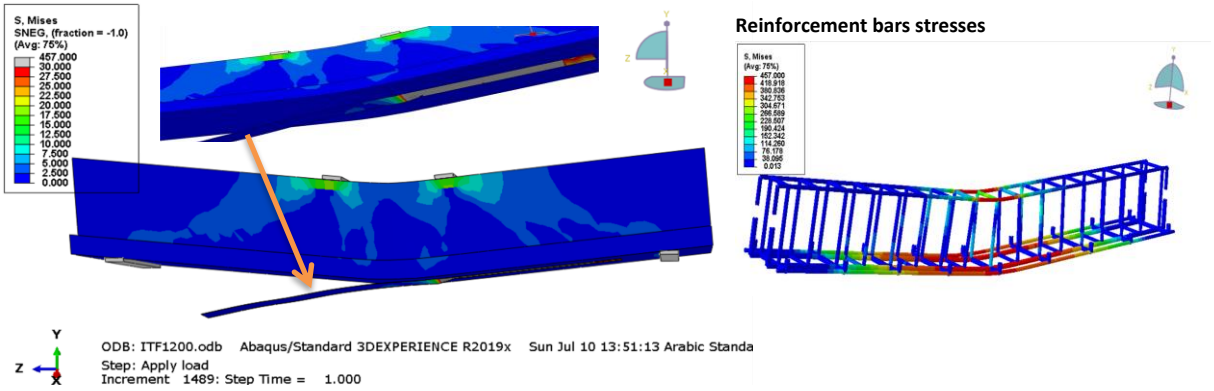

(c) ITF1200 beam

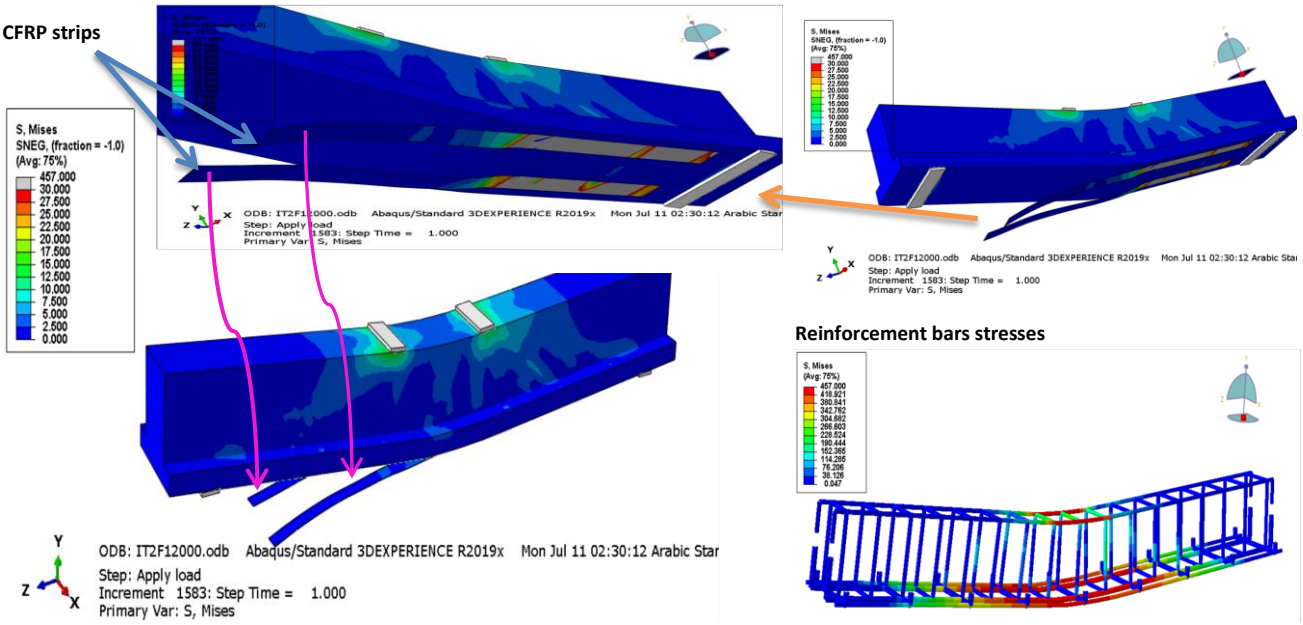

(d) IT2F1200 beam

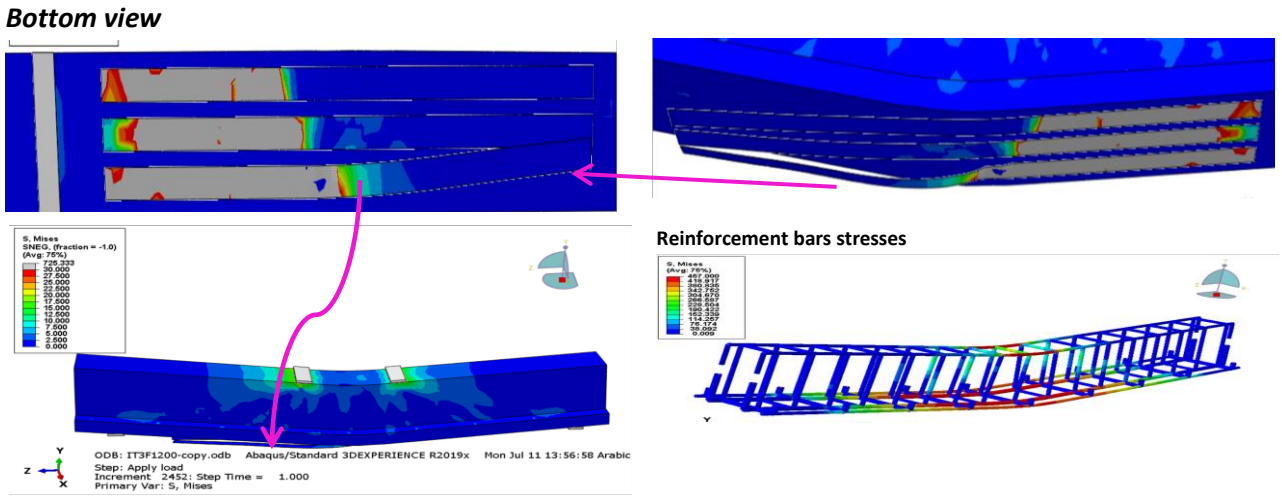

(e) IT3F1200 beam

Figure (5-12): Stresses distribution of FEM for strengthening beams with CFRP strips (continued)

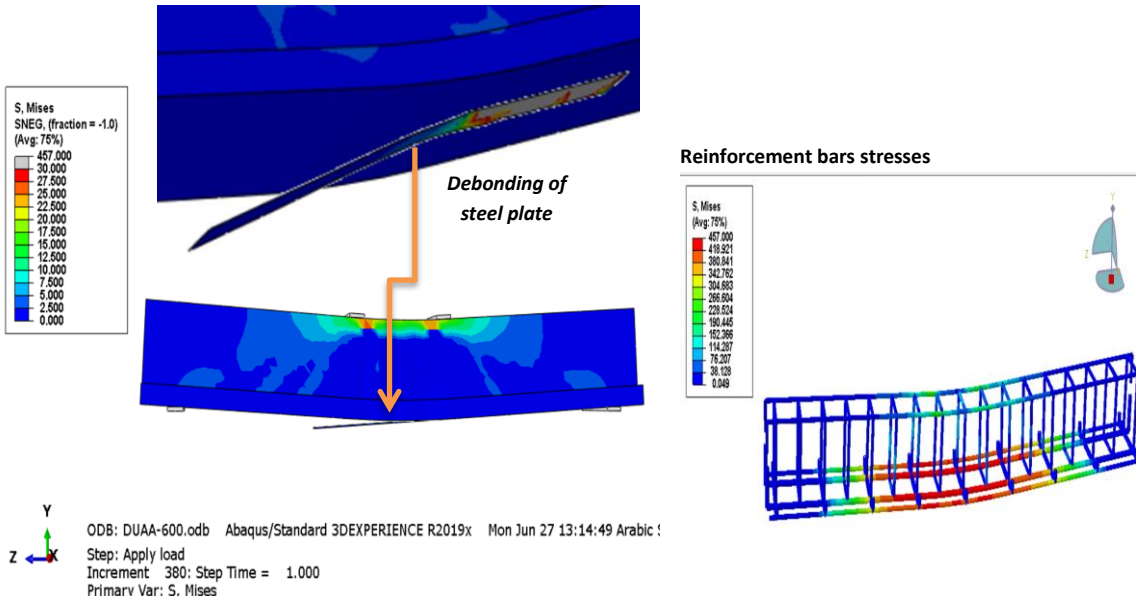

(a) ITS600 beam

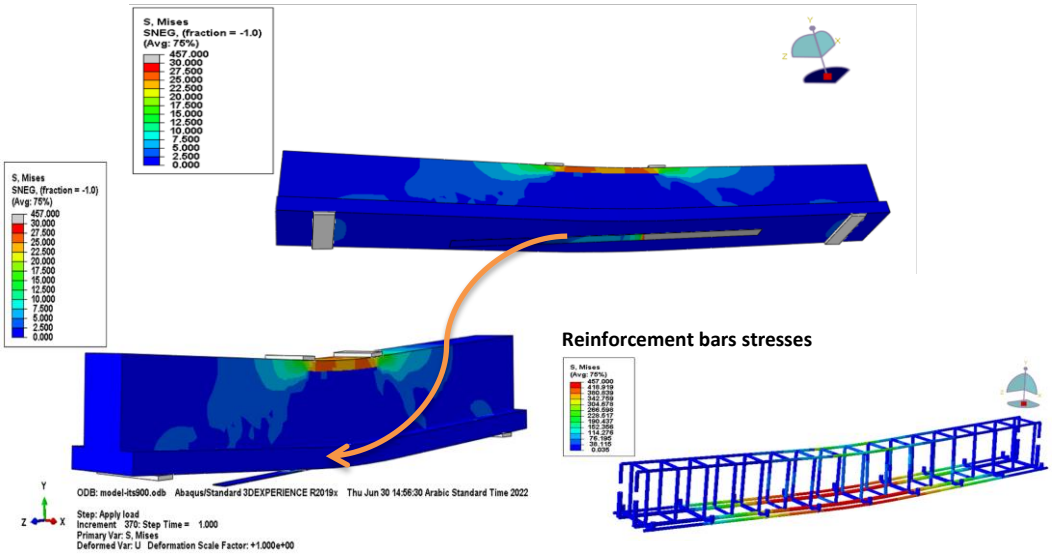

(b) ITS900 beam

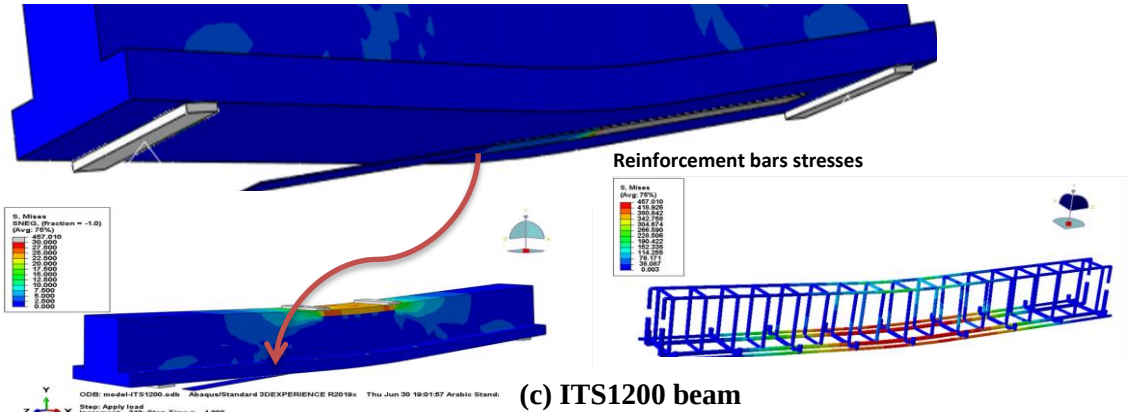

(c) ITS1200 beam

Figure (5-13): Stresses distribution of FEM for strengthening beams with steel plates (continue)

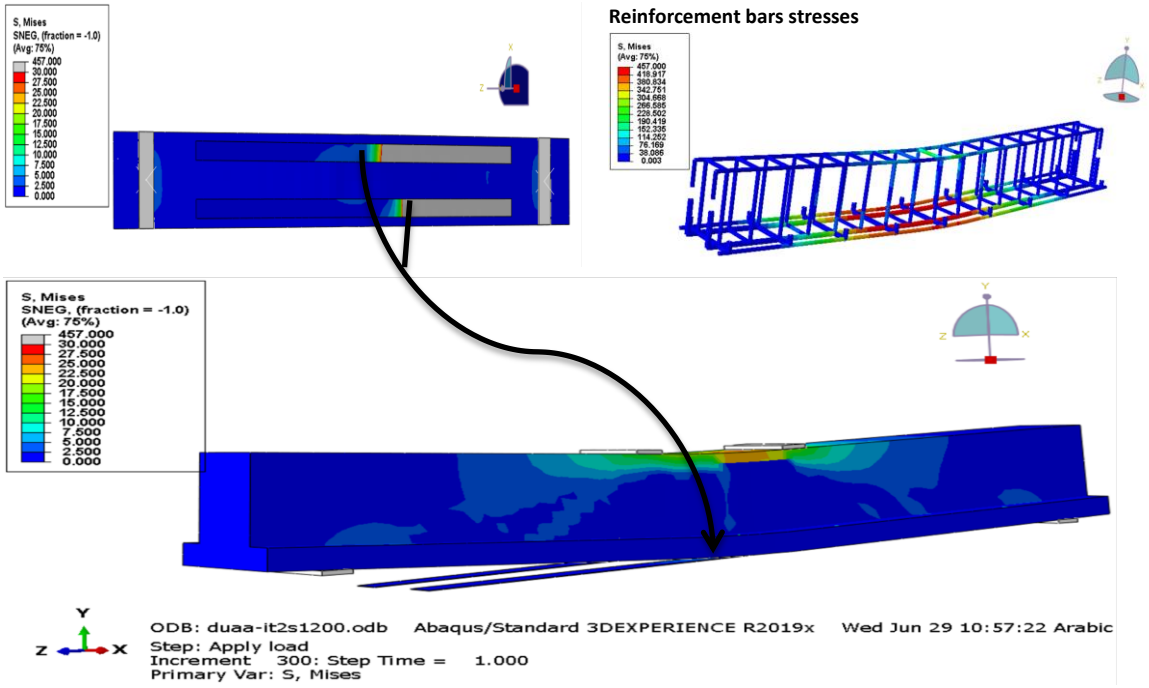

(d) IT2S1200 beam

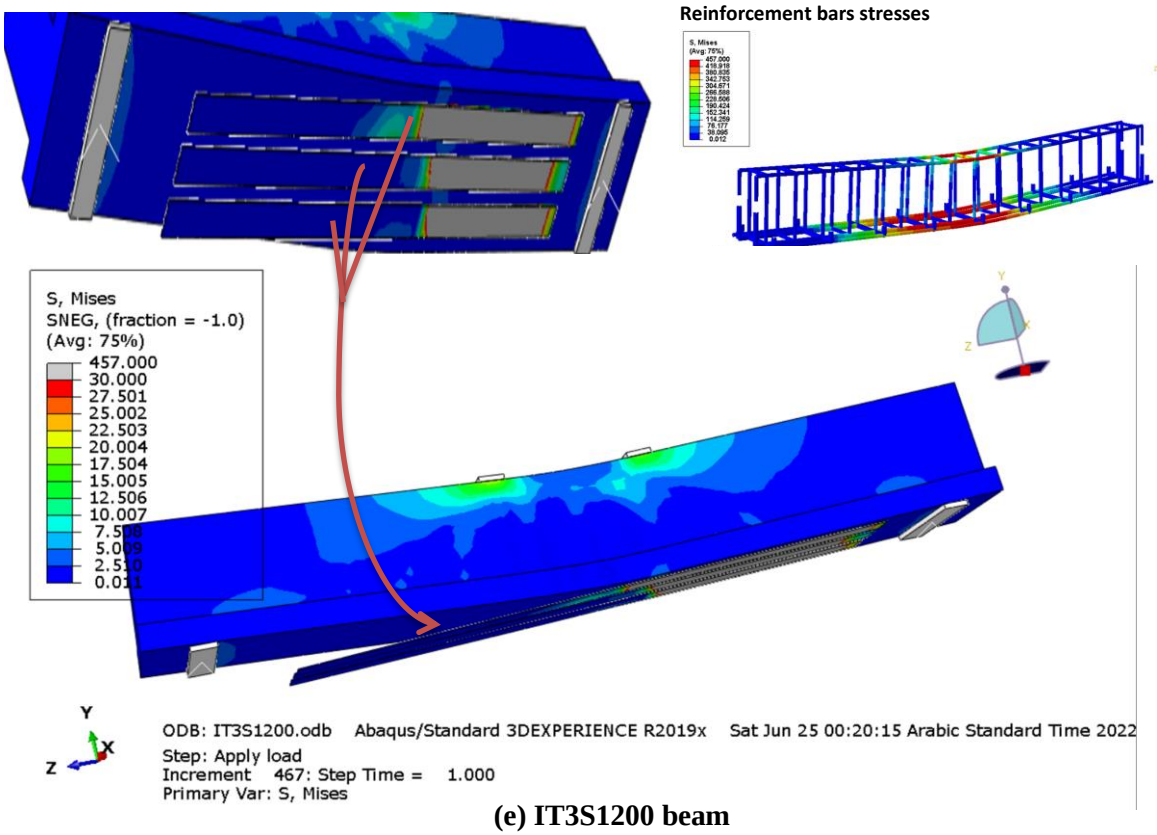

(e) IT3S1200 beam

Figure (5-13): Stresses distribution of FEM for strengthening beams with steel plates (continued)

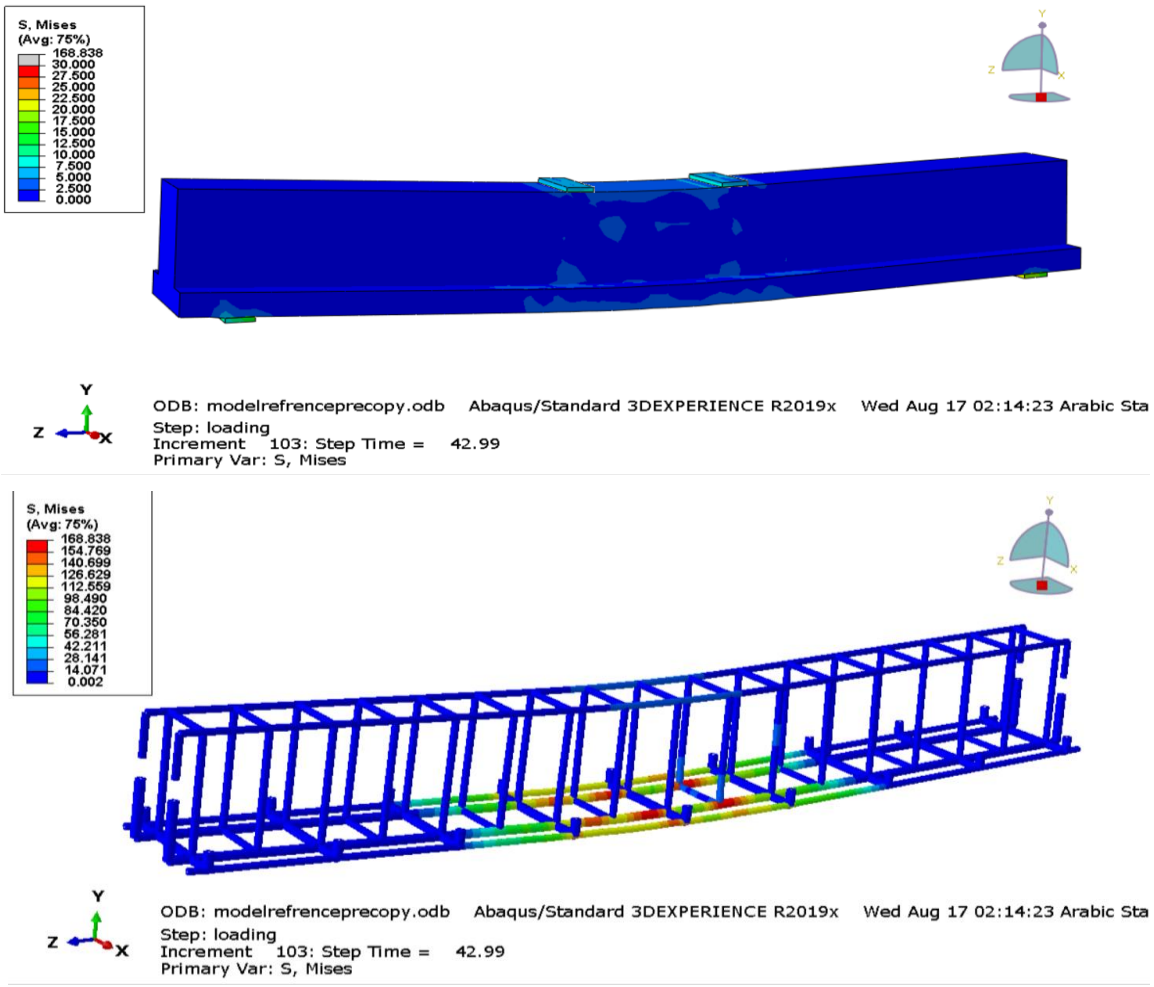

Figure (5-14): Stresses distribution of FEM before repair beam

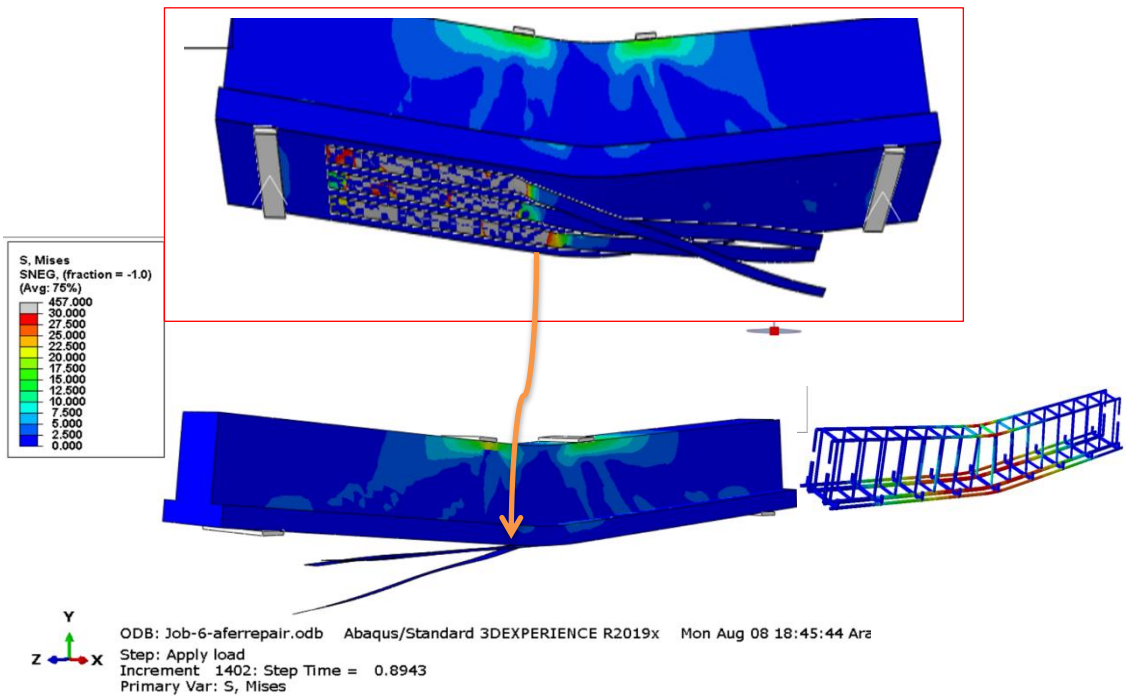

Figure (5-15): Stresses distribution of FEM after repair beam by CFRP strips (IT3FR1200)

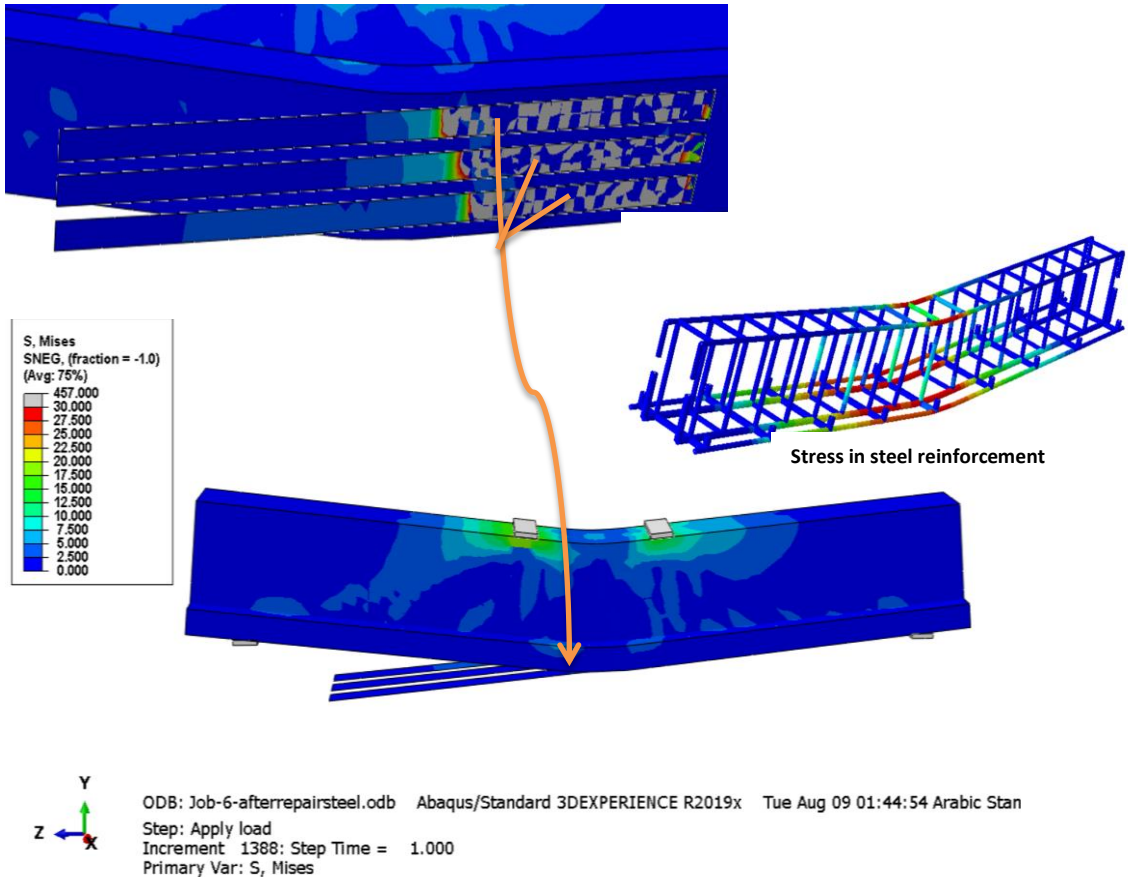

Figure (5-16): Stresses distribution of FEM after repair beam by steel plates (IT3SR1200)

5.8.3 Crack Pattern and Modes of Failure

The crack propagation patterns obtained from FEM analysis are similar to the crack propagation patterns recorded in the experimental study. Figures (5-17) to (5-22) show the comparison of crack patterns in FEM with experimental specimens for each total of (control specimen) and specimens strengthened or repaired with CFRP strips or steel plates. According to the observations made in the experimental work, the first cracks occurred in all cases in the bending regions. With the increase in load, cracks develop, newer cracks are formed and the older cracks become deeper in the areas of flexural. At the end, the failure observed in FEM for all beam specimens was the same as the experimental failure.

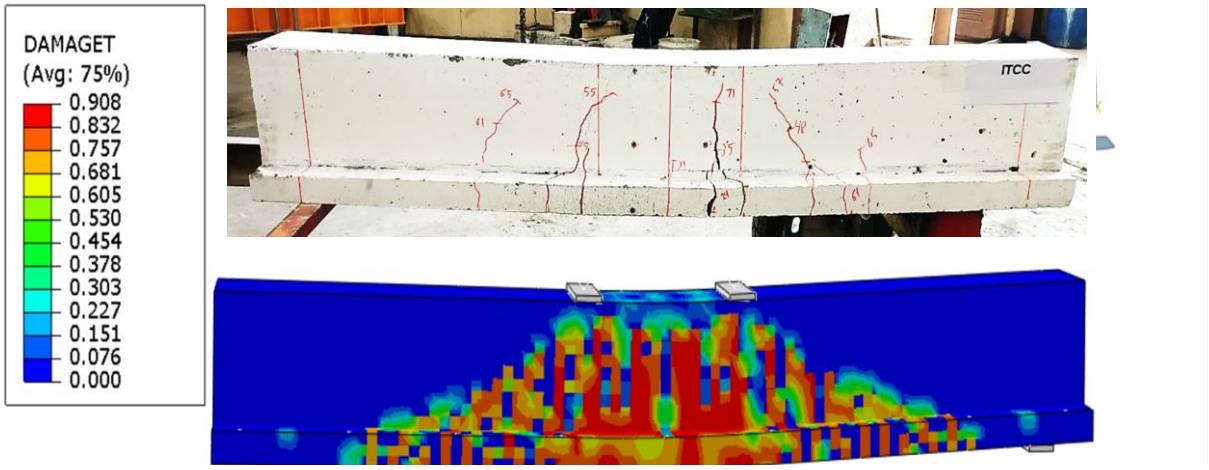

Figure (5-17): Cracking patterns of FEM versus experimental study for flexural beam (ITCC)

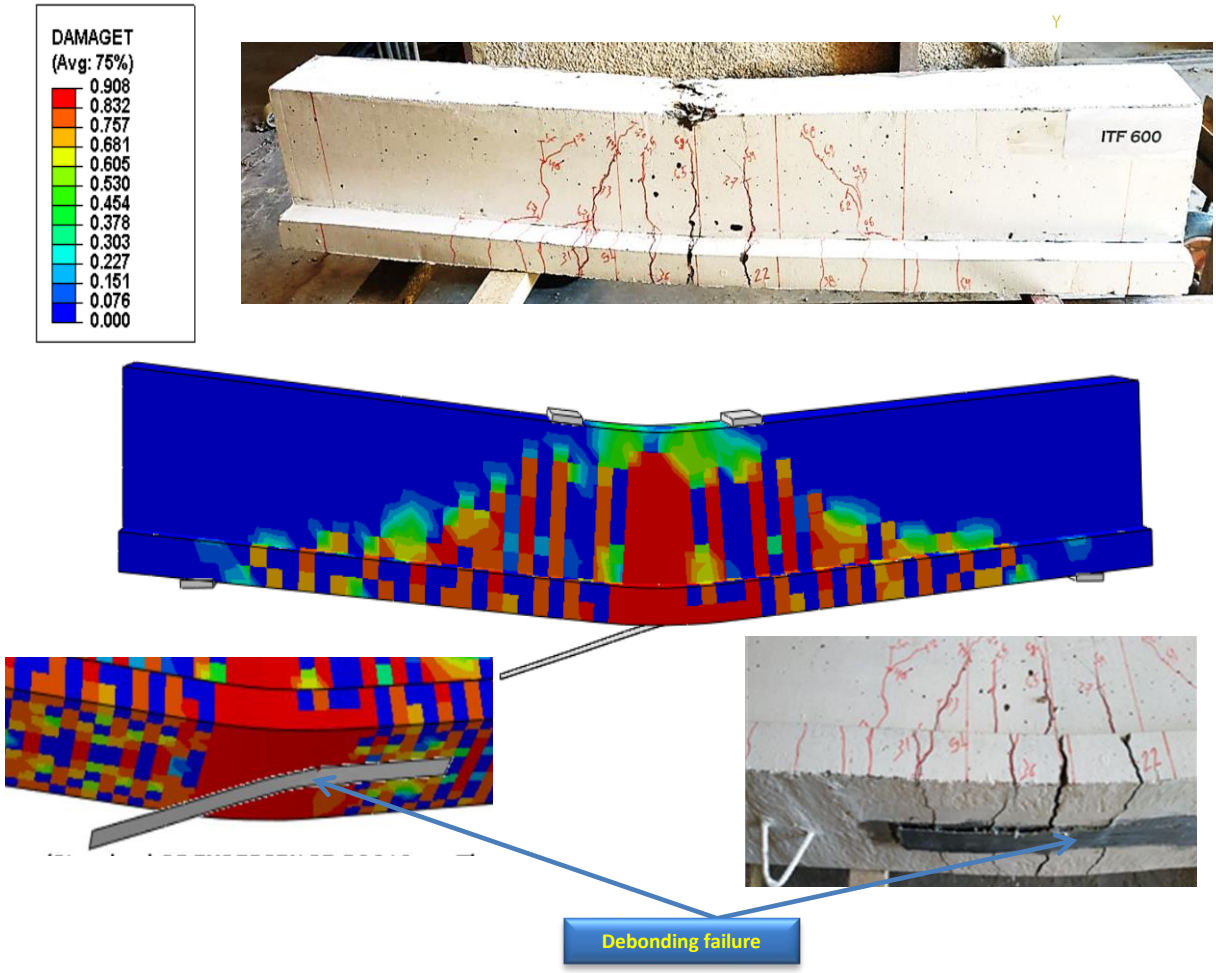

(a) ITF600 beam

Figure (5-18): Cracking patterns of FEM versus experimental study for flexural beams strengthening with CFRP strips (group one) (continue)

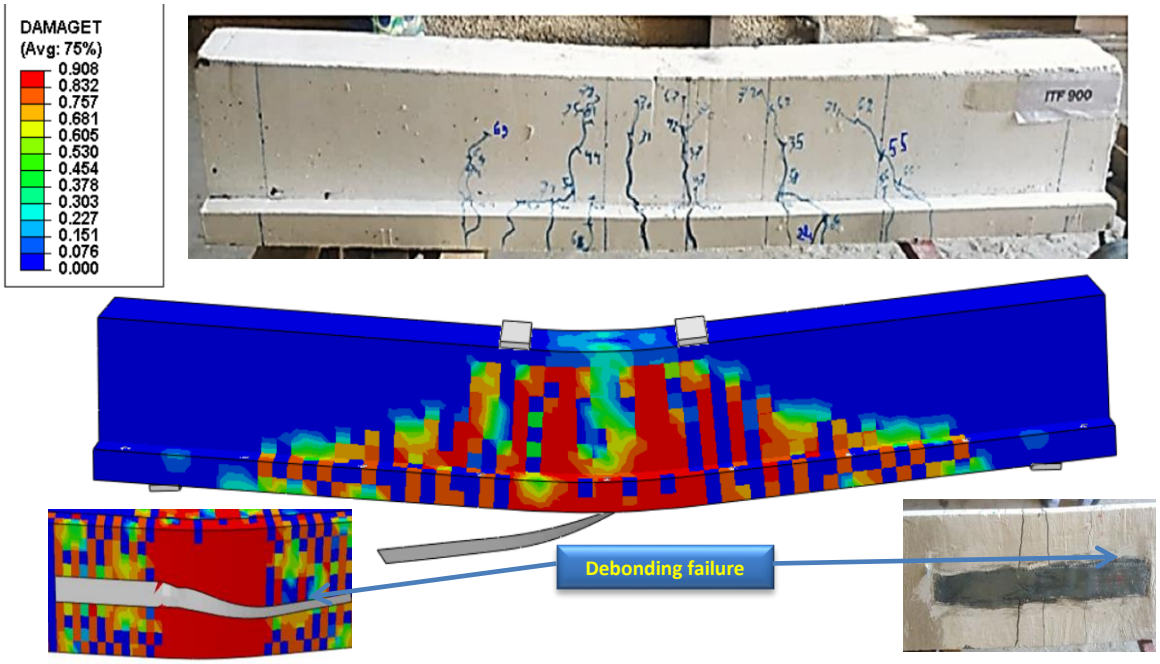

(b) ITF900 beam

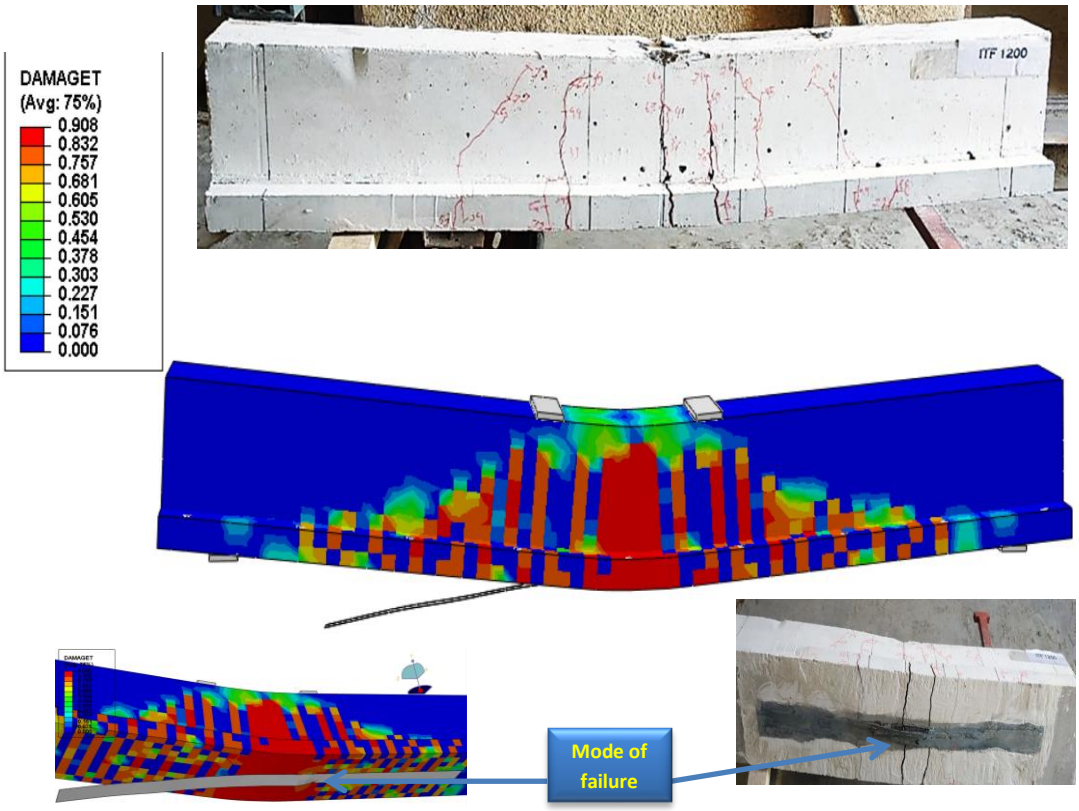

(c) ITF1200 beam

Figure (5-18): Cracking patterns of FEM versus experimental study for flexural beams strengthening with CFRP strips (group one) (continue)

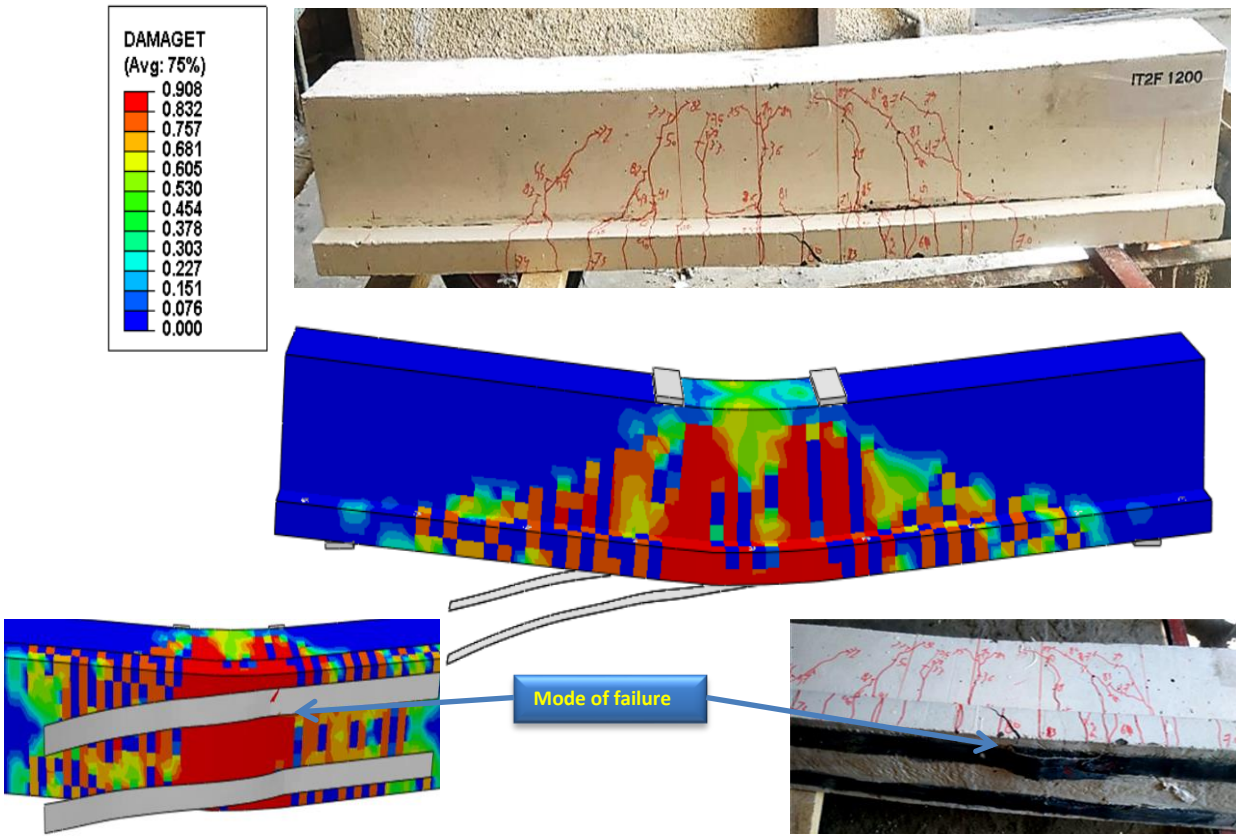

(d) IT2F1200 beam

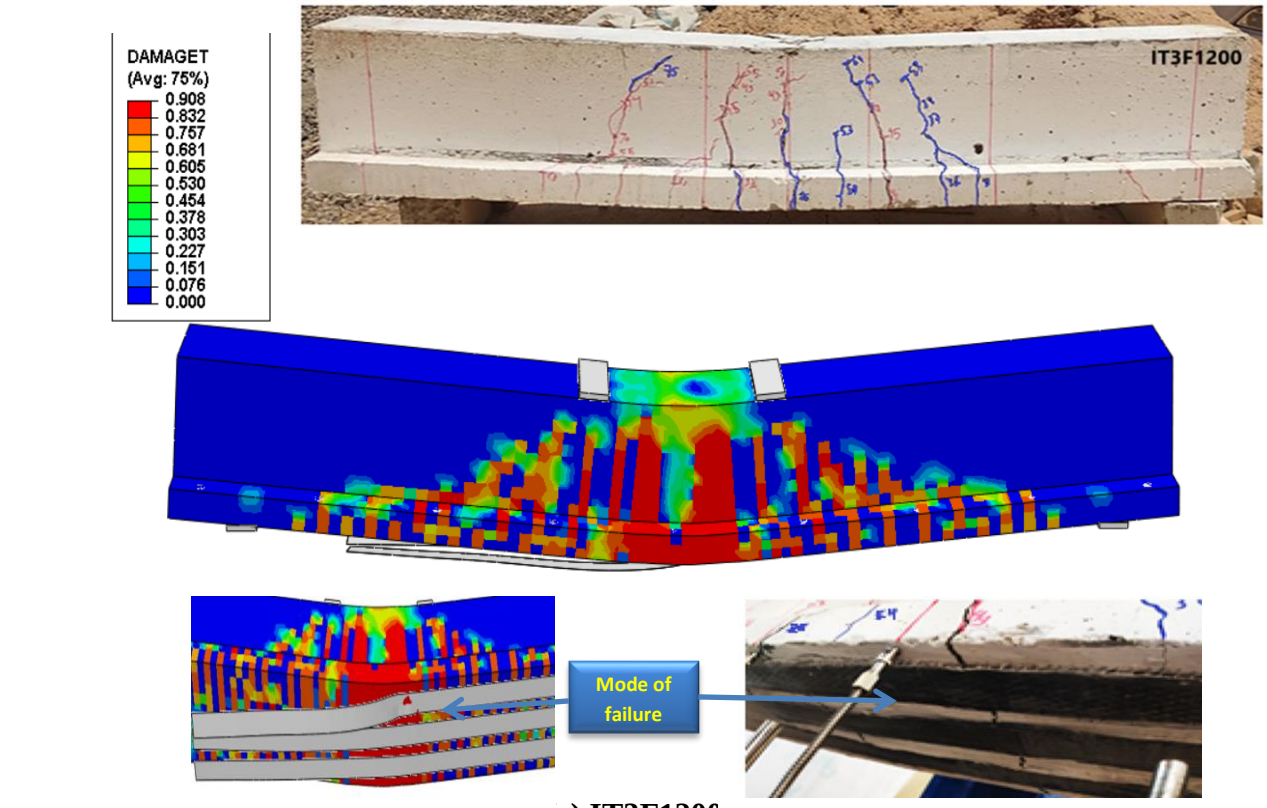

(e) IT3F1200 beam

Figure (5-18): Cracking patterns of FEM versus experimental study for flexural beams strengthening with CFRP strips (group one) (continued)

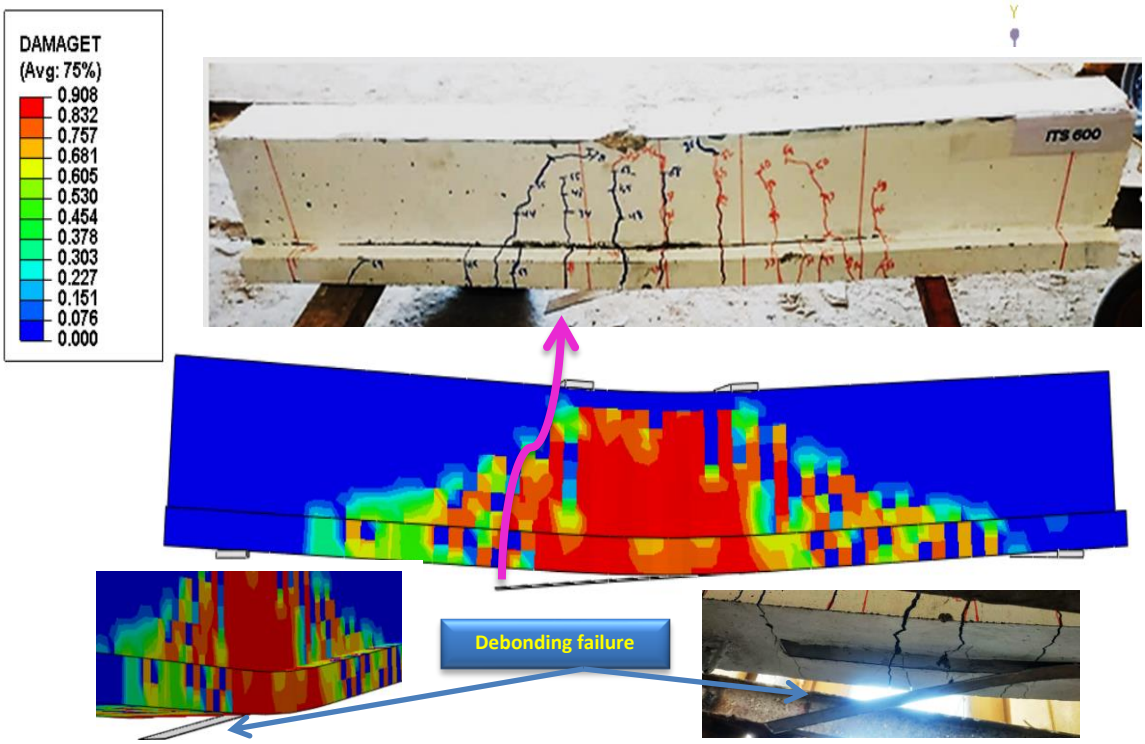

(a) ITS600 beam

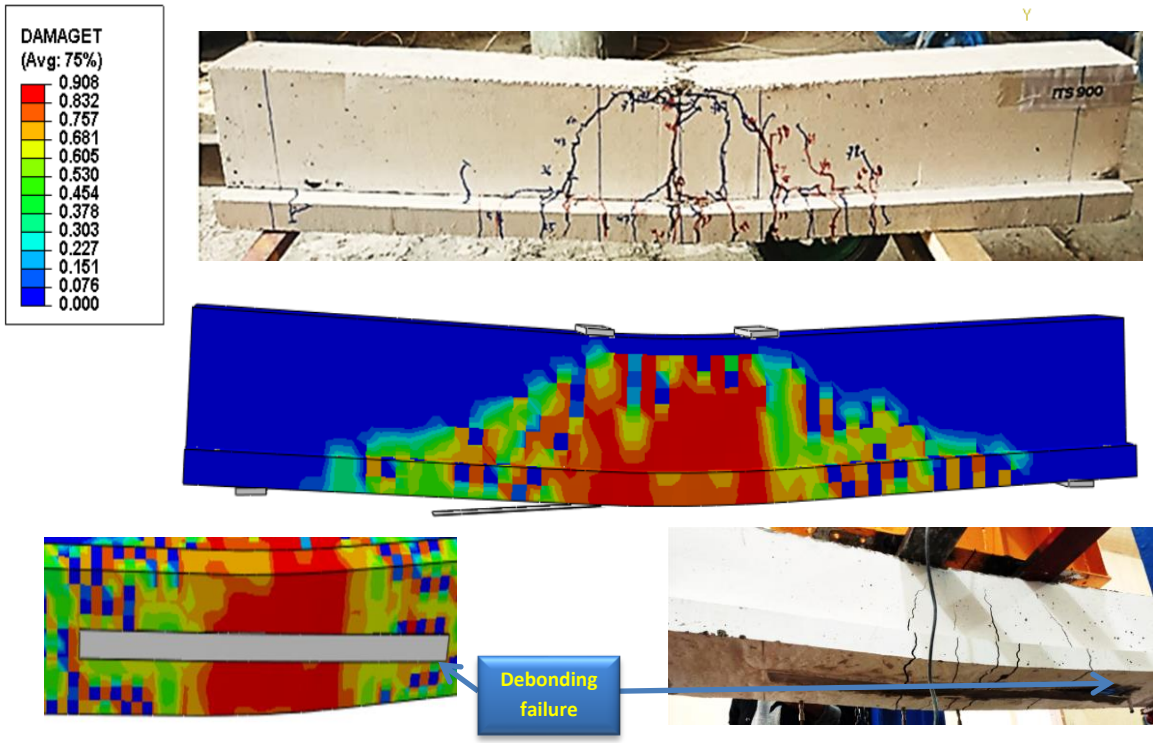

(b) ITS900 beam

Figure (5-19): Cracking patterns of FEM versus experimental study for flexural beams strengthening with steel plates (group two) (continue)

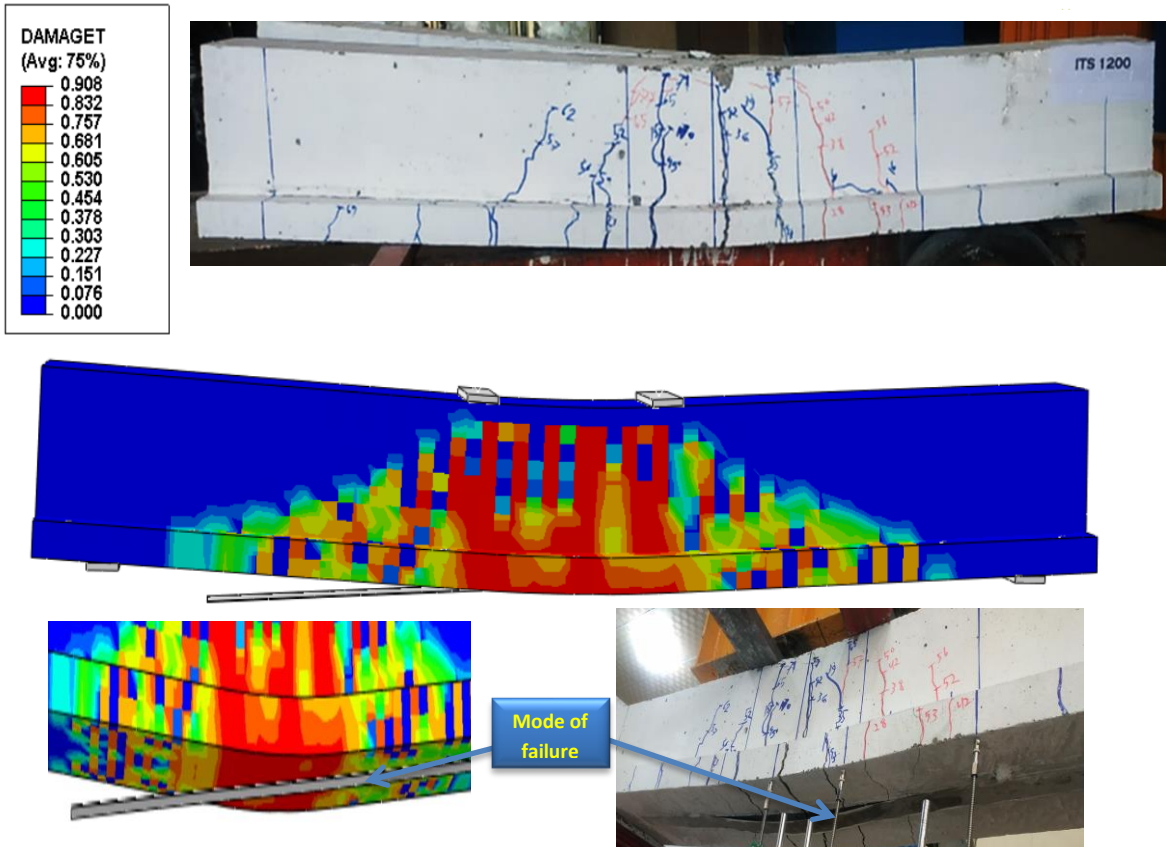

(c) ITS1200 beam

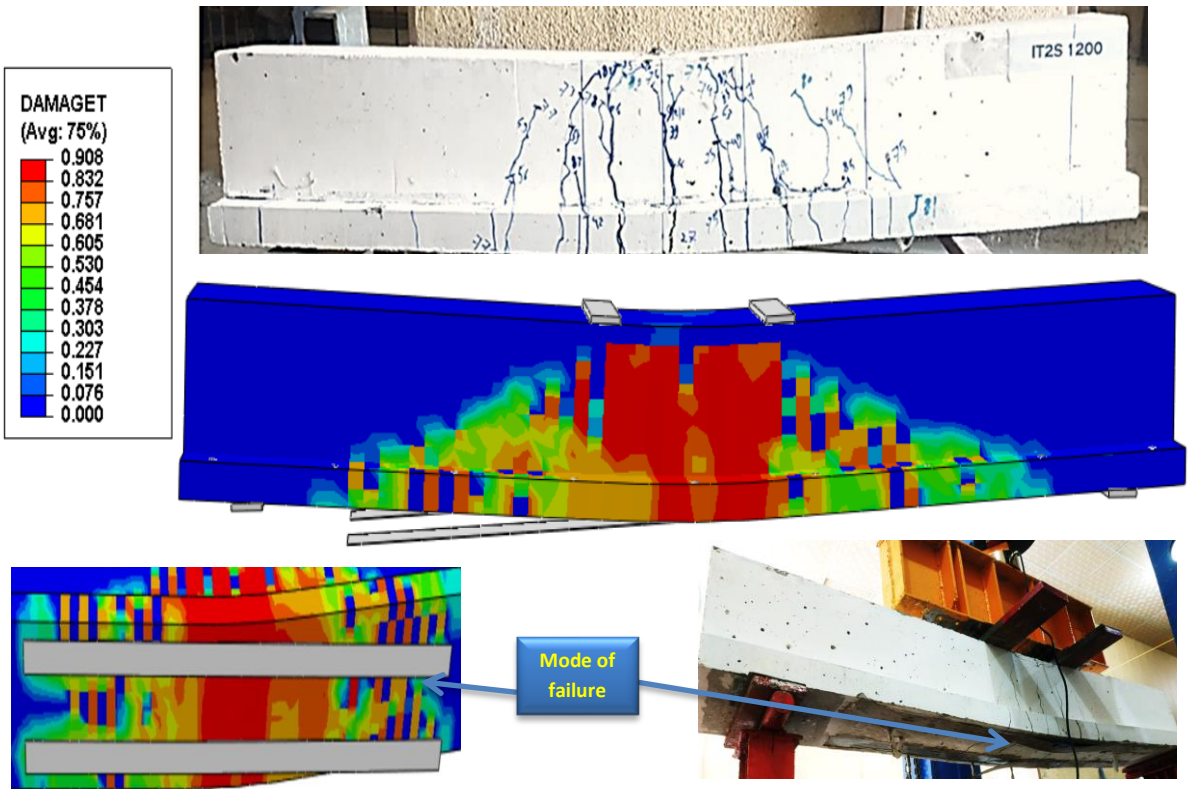

(d) IT2S1200 beam

Figure (5-19): Cracking patterns of FEM versus experimental study for flexural beams strengthening with steel plates (group two) (continue)

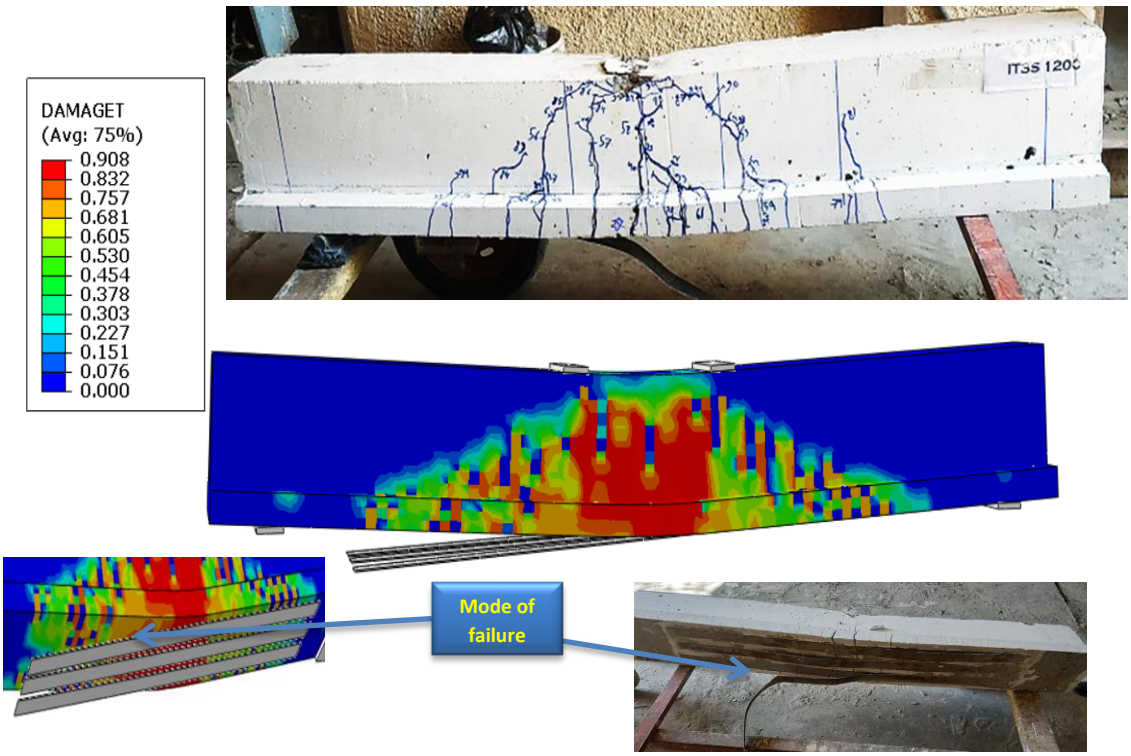

(e) IT3S1200 beam

Figure (5-19): Cracking patterns of FEM versus experimental study for flexural beams strengthening with steel plates (group two) (continued)

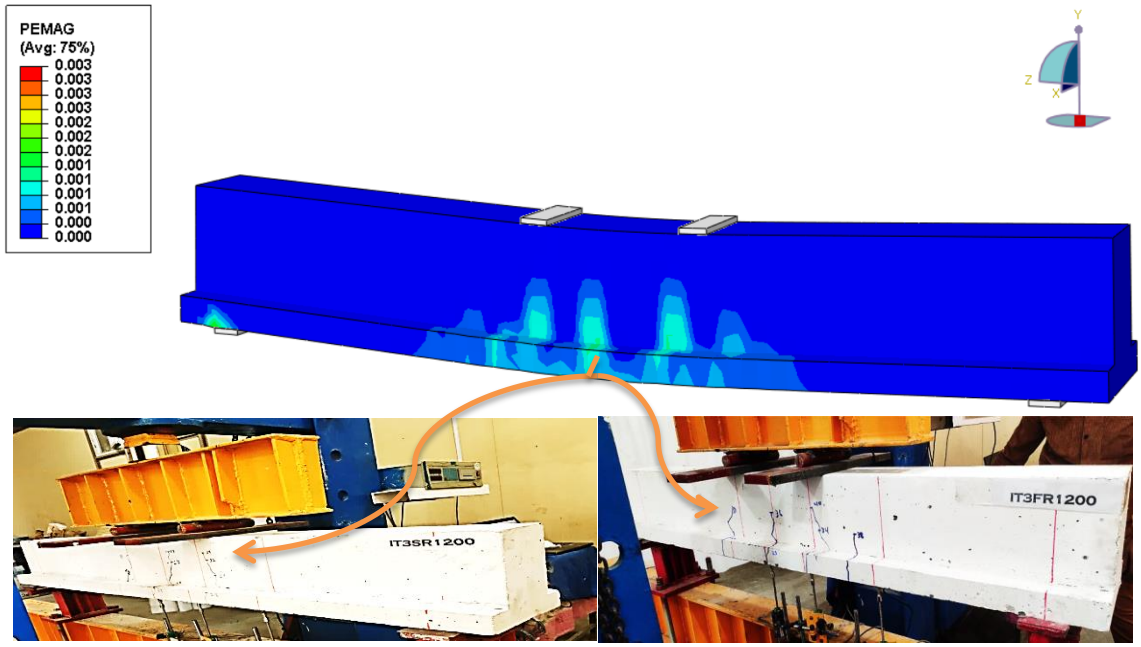

Figure (5-20): Cracking patterns of FEM versus experimental study for flexural beams (before the repair) with CFRP strips (IT3FR1200) and steel plates (IT3SR1200)

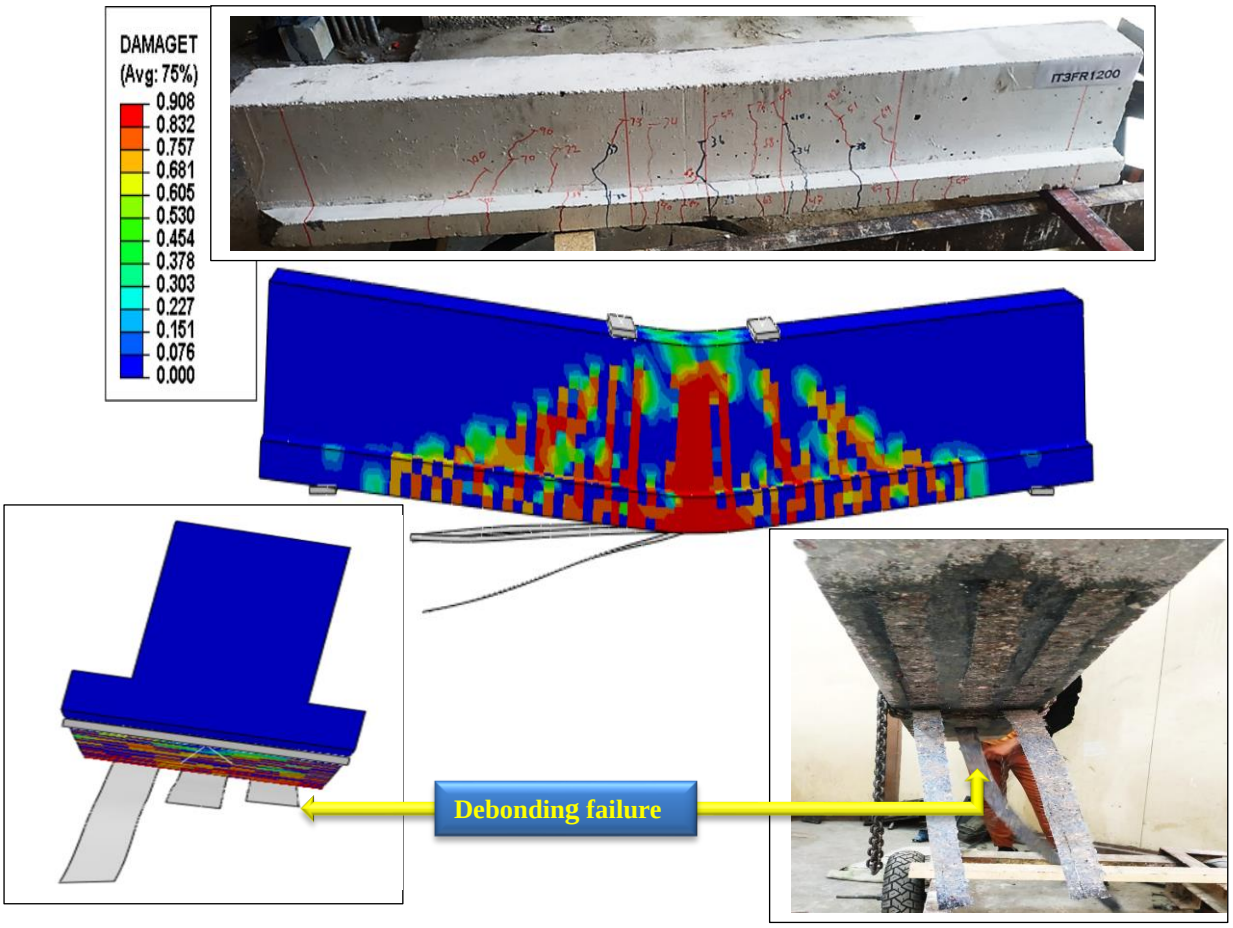

Figure (5-21): Cracking patterns of FEM versus experimental study for flexural beam (after repair) with CFRP strips (IT3FR1200)

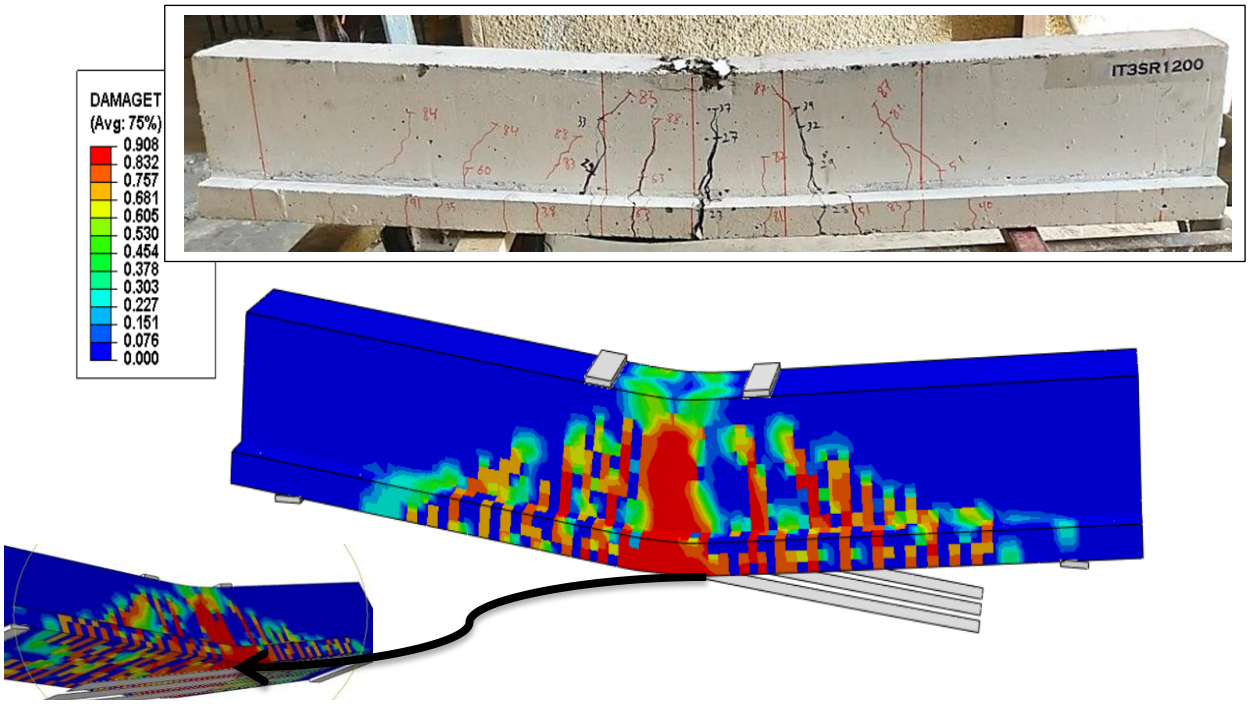

Figure (5-22): Cracking patterns of FEM versus experimental study for flexural beam (after repair) with steel plates (IT3SR1200)

5.9 Parametric study

In this study, the use of the FE model is developed in order to predict and know more details of the understanding of the behavior of the inverted T beams. The ABAQUS program achieved an acceptable level of accuracy to conduct a parametric study for the purpose of studying the effect of some variables on the behavior of the inverted T beam, which was not studied in the experimental program. The parameters that have been studied are as follows:

1- Increase the strengthening length of CFRP strips and also, increase the strengthening length of steel plates.

2- Increase the strengthening width of the CFRP sheet.

3- Increase the thickness of the steel plates to (a) 2mm and (b)3mm.

4- Increase the number of layers of (CFRP) sheets.

The specimens developed and used in the (ABAQUS) program were shown in Table (5-5) as follows:

Table (5-5): Specimens developed symbols

Symbol	Details
IT3F1500	**Inverted T beam three CFRP strips strengthening length 1500mm.**
IT3S1500	**Inverted T beam three steel plates strengthening length 1500mm.**
ITF1500-w250	**Inverted T beam CFRP sheets strengthening length 1500mm strengthening width 250mm.**
ITS1200-2th	**Inverted T beam steel plates strengthening length 1200mm-2mm thickness numerical model.**
ITS1200-3th	**Inverted T beam steel plates strengthening length 1200mm-3mm thickness.**
IT3F1200-2La	**Inverted T beam three CFRP strips strengthening length 1200mm-2 layers of CFRP strips.**

5.9.1 Increase the strengthening length

The best strengthening length selected from the numerical specimens, which was estimated at a length of 1200 mm, was developed to the length of the strengthening possessed by the analytical specimens, which was estimated at a length of 1500 mm, for the purpose of discovering the effect of increasing the length of the strengthening from CFRP strips or steel plates on the behavior of the inverted T-beams. The comparison between the beams on ultimate load and ultimate deflection is shown in Table (5-6). Figure (5-23) explain the behavior of beams at the ultimate stage.

Table (5-6): Comparison between the beams on ABAQUS results for specimens (IT3F1500, IT3F1200, IT3S1500 and IT3S1200)

Specimens	Load Capacity kN	Deflection Capacity mm	Difference in Ultimate Load %	Difference in Ultimate Deflection%
IT3F1500	108.073	29.33	1.67	12.55
IT3F1200	106.301	26.06		
IT3S1500	97.795	22.89	3.27	9.05
IT3S1200	94.696	20.99		

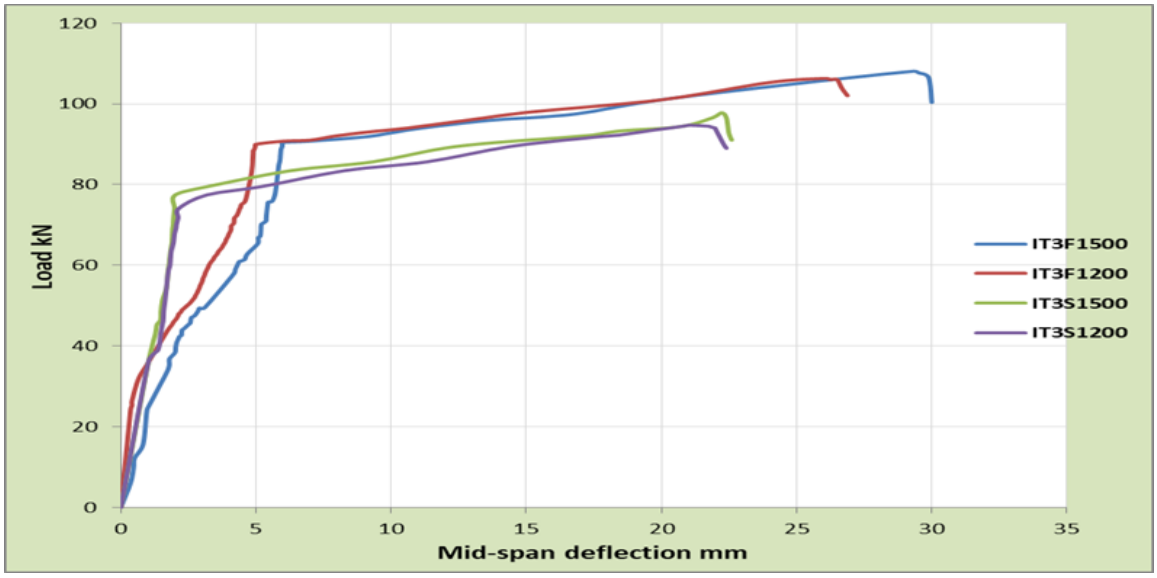

Figure (5- 23): ABAQUS results for load-deflection response of beams IT3F1500, IT3F1200, IT3S1500 and IT3S1200

When the strengthened beam with a length of 1500mm of (CFRP) strips (IT3F1500) is compared to the specimen (IT3F1200), the value of load capacity increases (1.67%), and the value of deflection capacity increases (12.55%). Also, when the strengthened beam with a length of 1500mm of steel plates (IT3S1500) is compared to the specimen (IT3S1200), the value of load capacity increases (3.27%), and the value of deflection capacity increases (9.05%). The beam specimens (IT3F1500 and IT3S1500) don't build and tested experimentally due to the time and high cost required, so the beam specimens were completed through the ABAQUS program. Indeed, increasing the strengthening length of (CFRP) strips increased load and deflection. As a result, the beam specimens (IT3F1500 and IT3S1500) give the best result when compared to the other specimens (IT3F1200 and IT3S1200).

Figure (5-24) and Figure (5-25) shows the principle stress distribution and crack pattern at the ultimate load formed by the FEM for flexural beams (IT3F1500 and IT3S1500).

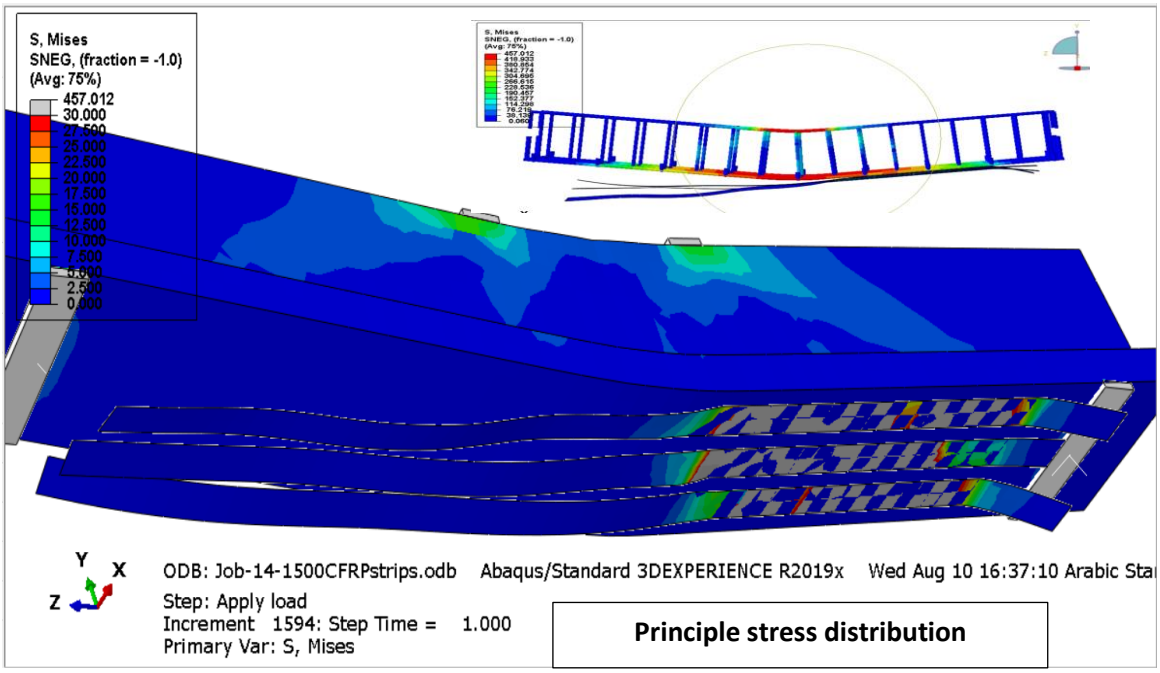

Figure (5-24): Principle stress distribution and crack pattern at ultimate load formed by the FEM for flexural beams (IT3F1500) (continue)

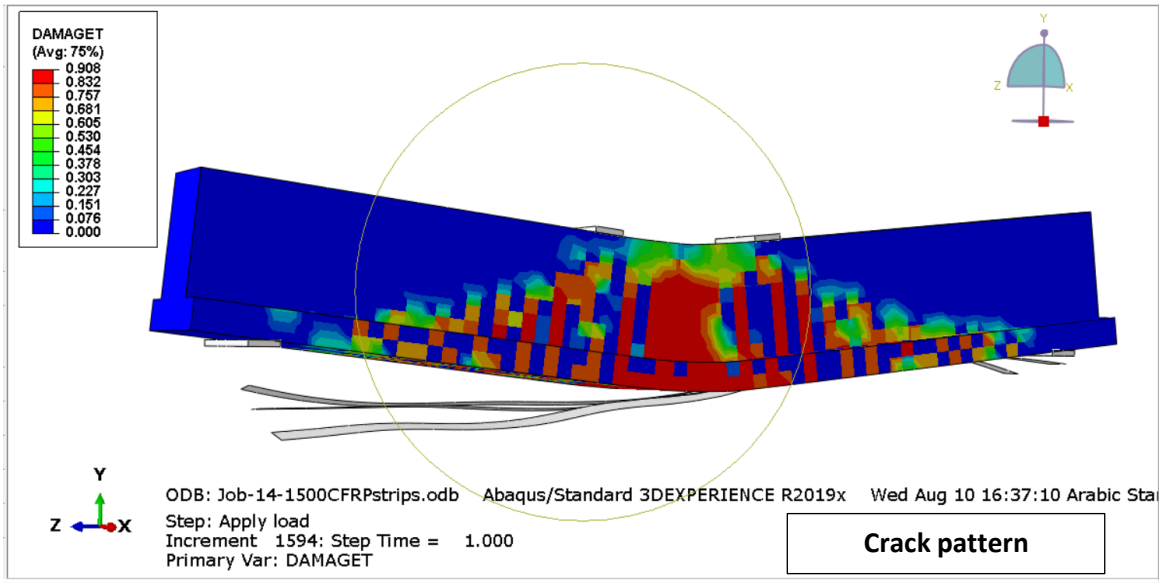

Figure (5-24): Principle stress distribution and crack pattern at ultimate load formed by the FEM for flexural beams (IT3F1500) (continued)

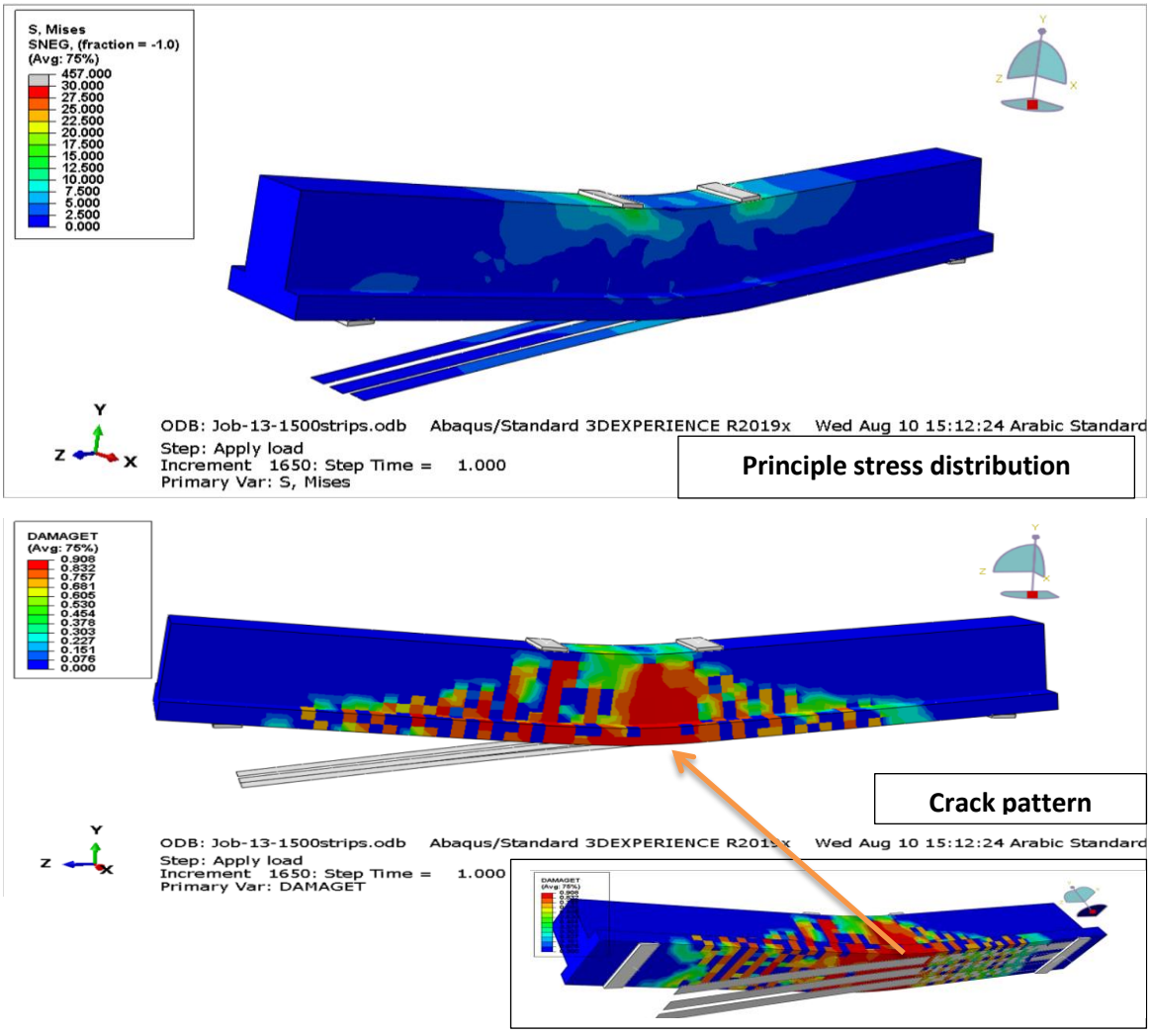

Figure (5-25): Principle stress distribution and crack pattern at ultimate load formed by the FEM for flexural beams (IT3S1500)

5.9.2 Increase the strengthening width of the CFRP sheet

With the development of the strengthening length to 1500 mm in specimen IT3F1500 that was implemented in the ABAQUS program to obtain the best result for the length of the strengthening, and as mentioned in paragraph (5.9.1), in this paragraph, the width of the strengthening is developed to 250 mm on the width of the inverted T beam with fixing the length of the strengthening 1500 mm to obtain the best and most accurate results from the width and total length of the reinforcement. The comparison between the beams on ultimate load and ultimate deflection is shown in Table (5-7). Figure (5-26) explain the behavior of beams at the ultimate stage.

Table (5-7): Comparison between the beams on ABAQUS results for specimens (IT3F1500-w250 and IT3F1500)

Specimens	Load Capacity kN	Deflection Capacity mm	Difference in Ultimate Load %	Difference in Ultimate Deflection%
IT3F1500-w250	118.407	32.21	9.56	9.82
IT3F1500	108.073	29.33		

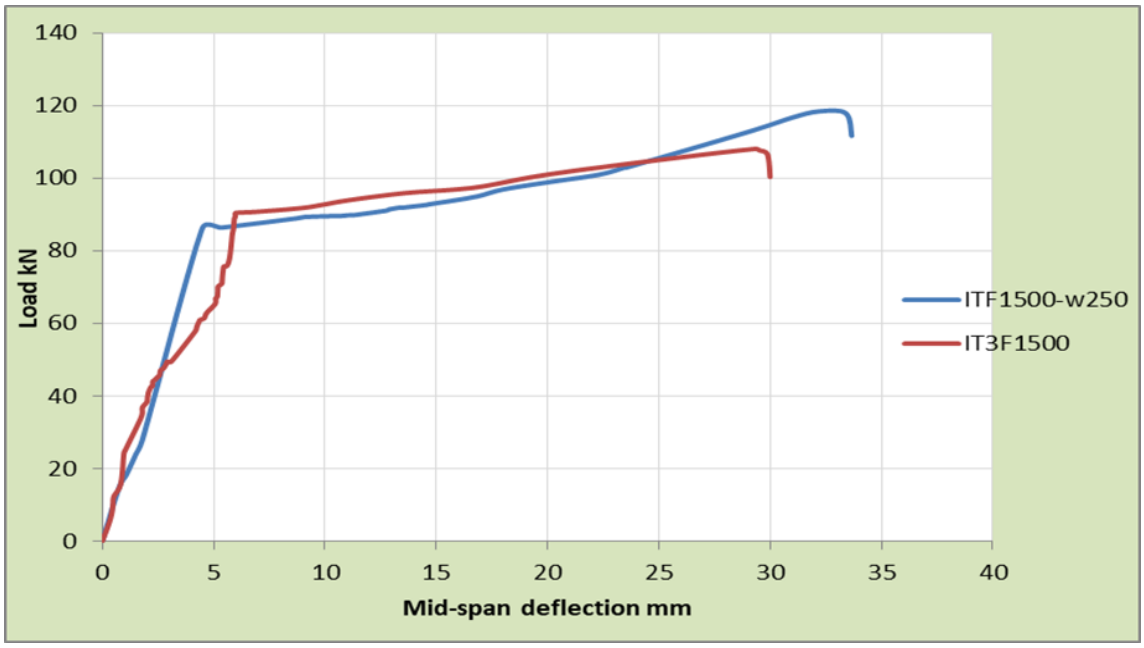

Figure (5- 26): ABAQUS results for load-deflection response of beams ITF1500-w250 and IT3F1200

When the strengthened beam with a length of 1500mm and width of 250mm of (CFRP) sheets (ITF1500-w250) with compared to the specimen (IT3F1500), the value of load capacity increases (9.56%), and the value of capacity deflection increases (9.82%). The beam specimens (ITF1500-w250) don't build and tested experimentally due to the time and high cost required, so the beam specimen was completed through the ABAQUS program. Indeed, increasing the strengthening width of the (CFRP) sheet increased load and deflection. As a result, the beam specimens (ITF1500-w250) give the best result when compared to the other specimen (IT3F1500).

Figure (5-27) shows the principle stress distribution and crack pattern at the ultimate load formed by the FEM for flexural beams (ITF1500-w250).

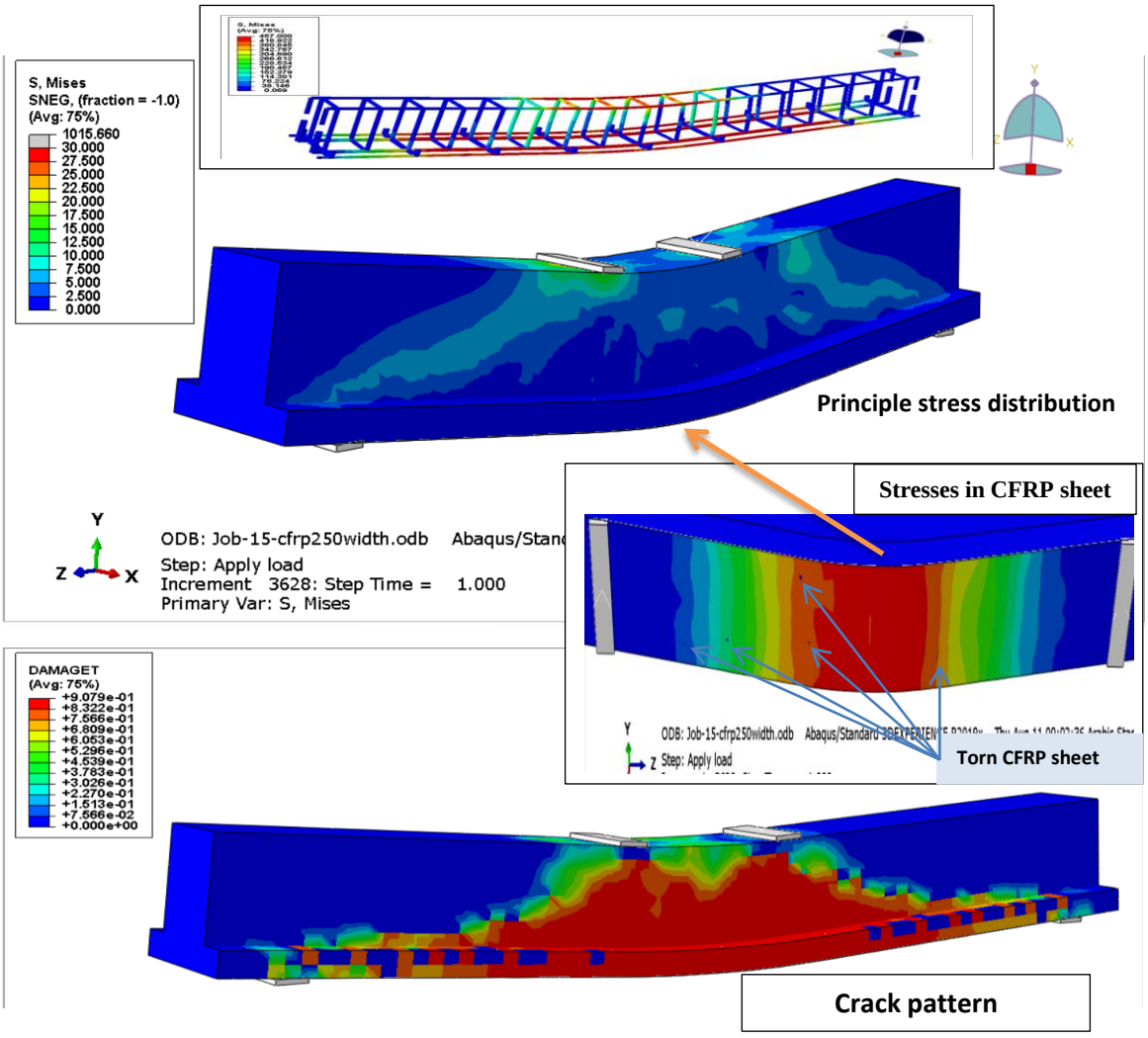

Figure (5-27): Principle stress distribution and crack pattern at ultimate load formed by the FEM for flexural beams (ITF1500-w250)

5.9.3 Increase the thickness of the steel plates to (a) 2mm and (b) 3mm

The best thickness selected for experimental specimens according to previous research is estimated at 0.8 mm. This thickness was developed by the FEM analytical method to know the effect of increasing the thickness on the behavior of the inverted T beams. The suggested thickness used in FEM analytical was (a) 2mm and (b) 3mm. The comparison between the beams on ultimate load and ultimate deflection is shown in Table (5-8). Figure (5-28) explain the behavior of beams at the ultimate stage.

Table (5-8): Comparison between the beams on ABAQUS results for specimens (IT3S1200-2th, IT3S1200) and (IT3S1200-3th, IT3S1200)

Specimens	Load Capacity kN	Deflection Capacity mm	Difference in Ultimate Load %	Difference in Ultimate Deflection%
IT3S1200-2th	81.069	13.12	-14.39	-37.48
IT3S1200	94.696	20.99		
IT3S1200-3th	82.243	13.24	-13.15	-36.92
IT3S1200	94.696	20.99		

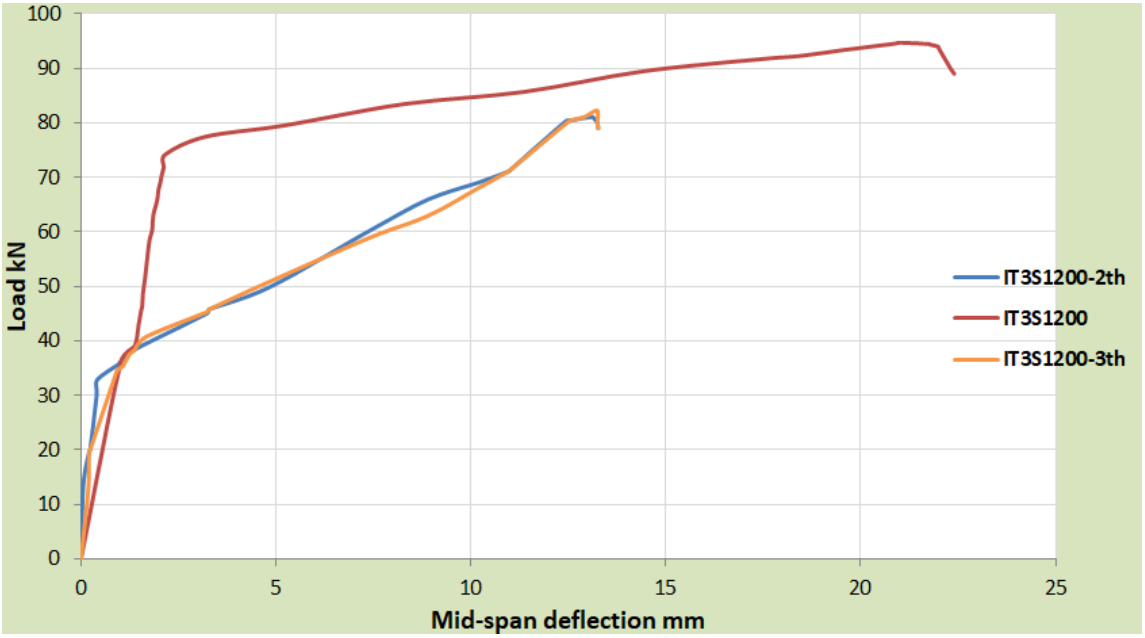

Figure (5- 28): ABAQUS results for a load-deflection response of beams IT3F1200-2th, IT3S1200 and IT3S1200-3th

In the FEM method, when a steel plate was used to strengthen the beam with a thickness of 2 mm and 3 mm, similar results were observed in terms of load and mid-span deflection between beams strengthening with steel plates with thicknesses of 2 mm and 3 mm. The results of the beams strengthened with thicknesses of 2 mm and 3 mm were compared with the numerical results for the beam strengthened with steel plates with thicknesses of 0.8 mm, the value of load capacity decreased to (-14.39% and -13.15%) respectively, also the value deflection capacity decreased to (37.48% and -36.92%) respectively.

Figure (5-29) and Figure (5-30) shows the principle stress distribution and crack pattern at the ultimate load formed by the FEM for flexural beams (ITF1500-2th and ITF1500-3th) respectively.

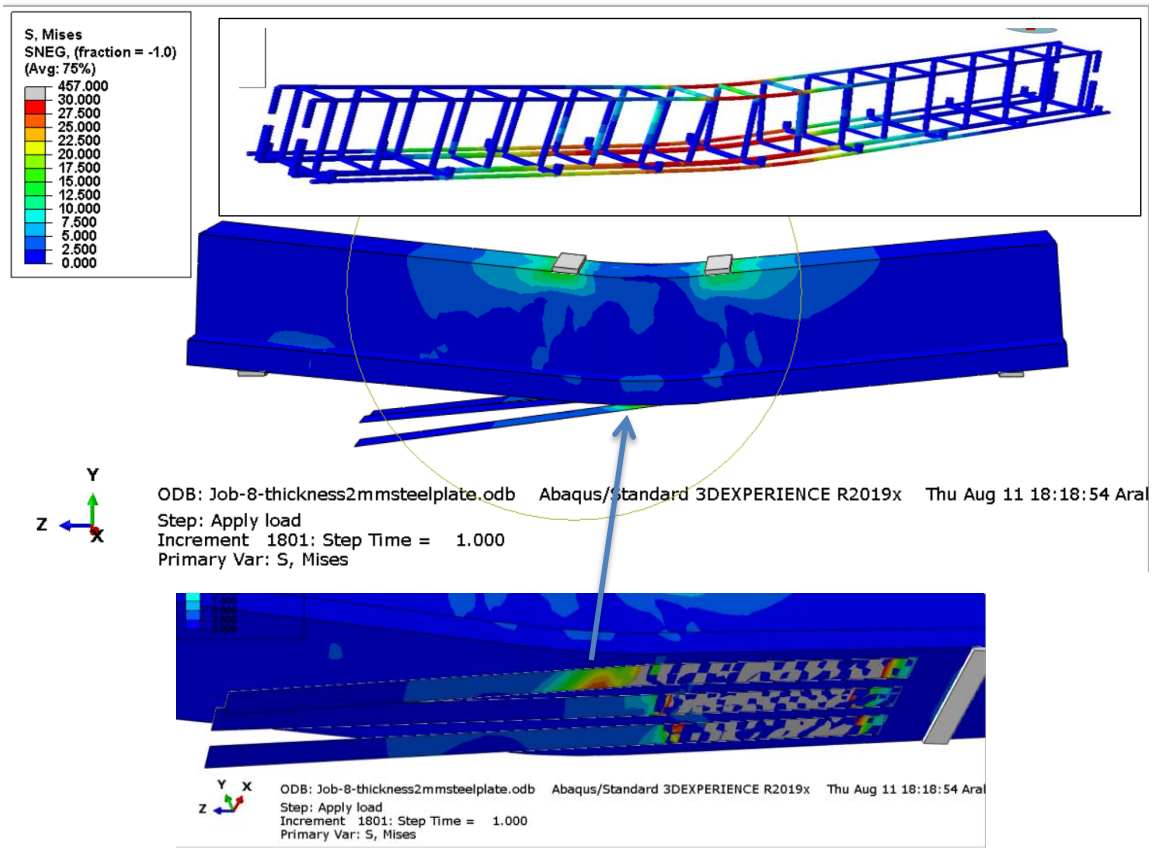

Figure (5-29): Principle stress distribution and crack pattern at ultimate load formed by the FEM for flexural beams (IT3S1200-2th) (continue)

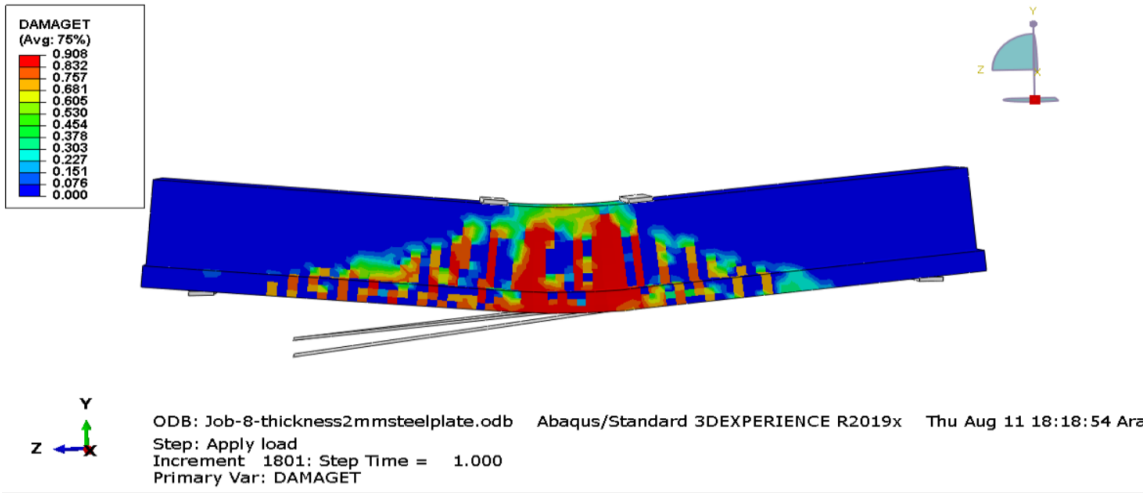

Figure (5-29): Principle stress distribution and crack pattern at ultimate load by FEM for flexural beam (IT3S1200-2th) (continued)

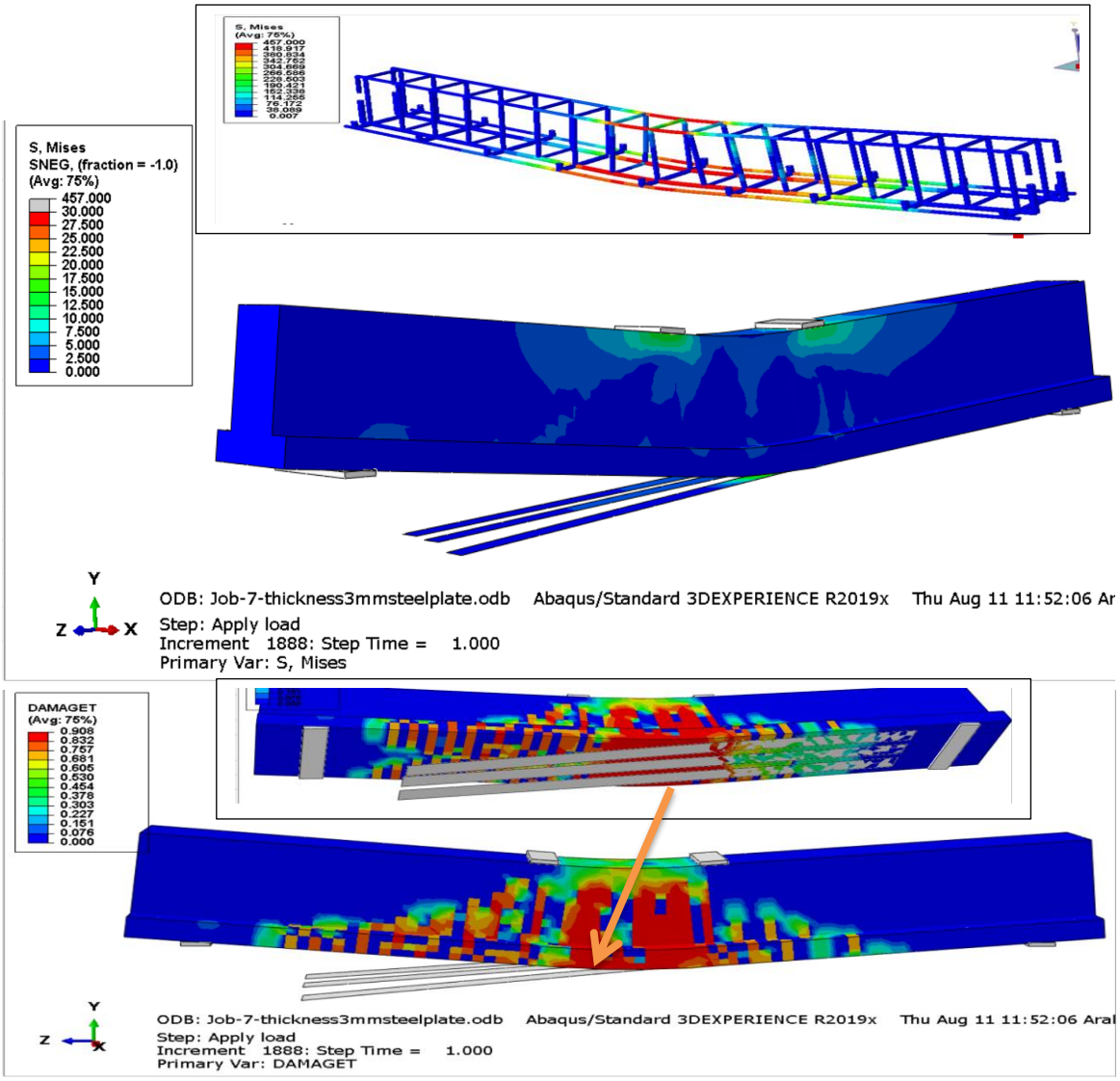

Figure (5-30): Principle stress distribution and crack pattern at ultimate load by FEM for flexural beam (IT3S1200-3th)

5.9.4 Increase the number of layers of (CFRP) sheets

For the study, the effect increased the thickness of the CFRP sheets by using double layers of CFRP sheets on the behavior of the inverted T beam. Therefore, the specimen (IT3F1200-2La) is taken and compared with the analytical specimen IT3F1200. The comparison between the beams on ultimate load and ultimate deflection is shown in Table (5-9). Figure (5-31) shows the behavior of beams at the ultimate stage.

Table (5-9): Comparison between the beams on ABAQUS result for the specimen (IT3F1200-2La and IT3F1200)

specimens	Load capacity kN	Deflection capacity mm	Difference in ultimate load%	Difference in ultimate deflection%
IT3F1200-2La	112.010	14.21	5.37	-45.47
IT3F1200	106.301	26.06		

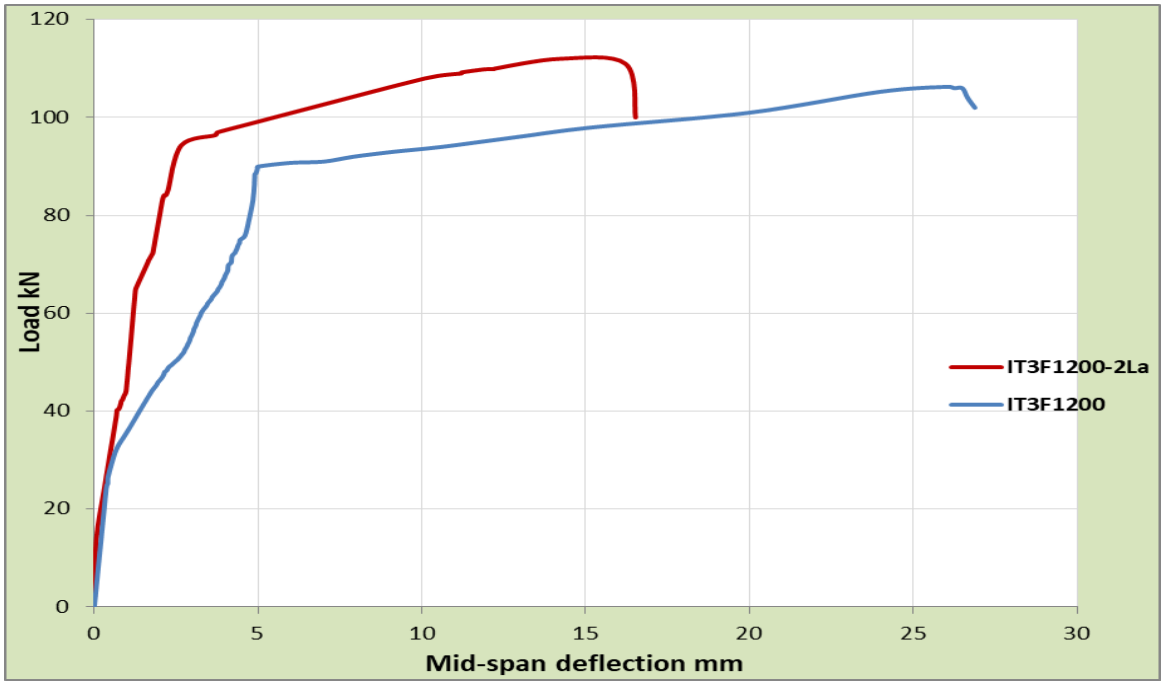

Figure (5- 31): ABAQUS results for a load-deflection response of beams IT3F1200-2La and IT3F1200

From comparing results between IT3F1200-2La and IT3F1200 specimens in a Table (5-9), appeared that the value of load capacity increased to (5.37%) while the value of the deflection capacity decreased to (45.47%). Don't apply the IT3F1200-2La in experimental work because it required added time and height cost, so this specimen study and completed in ABAQUS program software. It was concluded from the use of a double layer of CFRP sheets to increase the thickness of the layer, that the load increased and the deflection decreased.

Figure (5-32) shows the principle stress distribution and crack pattern at ultimate load formed by FEM for flexural beam IT3F1200-2La.

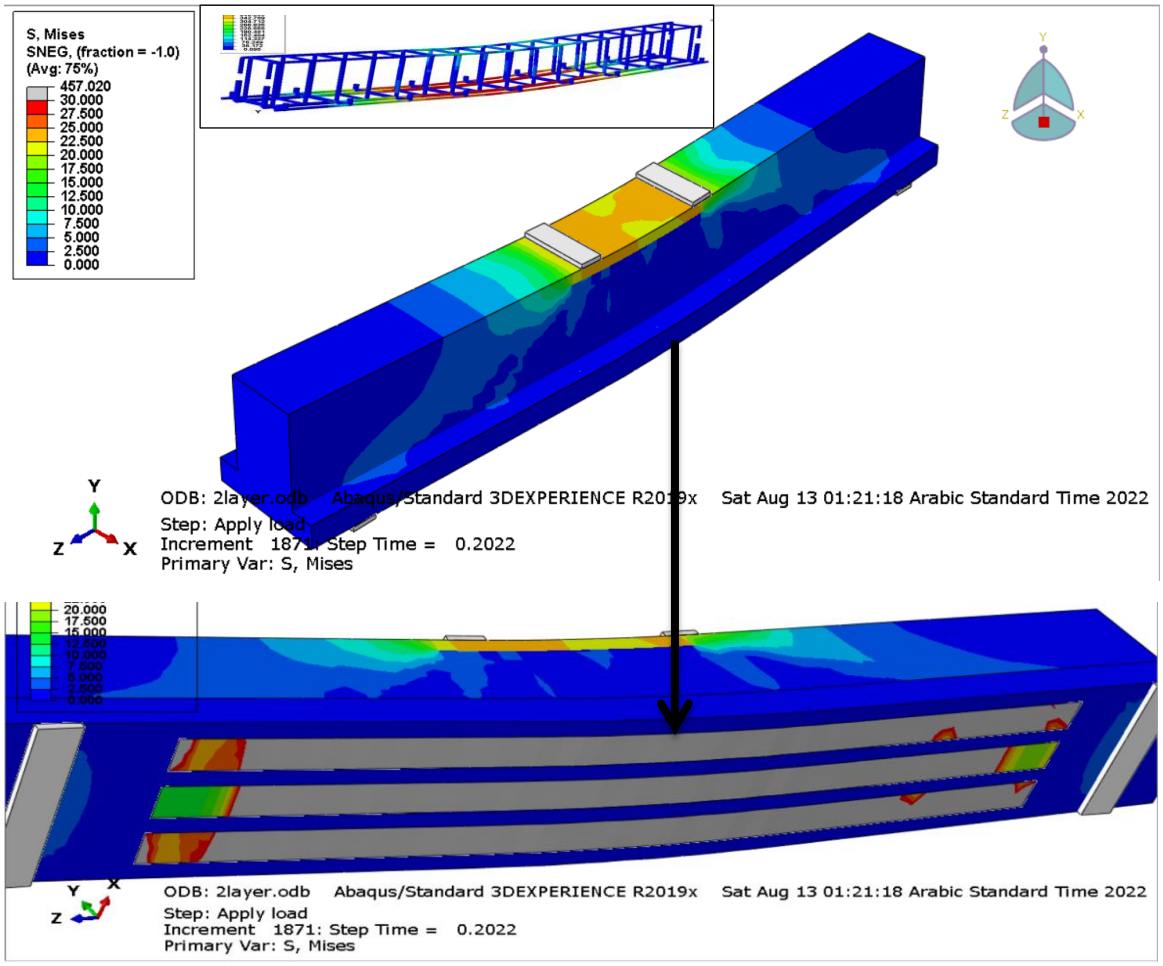

Figure (5-32): Principle stress distribution and crack pattern at ultimate load by FEM for flexural beam (IT3F1200-2La) (continue)

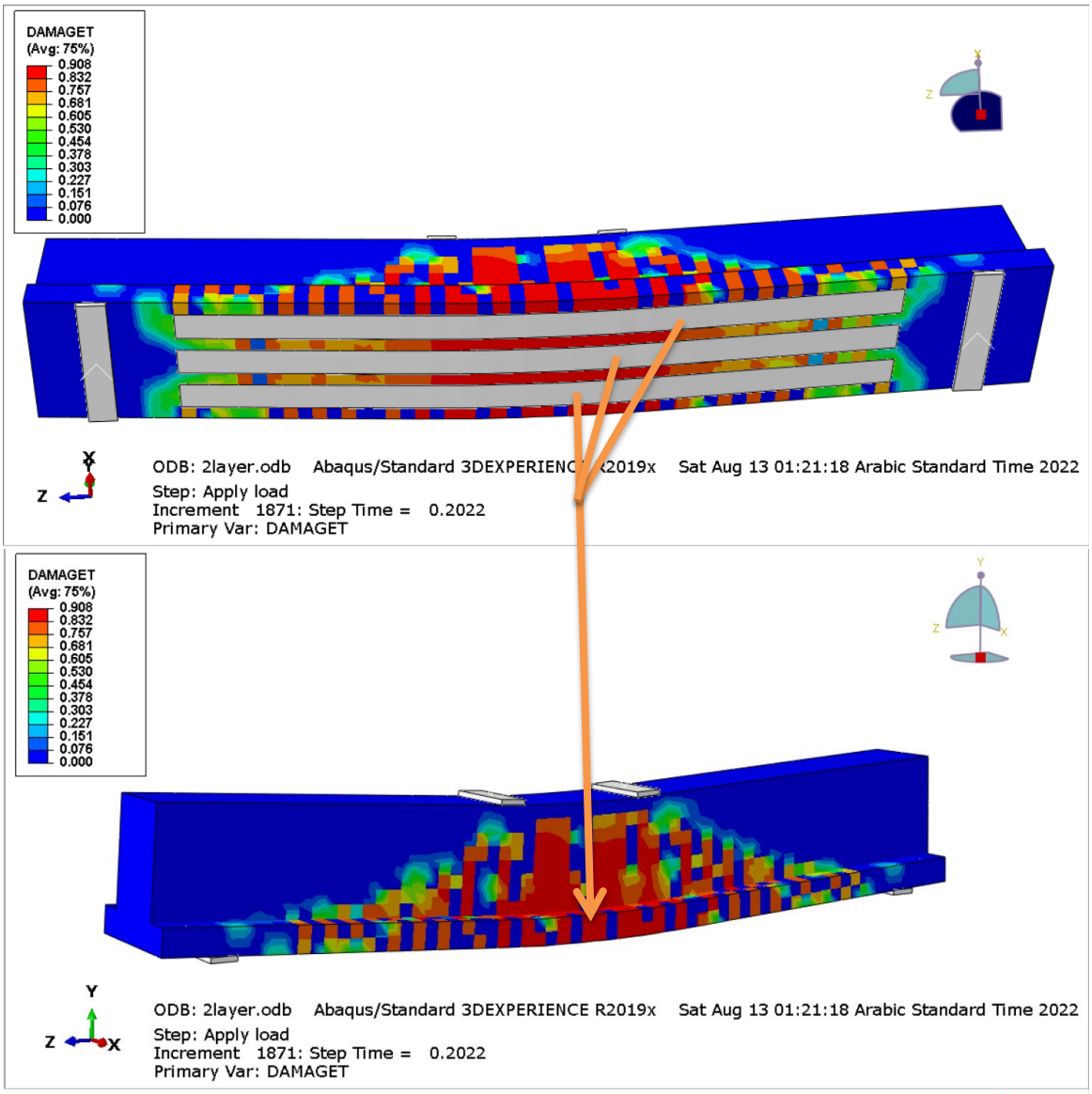

Figure (5-32): Principle stress distribution and crack pattern at ultimate load by FEM for flexural beam (IT3F1200-2La) (continued)

CHAPTER SIX

CONCLUSIONS AND RECOMMENDATIONS

*6.*1General

The main objective of this study is to study the flexural behavior of normal concrete simply supported inverted T beams retrofitted (strengthened and repaired) with (EBR CFRP strips or EBR steel plates). This thesis includes an experimental program in addition to the finite element model software using (ABAQUS standard/Explicit 2019) that develops to predict the flexural behavior of those tested RC beams. In this chapter, the conclusions drawn from the experimental and analytical findings are described and known. Also in this chapter suggestions are made for additional work in the future.

*6.*2 Conclusions

Depending on the overall results obtained from the experimental work and finite element analysis of externally retrofitted (strengthened and repaired) reinforced concrete inverted T beams with CFRP strips or steel plates failing in flexural, conclusions can be drawn as follows:

6.2.1 Conclusions from Experimental Work

1) In general, higher ultimate loads are achieved for inverted T beams strengthened with CFRP strips compared with (unstrengthened) control inverted T beam. The ultimate load increased by (10.2% to 45.4%). Also, For inverted T beams were strengthened with steel plates compared with (unstrengthened) control inverted T beam. The ultimate load increased by (0.7% to 31.1%).

2) For inverted T beams repaired with CFRP strips in flexural, the ultimate load increased by (39.3%) with respect to the ultimate load of the control inverted T beam. Also, For inverted T beams repaired with steel plates in flexural, the ultimate load increased by (29.6%) with respect to an ultimate load of control inverted T beam.
3) The presence of CFRP strips led to a decrease in the width of the cracks. The average of this decrease was about (16% to 69%) of the crack width in the control inverted T beam at ultimate load levels. Also, in the case of the presence of a steel plate, the average decrease in the width of the crack was about (17% to 39%) of the crack width in the control inverted T beam at ultimate load levels.
4) In general, all the inverted T beam deflections strengthened by steel plate were increased at load capacity if compared to the ITCC control beam while IT3S1200 beam deflection was convergent. As for the deflections of the beam strengthened with CFRP strips, the two beams (ITF600 and IT3F1200) recorded the highest deflection if they were compared to the control beam, As for the rest of the beams, the deflection values were recorded as lower compared to the beam control. Finally, the repair group recorded the highest deflection of the beam repaired with steel plates compared to the control beam.
5) The nature of the failure in all inverted T-beams is ductile according to what has been designed and according to the requirements of the ACI Code 318, 2019.
6) A more stiffness response was observed for the inverted T-beams retrofitted (strengthened and repaired) with steel plates or CFRP strips compared to the control beam.

7) Each inverted T beam retrofitted (strengthened and repaired) with CFRP strips or steel plates gave lower values of the ductility index when compared to the control beam specimen.
8) The percentage of increase in the load carrying capacity of the repaired inverted T beams (IT3FR1200 and IT3SR1200) is almost similar to that of the corresponding strengthened inverted T beams (IT3F1200 and IT3S1200) respectively.
9) In each tested inverted T beams considered in the present study, the failure mode of strengthened or repaired inverted T beams was flexural cracks causing debonding from the middle of the beam or its end or rupture of CFRP strips or steel plates located in the flexural zone at ultimate load level.
10) The strength of inverted T beams increased with strengthening length and width increased as compared with the response of the control inverted T beam, where the optimal ratio of effective length or effective width for CFRP strips or steel plates in all cases and in order to increase the ultimate load capacity was 80% and 60% respectively of the total length and width of the span, and this has been chosen as the maximum optimum increase in length and width for the purpose of taking into account the cost of materials.
11) The best results reflected the good ability to increase the load capacity of carbon fiber in retrofitting at a rate of (45.4%) by using three strips of CFRP dimensions [length (1200mm) and width (150mm)], as well as the case with the strengthened using steel plates, where the increase in the load capacity is (31.1%). This indicates that the dimensions of the length are 1200 mm and the width is 150 mm, an important, clear, and effective factor in increasing the resistance to inverted T-beam.
12) It was found that the CFRP strips used in the repair of the

inverted T beam gave better and higher results in terms of the ultimate load, crack width compared to the inverted T beam repaired by steel plates.

13) The technique of retrofitting (strengthening and repairing) by using steel plates gave a clear development in the energy absorption capacity compared to the control beam, while the retrofitted (strengthened and repaired) beams with CFRP strips technology gave similar values and lower values than the energy absorption capacity, except for beams ITF600 and IT3F1200 which gave higher values compared to control beam.

14) All inverted T beam specimens, whether strengthened or repaired, had a higher ultimate load and a higher load at the initiation of the first flexural crack (first crack load) compared to the control inverted T beam specimen. This is evidence that the use of CFRP strips or steel plates in retrofits has an effective role in the development of the strength of the structure as well as an effective role in delaying the appearance of the first crack.

6.2.2 Conclusions from the Finite Element Model

1) The 3D finite element model (ABAQUS 2019) used in the current study is capable to simulate the behavior of externally retrofitted reinforced concrete inverted T beams strengthened and repaired with CFRP strips or steel plates in flexural. The correct choice used in material modeling was one of the important choices used in this analytical program. Good agreement of FEM analytical results for ultimate load, load-deflection curves, and mid-span deflection with the results of experimental work. The ratio of numerical results to experimental results was (-8.62% decrease to 7.51% increase) in

ultimate loads and (-15.04% decrease to 12.28% increase) in maximum mid-span deflections at ultimate loads.

2) The crack patterns seen in the FEM models are similar to the crack patterns that occurred in the experimental study.
3) To compare the best case for strengthening by CFRP strips (in the percentage of the length of 80% and width of 60%), the results were an increase in the ultimate load value of about (40.31%), as well as the case when using the strengthening technique by steel plate, the results were an increase in the ultimate load value about (24.99%).
4) Also, when comparing the best method for repairing by CFRP strips or steel plates (in the percentage of the length of 80% and width of 60%), the models repaired with CFRP strips gave the highest increase in the value of the ultimate load capacity, while the models repaired with steel plate recorded a higher increase in the value of the deflection capacity.
5) The high ability of the cohesive model to represent the bonding behavior between CFRP sheets and concrete or between steel plates and concrete.
6) When comparing the results with the value of the length of the reinforcement of 1200 mm, increasing the length of the strengthening for CFRP strips or steel plates to a value of (1500 mm) reflects the good ability of this length to increase the load capacity to (1.67%) in the beams reinforced with externally CFRP strips and to (3.27%) in the beams reinforced externally with steel plates, and increased the mid-span deflection to (12.55%) in the beams reinforced with externally CFRP strips and (9.05%) in the beams reinforced externally with steel plates respectively.
7) Compared with model IT3F1500 with a width of 150 mm, the use of the total strengthening width of 250 mm for model IT3F1500-w250 on

the flange width of the beam gave an effective and sufficient role in increasing the ultimate load capacity to (9.56%) and increasing the maximum mid-span deflection capacity to (9.82%).

8) Increasing the number of CFRP layers to double layers in model IT3F1200-2La for the purpose of increasing the thickness of the CFRP strips increased the load capacity to (5.37%) and decreased the mid-span deflection capacity to (45.47%). While a decrease was observed in the ultimate load capacity and maximum mid-span deflection in the case of increasing the thickness of the steel plate to (2 mm) and (3 mm) compared to the thickness of the steel plate (0.8 mm).

6.3 Recommendations for Future Work

Retrofitting (strengthening and repairing) the structural behavior of reinforced concrete inverted T beams are done by flexural CFRP strips or steel plates requires further investigation. The following recommendations are proposed.

1) A similar experimental program can be made to enhance the T, I, or L section reinforced concrete simply supported beams or inverted T section reinforced concrete continuous beams.
2) Experimental work so as to check the maximum and minimum spacing between strips of CFRP or steel plates can be implemented.
3) Experimental work can be done similarly to repair fire-reinforced concrete beams.
4) Shear strengthening of damaged reinforced concrete inverted T beams.
5) An experimental program for studying the behavior of inverted T beams with high-strength concrete or lightweight concrete

strengthened or repaired with EBR CFRP strips or EBR steel plates or Near Surface Mounted (NSM) CFRP composites.

6) Experimental study on the structural behavior of prestressed reinforced concrete beams reinforced with carbon fiber or steel plate compounds.
7) The same experimental work can be done to find out the behavior of beams strengthened by CFRP strips or steel plates under dynamic or impact loading.
8) The same experimental program is done with strengthening or repair by a hybrid steel plate and carbon fiber reinforced polymer sheet.
9) Studying the behavior of the inverted T-beam by making openings in the inverted T beams, for example, making an opening in the web or the flange or both, and then the places surrounded by the openings are strengthened by carbon fiber reinforced polymer composites.
10) A study of the behavior of the inverted T-beam when the load is placed on the flange with strengthening with CFRP strips and steel plates.

REFERENCES

1. Choo, B. S., & MacGinley, T. J. (2018). "Reinforced concrete: design theory and examples". CRC Press.
2. A.Texas, (2018) "Strengthening of Existing Inverted-T Ben Cap—Volume1: Preliminary Design" Technical Report 0-6893-Vol1, Project performed in cooperation with the Texas Department of Transportation and the Federal Highway Administration. URL: http://tti.tamu.edu/documents/0-6893-R1-Vol1.pdf .
3. Kronal Rajput, (2020),"What Inverted Beam/ Advantage Inverted Beam/ Purpose of Inverted Beam". Civil Jungle, https://civiljungle-com.translate.google.
4. NORDIMPIANTI SYSTEM SRL Via Erasmo Piaggio, 19/A 66100 Chieti (CH) - Italy.info@nordimpianti.com .www.nordimpianti.com.
5. ECT Team, Purdue, "Precast Inverted T Beam" (2007). ECT Fact Sheets. Paper 33. http://dx.doi.org/10.5703/1288284315742 .
6. Shash, A. A. (2005). "Repair of concrete beams–a case study". Construction and Building Materials, 19(1), 75-79.
7. Nordin, H., (2003),"Flexural Strengthening of Concrete Structures with Prestressed Near Surface Mounted CFRP Rods", Licentiate Thesis. Lulea University of Technology, Lulea, Sweden.
8. Bakhoum, M. M. (Ed.). (2010). Case Studies of Rehabilitation, Repair, Retrofitting, and Strengthening of Structures (Vol.12). IABSE.
9. Gorai, S., & Maiti, P. R. (2016). "Advanced retrofitting techniques for reinforced concrete structures": a state-of-the-art review. i-Manager's Journal on Structural Engineering, 5(1), 36.
10. Catalin Andrei Neagoe, (2011), "Concrete Beams Reinforced with CFRP Laminates", Etseccpb-upc.

11. Mukhopadhyaya, P., and Swamy, N., (2001),"Interface Shear Stress:A New Design Criterion for Plate Debonding" Journal of Composites for Construction, Vol.5, No.1, pp. 35-43.
12. Siddika A, Al Mamun MA, Alyousef R, Amran YHM (2019), "Strengthening of reinforced concrete beams by using fiberreinforced polymer composites": a review. J Build Eng 25:100798. https://doi.org/10.1016/j.jobe.2019.
13. Al-Gemeel AN, Zhuge Y (2019), "Using textile reinforced engineered cementitious composite for concrete columns confinement". Compos Struct210:695–706. https://doi.org/10.1016/j.compstruct.2018.11.093 .
14. Huang L, Zhao L, Yan L (2018), "Flexural performance of RC beams strengthened with polyester FRP composites". Int J Civ Eng 16:715 724. https://doi.org/10.1007/s40999-016-0140-0 .
15. Al-Mahaidi R, Kalfat R (2018)," Methods of structural rehabilitation and strengthening. Rehabilitation of concrete structures with fiberreinforced polymer Elsevier ", New York, pp 7-13.
16. Federico M. Mazzolani (2001), "The Use of FRP Materials for The Seismic Upgrading of Existing RC Structures" University degli, Facoltà di Ingegneria.
17. Bai, J. (Ed.). (2013). "Advanced fibre-reinforced polymer (FRP) composites for structural applications". Elsevier.
18. Hollaway, L. C., & Leeming, M. (Eds.). (1999). "Strengthening of reinforced concrete structures: Using externally-bonded FRP composites in structural and civil engineering" . Elsevier.
19. ACI Committee 440, (2017), "Guide for the Design and Construction of Externally Bonded FRP Systems for Strengthening of Concrete Structures", American Concrete Institute, 2017, Michigan, USA.

20. Mahfouz, I., (2005) ,"The Utilization of Fiber Reinforced polymers, FRP in Egypt", International workshop on innovations in materials and design of civil infrastructure, December, Cairo, Egypt.
21. "Fiber reinforced strengthening strip", Technical data of Strong well Company, www.strongwell.com .
22. Abdul Redha, D., A., (2011), "Flexural behavior of steel fiber self-compacting concrete beams". M. Sc. Thesis, College of Engineering, University of Babylon, Iraq.
23. Resheq, A. S., (2010), "Strengthening of Continuous Reinforced Concrete Beams by CFRP Laminates", Ph.D. thesis, The Building and Construction Engineering Department of the University of Technology, Iraq.
24. Carolin, A., (2003), "Carbon Fiber Reinforced Polymers for Strengthening of Structural Elements", Ph. D. Thesis, Lulea University of Technology, Lulea, Sweden.
25. Siddh, S. P., Y. D. Patil, and H. S. Patil,(2017). "Experimental studies on behaviour of composite slab with profiled steel sheeting". Materials Today: Proceedings 4.9: 9792-9796.
26. L'Hermite, R., and Bresson, J. (1967). "Concrete reinforced with glued plates". Proc., RILEM Int. Symp. Synthetic Resins in Building Construction, Eyrolles, Paris, 175–203.
27. Bloxham JW. (1980). "Investigation of the flexural properties of reinforced concrete beams strengthened by externally bonded steel plate", PhD thesis Sheffield University.
28. B. B. Adhikary and H. Mutsuyoshi, (2006) ,"Shear strengthening of reinforced concrete beams using various techniques", Construction and Building Materials, Vol. 20, 366–373, 2006.

29. Wang J J, Tao M X, Zhou M, Nie X. (2018)," Force transfer mechanism in RC beams strengthened in shear by means of steel plated concrete". Engineering Structures, 171: 56–7.
30. Raithby KD. (1982), "Strengthening of concrete bridge decks with epoxy bonded steel plates". Int J Adhes ;115(04):115–8.
31. Swamy RN, Jones R, Bloxham JW. (1987), "Structural behaviour of reinforced concrete beams strengthened by epoxy-bonded steel plates". Struct Engr ;65A(2):59–68.
32. M.Z. Jumaat and A. Alam. (2008), "Experimental and Analytical Investigation on the structural Behaviour of Steel plate and CFRPREFERENCES 69Laminate Flexurally Strengthenend Reinforced Concrete Beams". Journal of Applied Sciences 8 (23): 4383.
33. Eray Ozbek, Meryem Bocek and Sabahattin Aykac.(2016) "Strengthening of RC Beams with Solid Steel Plates" .Athens Journal of Technology & Engineering, December.
34. Furlong, R.W., Ferguson, P.M., and Ma, J.S. (1971). "Shear and Anchorage Study of Reinforcement in Inverted T-beam Bent-Cap Girders". TxDOT Report #113-4, Center for Highway Research, The University of Texas at Austin, Austin, TX.
35. Furlong, R.W., and Mirza, S.A. (1974). "Strength and Serviceability of Inverted T-beam Bent-Caps Subject to Combined Flexure, Shear, and Torsion". TxDOT Report #153-1F, Center for Highway Research, University of Texas at Austin, Austin, TX.
36. Deifalla, A., and Ghobarah, A. (2014). "Behavior and Analysis of Inverted T-shaped RC Beams under Shear and Torsion," Engineering Structures, Vol. 68, pp. 57–70.
37. Ching, Francis D.K. (1995). A Visual Dictionary of Architecture. New York: John Wiley and Sons. p. 203. ISBN 978-0-471-28451-2.

38. Wiley.J, "T-beam - Wikipedia," A Visual Dictionary of Architecture. p. 203, 1995, [Online]. Available: https://en.wikipedia.org/wiki/T-beam .
39. Ambrose, James; Tripeny, Patrick (2007). Simplified design of concrete structures (8th ed.). Chichester: Wiley. p. 104. ISBN 978-0-470-04414-8. Retrieved 26 April 2015.
40. Chajes, Michael J.; Januszka, Ted F.; Mertz, Dennis R.; Thomson, Theodore A. Jr.; Finch, William W. Jr. (1 May 1995). "Shear Strengthening of Reinforced Concrete Beams Using Externally Applied Composite Fabrics". ACI Structural Journal. 92 (3). doi:10.14359/1130. Retrieved 26 April 2015.
41. Bryson, J., & Carpenter, E. F. (1970). "Flexural Behavior of Prestressed Concrete Composite Tee-beams". (Vol. 31). US National Bureau of Standards.
42. Hanson, N. W. (1980). "Prestressed Concrete Prisms as Reinforcement for Crack Control", Journal of the Prestressed Concrete Institute.
43. Ghailan, D. B. (2014). "T-Beam behavior in flexure with different layers of concrete in web and flange ". Kufa Journal of Engineering, 2(1).
44. Choi, H. T. (2008). "Flexural behaviour of partially bonded CFRP strengthened concrete T-beams". Licentiate Thesis. A thesis presented to the University of Waterloo in fulfillment.
45. M. Harshal and S. Rao Khode, (2019). "Advanced Retrofitting Techniques for Reinforced Concrete Structures: A State of an Art Technical Review," Int. J. Innov. Res. Sci., vol. 8, pp. 10127–10150, doi: 10.15680/IJIRSET.2019.0810039 .

46. Wolf, R., and Miessler, H. J., 1978, "HLV-Spannglieder in der praxis," Erfahrunggen Mit Glasfaserverbundstaben Beton, V. 2, pp. 44-51.
47. Meier, U., 1987 "Bridge Repair with High Performance Composite Material", Material and Technical, Vol.14, pp. 125-128 (in German).
48. Farouk, I.A., 2008 , "Retrofit of Shear Critical R.C Beam with Carbon Fiber Reinforced Polymer sheet", PhD thesis, University of Technology, Iraq, pp.152.
49. Meier, U.; Deuring, M.; Meier, H.; and Schwengler, G., 1992, "Strengthening of Structures with CFRP Laminates," Research and Applications in Switzerland, Proceedings of the 1st International Conference on Advanced Composite Material in Bridges and Structures, Sherbrooke, Quebec, pp. 243-251.
50. Arduini, M., and Nanni, A., (1997), "Behavior of precracked RC beams strengthened with carbon FRP sheets", ASCE Journal of Composites for Construction, Vol. 1, No. 2, pp. 63-70.
51. Shahawy, M., and Beitelman, T.E. (1999). "Static and Fatigue Performance of RC Beams Strengthened with CFRP Laminates," Journal of Structural Engineering, Vol. 125, No. 6, pp. 613–621.
52. Alagusundaramoorthy, P., Harik, I. E., & Choo, C. C. (2003). "Flexural behavior of R/C beams strengthened with carbon fiber reinforced polymer sheets or fabric". Journal of composites for Construction, 7(4), 292-301.
53. Esfahani, M. R., Kianoush, M. R., & Tajari, A. R. (2007). "Flexural behaviour of reinforced concrete beams strengthened by CFRP sheets. Engineering structures", 29(10), 2428-2444.
54. Thiemamn, Z. (2009). "Pretest 3-D Finite Element Analysis of the Girder-to-Cap-Beam Connection of an Inverted-Tee Cap Beam

Designed for Seismic Loadings", Master's Thesis, Iowa State University.

55. Yousif, Z. M. (2012). "RC Beams Strengthening by Carbon Fiber Reinforced Polymer Against Two Points Load Divergence". Journal of Engineering and Development, 16, 266-280.
56. Hussein, H. A., & Razzaq, Z. (2017)." Prestressed Concrete Inverted Tee Beams With CFRP for Building Structures". Global Journal of Research In Engineering.
57. Ayssar Al-Khafaji and Hani Salim. (2020). "Flexural strengthening of RC continuous T-Beams using CFRP. Fibers", 8(6), 41, www.mdpi.com/journal/fibers
58. Ritchie PA, Thomas DA, Lu LW,(1991). Connely GM. "External reinforcement of concrete beams using fiber reinforced plastics". ACI Structural Journal ;88(4):490–500.
59. Saadatmanesh H, Ehsani MR.(1991). "RC beams strengthened with GFRP plates". I: Experimental study. Journal of Structural Engineering ;117(11): 3417–33.
60. Triantafillou RC, Plevris N. (1992) "Strengthening of RC beams with epoxy bonded fiber-composite materials". Materials and Structures ;25: 201–11.
61. Chajes MJ, Thomson TA, Januszka TF, Finch Jr WW. (1994). "Flexural strengthening of concrete beams using externally bonded composite materials". Construction and Building Materials ;8(3):191–201.
62. Sharif A, Al-Sulaimani GJ, Basunbul IA, Baluch MH, Ghaleb BN. (1994). "Strengthening of initially loaded reinforced concrete beams using FRP plates". ACI Structural Journal ;91(2):160–8.
63. Hefferman PJ, Erki MA. (1996). "Equivalent capacity and efficiency of reinforced concrete beams strengthened with carbon fiber

reinforced plastic sheets". Canadian Journal of Civil Engineering ;23:21–9.

64. Shahawy MA, Arockiasamy M, Beitelman T, Sowrirajan R. (1996). "Reinforced concrete rectangular beams strengthened with CFRP laminates". Composites: Part B ;27B:225–33.
65. Takeda K, Mitsui Y, Murakami K, Sakai H, Nakamura M. (1996). "Flexural behavior of reinforced concrete beams strengthened with carbon fiber sheets". Composites: Part A ;27A:981–7.
66. Arduini M, Nanni A. (1997). "Behavior of pre-cracked RC beams strengthened with carbon FRP sheets". Journal of Composites for Construction, ASCE ;1(2):63–70.
67. Malek AM, Saadatmanesh H, Ehsani MR. (1998). "Prediction of failure load of R/C beams strengthened with FRP plate due to stress concentration at the plate end". ACI Structural Journal ;95(1):14252.
68. Grace NF, Soliman AK, Abdel-Sayed G, Saleh KR. (1998). "Behavior and ductility of simple and continuous FRP reinforced beams". Journal of Composites for Construction, ASCE ;2(4):186-94.
69. GangaRao HVS, Vijay PV. (1998) . "Bending behavior of concrete beams wrapped with carbon fabric". Journal of Structural Engineering, ASCE ;124(1): 3–10.
70. Ross CA, Jerome DM, Tedesco JW, Hughes ML. (1999). "Strengthening of reinforced concrete beams with externally bonded composite laminates". ACI Structural Journal;96(2):212–20.
71. Bonacci JF, Maalej M. (2000). "Externally bonded fiber-reinforced polymer for rehabilitation of corrosion damaged concrete beams". ACI Structural Journal ;97(5):703–11.
72. Maalej M, Bian Y. (2001). "Interfacial shear stress concentration in FRPstrengthened beams". Composite Structures ;54:417–26.

73. Nguyen DM, Chan TK, Cheong HK. (2001). "Brittle failure and bond development length of CFRP-concrete beams". Journal of Composites for Construction, ASCE ;5(l):12–7.
74. Rahimi H, Hutchinson A. (2001). "Concrete beams strengthened with externally bonded FRP plates". Journal of Composites for Construction, ASCE ; 5(1):44–56.
75. Ye JQ. (2001). "Interfacial shear transfer of RC beams strengthened by bonded composite plates". Cement and Concrete Composites ;23:411–7.
76. Lau KT, Dutta PK, Zhou LM, Hui D. (2001). "Mechanics of bonds in an FRP bonded concrete beam". Composites Part B: Engineering ;32: 491–502.
77. Sebastian WM. (2001). " Significance of mid-span debonding failure in FRP-plated concrete beams". Journal of Structural Engineering, ASCE ;127(7): 792–8.
78. Teng JG, Smith ST, Yao J, Chen JF. (2003) ."Intermediate crack-induced debonding in RC beams and slabs". Construction and Building Materials ;17:447–62.
79. Jones, R., Swamy, R. N. and Charif, A. (1998), "Plate Separation and Anchorage of Reinforced Concrete Beams Strengthened by Epoxy-Bonded Steel Plates " , The Structural Engineering, vol. 66, No. 5, pp. 85-94.
80. Adhikary, B. B., & Mutsuyoshi, H. (2002). "Numerical simulation of steel-plate strengthened concrete beam by a non-linear finite element method model". Construction and Building Materials, 16(5), 291-301.
81. Jumaat, M. Z., & Alam, M. A. (2008). "Behaviour of U and L shaped end anchored steel plate strengthened reinforced concrete beams". European Journal of Scientific Research, 22(2), 184-196.

82. Rakgate, S. M., & Dundu, M. (2018). "Strength and ductility of simple supported R/C beams retrofitted with steel plates of different width-to-thickness ratios". Engineering structures, 157, 192-202.
83. Jumaat, M. Z., & Alam, M. A. (2008). "Behaviour of U and L shaped end anchored steel plate strengthened reinforced concrete beams". European Journal of Scientific Research, 22(2), 184-196.
84. Ercan, E., Arisoy, B., & ÇİFTÇİOĞLU, A. Ö. (2018). "EXPERIMENTAL AND NUMERICAL ANALYSIS OF REINFORCED CONCRETE BEAM STRENGTHENED USING CARBON FIBER REINFORCED PLASTIC SHEETS AND BOLTED STEEL PLATE". Sigma: Journal of Engineering & Natural Sciences/Mühendislik ve Fen Bilimleri Dergisi, 36(1).
85. Hussain, M., Sharif, A., Baluch, I. B. M., & Al-Sulaimani, G. J. (1995). "Flexural behavior of precracked reinforced concrete beams strengthened externally by steel plates". Structural Journal, 92(1), 14-23.
86. Benjeddou, O., Ouezdou, M. B., & Bedday, A. (2007). "Damaged RC beams repaired by bonding of CFRP laminates". Construction and building materials, 21(6), 1301-1310.
87. Gao B, Kim JK, Christopher KY. (2004) "Experimental study on RC beams with FRP strips bonded with rubber-modified resins". Comp Sci Tech;64(16):2557–64.
88. Hawileh, R., Al-Tamimi, A. K., Abdalla, J. A., & Wehbi, M. H. (2011). "Retrofitting pre-cracked RC beams using CFRP and epoxy injections". In Key Engineering Materials (Vol. 471, pp. 692-696). Trans Tech Publications Ltd.
89. Meikandaan, T., & Murthy, A. R. (2017). "Study of damaged RC beams repaired by bonding of CFRP laminates". Technology, 8(2), 470-486.

90. Sandile D Ngidi and Morgan Dundu. (2017). "Flexural behavior of precracked reinforced concrete beams strengthened externally by steel plates". Structural Journal, 92(1), 14-23.
91. Yu, F., Zhou, H., Jiang, N., Fang, Y., Song, J., Feng, C., & Guan, Y. (2020). "Flexural experiment and capacity investigation of CFRP repaired RC beams under heavy pre-damaged level". Construction and Building Materials, 230, 117030.
92. Iraqi Specification Standards "Portland Cement IQS No. (5)," Central Agency for Standardization and Quality Control, Planning Council, Baghdad, IRAQ, 1984 (in Arabic)
93. Iraqi Specification Standards "Aggregate from Natural Sources for Concrete and Construction IQS No. (45)," Central Agency for Standardization and Quality Control, Planning Council, Baghdad, IRAQ, 1984 (in Arabic).
94. ASTM A615, 2009 ",Standard Specification for Deformed and Plain Carbon-Steel Bars for Concrete Reinforcement (ASTM A615-09)". West Conshohocken, PA: ASTM International.
95. A. Hillerborg, 1985"The theoretical basis of a method to determine the fracture energy of concrete," Mater. Struct., vol. 18, no. 4, p. 291–296.
96. ASTM, E. 9. (2001). Standard test methods for tension testing of metallic materials. Annual book of ASTM standards. ASTM.
97. ACI Committee 211, "Standard practice for selecting proportions for normal, heavyweight and mass concrete, ACI 211.1-97," ACI Manual of Concrete Practice, American Concrete Institute, Detroit, 1997.
98. ASTM C 143/C 143M-15, "Standard Test method for Slump of Hydraulic Cement Concrete", Book of ASTM Standards, American Society for Testing and Materials, 2015, pp.1-4.

99. BS 1881: Part 116, "Method for Determination of Compressive Strength of Concrete Cubes", British Standards Institution, 1989.
100. ASTM C 39/C 39M-15a, "Standard Test Method for Compressive Strength of Cylindrical Concrete Specimens", Annual Book of ASTM Standards, American Society for Testing and Materials,2016, pp.1-7.
101. ASTM C 496/C 496M-11, "Standard Test Method for Splitting Tensile Strength of Cylinder Concrete Specimens", Annual Book of ASTM Standards, American Society for Testing and Materials, 2011, pp. 1-5.
102. ASTM C 78-15a, "Standard Test Method for Flexural Strength of Concrete (Using Simple Beam with Third-Point Loading)", Annual Book of ASTM Standards, American Society for Testing and Materials, 2010, pp. 1-4.
103. Mansur, M. A. "Design of reinforced concrete beams with web openings," In Proceedings of the 6th Asia-Pacific structural engineering and construction conference (ASPEC 2006), pp. 5-6.2006.
104. Tayşi, N., Abdoalhadi, A. A., & Arnao't, F. H. (2017). Investigation Of Ductility Of Pva Fiber Reinforced Beams.
105. Muthuswamy, K.R, and Thirugnanam G.S. 2014, "Structural Behaviour of Hybrid Fibre Reinforced Concrete Exterior Beam-Column Joint Subjected to Cyclic Loading". International Journal of Civil and Structural Engineering.
106. Joshi, S., Paul, S., Balakrishnan, B., & Menon, D. (2015, December). Moment curvature relation of reinforced concrete T-beam sections: Numerical and experimental studies. In Third International Conference on Advances in Civil, Structural and Construction Engineering, Rome, Italy.

107. Alasadi, S., Shafigh, P., & Ibrahim, Z. (2020). Experimental Study on the Flexural Behavior of over Reinforced Concrete Beams Bolted with Compression Steel Plate: Part I. Applied Sciences, 10(3), 822.
108. Meng, Xianzhe. 2016, "Shear strengthening of prestressed hollow core slabs using externally bonded Carbon Fiber Reinforced Polymer sheets.", M.Sc. Thesis, Windsor's University, Canada.
109. Bahij, Sifatullah, et al. 2018 ,"Numerical investigation of the shear behavior of reinforced ultra-high-performance concrete beams," Structural Concrete, PP. 305-317.
110. Alfaidi, H. (2021). Finite Element Modelling of RC Beams Strengthened with Prestressed NSM CFRP Plate (Master's thesis, University of Waterloo).
111. Wu, Yuanli. 2015, "Shear Strengthening of Single Web Prestressed Hollow Core Slabs Using Externally Bonded FRP Sheets", M.Sc. Thesis, Windsor's University, Canada.
112. Raza, A., & Ahmad, A. (2020). Prediction of axial compressive strength for FRP-confined concrete compression members. KSCE Journal of Civil Engineering, 24(7), 2099-2109.
113. Bsisu, K. A. D., Hussein, H. H., & Sargand, S. M. (2017). The use of Hashin damage criteria, CFRP–concrete interface and concrete damage plasticity models in 3D finite element modeling of retrofitted reinforced concrete beams with CFRP sheets. Arabian Journal for Science and Engineering, 42(3), 1171-1184.
114. Metwally IM" 2014, Nonlinear analysis of concrete deep beam reinforced with GFRP bars using finite element method" , Malaysian Journal of Civil Engineering, PP. 224–250.

ANALYSIS OF REINFORCED CONCRETE BEAMS

Each beams are designed according to ACI-Code 318M-19. The control beam is designed in such a method to ensure the failure of flexural with a tensile mode of failure.

1- To check the dimensions

➢ **For the purpose of verifying dimensions of the beams according to (ACI 318, section 8.10.20):**

a) $\mathbf{b \le \frac{span}{4}}$

$250 \le \frac{1500}{4} = 375\text{mm} \quad \therefore O.K.$

b) $\mathbf{\frac{b-bw}{2} \le 8hf}$

$\frac{250-150}{2} = 50 \le 8(50) = 400\text{mm} \quad \therefore O.K.$

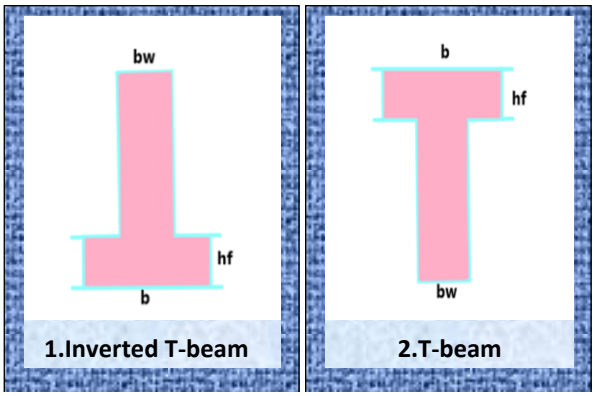

Figure (A-1):Shape of beams

2- Location of neutral axes (N.A)

$$C = \frac{\sum Ai\ yi}{\sum Ai}$$

$$C = \frac{(150*200*100)+(50*250*225)}{(150*200)+(50*250)}$$

C=137mm.

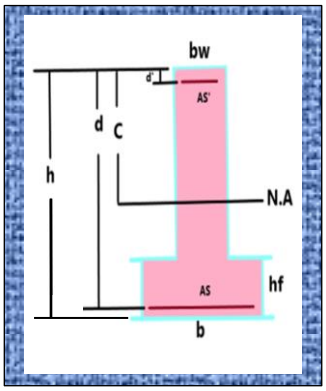

Figure (A-2): Details inverted T-beam

3- Effective depth calculation

$y' = \frac{\sum Ai\ yi}{\sum Ai}$ (y': steel reinforcement center)

$$= \frac{\left(2*\frac{\pi}{4}*8^2\right)*4+\left(2*\frac{\pi}{4}*6^2\right)*3}{\left(2*\frac{\pi}{4}*8^2\right)+\left(2*\frac{\pi}{4}*6^2\right)}$$

y'=3.64mm

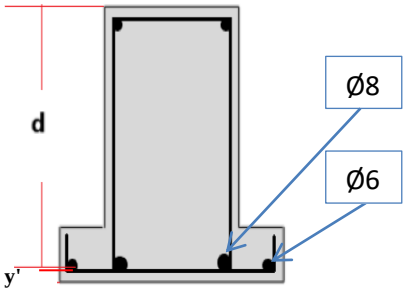

Figure (A-3): Effective depth calculation

d=h – cover – d stirrup - 3.64 (d: effective depth)

=250-20-6-3.64 ⟶ d=220.36mm

4- To check shallow beam

$\frac{a}{d}$ (a: the distance from one of the supports to one of the loads)

$=\frac{600}{220.36}$ ⟶ $\frac{a}{d} = 2.72 > 2$ *O.K* ⟶ according to ACI-Code 318M-19

5- Check flexural capacity of section

The control beam consists of two bars of Ø8mm and two bars of Ø6mm as flexural reinforcement at depth (d=220.36mm) and 2Ø6 mm as top reinforcement at depth. The width of the cross-section for the flange of this beam (bf=250 mm), the width web (bw=150mm), and the total height (h=200 mm). The shear span is reinforced with Ø6mm@100mm. The concrete compressive strength (fc') is equal to 30 MPa.

$$\rho = \frac{As}{bw*d}$$

$$= \frac{\left(2*\frac{\pi}{4}*8^2\right)+\left(2*\frac{\pi}{4}*6^2\right)}{150*220.36} \longrightarrow \rho=0.00475$$

$\rho_{max}=0.85*\beta_1*\frac{fc'}{fy}*(\frac{\varepsilon cu}{\varepsilon cu+0.004})$ ⟶ $\beta 1=0.85$ ⟶ fc'=30 Mpa

$=0.85*0.85*\frac{30}{420}*(\frac{0.003}{0.003+0.004})$

$\rho max=0.02212$

$\rho < \rho max$ ∴Singly Reinforced section analysis

$$\rho min=max\ (\frac{1.4}{fy}, \frac{\sqrt{fc'}}{4*fy})$$

ρ_{min}= max($\frac{1.4}{420}$, $\frac{\sqrt{30}}{4*420}$) = (0.00333, 0.00326) = 0.00333

[$\rho min < \rho < \rho$max] $\therefore$ *O.K.*

$\rho_b = 0.85 * \beta_1 * \frac{fc'}{fy} * (\frac{600}{600+fy})$

$= 0.85 * 0.85 * \frac{30}{420} * \frac{600}{600+420}$ ⟶ ρb=0.03036

$\rho < \rho b$ ⟶ $\therefore$under reinforce section (tensile failure)

$a = \frac{As\ fy}{0.85\ fc' bw}$

$= \frac{\left[\left(2 * \frac{\pi}{4} * 8^2\right) + \left(2 * \frac{\pi}{4} * 6^2\right)\right] * 420}{085 * 30 * 150}$ ⟶ a=17.248mm

➢ **Calculation of Internal Moment**

Mn=As fy $(d - \frac{a}{2})$

$= [[\left(2 * \frac{\pi}{4} * 8^2\right) + \left(2 * \frac{\pi}{4} * 6^2\right)] * 420 * (220.36 - \frac{17.248}{2})] * (10\hat{} - 6)$

Mn=13.969 kN.m

➢ **Calculation of External Moment**

From figure (A-4) of shape bending moment diagram

External Moment = Internal Moment

0.3p=13.969

P=46.563 kN

$\therefore$ P < Maximum load carrying by machine $\therefore$ *Ok.*

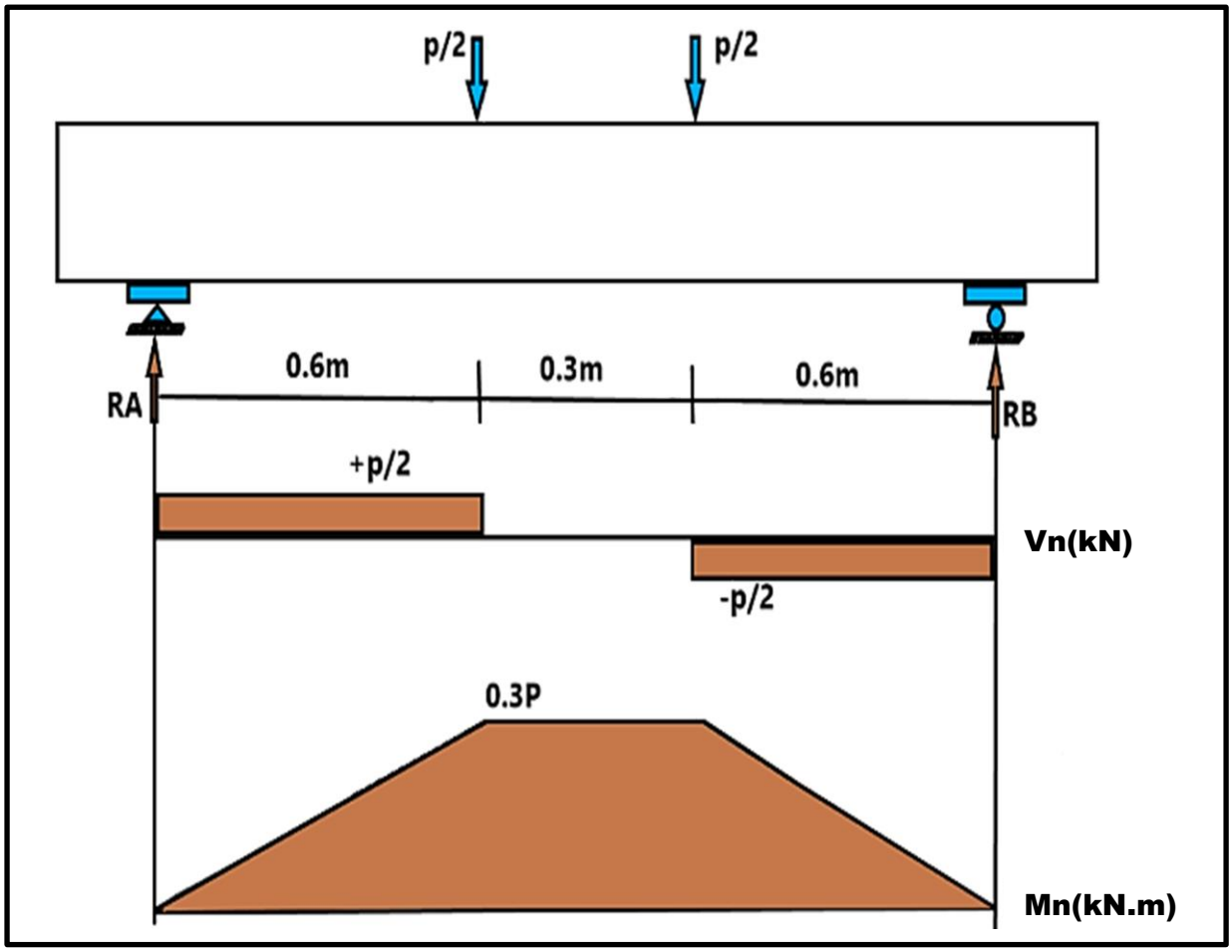

Figure (A-4): Bending moment and Shear force diagram

6- Check shear capacity of section

Vc= $\frac{1}{6}\sqrt{f'c}$ b_wd… … … **(ACI 11 – 3)**

Where:

Vc= Shear force carrying by concrete.

bw=web width

d=ffective depth

Vc=$[\frac{1}{6}\sqrt{30} * 150 * 220.36] * (10\text{^} - 3)$

Vc=30.778 kN

$Vs = \frac{d}{s} A_v f_y$ ACI 11.5.6.2 $\leq \frac{2}{3} \sqrt{fc'}$ $b_w d = 4Vc$ ….. **(ACI 11.5.6.9)**

Where:

Vs = Shear force carrying by stirrup

Av =Area of two legs of stirrups

S=Spacing of stirrups

Use Ø6@ 100mm a long span of beam

$Vs=\frac{220.36}{100} *(2*\frac{\pi}{4} * 6^2) * 420*(10\text{^-}3)$

Vs=52.336 kN

Vs<4Vc ⟶ 52.336 kN<123.112 kN ⟶ ∴O.K.

Vn = (Vs + Vc)

Where:

Vn = nominal shear capacity of section

Vn= (52.336+30.778)

=83.114 kN

From figure (A-4) of shape shear force diagram

External shear force(from shear force diagram) =internal shear force(Vn)

0.5p=83.114

P=166.228 kN

Pu=0.75*166.228

∴shear failure load > flexural failure load

∴Flexural tension failure control

$Sc_{min}=\begin{cases} db = 8mm \\ 25mm \\ \frac{4}{3}\ max.size\ of\ agg. \end{cases}$ =25mm

$Sc=\frac{b-2cover-2stirrup-ndbar}{n-1}$

$=\frac{150-2(20)-2(6)-2(8)}{2-1}$

Sc=82mm > Sc_{min} ∴O.K.

Details :

db=diameter of main bar

Sc=clear spacing between bars

n= number the main diameter of bar

max. size of agg.=maximum size of aggregate

***Details of the reinforcement of the analyzed beam are shown in figure (A-5).

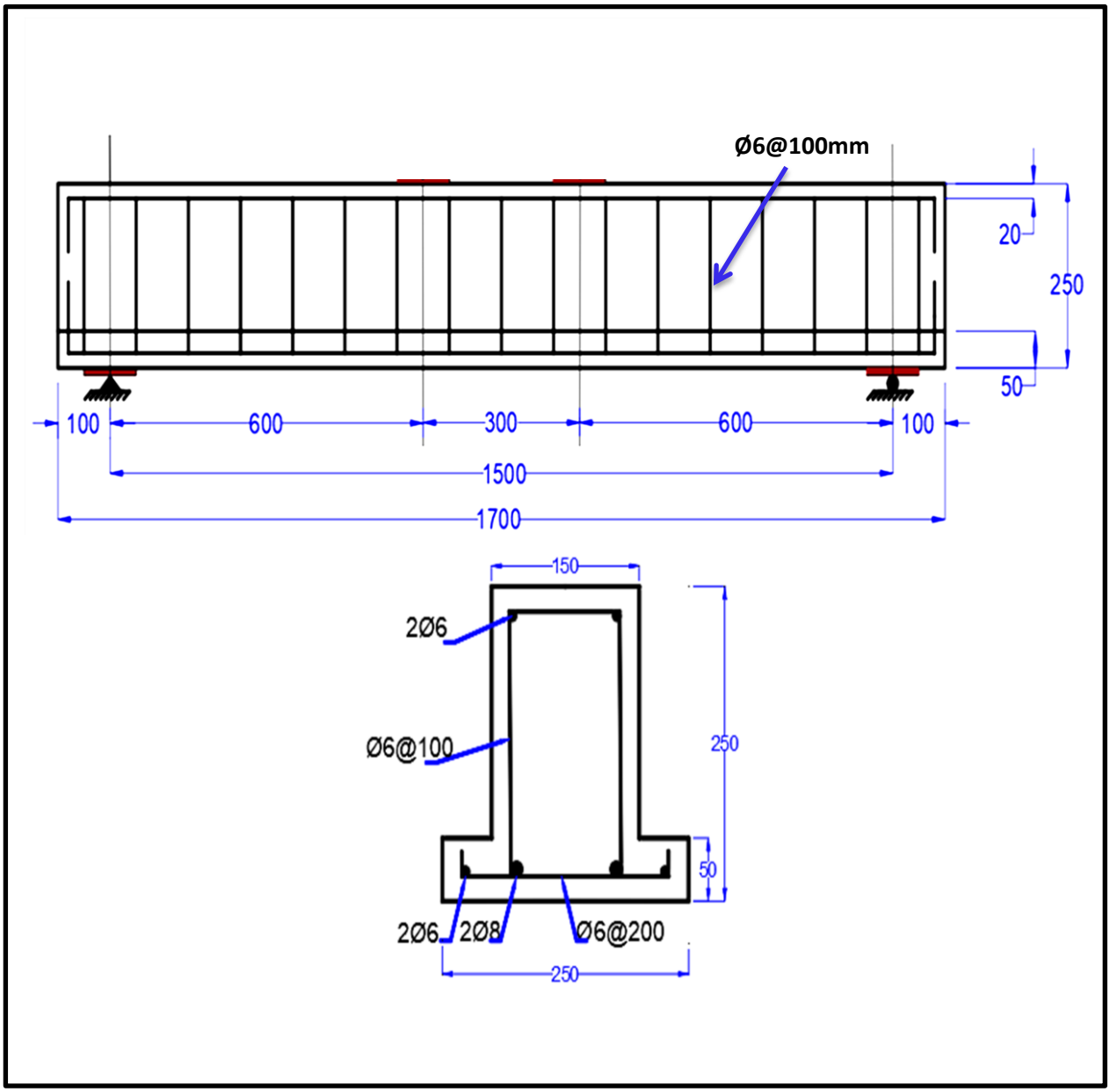

Figure (A-5): Details of the reinforcement of the analyzed beam

MODELLING OF MATERIAL PROPERTIES IN FINITE ELEMENT ANALYSIS

B.1 Introduction

The main components of an inverted T beam are the concrete and the steel reinforcement bars embedded inside the concrete. Moreover, the EBR-steel plates, the EBR-CFRP sheets, and the adhesive layer connecting steel plates or CFRP sheets to beams are strengthened or repaired by the steel plates or CFRP sheets technique. It is important to simulate the material behavior of all components to provide an actual model of reinforced concrete inverted T beams.

B.2 Material models:

B.2.1 Concrete

Concrete damaged plasticity (CDP) was one of the methods chosen to simulate concrete behavior in ABAQUS software. The CDP is able of modeling each structural type such as unreinforced or reinforced concrete or quasi-brittle materials subjected to cyclic, monotonic, or dynamic loads. This model is dependent on a coupled damage plasticity notion and the multi-axial behavior of concrete in the damaged plasticity model governs by a yield surface, which was proposed by **(Lubliner et al.) [1]**. Two supposed main failure mechanisms in this model such as compressive crushing and tensile cracking of concrete. Degradation of concrete for both tension and compression behavior in dynamic and cyclic loadings is a calculation by defining two scalar parameters; compressive damage parameter (dc) and tensile damage parameter (dt).

B.2.1.1 Uniaxial Tensile and Compressive Behavior of Concrete

It is clear from figure (B-1), under uniaxial tension that the stress is with an elastic linear relationship with strain, so the stress increases with strain up to the ultimate tensile strength, Subsequently, microscopically micro-cracks are formed with a tension softening response. In the ABAQUS program, there are different ways of defining the tension softening response; stress-displacement, stress-strain, or by utilization of fracture energy **[2]**.

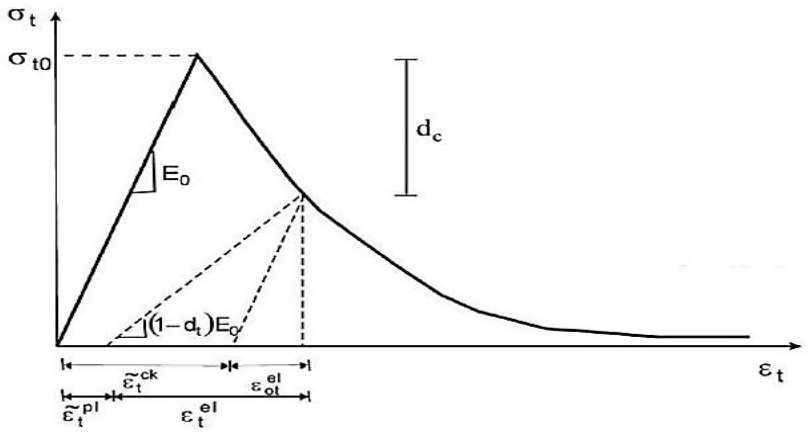

Figure (B-1): Uniaxial tensile behavior of concrete [3]

In ABAQUS, to know the tensile stress-strain relation of concrete, the following entries must be used; stress (σt), young's modulus (E_0), the damage parameter values (dt), and cracking strain ($\varepsilon t^{\sim ck}$) values for the suitable concrete grade. The cracking strain ($\varepsilon t^{\sim ck}$) must be calculated from the total strain using the following equation (B-1):

$$\boldsymbol{\varepsilon t^{\sim ck} = \epsilon t - \varepsilon o t^{el}} \qquad \textbf{(B-1)}$$

Where:

$\epsilon o t^{el} = \sigma t / Eo$, the elastic strain corresponding to the undamaged material

$\varepsilon t = total\ tensile\ strain$

Figure (B-2) explains the uniaxial compressive behavior of concrete, a linear elastic relationship between stress-strain until the yield is initial. Nonlinear is formed after the failure of the connection between cement paste and aggregates. The plastic response is defined when stresses major than ultimate strength, stress hardening, and strain softening. In other words, strain increases while the corresponding compressive stress decreases [3].

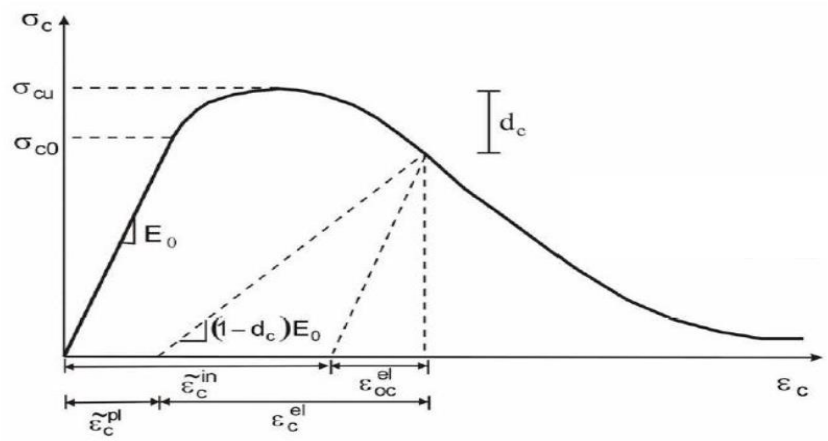

Figure (B-2): Uniaxial compressive behavior of concrete [3]

In ABAQUS, to know the compression stress-strain relation of concrete the following entries must be used; the stresses (σc), inelastic strains ($\varepsilon c^{\sim in}$) corresponds to stress values and damage properties (dc) with inelastic strains in tabular Formula. So that, total strain values should be converted to the inelastic strains using Eq. (B-2):

$$\boldsymbol{\varepsilon c^{\sim in} = \epsilon_c - \varepsilon oc^{el}} \quad \textbf{(B-2)}$$

Where:

$\boldsymbol{\varepsilon oc^{el}} = \sigma c/Eo$, the elastic compression strain corresponding to the undamaged material.

εc = compressive strain in concrete

The following equations were utilized in obtaining the damage and compression parameters which were developed successfully by **(Birtel and Mark) [4]**. The level of damage parameters is represented by values ranging from 0 (no damage) to 1 (fully damaged).

$$d_c = 1 - \frac{\sigma_c E_c^{-1}}{\varepsilon_c^{pl}(1/b_c - 1) + \sigma_c E_c^{-1}} \quad \text{(B-3)}$$

$$d_t = 1 - \frac{\sigma_t E_c^{-1}}{\varepsilon_t^{pl}(1/b_t - 1) + \sigma_t E_c^{-1}} \quad \text{(B-4)}$$

$$\varepsilon_c^{pl} = b_c \, \tilde{\varepsilon}_c^{in} \quad \text{(B-5)}$$

$$\varepsilon_t^{pl} = b_t \, \tilde{\varepsilon}_t^{ck} \quad \text{(B-6)}$$

The **(Birtel and Mark) [4]** suggested bt=0.1 and bc=0.7.

B.2.1.2 Concrete Damaged Plasticity Parameters in Triaxial Loading State

Completing the description of the plasticity behavior of concrete requires entering five parameters into the ABAQUS program as follows:

Ψ, Dilation angle: the angle of inclination of the failure surface in the direction hydrostatic axis. Physically, the dilation angle (Ψ) is the internal friction angle. The maximum value of the dilation angle is (56.3 degrees), and its lowest value is close to (zero) **[5]**.

Fb0/fc0: is the proportion of initial equiaxial compressive yield stress and initial uniaxial compressive yield stress **[5]**. The default value used in ABAQUS software is (1.16).

ϵ: Plastic potential eccentricity, is defined as a small positive value and can be calculated as the ratio of tensile strength to compressive strength. In the CDP model it is desirable to assume (ϵ = 0.1) **[5].**

K: defined as the ratio of the second stress invariant in the tensile meridian to compressive meridian for any value of the pressure invariant at initial yield. It is utilized to define the multi-axial behavior of concrete and is (0.5<Kc≤1) **[5]**. The default value used in ABAQUS is (0.667).

μ: is the viscosity parameter. contribute to converging in an ABAQUS/Standard but it does not affect the ABAQUS/Explicit analysis. According to (Malm) **[6]**, the μ must be equal to (10-7) because in comparison with characteristic time increments it should be small.

B.2.1.3 Concrete Model Properties for FEM Analysis

The parameters of concrete material used in the (CDP) model are as follows: the tensile and compressive strengths of concrete, Poisson's ratio (v), and the modulus of elasticity (E_0). Use the unconfined stress-strain relationship model as proposed by **(Popovics) [7]** to simulate concrete with normal compressive strength. This relationship depends on the concrete cylinder strength, As shown in the equations (B-7) and (B-8).

$$\frac{f_c}{\hat{f_c}} = \frac{n\times\left[\frac{\varepsilon_c}{\varepsilon_{co}}\right]}{(n-1)+\left[\frac{\varepsilon_c}{\varepsilon_{co}}\right]^n} \qquad \text{(B-7)}$$

$$n = (0.4\times10^{-3}\times\hat{f_c}(psi)) + 1.0 \qquad \text{(B-8)}$$

Where:

fc'= the compressive strength of cylinder at maximum stress.

ϵ_{co}= strain of concrete at maximum stress.

n = a curve-fitting factor.

On the other hand, the stress-strain relationship (σ-ε) is linear to uniaxial tensile strength and then determined utilizing the exponential function in the following equation (B-9) **[8]**:

$$\sigma = f_t \times \left[\frac{\varepsilon_t}{\varepsilon}\right]^{(0.7+1000\varepsilon)} \quad , \ \varepsilon_t = \frac{f_t}{E_o} \qquad \text{(B-9)}$$

B.2.2 Steel Reinforcement

It was used the plasticity model For steel reinforcement depending on the use of elastic-plastic hardening material. The required input parameters in ABAQUS software are defined for the material behavior of steel bars, which contains density, elastic behavior which includes (Young's modulus and Poisson's ratio), and plastic behavior which includes (yield stress and plastic strain).

B.2.3 CFRP

The CFRP composite sheet was modeled as an orthotropic elastic material, and relationships of stress with strain were represented by the expression below:

$$\begin{bmatrix}\sigma_1\\ \sigma_2\\ \sigma_3\\ \tau_{12}\\ \tau_{13}\\ \tau_{23}\end{bmatrix} = \begin{bmatrix} D_{1111} & D_{1122} & D_{1133} & 0 & 0 & 0 \\ & D_{2222} & D_{1212} & 0 & 0 & 0 \\ & & D_{3333} & 0 & 0 & 0 \\ & & & D_{1212} & 0 & 0 \\ & Sym. & & & D_{1313} & 0 \\ & & & & & D_{2323} \end{bmatrix} \begin{bmatrix}\varepsilon_{11}\\ \varepsilon_{22}\\ \varepsilon_{33}\\ \gamma_{12}\\ \gamma_{13}\\ \gamma_{23}\end{bmatrix} \qquad \textbf{B-10}$$

Equations below described the expression of the stiffness matrix which consisted of nine independent elastic stiffness parameters (D_{ijkl}) **[9]**

$$D_{1111} = E_1(1 - \nu_{23}\nu_{32})\gamma, \quad \text{B-11}$$

$$D_{2222} = E_2(1 - \nu_{13}\nu_{31})\gamma, \quad \text{B-12}$$

$$D_{3333} = E_3(1 - \nu_{12}\nu_{21})\gamma, \quad \text{B-13}$$

$$D_{1122} = E_1(\nu_{21} - \nu_{31}\nu_{23})\gamma = E_2(\nu_{12} - \nu_{32}\nu_{13})\gamma, \quad \text{B-14}$$

$$D_{1133} = E_1(\nu_{31} - \nu_{21}\nu_{32})\gamma = E_3(\nu_{13} - \nu_{12}\nu_{23})\gamma, \quad \text{B-15}$$

$$D_{2233} = E_2(\nu_{32} - \nu_{12}\nu_{31})\gamma = E_3(\nu_{23} - \nu_{21}\nu_{13})\gamma, \quad \text{B-16}$$

$$D_{1212} = G_{12}, \quad D_{1313} = G_{13}, \quad D_{2323} = G_{23} \quad \text{B-17}$$

$$\gamma = \frac{1}{1-\nu_{12}\nu_{21}-\nu_{23}\nu_{32}-\nu_{31}\nu_{13}-2\nu_{21}\nu_{32}\nu_{13}} \quad \text{B-18}$$

B.2.4 Modelling of Interaction

B.2.4.1 Linear elastic traction-separation behavior

Initially displays the traction-separation model linear elastic behavior, then the damage begins to form and develops. In 3D FEM analysis, the concept of initiation of the damage is expressed in terms of an elastic matrix, this matrix is consist of the nominal traction stress vector, t, is consist of three components: t_n, ts, and t_t, which are described in the interface plane's normal and the two shear traction stresses along the local first and second directions, respectively. This matrix can be seen in the description below:

$$t = \begin{Bmatrix} t_n \\ t_s \\ t_t \end{Bmatrix} = \begin{bmatrix} K_{nn} & K_{ns} & K_{nt} \\ K_{ns} & K_{ss} & K_{st} \\ K_{nt} & K_{st} & K_{tt} \end{bmatrix} \begin{Bmatrix} \epsilon_n \\ \epsilon_s \\ \epsilon_t \end{Bmatrix} = K\epsilon \quad \text{B-19}$$

The nominal strains are the corresponding separations, represented by δn, δs, and δt, divided by the initial constitutive thickness, denoted by T_D. The initial constitutive thickness T_D was assumed to be equal to unity. Therefore, the

nominal strain components are equivalent to the relative displacement components.

$$\epsilon_n = \frac{\delta_n}{T_0}, \quad \epsilon_s = \frac{\delta_s}{T_0}, \quad \epsilon_t = \frac{\delta_t}{T_0}, \qquad \text{(B-20)}$$

B.2.4.2 Damage modeling

B.2.4.2.1 Damage initiation

There several damage initiation criteria are available, including:

1. Maximum nominal stress criterion.
2. Maximum nominal separation criterion.

1. Maximum nominal stress criterion

The damage initiates, when the maximum nominal stress ratio equals one as shown in the criterion below:

$$max\left\{\frac{\langle t_n \rangle}{t_n^0}, \quad \frac{t_s}{t_s^0}, \quad \frac{t_t}{t_t^0}\right\} = 1 \qquad \text{B-21}$$

2. Maximum nominal separation criterion

The damage initiates, when the maximum nominal strain ratio equals one as shown in the criterion below:

$$max\left\{\frac{\langle \epsilon_n \rangle}{\epsilon_n^0}, \quad \frac{\epsilon_s}{\epsilon_s^0}, \quad \frac{\epsilon_t}{\epsilon_t^0}\right\} = 1 \qquad \text{B-22}$$

B.2.4.2.2 Damage evolution

The rate of deterioration of coherent toughness begins when the law of damage progression begins once the damage initiation criterion is met. The damage variable (D) represents the total amount of damage to the contact surface, this variable must be a number that specifies the extent of damage with a range of 0 if no damage is done and 1 if the item has lost its full

power. The response of evolution to damage is estimated by the following criteria:

A. Evolution based on effective displacement

This evolution is determined by the difference in potency displacement at complete failure (δ_t^f), relative to effective displacement at starting damage (δ_t^0). The decrease in the degree of stiffness is achieved through developing damage, three methods can be used.

A.1 Linear damage evolution: Reduces damage variable (D), to the equation offered by **Camanho and Dávila [10]** [equation (B-23)] for linear softening when ABAQUS has used an evolution of this variable as shown in figure (B-3).

$$D = \frac{\delta_t^f(\delta_t^m - \delta_t^0)}{\delta_t^m(\delta_t^f - \delta_t^0)} \qquad \textbf{(B-23)}$$

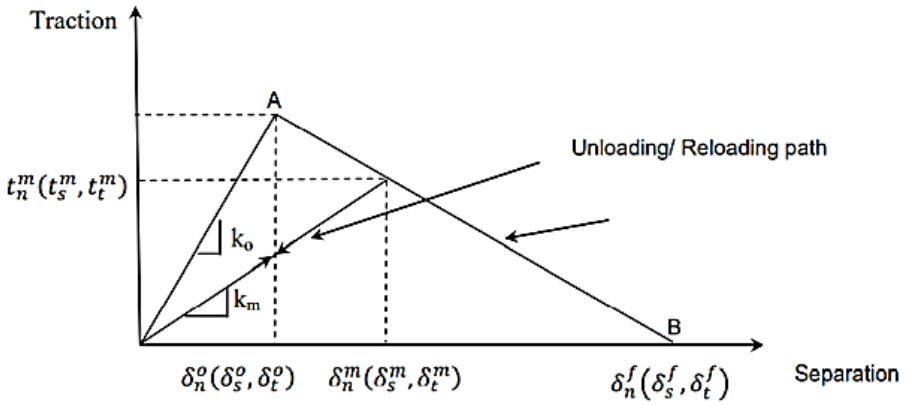

Figure (B-3): Typical traction-separation response [11]

A.2 Exponential damage evolution: Reduces damage variable (D), to the equation (B-24) **[12]** For exponential softening when ABAQUS has used an evolution of this variable as shown in figure (B-4).

$$D = 1 - \left\{\frac{\delta_t^o}{\delta_t^m}\right\}\left\{1 - \frac{1-\exp\left(-\alpha\left(\frac{\delta_t^m - \delta_t^o}{\delta_t^f - \delta_t^o}\right)\right)}{1-\exp(-\alpha)}\right\} \quad \textbf{(B-24)}$$

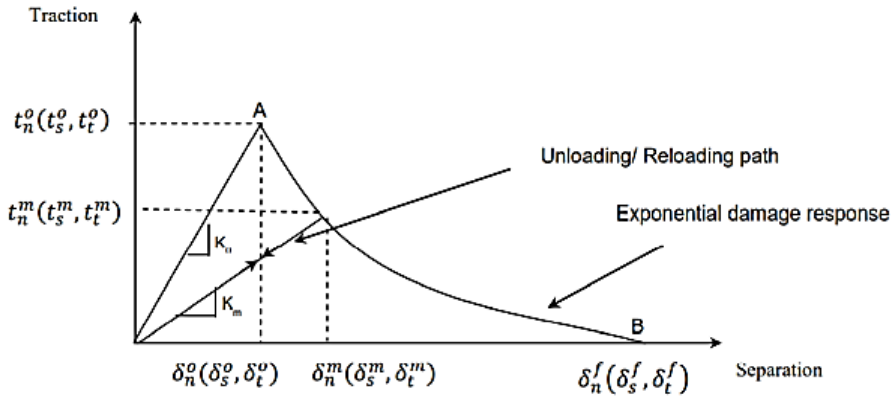

Figure (B-4): Typical traction-separation response [12]

A-3 Tabular damage evolution: It is represented directly by the scheduling function, which depicts the difference between effective displacement and effective displacement at initiation. As shown in figure (B-5) **[12]**, assessing the damage variable D is As follows:

$$D = \frac{T_{eff} - T_m}{T_{eff}} \quad \textbf{(B-25)}$$

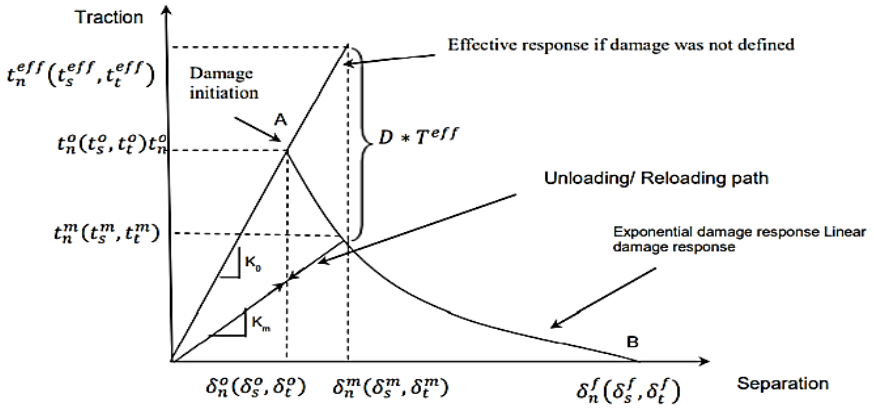

Figure (B-5): Typical traction-separation response [12]

B. Evolution based on energy

This evolution is defined by the energy dissipated as a result of the process of damage, also known as fracture energy. This evolution is

estimated by the area under the traction separator curve. It can be defined in ABAQUS software as a linear or exponential softening behavior depending on the mechanical properties of the materials.

B-1 Linear damage evolution: ABAQUS software uses the damage evolution variable for a linear softening by depending on the effective displacement equation, however (δ_t^f) is calculated by this expression:

$$\delta_t^f = \frac{2G^C}{t_t^0} \quad \textbf{(B-26)}$$

Where:

(G^c) is the mixed-mode fracture energy, [(G^c) = Gn+ Gt+ Gs]. Gn, Gt, and Gs return to the work done by traction in the normal, first, and second shear directions, as well as its conjugate relative displacement ($\delta t0$) is the effective traction at damage initiation in the first direction.

B-2 Exponential damage evolution: ABAQUS uses an evolution of the damage variable depending on the below formula for exponential softening

$$D = \int_{\delta_t^0}^{\delta_t^f} \frac{T_{eff} d\delta}{G^C - G_0} \quad \textbf{(B-27)}$$

Where:

(Teff) is the effective traction at damage initiation.

(G0) is the elastic energy at damage initiation.

(δ_t^0) is the effective traction at damage initiation in the first direction.

Determination of unloading/reloading stiffness is done by the following formula: $K_m = (1\text{-}D)\, K_0$

References

1) Lubliner, J., Oliver, J., Oller, S., and Oñate, E., "A plastic-damage model for concrete," International Journal of Solids and Structures, 25(3), pp. (299-326), 1989, doi: https://doi.org/10.1016/0020-7683(89)90050-4.
2) Hibbitt, Karlsson, & Sorensen, "ABAQUS User's Manual". Pawtucket, 6th Edition, 2010.
3) Jankowiak, Tomasz, and Tomasz Lodygowski, "Identification of parameters of concrete damage plasticity constitutive model," Foundations of civil and environmental engineering, pp. 53-69, 2005.
4) Birtel, V., and P. Mark, "Parameterised finite element modeling of RC beam shear failure," ABAQUS users' conference. 2006.
5) Kmiecik, P., and M. Kamiński, "Modelling of reinforced concrete structures and composite structures with concrete strength degradation taken into consideration," Archives of civil and mechanical engineering, pp. 623-636, 2011.
6) Malm, R., "Shear cracks in concrete structures subjected to in-plane stresses," Lic. thesis, Royal Institute of Technology (KTH), Stockholm, Sweden, 2006.
7) S. Popovics, "A numerical approach to the complete stress-strain curves of concrete," Cement and Concrete Research, vol. 3, no. 5, pp. 583-599, 1973.
8) Dere, Y., & Koroglu, M., A., "Nonlinear FE Modeling of Reinforced Concrete, "International Journal of Structural and Civil Engineering Research, Vol. (6), No.1, pp.(71-74), 2017.
9) J. Lubliner, J. Oliver, S. Oller, and E. Oñate. A plastic-damage model for concrete. Int. J. Solids Struct., vol. 25, no. 3, pp. 299–326, 1989.

10) Camanho, P. P., & Dávila, C. G. (2002). Mixed-mode decohesion finite elements for the simulation of delamination in composite materials (No. NAS 1.15: 211737).

11) Abaqus 2011. Theory Manual, User Manual, and Example Manual, Version 6.10, Providence, RI.

12) Hibbitt, H., Karlsson, B., & Sorensen, P. J. D. S. S. C. P. (2011). Abaqus analysis user's manual version 6.10. Dassault Systèmes Simulia Corp.: Providence, RI, USA.

Properties of CFRP sheets (Sikawarp-300C)

BUILDING TRUST

PRODUCT DATA SHEET

SikaWrap®-300 C

WOVEN UNIDIRECTIONAL CARBON FIBRE FABRIC, DESIGNED FOR STRUCTURAL STRENGTHENING APPLICATIONS AS PART OF THE SIKA® STRENGTHENING SYSTEM

DESCRIPTION

SikaWrap®-300 C is a unidirectional woven carbon fibre fabric with mid-range strengths, designed for installation using the dry or wet application process. Suitable for use in hot and tropical climatic conditions.

USES

SikaWrap®-300 C may only be used by experienced professionals.
Structural strengthening of reinforced concrete, masonry, brickwork and timber elements or structures, to increase flexural and shear loading capacity for:

- Improved seismic performance of masonry walls
- Replacing missing steel reinforcement
- Increasing the strength and ductility of columns
- Increasing the loading capacity of structural elements
- Enabling changes in use / alterations and refurbishment
- Correcting structural design and / or construction defects
- Increasing resistance to seismic movement
- Improving service life and durability
- Structural upgrading to comply with current standards

CHARACTERISTICS / ADVANTAGES

- Multifunctional fabric for use in many different strengthening applications
- Flexible and accommodating of different surface planes and geometry (beams, columns, chimneys, piles, walls, soffits, silos etc.)
- Low density for minimal additional weight
- Extremely cost effective in comparison to traditional strengthening techniques

APPROVALS / STANDARDS

- Poland: Technical Approval ITB AT-15-5604/2011: Zestaw wyrobów Sika CarboDur do wzmacniania i napraw konstrukcji betonowych.
- Poland: Technical Approval IBDiM Nr AT/2008-03-0336/1, Płaskowniki. pręty, kształtki i maty kompozytowe do wzmacniania betonu o nazwie handlowej: Zestaw materiałów Sika CarboDur® do wzmacniania konstrukcji obiektów mostowych.
- USA: ACI 440.2R-08, Guide for the Design and construction of Externally Bonded FRP Systems for strengthening concrete structures, July 2008.
- UK: Concrete Society Technical Report No. 55, Design guidance for strengthening concrete structures using fibre composite material, 2012.

PRODUCT INFORMATION

Construction	Fibre orientation Warp Weft	0° (unidirectional) Black carbon fibres 99 % White thermoplastic heat-set fibres 1 %
Fibre Type	Selected mid-range strength carbon fibres	
Packaging	**Fabric length per roll**	**Fabric width**
	≥ 100 m	500 mm
Shelf life	24 months from date of production	

Product Data Sheet
SikaWrap®-300 C
May 2017, Version 01.01
020206020010000011

Storage conditions	Store in undamaged, original sealed packaging, in dry conditions at temperatures between +5 °C and +35 °C. Protect from direct sunlight.	
Dry Fibre Density	1.82 g/cm³	
Dry Fibre Thickness	0.167 mm (based on fibre content)	
Area Density	304 g/m² ± 10 g/m² (carbon fibres only)	
Dry Fibre Tensile Strength	4 000 N/mm²	(ISO 10618)
Dry Fibre Modulus of Elasticity in Tension	230 000 N/mm²	(ISO 10618)
Dry Fibre Elongation at Break	1.7 %	(ISO 10618)

TECHNICAL INFORMATION

Laminate Nominal Thickness	0.167 mm		
Laminate Nominal Cross Section	167 mm² per m width		
Laminate Tensile Strength	Average 3 500 N/mm²	Characteristic 3 200 kN/mm²	(EN 2561*) (ASTM D 3039*)
Laminate Modulus of Elasticity in Tension	Average 225 kN/mm²	Characteristic 220 kN/mm²	(EN 2561*)
	Average 220 kN/mm²	Characteristic 210 kN/mm²	(ASTM D 3039*)
	* modification: sample with 50 mm Values in the longitudnal direction of the fibres Single layer, minimum 27 samples per test series		
Laminate Elongation at Break in Tension	1.56 % 1.59 %		(EN 2561) (ASTM D 3039)
Tensile Resistance	Average 585 N/mm	Characterstic 534 N/mm	(EN 2561) (ASTM D 3039)
Tensile Stiffness	Average 37.6 MN/m 37.6 kN/m per ‰ elongation	Characteristic 36.7 MN/m 36.7 kN/m per ‰ elongation	(EN 2561)
	Average 36.7 MN/m 36.7 kN/m per ‰ elongation	Characteristic 35.1 MN/m 35.1 kN/m per ‰ elongation	(ASTM D 3039)

SYSTEMS

System Structure

The system build-up and configuration as described must be fully complied with and may not be changed.

Concrete substrate adhesive primer	Sikadur®-330
Impregnating / laminating resin	Sikadur®-330 or Sikadur®-300
Structural strengthening fabric	SikaWrap®-300 C

For detailed information on Sikadur®-330 or Sikadur®-300, together with the resin and fabric application details, please refer to the Sikadur®-330 or Sikadur®-300 Product Data Sheet and the relevant Method Statement.

APPLICATION INFORMATION

Consumption

Dry application with Sikadur®-330	
First layer including primer layer	1.0 - 1.5 kg/m²
Following layers	0.8 kg/m²
Wet application with Sikadur®-300	
Primer layer	0.4 - 0.6 kg/m²
Fabric layers	0.6 kg/m²

Please also refer to the relevant Method Statement for further information.

APPLICATION INSTRUCTIONS

SUBSTRATE QUALITY

Minimal substrate tensile strength: 1.0 N/mm² or as specified in the strengthening design.
Please also refer to the relevant Method Statement or further information.

SUBSTRATE PREPARATION

Concrete must be cleaned and prepared to achieve a laitance and contaminant free, open textured surface. Please also refer to the relevant Method Statement for further information.

APPLICATION METHOD / TOOLS

The fabric can be cut with special scissors or a Stanley knife (razor knife / box-cutter knife). Never fold the fabric.
SikaWrap®-300 C is applied using the dry or wet application process.
Please refer to the relevant Method Statement for details on the impregnating / laminating procedure

LIMITATIONS

- SikaWrap®-300 C shall only be applied by trained and experienced professionals.
- A specialist structural engineer must be consulted for any structural strengthening design calculation.
- SikaWrap®-300 C fabric is coated to ensure maximum bond and durability with the Sikadur® adhesives / impregnating / laminating resins. To maintain and ensure full system compatibility, do not interchange different system components.
- SikaWrap®-300 C can be over coated with a cementitious overlay or other coatings for aesthetic and / or protective purposes. The over coating system selection is dependent on the exposure and the project specific requirements. For additional UV light protection in exposed areas use Sikagard®-550 W Elastic (G) or Sikagard®-680 SG.
- Please refer to the Method Statement of SikaWrap® manual dry application, SikaWrap® manual wet application or SikaWrap® machine wet application for further information, guidelines and limitations.

BASIS OF PRODUCT DATA

All technical data stated in this Data Sheet are based on laboratory tests. Actual measured data may vary due to circumstances beyond our control.

LOCAL RESTRICTIONS

Please note that as a result of specific local regulations the declared data and recommended uses for this product may vary from country to country. Please consult the local Product Data Sheet for the exact product data and uses.

ECOLOGY, HEALTH AND SAFETY

This product is an article as defined in article 3 of regulation (EC) No 1907/2006 (REACH). It contains no substances which are intended to be released from the article under normal or reasonably foreseeable conditions of use. A safety data sheet following article 31 of the same regulation is not needed to bring the product to the market, to transport or to use it. For safe use follow the instructions given in this product data sheet. Based on our current knowledge, this product does not contain SVHC (substances of very high concern) as listed in Annex XIV of the REACH regulation or on the candidate list published by the European Chemicals Agency in concentrations above 0.1 % (w/w)

LEGAL NOTES

The information, and, in particular, the recommendations relating to the application and end-use of Sika products, are given in good faith based on Sika's current knowledge and experience of the products when properly stored, handled and applied under normal conditions in accordance with Sika's recommendations. In practice, the differences in materials, substrates and actual site conditions are such that no warranty in respect of merchantability or of fitness for a particular purpose, nor any liability arising out of any legal relationship whatsoever, can be inferred either from this information, or from any written recommendations, or from any other advice offered. The user of the product must test the product's suitability for the intended application and purpose. Sika reserves the right to change the properties of its products. The proprietary rights of third parties must be observed. All orders are accepted subject to our current terms of sale and delivery. Users must always refer to the most recent issue of the local Product Data Sheet for the product concerned, copies of which will be supplied on request.

SIKA NORTHERN GULF
Bahrain / Qatar / Kuwait
Tel: +973 177 38188
sika.gulf@bh.sika.com
gcc.sika.com

SIKA SOUTHERN GULF
UAE / Oman / SIC
Tel: +971 4 439 8200
info@ae.sika.com
gcc.sika.com

SIKA SAUDI ARABIA
Riyadh / Jeddah / Dammam
Tel: +966 11 217 6532
info@sa.sika.com
gcc.sika.com

SikaWrap-300C_en_AE_(05-2017)_1_1.pdf

Product Data Sheet
SikaWrap®-300 C
May 2017, Version 01.01
020206020010000011

BUILDING TRUST

Properties of adhesives

A. Epoxy Sikadur®-330 for CFRP sheets adhesive

BUILDING TRUST

PRODUCT DATA SHEET

Sikadur®-330

2-COMPONENT EPOXY IMPREGNATION RESIN

DESCRIPTION

Sikadur®-330 is a 2-component, thixotropic epoxy based impregnating resin and adhesive.
Suitable for use in hot and tropical climatic conditions.

USES

Sikadur®-330 may only be used by experienced professionals.
Sikadur®-330 is used as:
- Impregnation resin for SikaWrap® fabric reinforcement for the dry application method
- Primer resin for the wet application system
- Structural adhesive for bonding Sika® CarboDur® plates into slits

CHARACTERISTICS / ADVANTAGES

- Easy mix and application by trowel and impregnation roller
- Manufactured for manual saturation methods
- Excellent application behaviour to vertical and overhead surfaces
- Good adhesion to many substrates
- High mechanical properties
- No separate primer required

APPROVALS / STANDARDS

- Avis Technique N° 3/10-669 (annule et remplace N° 3/07-502) Sika® CarboDur®, SikaWrap®
- Road and Bridges Research Institute (Poland): IBDiM No AT/2008-03-336/1
- Adhesive for structural bonding tested according to EN 1504-4

PRODUCT INFORMATION

Chemical base	Epoxy resin
Packaging	5 kg (A + B)
Colour	Component A: white paste Component B: grey paste Components A + B: light grey paste
Shelf life	24 months from date of production
Storage conditions	Store in original, unopened, sealed and undamaged packaging in dry conditions at temperatures between +5 °C and +30 °C. Protect from direct sunlight.
Density	~1.30 kg/l (mixed component A + B mixed) (+23 °C)
Viscosity	Shear rate: 50/s

Temperature	Viscosity
+10 °C	~10 000 mPas
+23 °C	~6 000 mPas
+35 °C	~5 000 mPas

Product Data Sheet
Sikadur®-330
February 2017, Version 02.01
020206040010000004

TECHNICAL INFORMATION

Modulus of Elasticity in Flexure	~3 800 N/mm² (7 d, +23 °C)	(DIN EN 1465)
Tensile Strength	~30 N/mm² (7 d, +23 °C)	(ISO 527)
Modulus of Elasticity in Tension	~4 500 N/mm² (7 d, +23 °C)	(ISO 527)
Elongation at Break	~0.9 % (7 d, +23 °C)	(ISO 527)
Tensile Adhesion Strength	Concrete fracture (> 4 N/mm²) on sandblasted substrate	(EN ISO 4624)
Coefficient of Thermal Expansion	4.5 × 10⁻⁵ 1/K (Temperature range -10 °C min. / +40 °C max.)	(EN 1770)
Glass Transition Temperature	Curing time: 30 d; Curing temperature: +30 °C; TG: +58 °C	(EN 12614)
Heat Deflection Temperature	Curing time / Curing temperature / HDT: 7 d / +10 °C / +36 °C; 7 d / +23 °C / +47 °C; 7 d / +35 °C / +53 °C. Resistant to continuous exposure up to +45 °C.	(ASTM D 648)
Service Temperature	-40 °C min. / +45 °C max.	

SYSTEMS

System Structure	Substrate primer: Sikadur®-330. Impregnating / laminating resin: Sikadur®-330. Structural strengthening fabric: SikaWrap® type to suit requirements.

APPLICATION INFORMATION

Mixing ratio	Component A : Component B = 4 : 1 (by weight) When using bulk material the exact mixing ratio must be safeguarded by accurately weighing and dosing each component.
Consumption	See the "Method Statement for SikaWrap® manual dry application" Guide: 0.7 - 1.5 kg/m²
Ambient Air Temperature	+10 °C min. / +35 °C max.
Dew Point	Beware of condensation. Substrate temperature during application must be at least 3 °C above dew point.
Substrate Temperature	+10 °C min. / +35 °C max.
Substrate Moisture Content	< 4 % pbw

Product Data Sheet
Sikadur®-330
February 2017, Version 02.01
020206040010000004

BUILDING TRUST

Pot Life (EN ISO 9514)

Temperature	Pot life	Open time
+10 °C	~90 min (5 kg)	~90 min
+23 °C	~60 min (5 kg)	~60 min
+35 °C	~30 min (5 kg)	~30 min

The pot life begins when the resin and hardener are mixed. It is shorter at high temperatures and longer at low temperatures. The greater the quantity mixed, the shorter the pot life. To obtain longer workability at high temperatures, the mixed adhesive may be divided into portions. Another method is to chill components A and B before mixing them (not below +5 °C).

APPLICATION INSTRUCTIONS

SUBSTRATE QUALITY

Substrate must be sound and of sufficient tensile strength to provide a minimum pull off strength of 1.0 N/mm² or as per the requirements of the design specification.
See also the "Method Statement for SikaWrap® manual dry application".

SUBSTRATE PREPARATION

See the "Method Statement for SikaWrap® manual dry application".

MIXING

Pre-batched units:
Mix components A+B together for at least 3 minutes with a mixing spindle attached to a slow speed electric drill (maximum 300 rpm) until the material becomes smooth in consistency and a uniform grey colour. Avoid aeration while mixing. Then, pour the whole mix into a clean container and stir again for approximately 1 more minute at low speed to keep air entrapment at a minimum. Mix only that quantity which can be used within its pot life.

Bulk packing, not pre-batched:
First, stir each component thoroughly. Add the components in the correct proportions into a suitable mixing pail and stir correctly using an electric low speed mixer as above for pre-batched units.

APPLICATION METHOD / TOOLS

See the "Method Statement for SikaWrap® manual dry application".

CLEANING OF TOOLS

Clean all equipment immediately with Sika® Colma Cleaner. Cured material can only be removed mechanically.

LIMITATIONS

Sikadur®-330 must be protected from rain for at least 24 hours after application.
Ensure placement of fabric and laminating with roller takes place within open time.
At low temperatures and / or high relative humidity, a tacky residue (blush) may form on the surface of the cured Sikadur®-330 epoxy. If an additional layer of fabric or a coating is to be applied onto the cured epoxy, this residue must first be removed with warm, soapy water to ensure adequate bond. In any case, the surface must be wiped dry prior to application of the next layer or coating.
For application in cold or hot conditions, pre-condition material for 24 hours in temperature controlled storage facilities to improve mixing, application and pot life limits.
For further information on over coating, number of layers or creep, please consult a structural engineer for calculations and see also the "Method Statement for SikaWrap® manual dry application".
Sikadur® resins are formulated to have low creep under permanent loading. However due to the creep behaviour of all polymer materials under load, the long term structural design load must account for creep. Generally the long term structural design load must be lower than 20 to 25 % of the failure load. Please consult a structural engineer for load calculations for the specific application.

BASIS OF PRODUCT DATA

All technical data stated in this Data Sheet are based on laboratory tests. Actual measured data may vary due to circumstances beyond our control.

LOCAL RESTRICTIONS

Please note that as a result of specific local regulations the declared data and recommended uses for this product may vary from country to country. Please consult the local Product Data Sheet for the exact product data and uses.

ECOLOGY, HEALTH AND SAFETY

For information and advice on the safe handling, storage and disposal of chemical products, users shall refer to the most recent Safety Data Sheet (SDS) containing physical, ecological, toxicological and other safety-related data.

Product Data Sheet
Sikadur®-330
February 2017, Version 02.01
020206040010000004

BUILDING TRUST

B. Epoxy Sikadur®-31 CF Slow for steel plate adhesive

BUILDING TRUST

PRODUCT DATA SHEET

Sikadur®-31 CF Slow

2-COMPONENT THIXOTROPIC EPOXY ADHESIVE

DESCRIPTION

Sikadur®-31 CF Slow is a moisture tolerant, thixotropic, structural 2-component adhesive and repair mortar, based on epoxy resins and special fillers for use at higher temperatures between +25 °C and +45 °C.

USES

Sikadur®-31 CF Slow may only be used by experienced professionals.
As a structural adhesive and mortar for:
- Concrete elements
- Hard natural stone
- Ceramics, fibre cement
- Mortar, Bricks, Masonry
- Steel, Iron, Aluminium
- Wood
- Polyester, Epoxy
- Glass

As a fast setting rapid repair adhesive and mortar:
- Corners and edges
- Holes and void filling
- For vertical and overhead use

Joint filling and crack sealing:
- Joint arris repair and crack sealing

CHARACTERISTICS / ADVANTAGES

Sikadur®-31 CF Slow has the following advantages:
- Easy to mix and apply
- Very good adhesion to most construction materials
- High strength adhesive
- Thixotropic: non-sag in vertical and overhead applications
- Hardens without shrinkage
- Different coloured components (for mixing control)
- No primer needed
- High initial and ultimate mechanical strength
- Good abrasion resistance
- Impermeable to liquids and water vapour
- Good chemical resistance

PRODUCT INFORMATION

Composition	Epoxy resin	
Packaging	30 kg (A+B) 6 kg (A+B) 1.2 kg (A+B)	Pre-batched unit Pre-batched unit Pre-batched unit box of 6 x 1.2 kg
Colour	Component A: grey Component B: black Components A+B mixed: concrete grey	
Shelf life	24 months from date of production	
Storage conditions	Store in original, unopened, sealed and undamaged packaging in dry conditions at temperatures between +15 °C and +30 °C. Protect from direct sunlight.	
Density	1.93 ± 0.1 kg/L (component A+B mixed) (at +23 °C) (evacuated)	

Product Data Sheet
Sikadur®-31 CF Slow
December 2018, Version 01.02
020204030010000041

TECHNICAL INFORMATION

Compressive Strength (DIN EN 196)

Curing time	Curing temperature +25 °C	+35 °C	+45 °C
1 day	~ 35 - 45 N/mm²	~ 40 - 50 N/mm²	~ 43 - 53 N/mm²
3 days	~ 42 - 52 N/mm²	~ 44 - 54 N/mm²	~ 49 - 59 N/mm²
7 days	~ 47 - 57 N/mm²	~ 49 - 59 N/mm²	~ 52 - 62 N/mm²

Modulus of Elasticity in Compression ~ 2 600 N/mm² (14 days at +23 °C) (ASTM D 695)

Tensile Strength in Flexure (DIN EN 196)

Curing time	Curing temperature +25 °C	+35 °C	+45 °C
1 day	~ 15 - 25 N/mm²	~ 15 - 25 N/mm²	~ 15 - 25 N/mm²
3 days	~ 20 - 30 N/mm²	~ 15 - 25 N/mm²	~ 20 - 30 N/mm²
7 days	~ 22 - 32 N/mm²	~ 22 - 32 N/mm²	~ 23 - 33 N/mm²

Tensile Strength (DIN EN 196)

Curing time	Curing temperature +25 °C	+35 °C	+45 °C
1 day	~ 4 - 8 N/mm²	~ 9 - 15 N/mm²	~ 10 - 16 N/mm²
3 days	~ 9 - 15 N/mm²	~ 10 - 16 N/mm²	~ 13 - 19 N/mm²
7 days	~10 - 16 N/mm²	~ 10 - 16 N/mm²	~ 14 - 20 N/mm²

Modulus of Elasticity in Tension ~ 3 000 N/mm² (14 days at +23 °C) (ISO 527)

Elongation at Break 0.6 ± 0.1 % (7 days at +35 °C) (ISO 527)

Tensile Adhesion Strength (EN ISO 4624, EN 1542, EN 12188 at +35 °C)

Curing time	Substrate	Adhesion strength
7 days	Concrete dry	~2 N/mm² *
7 days	Concrete moist	~2 N/mm² *
7 days	Steel	~12 N/mm²

* 100% concrete failure

Shrinkage Hardens without shrinkage.

Coefficient of Thermal Expansion 7.9 x 10^{-5} per °C (Temp. range +23 °C – +60 °C) (EN 1770)

Heat Deflection Temperature (ISO 75)

Curing time	Curing temperature	HDT
7 days (thickness 10 mm)	+35 °C	+50 °C

APPLICATION INFORMATION

Mixing Ratio Component A : component B = 2 : 1 by weight

Consumption The consumption of Sikadur®-31 CF Slow is ~1.9 kg/m² per mm of thickness.

Layer Thickness 30 mm max.
When using multiple units, one after the other. Do not mix the following unit until the previous one has been used in order to avoid a reduction in handling time.

Sag Flow On vertical surfaces it is non-sag up to 15 mm thickness. (EN 1799)

Product Temperature Sikadur®-31 CF Slow can be applied at temperatures between +25 °C and +45 °C.

Ambient Air Temperature +25 °C min. / +45 °C max.

Dew Point Beware of condensation.
Substrate temperature during application must be at least 3 °C above dew point.

Substrate Temperature +25 °C min. / +45 °C max.

Substrate Moisture Content Substrate must be dry or mat damp (no standing water)
Brush the adhesive well into the substrate

Pot Life (EN ISO 9514)

Temperature	Potlife*	Open time
+25 °C	~ 120 min	—
+35 °C	~ 70 min	—
+45 °C	~ 45 min	~ 60 min

* 200 g
The potlife begins when the resin and hardener are mixed. It is shorter at high temperatures and longer at low temperatures. The greater the quantity mixed, the shorter the potlife. To obtain longer workability at high temperatures, the mixed adhesive may be divided into portions. Another method is to chill components A+B before mixing them (not below +5 °C).

APPLICATION INSTRUCTIONS

SUBSTRATE QUALITY

Mortar and concrete must be older than 28 days. (depends on minimal requirement of strengths).
Verify the substrate strength (concrete, masonry, natural stone).
The substrate surface (all types) must be clean, dry or mat damp (no standing water) and free from contaminants such as dirt, oil, grease, existing surface treatments and coatings etc..
Steel substrates must be de-rusted similar to Sa 2.5
The substrate must be sound and all loose particles must be removed.

SUBSTRATE PREPARATION

Concrete, mortar, stone, bricks: Substrates must be sound, dry or mat damp (no standing water), clean and free from laitance, ice, standing water, grease, oils, old surface treatments or coatings and all loose or friable particles must be removed to achieve a laitance and contaminant free, open textured surface.
Steel: Must be cleaned and prepared thoroughly to an acceptable quality i.e. by blastcleaning and vacuum.
Avoid dew point conditions.

MIXING

Pre–batched units:
Mix components A+B together for at least 3 minutes with a mixing spindle attached to a slow speed electric drill (max. 300 rpm) until the material becomes smooth in consistency and a uniform grey colour.
Avoid aeration while mixing. Then, pour the whole mix into a clean container and stir again for ~ 1 minute at low speed to keep air entrapment at a minimum. Mix only that quantity which can be used within its pot life.

APPLICATION METHOD / TOOLS

When using a thin layer adhesive, apply the mixed adhesive to the prepared surface with a spatula, trowel, notched trowel, (or with hands protected by gloves).
When applying as a repair mortar use some formwork.
When using for bonding metal profiles onto vertical surfaces, press uniformly using props for at least 12 hours, dependent on the layer thickness applied (not more than 5 mm) and the room temperature.
Once hardened check the adhesion by tapping with a hammer.

CLEANING OF EQUIPMENT

Clean all tools and application equipment with Sika® Colma Cleaner immediately after use. Hardened / cured material can only be mechanically removed.

IMPORTANT CONSIDERATIONS

Sikadur® resins are formulated to have low creep under permanent loading. However due to the creep behaviour of all polymer materials under load, the long term structural design load must account for creep. Generally the long term structural design load must be lower than 20–25 % of the failure load.
A structural engineer must be consulted for load calculations for the specific application.

BASIS OF PRODUCT DATA

All technical data stated in this Data Sheet are based on laboratory tests. Actual measured data may vary due to circumstances beyond our control.

Product Data Sheet
Sikadur®-31 CF Slow
December 2018, Version 01.02
020204030010000041

BUILDING TRUST

LOCAL RESTRICTIONS

Note that as a result of specific local regulations the declared data and recommended uses for this product may vary from country to country. Consult the local Product Data Sheet for the exact product data and uses.

ECOLOGY, HEALTH AND SAFETY

For information and advice on the safe handling, storage and disposal of chemical products, users shall refer to the most recent Safety Data Sheet (SDS) containing physical, ecological, toxicological and other safety-related data.

LEGAL NOTES

The information, and, in particular, the recommendations relating to the application and end-use of Sika products, are given in good faith based on Sika's current knowledge and experience of the products when properly stored, handled and applied under normal conditions in accordance with Sika's recommendations. In practice, the differences in materials, substrates and actual site conditions are such that no warranty in respect of merchantability or of fitness for a particular purpose, nor any liability arising out of any legal relationship whatsoever, can be inferred either from this information, or from any written recommendations, or from any other advice offered. The user of the product must test the product's suitability for the intended application and purpose. Sika reserves the right to change the properties of its products. The proprietary rights of third parties must be observed. All orders are accepted subject to our current terms of sale and delivery. Users must always refer to the most recent issue of the local Product Data Sheet for the product concerned, copies of which will be supplied on request.

PT. Sika Indonesia Head Office and
Jl. Raya Cibinong-Bekasi Km.20
Limusnunggal-Cileungsi
Bogor 16820-Indonesia
Tel. +62 21 8230025, Fax +62 21 8230026
Web: idn.sika.com
Email: sikacare@id.sika.com

الخلاصة

ان الغرض الرئيسي من هذا البحث هو التحري عن سلوك وأداء اعتاب (T) المقلوبة من الخرسانة المسلحة باستخدام مجموعة متنوعة من التعديل التحديثي (التقوية والتصليح) بواسطة تقنية الربط الخارجي (EBR) بشرائح الياف الكاربون (CFRP) أو الالواح الفولاذية لترقية الهياكل الحالية وزيادة قدرتها على الانثناء. تكونت الدراسة البحثية الحالية من جزأين. الجزء الاول تضمن الجزء العملي لتهيئة وفحص ثلاث عشر من العتبات الخرسانية المسلحة لأعتاب (T) المقلوبة مقسمة الى ثلاثة مجاميع بالإضافة الى العتب المرجعي او عتب السيطرة. المجموعة الاولى تألفت من خمسة اعتاب (T) المقلوبة مقواة بالربط الخارجي لشرائح الياف الكاربون (CFRP) لبيان تأثير الطول الفعال والعرض الفعال لشرائح الياف الكاربون (CFRP) على تصرف العتبات و سعة التحمل. المجموعة الثانية تألفت من خمسة اعتاب (T) المقلوبة مقواة بالربط الخارجي للألواح الفولاذية لبيان تأثير الطول الفعال والعرض الفعال للألواح الفولاذية على تصرف العتبات ومقدار التحمل. أما المجموعة الثالثة تألفت من عتبين (T) المقلوبة للتحري على تحمل وتصرف اعتاب (T) المقلوبة المتشققة والمصلحة بواسطة تقنية الربط الخارجي (EBR) لشرائح الكاربون فايبر (CFRP) او الالواح الفولاذية. جميع أعتاب (T) المقلوبة كان لها نفس الابعاد ونفس قضبان حديد التسليح للشد والضغط والقص. فحصت جميع أعتاب (T) المقلوبة تحت ظروف الاسناد البسيط. الاعتاب في المجموعة الاولى والثانية تم فحصها الى مرحلة الفشل بينما الاعتاب في المجموعة الثالثة فسلط عليها الحمل الى مرحلة التشقق وبعد تصليحها سلط عليها الحمل الى مرحلة الفشل. النتائج العملية اظهرت بان استخدام تقنية التقوية بالربط الخارجي بشرائح الكاربون فايبر أو الألواح الفولاذية حسنت من سلوك وسعة التحمل للأعتاب الخرسانية المسلحة (T) المقلوبة. وان نسبة زيادة تحمل اعتاب (T) المقلوبة المقواة بشرائح الياف الكاربون فايبر تراوحت بين 10.2% و 45.4% من مقدار تحمل العتب المصدري (العتب غير المقوى), وان نسبة زيادة تحمل اعتاب (T) المقلوبة المقواة بالألواح الفولاذية تراوحت بين 0.7% و 31.1% من مقدار تحمل العتب المصدري (العتب غير المقوى). و لوحظ بان النموذج المقوى بشرائح الكاربون فايبر بقياس طول وعرض (1200ملم و150 ملم) على التوالي اعطى اعلى زيادة بالحمل الاقصى عند المقارنة مع الانواع الاخرى من الاعتاب المقواة بشرائح الكاربون فايبر. ايضا اظهرت النتائج مقاومة انثناء عالية عند استخدام تقنية التقوية بشرائح الكاربون فايبر بالمقارنة مع النوع الاخر من تقنية التقوية بواسطة الالواح الفولاذية. النتائج العملية أيضا تضمنت دراسة تأثير الالواح الفولاذية والياف الكاربون في اعادة تأهيل اعتاب (T) المقلوبة

الخرسانية المسلحة, فقد عكست تلك النتائج القابلية الجيدة للألواح الفولاذية والياف الكاربون في تأهيل الأعتاب المتضررة حيث زادت قابلية التحمل للأعتاب بنسب تتراوح بين (29.6% و 39.3%)مقارنة بالعتب المصدري. وأظهرت النتائج بأن الطريقة المفضلة لأعاده تأهيل الاعتاب الخرسانية المسلحة لأعتاب (T) المقلوبة كانت بأستخدام شرائح الكاربون فايبر بالمقارنة مع الالواح الفولاذية. الجزء الثاني تضمن الدراسة باستعمال التحليل اللاخطي بواسطة طريقة العناصر المحددة لاقتراح التصرف اللاخطي للأعتاب الخرسانية المسلحة (T) المقلوبة. تم تمثيل النماذج العددية بأستخدام برنامج ABAQUS Standard/Explicit 2019. طريقة العناصر المحددة أعطت نتائج ذات تقارب جيد مع النتائج العملية حيث كان الاختلاف في مقدار التحمل الاقصى لجميع عتبات التعديل التحديثي يتراوح بين 8.62%- الى 7.51%. وأيضا تم الحصول على توافق جيد بين منحنيات القوة-الهطول في الجزء التحليلي والجزء العملي.

أيضا تم استخدام برنامج ABAQUS Standard/Explicit 2019 لتطور الدراسة اكثر ولإعطاء المزيد من النتائج لفهم السلوك الحقيقي لتحليل العتبات الخرسانية المسلحة المقلوبة ذات الشكل (T) المعدلة بواسطة لوح فولاذي خارجي أو بوليمر مقوى بألياف الكاربون (CFRP).

جمهورية العراق
وزارة التعليم العالي و البحث العلمي
جامعة بابل
كلية الهندسة
قسم الهندسة المدنية

تصرف الاعتاب الخرسانية المسلحة بشكل حرف T مقلوب والمقواة باستخدام تقنيات تقوية مختلفة

رسالة
مقدمة إلى مجلس كلية الهندسة / جامعة بابل
وهي جزء من متطلبات نيل درجة الماجستير في الهندسة
/الهندسة المدنية/ إنشاءات

من قبل

دعاء ماجد شاكر حمزة

بكالوريوس علوم في الهندسة المدنية (2015) م

أشراف

أ. م . د : محمد جواد كاظم

1444هـ **2023م**